IRF5 and the metabolic adaptations of adipose tissue macrophages upon metabolic stress

Lucie Orliaguet

Sorbonne Université

Ecole doctorale ED 394 – Physiologie, physiopathologie et thérapeutique

Equipe IMMEDIAB « Immunité et Métabolisme du Diabète »
Institut Necker Enfants Malades

IRF5 and the metabolic adaptations of adipose tissue macrophages upon metabolic stress

Lucie Orliaguet

Thèse de doctorat de Sciences

Dirigée par Dr Nicolas Venteclef

Présentée et soutenue publiquement le 7 juillet 2022

Devant un jury composé de :

- Bruno Fève, PU-PH, Paris, *Président du jury*
- Ganna Panasyuk, DR INSERM, Paris, *Rapporteur*
- Stoyan Ivanov, CR INSERM, Nice, *Rapporteur*
- Soraya Taleb, DR INSERM, Paris, *Examinateur*
- Jennifer Rieusset, DR INSERM, Lyon, *Examinateur*
- Nicolas Venteclef, DR INSERM, Paris, *Directeur de Thèse*
- Fawaz Alzaid, CR INSERM, Koweït, *Membre invité*

Abstract

IRF5 and the metabolic adaptations of adipose tissue macrophages upon metabolic stress

Obesity and type 2 diabetes (T2D) are growing pandemics. These diseases are of both etiologies : metabolic and inflammatory. The abnormal and ectopic accumulation of fat in the organism leads to the accumulation and activation of tissue resident immune cells, and particularly adipose tissue macrophages (ATM). This phenomenon is the starting point of the so-called metabolic inflammation or metainflammation which is a sterile, systemic and low-grade inflammation. This pro-inflammatory environment favors the progression of obesity and its complications. Type 1 interferon signaling, mediated by the pro-inflammatory transcription factor interferon regulatory factor (IRF) 5, plays a key role in the activation of ATMs during the pathogenesis of obesity and T2D. Interestingly, an emerging field of research places cellular metabolism at the center of immune-effector function. M1 macrophages display an increase of glycolysis while M2 macrophages rely on oxidative respiration to produce energy. This thesis focuses on the potential role of IRF5 in the bioenergetic adaptations of macrophages upon a metabolic stress remains to be elucidated.

Mice with a specific myeloid deletion of IRF5 (IRF5-KO) were fed with a high fat diet to mimic a metabolic stress. Analysis of the bioenergetic and transcriptional profile of IRF5-KO and wild-type ATMs revealed an IRF5-dependent metabolic adaptation of the ATMs, characterized by an increase of the mitochondrial activity. Combined analysis of RNA-seq and ChIP-seq data identified IRF5 as a transcriptional regulator of metabolic pathways. Moreover, IRF5 represses the expression of the *Growth Hormone Inducible Transmembrane Protein*, a mitochondrial protein. This transcriptional repression favors mitochondrial cristae disruption and triggers AT maladaptation to caloric excess. Interestingly, this novel and non-canonical IRF5-GHITM axis extends to ATMs and monocytes from T2D and/or obese patients.

In parallel, I have also studied the importance of cellular metabolism in macrophage polarization *in vitro* and in other context of sterile inflammation. Overall, this thesis underlies the powerful function of cellular metabolism in controlling macrophage activation.

Keywords : obesity, immunometabolism, metainflammation, macrophages, mitochondria

Acknowledgements

Aux membres du jury,
Je tiens à remercier l'ensemble des membres de mon jury de thèse. Un grand merci au **Pr Bruno Fève** pour avoir accepté de présider mon jury de thèse. Sincères remerciements au **Dr Ganna Panasyuk** et au **Dr Stoyan Ivanov** pour leur disponibilité, au temps consacré à ce manuscrit ainsi que pour leurs remarques pertinentes et leurs conseils. Enfin, je tiens à remercier **Dr Soraya Taleb** pour ses commentaires constructifs tout au long de ma thèse ainsi que **Dr Jennifer Rieusset** pour sa précieuse aide sur le projet IRF5. Merci d'avoir accepté d'examiner mon travail de thèse.

A mes directeurs de thèse,
Nicolas, Fawaz, immense merci pour l'opportunité que vous m'avez offerte à l'issue de ma L3, de poursuivre ce projet IRF5. Merci pour votre confiance et votre soutien.
Fawaz, sincère merci pour ton accompagnement tout au long de cette aventure qu'est la thèse. Merci pour tes conseils avisés, tes corrections ainsi que ta disponibilité et ta patience au quotidien, et ce depuis mon premier stage.
Nicolas, un grand merci pour ton dynamisme, ton exigence, tout en étant bienveillant, ton implication dans ce projet et plus généralement dans la vie du labo. Ta passion pour la Science a grandement contribué à mon parcours depuis notre rencontre en 2015. Merci d'avoir toujours été présent depuis mes débuts.

A l'ensemble de l'équipe IMMEDIAB,
Je suis ravie d'avoir pu vous côtoyer tout au long de ma thèse, merci pour votre accueil, votre précieuse aide, vos conseils et ainsi que pour tous les moments en dehors du labo. Merci Elena, Charline P, Aude, Joy, Pauline, Charline G, Dina, Claire, JB, Marc, Louis, Jean-François, Jean-Pierre, Frédéric, Ronan, Gilberto et Samuel !
Merci tout particulier pour Elise, pour tes conseils, j'ai énormément appris grâce à toi !
Mention spéciale pour Tina, Raphaëlle, Diane, Amélie et Ronan qui m'ont tout particulièrement soutenue, toujours autour d'un goûter, gâteau, thé, repas ou verre ! Merci pour tous ces excellents moments passés ensemble, que je ne suis pas prête d'oublier.

Merci aux personnes passionnées et passionnantes qui m'ont donné l'envie de poursuivre en thèse, Ron, Marion, Emrah et tout particulièrement Holly et Jessica.

A mes amis,
Ma deuxième famille, avec qui j'ai partagé tellement de moments uniques et inoubliables. Et tout particulièrement à ceux qui m'entourent depuis presque 8 ans, Flora, Maylis, Claire, Rémi, Cyril, Gaétan, Alexandre Matthieu, Enzo, Charles, Guillaume M, Guillaume R. Je vous dois tant, merci pour votre humour, vos encouragements… J'espère pouvoir vous rendre dans les prochaines années tout le bonheur que vous avez pu m'apporter !
Pensées spéciales pour Louise, Sofia, Rémi et Ulysse, pour votre présence au quotidien !

A ma famille, à mes parents, à ma sœur,
Merci pour votre amour, votre soutien immuable. Merci d'avoir toujours cru en moi. Il m'est parfois difficile de reconnaitre à quel point je suis chanceuse de vous avoir dans ma vie, merci pour tout.

Table of contents

Abstract 1

Acknowledgements 2

Table of contents 3

Table of illustrations 6

Abbreviations 7

Introduction 8

Chapter I : Obesity, type-2 diabetes and metabolic inflammation 8

I. Definition & epidemiology 8

1. Definition of obesity 8
2. Obesity-associated complications 9
3. Obesity and T2D are major health issues 9
4. Animal models to study obesity and T2D 11

II. Adipose tissue biology 11

1. WAT depots 12
2. Functions of adipose tissue 12
3. Adipose tissue during obesity 14

III. The concept of metabolic inflammation 16

1. Obesity is associated with an inflammatory status 16
2. Macrophage are key actors of metabolic inflammation 17
3. Molecular basis of inflammation-induced insulin resistance 17

Chapter II : Macrophages and metabolic health 19

I. Macrophages : cells of the innate immune system 19

1. Overview 19
2. Origins and differentiation of macrophages 19
3. Macrophage functions and phenotypes 20
4. Activation of macrophages 21
   a) Transcriptional regulation of macrophage polarization 21
   b) Epigenetic remodeling 26
   c) Cellular metabolism 26

II. Interferon regulatory factors control macrophage activation 26

1. Overview 26
2. IRF5 and the pro-inflammatory activation of macrophages 27
   a) Physiological functions of IRF5 27
   b) Signaling and mechanisms of action 27
   c) Positive and negative regulation of IRF5 activity 28
   d) Dysregulated expression and activity of the IRF5 pathway 29

III. Adipose tissue macrophages and metabolic health 31

1. Origins and heterogeneity of ATMs 31
2. Roles of ATMs in AT homeostasis 31
   a) Immune function 31
   b) Maintenance of tissue homeostasis 32

3. Roles of ATMs in metabolic inflammation 34
a) Recruitment and proliferation of ATMs during obesity 34
b) Phenotype and activation of ATMs during obesity 34
c) Protective and deleterious functions of ATMs during obesity 35
Chapter III : Cellular metabolism of macrophages 38
I. Cellular metabolism : overview 38
1. Metabolic pathways 38
a) Glycolysis 38
b) The pentose phosphate pathway 39
c) Amino acids metabolism 39
d) Fatty acid metabolism 39
e) The TCA cycle 40
2. Mitochondria are a metabolic hub 40
a) Structure and function 41
b) Mitochondrial dynamics and metabolic regulation 42
3. Experimental approaches to interrogate cellular metabolism 43
II. Metabolic adaptations of pro-inflammatory (M1) macrophages 44
1. Glycolysis and PPP 44
2. TCA cycle 45
3. Fatty acid metabolism 46
4. Amino acids metabolism 46
III. Metabolic adaptations of anti-inflammatory (M2) macrophages 47
1. TCA cycle and OXPHOS 47
2. Fatty acid metabolism 47
3. Glycolysis 48
4. Amino acids metabolism 48
5. Pentose phosphate pathway 49
IV. Metabolic adaptations of tissue resident macrophages 49
1. Airway macrophages 50
2. Peritoneal macrophages 50
3. Adipose tissue macrophages 51
a) In physiology 51
b) During obesity 51
Results 53
Axis 1: IRF5 and ATMs metabolic adaptations upon metabolic stress 53
Hypothesis and aims of the study 53
Methods 54
Discussion and perspectives 115
Axis 2: Cellular metabolism and macrophage polarization 120
Hypothesis and aims of the study 120
Discussion and perspectives 132
Axis 3: Metabolic reprogramming of macrophages during gout and pseudo-gout flares 133
Hypothesis and aims of the study 133
Discussion and perspectives 144
Conclusion 145
Publications and presentations 147

Bibliography **148**

Appendix 1 ..... **163**

Appendix 2 ..... **186**

Résumé **205**

Table of illustrations

Figure 1: Prevalence of obesity and T2D 10
Figure 2: Lipogenesis and lipolysis in the AT 13
Figure 3: Adipose tissue dynamics during obesity 15
Figure 4: Molecular basis of inflammation-induced insulin resistance 18
Figure 5: Transcriptional regulation of M1 polarization 25
Figure 6: Transcriptional regulation of M2 polarization 25
Figure 7: IRF5 signaling pathway 28
Figure 8: Irf5 deletion is protective against insulin resistance in a murine model of diet-induced obesity 30
Figure 9: Subpopulations of adipose tissue macrophages upon obesity 37
Figure 10: Mitochondria are metabolic hub 42
Figure 11: Mitochondrial dynamics 43
Figure 12: Metabolic adaptations of M1 macrophages 47
Figure 13: Metabolic adaptations of M2 macrophages 49
Figure 14: Initiation of the inflammatory process during gout and pseudo-gout flares 134

Abbreviations

2-DG: 2-deoxy-glucose
AA: amino acid
AP-1: activated protein 1
AT: adipose tissue
ATM: adipose tissue macrophages
BMDM: bone-marrow derived macrophage
BMI: body mass index
CLS: crown-like structure
CPT: carnitine palmitoyltransferase
ETC: electron transport chain
FA: fatty acids
FAO: fatty acid oxidation
FAS: fatty acid synthesis
FFA: free fatty acids
GHITM: growth hormone inducible transmembrane protein
GLUT: glucose transporter
HIF: hypoxia-inducible factor
Hk: hexokinase
IDO1: indole-2,3-dioxygenase
IFN: interferon
IKK: IκB kinase
IL: interleukine
ILC: innate lymphoid cell
iNOS: inducible NO synthase
IRAK: Interleukine 1 receptor associated kinase
IRF: interferon regulatory factor
IRS-1 : insulin receptor substrate 1
ISRE: IFN sensitive response elements
JAK: janus kinase
JNK: c-Jun N-terminal kinase
KAP1: KRAB-associated protein 1
KLF: Krüppel like factor
LAM: lipid associated macrophage
LXR: liver X receptor
MCP: monocyte chemoattractant protein
MMe: metabolically activated macrophage
NCoR: nuclear receptor corepressor
NFκB: nuclear factor-kappa B
NLRP3: NOD-like receptor family, pyrin domain containing 3
OXPHOS: oxidative phosphorylation
PDGF: platelet-derived growth factor
PGC1β: PPARγ coactivator protein
PPAR: Peroxisome Proliferator-Activated Receptors
PPP: pentose phosphate pathway
PRR: pattern recognition receptor
ROS: reactive oxygen species
SAM: sympathetic neuron associated macrophage
SDH: succinate dehydrogenase
SLE: systemic lupus erythematosus
SOCS: suppressors of cytokine signaling
SREBP: Sterol Regulatory Element-binding Protein
STAT: signal transducer and activator of transcription
T2D: type-2 diabetes
TCA: tricarboxylic acid cycle
TG: triglycerides
TGFβ: transforming growth factor β
TLR: toll like receptor
TNFα: tumor necrosis factor α
TRAF6: tumor necrosis factor receptor associated factor 6
TRIM21: E3 ubiquitin ligase tripartite motif-containing protein 21
VAM: perivascular macrophages
VLDL: very-low density lipoproteins
WAT: white adipose tissue
αKG: α-ketoglutarate

As the saying goes, "*Tell me what you eat and I will tell you what you are*". This phrase was initially pronounced by the French gastronome Brillat-Savarin to underline the link between food and cultural identity of a given society. It was then used as a slogan to promote healthy diets. Nevertheless, if the interpretations and usages of this statement are diverse, it is now well established that food and nutrition not solely shape culture and identity at the societal level, but also physiology and the health of human body.

Indeed, food provides fuel for the organism and shapes all physiological processes, and notably the capacity for the organism to fight against an infection, namely immunity. Interestingly, the immune system is also involved in the maintenance of an healthy physiological state. Metabolism and immunity are tightly related. Unhealthy diets, poor in fibers and/or enriched in sugar and fat, and excess body weight are risk factors for disability and death. Therefore, the issue of malnutrition, in all its forms, is essential to ensure global health.

While the immune system and the metabolic homeostasis have long been studied separately, immunometabolism is an emerging field of research focusing on the reciprocal relationship between the immune system and the metabolic status. At the systemic level, metabolic status of the individual influences immune responses. Inversely, the immune system is involved in the maintenance of metabolic status and also in the development of metabolic disorders. At the cellular level, metabolism is a potent regulator of immune cell function.

This thesis, which falls at the crossroads of systemic and cellular immunometabolism, focuses on the metabolic adaptations of adipose tissue macrophages during early caloric excess.

Introduction

Chapter I : Obesity, type-2 diabetes and metabolic inflammation

I. Definition & epidemiology

1. Definition of obesity

Obesity is a highly complex condition characterized by an abnormal or excessive fat accumulation that may impair health according to the World Health Organization (WHO). Body mass index (BMI) is a metric (weight-for-height) is used as a surrogate marker for adiposity in adults. It is commonly used to classify overweight and obese adults. WHO characterizes obesity as an excessive fat accumulation that can impair health, with a BMI > 30

kg/m^2 (1). Overweight is for a BMI greater than or equal to 25 kg/m^2. Waist circumference is a more precise metric to assess fat repartition. The fundamental cause of obesity is chronic imbalance between energy expenditure and food intake. Globally, there is an increase of calorie intake due to consumption of high-fat and high-sugar processed food. This is associated with a decrease of physical activity, related to sedentary lifestyle. Overall, obesity promotes an expansion of adipose tissue (AT) to buffer the excess of nutrient.

2. Obesity-associated complications

People with obesity are more likely to develop a number of complications, including cardiovascular events, type-2 diabetes (T2D), non-alcoholic fatty liver disease, dementia, cancers, sleep apnea, osteoarthritis… Obesity also impairs immune function and increases the risk of severe infectious diseases.

Regarding T2D, which corresponds to chronic hyperglycemia due to defects in insulin production and sensitivity, the excess risk of T2D attributable to obesity is comprised between 30 and 53% (2). Obesity favors the establishment of an insulin-resistant state, which, when associated to pancreatic ß cell dysfunction, leads to the development of T2D. Approximately 80 to 90% of T2D-patients are overweight or obese. Moreover, T2D is associated with the development of a wide-range of complications such as hepatic comorbidities, retinopathies, neuropathies and nephropathies.

3. Obesity and T2D are major health issues

In 2021, WHO declared obesity as an ongoing pandemic. While for decades obesity has been associated with high-income countries, its prevalence is now rising in low- and middle-income countries (Figure 1). Worldwide, in 2016, 1.9 billion adults (39% of the adult population) were overweight and among them, 650 million were obese, which represents 13% of the general population. Strikingly, the prevalence of obesity has tripled over the last 40 years. More recently, the COVID-19 pandemic and the successive periods of lockdowns lead to a worsening of the childhood obesity pandemic. Indeed, in the US, the rate of BMI increase in children has doubled over the last two years, compared to pre-pandemic levels (3).

In addition, obesity and T2D are tightly related. According to WHO, the incidence of T2D has been multiplied by four in the last 30 years. Its prevalence has been increasing in low- and middle-income countries, where obesity is rising (Figure 1).

Obesity is associated with the development of several complications, which lead to a decrease of the quality of life and a reduction of life expectancy by 2.7 years on average according to the Organization for Economic Cooperation and Development (OECD). In particular, T2D was the ninth cause of death in 2019 and there was, between 2000 and 2016, a 5% increase in premature mortality from T2D. Moreover, the impact on health population will translate into an increase in health expenditure. Obesity and its associated comorbidities represent an economic burden for healthcare systems.

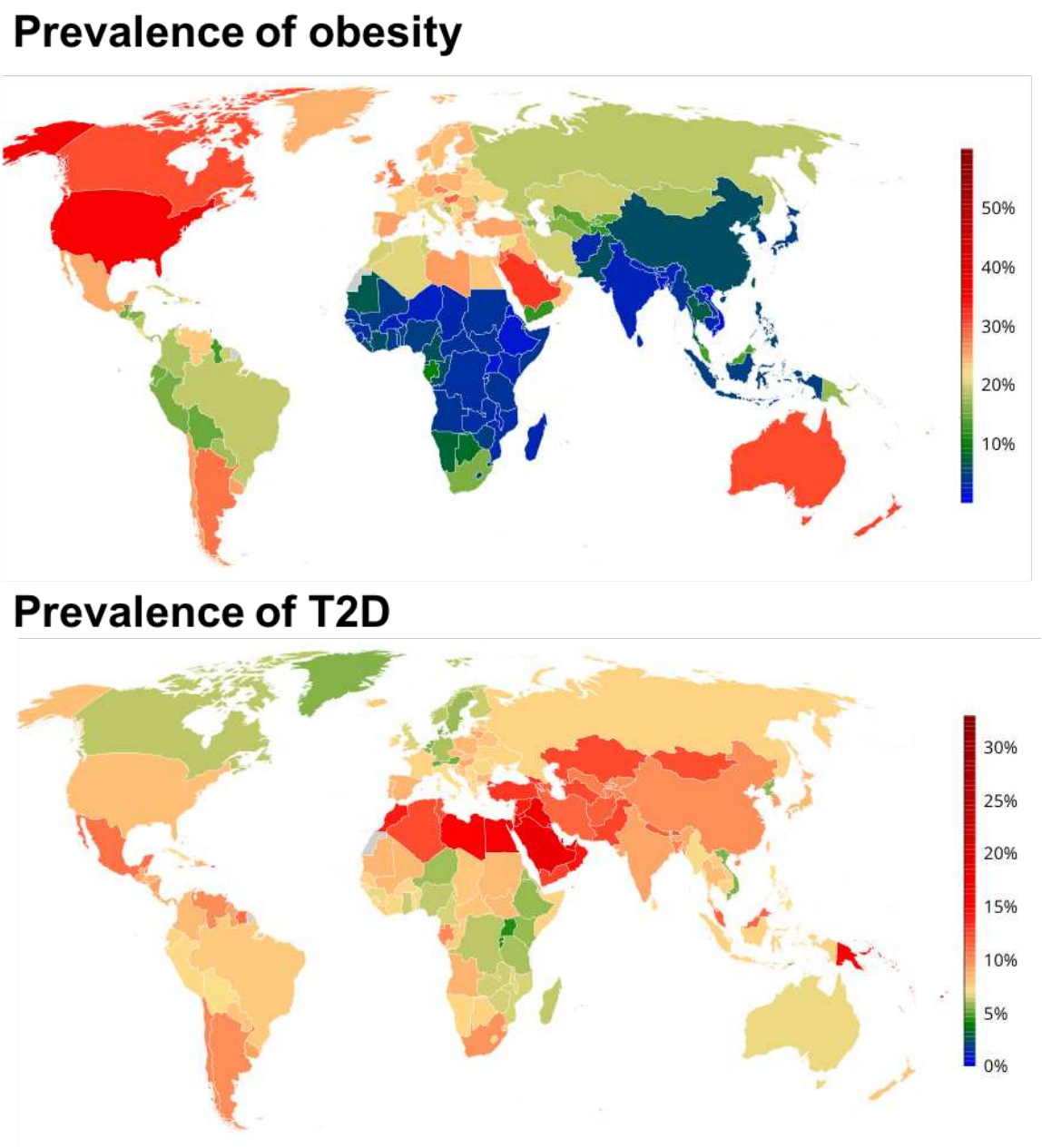

Figure 1: Prevalence of obesity and T2D
Obesity is defined by a BMI>30kg/m^2 and TD2 individuals are characterized by fasting plasma glucose ≥7.0 mmol/L, or history of diagnosis with diabetes, or use of insulin or oral

hypoglycaemic drugs) in men, in 2016. Data from WHO, © Copyright 2017 NCD Risk Factor Collaboration (ncdrisc.org)

Altogether, obesity, overweight and the associated complications are largely preventable. Public health policies to improve nutrition and promote physical activity could help to tackle this ongoing pandemic.

4. Animal models to study obesity and T2D

In the context of the growing pandemics of obesity and T2D, it is imperative to develop animal models to replicate human obesity, to study the mechanisms involved in the pathogenesis of obesity and its associated complications. Most of the studies have been performed on rodents. We can distinguish genetic models, related to one or several genetic mutations from non-genetic models, where obesity is induced surgically or by dietary interventions.

Most studied models of genetic obesity are linked to mutations in the leptin-melanocortin pathway. This signaling pathway encompasses different hormones and neuropeptides and regulates food intake and energy homeostasis (4). In particular, *Ob/ob* mice have a mutation in the gene encoding leptin while *db/db* mice are characterized by a mutation in the gene encoding leptin receptor. These two mice models become spontaneously obese but only *db/db* mice develop a frank insulin resistance. In addition, they differ in terms of AT and liver inflammation (5). Although these models are widely used, monogenic obesity only represent a small proportion of human obesity.

Non-genetic rodent models consist of surgical or dietary approaches. In rodents, surgical ablation of hypothalamic nuclei involved in the control of food intake is associated with hyperphagia and increased adiposity and can thus model obesity (6). Today, the gold-standard model to mimic human obesity is the dietary approach. The most widely used diets are composed of varying fat content, ranging from 10% (normal chow diet) to 60% (high fat diet (HFD)) of kcal from fat. Sucrose and different sources of fat can be used to mimic human physiology. One week of high fat feeding is enough to observe significant weight gain but most studies are based on longer periods to induce obesity and insulin resistance. High fat feeding is a powerful tool to replicate in rodents AT features of obese patients (7).

II. Adipose tissue biology

Over the course of developing obesity, AT expands. Mammals have different types of AT : white, beige and brown, with different localizations, structures and functions. In this manuscript, white AT (WAT) will be studied.

1. WAT depots

In humans, most of the AT is composed of WAT. WAT has the unique ability to expand and shrink in significant proportion as it can represent from 3% to 70% of total body weight in athlete or in obese individuals respectively.

We distinguish subcutaneous and visceral AT. Visceral or abdominal fat is located in the abdominal cavity, where we can find mesenteric AT around intestines, omental AT and perigonadal AT in rodents. Visceral fat is playing a central role in obesity, as it is associated with the development of insulin resistance and T2D. On the other hand, subcutaneous AT is located below the skin and is found in the neck, around the hips and thighs in women. Subcutaneous AT is less associated with obesity-associated complications and is usually considered as protective (8). However, a study performed on a cohort of non-obese T2D patients highlights a specific remodeling of subcutaneous AT, characterized by hypertrophic adipocytes compared to healthy controls. Adipocyte hypertrophy is due to a decrease in the differential capacity of progenitors and is associated with impaired insulin sensitivity (9).

Most of the AT is composed of adipocytes, associated with mesenchymal cells, endothelial cells, fibroblasts and immune cells which compose the stromal vascular fraction. White adipocytes are composed of one lipid droplet which occupies up to 90% of the cellular volume, few mitochondria and a peripheral nucleus. AT resident immune cells form a *bona fide* tissue-specific immune system, with its own particularities due to the micro-environment in which cells reside (10).

2. Functions of adipose tissue

WAT has long been seen as an inert organ that accumulates fat. WAT is a plastic and dynamic organ that respond to physiological stressors to store or to release lipids (lipolysis). In the AT, energy is stored under the form of triglycerides (TG) which are either synthesized from an excess of carbohydrates or coming from circulating TG.

De novo lipogenesis is a metabolic pathway allowing carbohydrates from the circulation to be converted into fatty acids (FA), which can then be stored as triglycerides. More precisely,

glucose is captured and metabolized through glycolysis, which leads to the production of pyruvate and glycerol-3-phosphate. Pyruvate can feed the mitochondria for the generation of citrate, which then serve as a substrate for fatty acid synthesis. Similarly to FA, glycerol-3-phosphate is a precursor for TG synthesis in the lipid droplet. Moreover, TG can also originate from the circulation where there are associated to lipoproteins. TG are hydrolyzed to generate free fatty acids (FFA) by the action of the lipoprotein lipase. FFA can enter the adipocytes and be esterified in TG in the lipid droplet (Figure 2). These mechanisms of energy storage are stimulated by insulin (11).

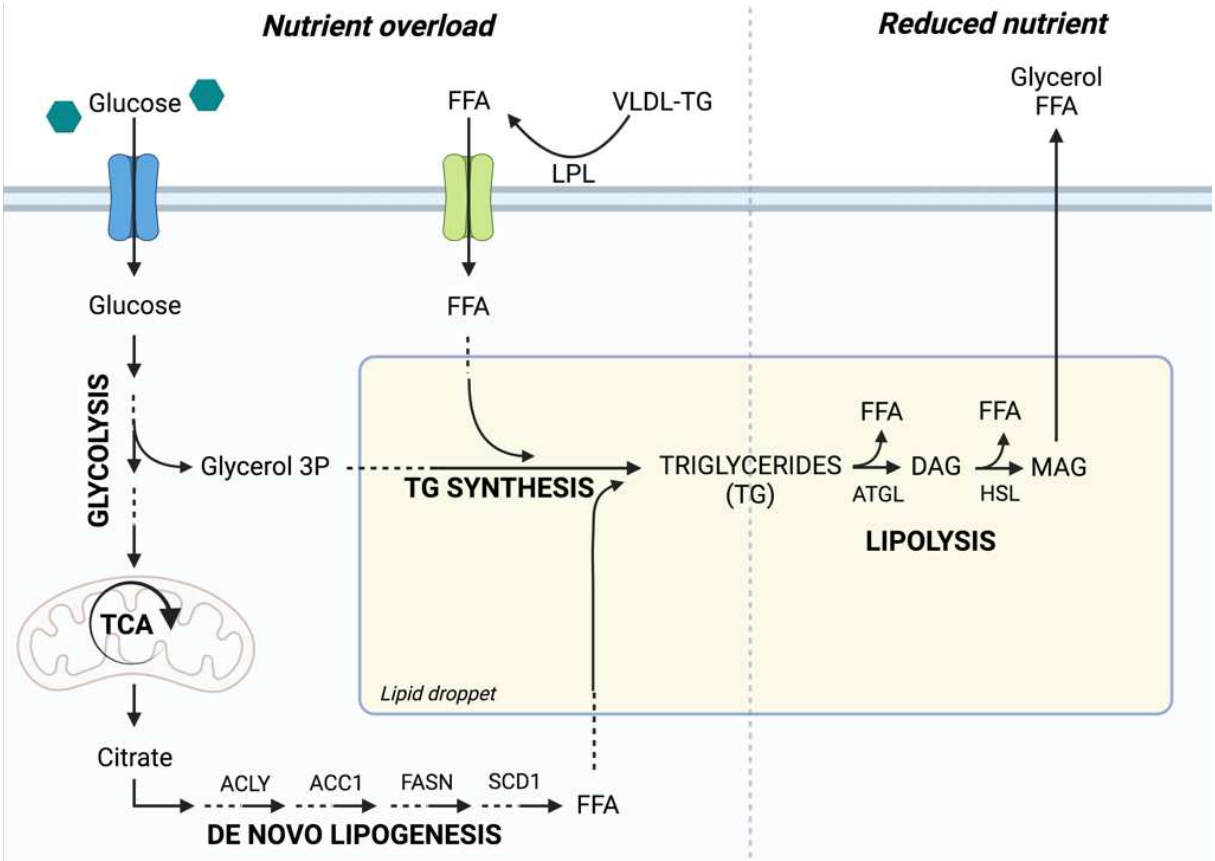

Figure 2: Lipogenesis and lipolysis in the AT
In a nutrient rich environment, adipocytes store energy. This process is mediated by de novo lipogenesis and by the uptake of free fatty acids (FFA), to give rise to the synthesis of triglycerides (TG). In conditions where nutrient availability is reduced (fasting for example), TG undergo lipolysis, which enables the production of FFA in the extracellular milieu.
VLDL-TG: very low density lipoproteins-TG, LPL: lipoprotein lipase, TCA: tricarboxylic acid cycle, ACLY: ATP citrate synthase, ACC1: acetyl-coA carboxylase 1, FASN: fatty acid synthase , SCD1: stearoyl-coA desaturase 1, ATGL: adipose TG lipase, DAG: diacylglycerol, HSL: hormone-sensitive lipase, MAG: monoacylglycerol

On the other hand, during periods of energy demands, such as fasting or exercise, TG undergo lipolysis. Through sequential enzymatic reactions, TG are hydrolyzed into glycerol and FA that

can be released into the circulation (Figure 2). This metabolic pathway is attenuated by insulin (12).

Moreover, AT can be considered as an endocrine organ. Indeed, AT synthetizes and secretes several factors, named adipokines, such as the metabolic hormones leptin and adiponectin and also the pro-inflammatory cytokines, namely tumor necrosis factor (TNF)- α and interleukine (IL)6 (13).

3. Adipose tissue during obesity

During energy surplus and obesity, AT expands. Two mechanisms are associated with AT growth : hypertrophy (increase of adipocyte size) and hyperplasia (increase of adipocyte number, due to *de novo* differentiation of pre-adipocytes into adipocytes).

Hypertrophy occurs before hyperplasia, to meet the need for additional fat storage. The recruitment of new cells is associated with the increase in fat mass. However, hypertrophy is the main contributor to the expansion of fat mass (14). Hypertrophic adipocytes have an impaired capacity to store dietary fat. Obesity is associated with insulin resistance, leading to a defect in stimulating lipogenesis (12). The development of single nucleus RNA-sequencing allowed a better and more precise comprehension of the dynamics and heterogeneity of pre- and adipocytes populations during obesity (15,16). In particular, one specific subpopulation of progenitors is increased with obesity. This population expresses markers of adipocytes and is characterized by a down-regulation of anti-adipogenic factors, which is in favor with an increased commitment in the adipocyte lineage. Adipocytes also represent an heterogeneous population. We can distinguish 3 subpopulations of adipocytes, with lipogenic adipocytes associated with *de novo* lipogenesis and insulin sensitivity, lipid scavenging adipocytes which uptake lipids rather than generating them and stressed-lipid scavenging adipocytes characterized by the expression of genes involved in stress response, notably hypoxia and cell death. Overall, with obesity, there is a switch from the lipogenic adipocytes towards the stressed-lipid scavenging adipocytes. This phenotypic switch is consistent with the development of AT insulin-resistance and the tissue deleterious microenvironment induced by obesity (16). Indeed, obese subjects exhibit lower AT blood flow and capillarization, inducing the formation of hypoxic areas and consequently cellular stress (17).

The expansion of fat mass during obesity is accompanied by infiltration and accumulation of immune cells, in particular macrophages. In addition, there is an increase of pro-inflammatory

cytokines production (13). With chronic obesity, AT undergoes major remodeling, with unresolved inflammation and fibrosis accumulation (18) (Figure 3).

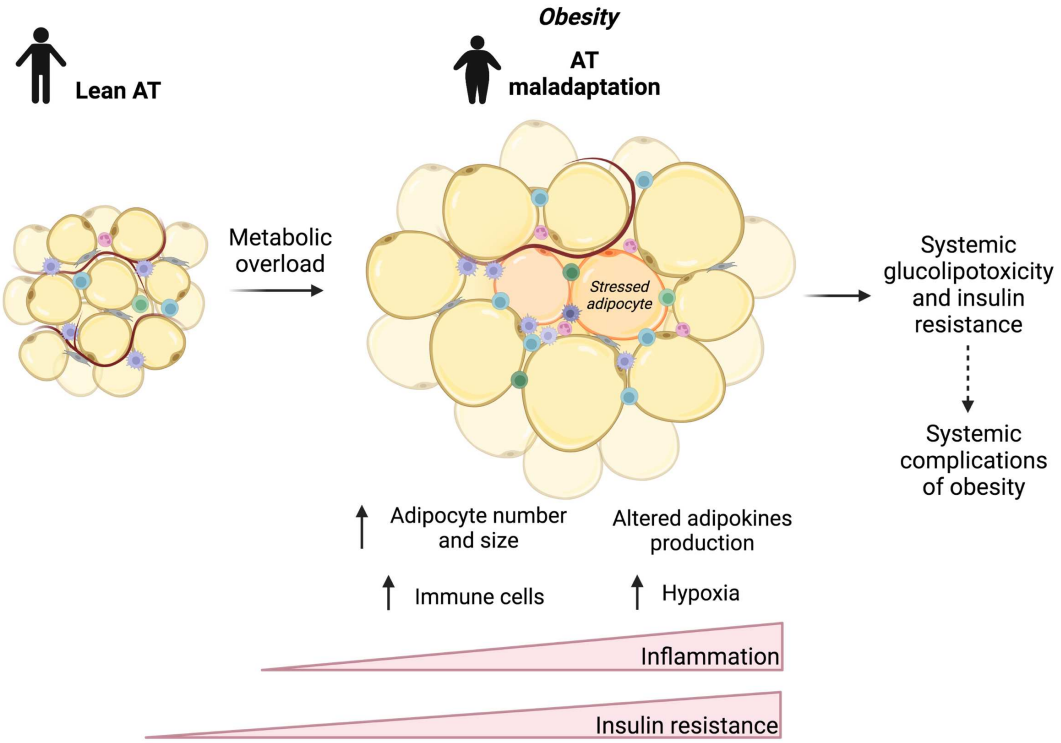

Figure 3: Adipose tissue dynamics during obesity
During obesity, AT expands due to hyperplasia and hypertrophy of adipocytes. In addition, obese AT is characterized by defects in vascularization, leading to hypoxia, immune cell recruitment, and notably macrophages, insulin resistance and a pro-inflammatory environment. This AT maladaptation can trigger disruption of systemic homeostasis with systemic insulin resistance and glucolipotoxicity which together favor the development of obesity-related complications.

AT maladaptation alters systemic homeostasis. Indeed, other tissues are chronically exposed to high levels of glucose or lipids, namely glucolipotoxic conditions. It favors ectopic lipid accumulation, a major site of which is the liver. This triggers the development of insulin resistance and non-alcoholic fatty liver disease, an hepatic comorbidity of obesity. Moreover, obese AT is associated with an altered production of adipokines, which can notably impair metabolic health (Figure 3). Notably, obese AT secrete mediators that can trigger pancreatic β cell failure (19) and stimulate hepatic production of glucose (gluconeogenesis), which favors hyperglycaemia (20).

AT is a dynamic organ that can respond to acute and physiological metabolic stress. However, metabolic overload is pathological and alters adipocytes dynamics, alongside with the recruitment of immune cells. Overall, AT maladaptation can alter systemic homeostasis.

III. The concept of metabolic inflammation

1. Obesity is associated with an inflammatory status

The first observation linking obesity and immunity dates back from 1966 when Hausberger noticed histological changes in the AT of obese mice, with an influx of immune cells and notably macrophages during obesity (21). Then, in 1983, Pekala *et al*. demonstrated *in vitro* that macrophages activated with endotoxins secrete molecules that induce adipocyte insulin resistance (22). Finally, the first evidence linking inflammation and metabolic health *in vivo* dates back to 1993 when Gokhan Hotamisligil and Bruce Spiegelman discovered that the pro-inflammatory cytokine TNFα was increasingly expressed in the adipose tissue of rodent models of obesity (23). Neutralizing TNFα action in obese rats leads to a significant increase in glucose uptake in response to insulin. This study showed that blocking a single cytokine can restore insulin sensitivity.

Moreover, in obese individuals, it is clearly established that there is an increased concentration of circulating pro-inflammatory cytokines, such as C-reactive protein (CRP) and TNFα (24).

Altogether, these studies lead to the concept of metabolic inflammation, or *metainflammation* (see https://metaflammation.org for further details) (25). Obesity is associated with a systemic, low-grade and sterile inflammation.

Inflammation is an adaptive response of the organism. Physiological purposes of inflammation depend on the trigger and include host defense against pathogens, tissue-repair and restoration of a homeostatic state. The molecular and cellular basis of inflammation are well described and macrophages are master regulators of this response. Unresolved and chronic inflammation is pathological (26).

As opposed to “classic” inflammatory response, triggers of metainflammation are not external nor coming from bacterial or viral infection but originate from chronic overnutrition and

metabolic stress. Metabolic inflammation is a key driver in the development of obesity-related complications (27).

2. Macrophage are key actors of metabolic inflammation

A decade later, in 2003, macrophages were identified as the main source of TNFα and other pro-inflammatory molecules (IL6 and NO, produced by the inducible NO synthase (iNOS)) in the context of obesity (28). Moreover, macrophages drastically accumulate in the AT of obese animals (21,28). The precise contributions of AT macrophages (ATM) to metabolic health and obesity will be further developed in Chapter II.

3. Molecular basis of inflammation-induced insulin resistance

The aforementioned studies emphasize the contributing role of inflammation in the development of obesity-induced insulin resistance.

At the molecular level, pro-inflammatory cytokines act through paracrine mechanisms on insulin sensitive cells such as adipocytes, causing the disruption of insulin signaling and thus insulin resistance (29). Physiologically, upon insulin binding to its receptor, the phosphorylation of tyrosine residues of insulin receptor substrate (IRS)-1 activates intracellular signaling pathways mediating insulin action (30).

In the context of metabolic inflammation, c-Jun N-terminal kinases (JNK)-1 and IκB kinase (IKK) are capable of interfering with insulin signaling by phosphorylating inhibitory serine/threonine residues of IRS-1, leading to insulin signaling disruption (31). Similar pathways involving JNK-1 and IKK can be activated through the binding of fatty acids on toll like receptors (TLR). Moreover, IL1β favors insulin resistance by repressing IRS-1 expression at both transcriptional and post-transcriptional levels, through IKK and nuclear factor-kappa B (NFκB) signaling (32). On the other side, IL6 signaling mediated by Janus kinase (JAK) and signal transducer and activators of transcription (STAT) controls the transcription of its own suppressor, known as suppressors of cytokine signaling (SOCS), notably SOCS3. The high levels of circulating IL6 induce increased expression of SOCS3 which physically interacts with tyrosine phosphorylated residues, and consequently inhibits the binding of IRS-1 with insulin receptor (33) (Figure 4).

While the role of inflammation in insulin resistance is clearly established, one report suggests that insulin resistance precedes inflammation within the AT of obese mice (34). Inflammation

and metabolic dysfunction are tightly linked but the precise causal relationship is incompletely understood.

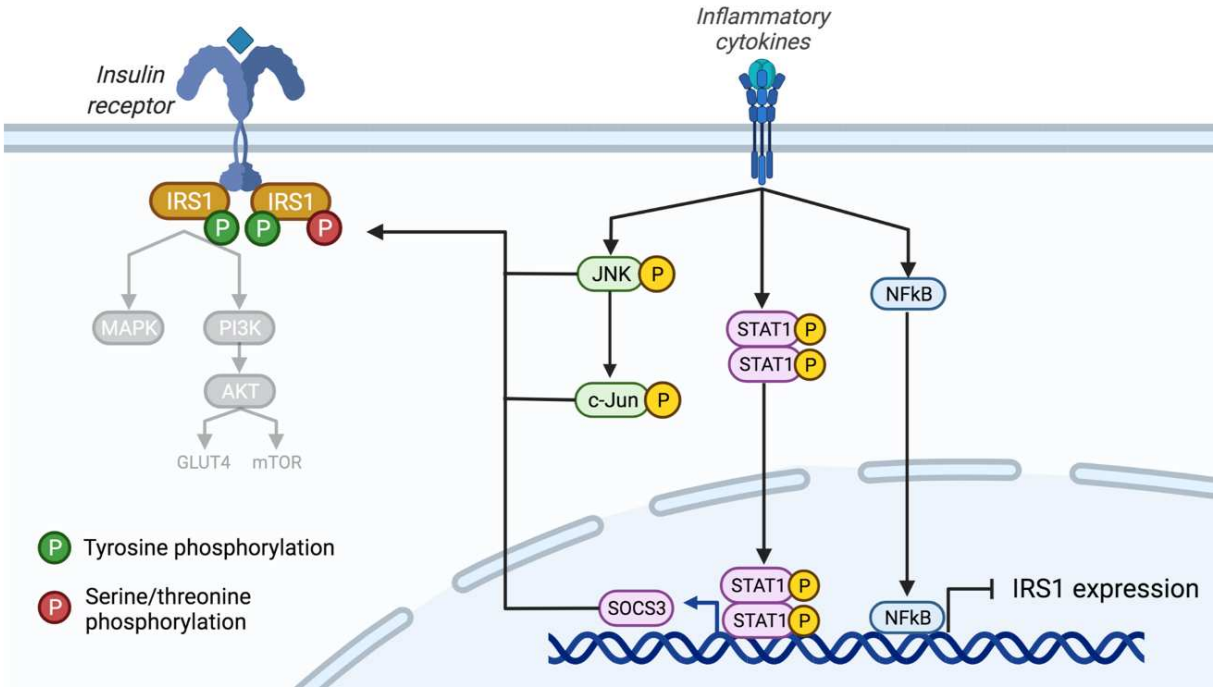

Figure 4: Molecular basis of inflammation-induced insulin resistance
Signaling cascades induced by pro-inflammatory cytokines alter insulin signaling, notably through inhibitory phosphorylation on serine/threonine residues of IRS1 and decreased expression of IRS1. P: phosphorylation.

Chapter II : Macrophages and metabolic health

I. Macrophages : cells of the innate immune system

1. Overview

Macrophages are myeloid cells from the innate immune system that were firstly identified by Metchnikoff as phagocytic cells. Phagocytosis is a cellular process associated with the innate immunological response against pathogens, but is also critical in the clearance of debris and tissue repair.

Macrophages are distributed throughout the organism and exert a wide range of functions. As part of the innate immune system and due to their phagocytic activities, they are key in host defense. They are involved in the initiation of immune response, but also in the resolution of inflammation by promoting wound repair. The view of macrophages as phagocytic entities is however restrictive. Recent advances in the field of macrophage biology revealed new functions for macrophages, notably in tissue homeostasis.

The macrophage population is broadly composed of two classes : tissue resident macrophages which play a key role in the maintenance of tissue homeostasis upon steady-state and infiltrating macrophages, which are found in response to an injury or in a pathological context. This population of infiltrating macrophages derives from circulating monocytes. Tissue resident macrophages populate a large variety of tissues. For example, Kupffer cells are found in the liver, microglia in the brain. Lungs, AT and the spleen are also populated by tissue resident macrophages.

Macrophages are commonly identified with the use of specific markers, namely CD68, CD64, MERTK, CD11b, along with the use of F4/80 in mice. Additional markers are used to identify specific tissue-resident macrophages subpopulations and different macrophage activation state.

2. Origins and differentiation of macrophages

It has long been thought that all tissue macrophages derive from circulating monocytes which differentiate into macrophage when they infiltrate tissues (35). Monocytes are circulating cells from the mononuclear phagocyte system. They are produced in the bone marrow, where hematopoietic stem cells produce myeloid committed precursors. These cells give rise to monocytes/macrophages and dendritic cells precursors, from which derive monocytes.

Monocytes can leave the bone marrow to enter circulation (36). Monocytes are heterogeneous and can be divided into classical (Ly6C^{hi} in mice, CD14^{+}CD16^{-} in humans) and non-classical monocytes (Ly6C^{lo} in mice, CD14^{dim}CD16^{+} in humans). Upon tissue injury or inflammation, monocytes are recruited, notably through the CCR2/CCL2 axis, to the site of tissue damage where they differentiate in macrophages or dendritic cells (35).

Over recent years, several publications shed light on the precise origin of tissue resident macrophages. With the use of genetic fate-mapping systems, monocyte depletion, parabiosis models, it has been shown that tissue resident macrophages are in fact established during embryonic state and their maintenance is independent of circulating blood monocytes (37–41). More precisely, there are two successive waves of hematopoiesis, in the yolk sac and in the fetal liver, giving rise to long-lived, self-maintaining tissue resident macrophages. The contribution of each of these hematopoietic waves is tissue-specific. Indeed, in the brain, microglia mostly originate from the yolk sac (37), while lung alveolar macrophages and Kupffer cells derive from the fetal liver (42).

3. Macrophage functions and phenotypes

Macrophages display a remarkable plasticity. They exert a wide range of functions from host defense to tissue homeostasis to remodeling.

First, macrophages have the capacity to quickly respond to environmental cues and to consequently adapt their functions. They sense changes in their microenvironment through the engagement of cell surface receptors, notably TLRs which are part of the larger family of pattern recognition receptors (PRR).

Similarly to lymphocytes, a dichotomy is currently used to describe macrophage polarization: M1, known as pro-inflammatory, classic macrophages vs. M2, anti-inflammatory, alternatively activated macrophages. The M1 subset's nomenclature derives from type-1 immunity (Th1/Th17) and is associated with the response and the production of interferon (IFN) γ. Classical macrophages have pro-inflammatory, microbicidal and antigen presenting capacities. They can notably produce pro-inflammatory cytokines such as TNFα, IL6, IL1β and reactive oxygen species (ROS). On the other side, M2 macrophages produce IL10, transforming growth factor (TGF) β in response to extracellular pathogens (parasites, helminths) and to the type-2 cytokines (IL4, IL5 and IL13) produced by adaptive immune cells upon Th2 polarization.

M2 macrophages are involved in immunoregulation, tissue repair and remodeling (43) and are associated with the later stages of resolving inflammation.

Although the M1/M2 dichotomy remains in use, it is increasingly recognized that a continuum of intermediate macrophage phenotypes exists in between the two states. Novel functional classifications are established according to the cytokine/chemokine secretion profile, transcription factor activation as well as predominant cellular metabolism (44). Omics analysis at the single cell level allow to decipher the heterogeneity and the diversity of the macrophage phenotypes and functions, notably within a tissue (45).

Regarding tissue resident macrophages and their roles in tissue homeostasis, beyond immune responses, this M1/M2 dichotomy is not appropriate. Tissues were initially thought to be rather uniform, leading to the concept that all tissue resident macrophages were similar across tissues. However, several studies gave precise insight on the diversity and the specificity of each tissue resident macrophages population. For example, peritoneal macrophages differ from red pulp macrophages due to the expression of specific transcription factors, GATA-6 and Spi-C respectively (46). Tissue resident macrophages perform organ-specific functions. Kupffer cells are involved in erythrocyte clearance, while alveolar macrophages are responsible for the degradation of surfactant and microglia have a key role in synapse remodeling (47). Moreover, within one tissue different subpopulations of tissue resident macrophages coexist, such as in the brain with microglia, perivascular and meningeal macrophages (48).

4. Activation of macrophages

Macrophages undergo activation and polarization in response to changes in their microenvironment, which can be sensed through TLRs. At the molecular level, macrophage activation is characterized by a specific transcriptional program, a remodeling of the epigenetic landscapes and an adaptation of their cellular metabolism. These three aspects are tightly interconnected.

a) Transcriptional regulation of macrophage polarization

Transcription factors are the key molecules to regulate the expression of specific genes involved in the activation of macrophages. They have ben intensively studied to understand macrophage polarization (49). Transcription factors are activated in response to cytokines,

TLR ligation by infectious pathogens, but also by metabolic stressors recognized as danger signals (DAMPs).

JAK-STAT pathway

The Janus-kinase (JAK)/signal transducer and activator of transcription (STAT) pathway is activated in response to several cytokines. JAKs bind to cytokine receptor and phosphorylate themselves, which favors the docking of STATs and their phosphorylation. Once phosphorylated, STATs dimerize and translocate into the nuclei where they bind to DNA. There are seven STAT molecules conserved in mammals. The nature of the stimuli defines which STATs are activated, the homo- or heterodimerization and thus the DNA binding elements.

A disruption in JAK/STAT signaling due to genetic deletion of STAT1 or 2 induces a defect in M1 polarization. STAT1 deficient macrophages lose their ability to respond to type II IFN (50) and in absence of STAT2, mice are more sensitive to viral infection (51). Moreover, STAT3 is involved in the production of IL10, and the anti-inflammatory polarization. However, in response to IL6, STAT3 favors a pro-inflammatory activation (49). STAT6 is the key transcription factor involved in M2 polarization, it is activated in response to IL4 and IL13. Its homodimerization and its binding to the chromatin leads to the transcription of genes encoding key M2 markers such as CD206, and the repression of pro-inflammatory genes (52).

Nuclear factor κ B (NFκB) pathway

NFκB is a family of transcription factors composed of different sub-units, namely p50, p52, p65, RelB and c-Rel. Upon steady state, NFκB proteins are sequestered in the cytoplasm by the IκB family. Canonically, upon activation of PRR or cytokine receptors, IκB is phosphorylated by IKK family members, leading to its proteasome-mediated degradation and NFκB nuclear translocation. NFκB is a master regulator of the expression of pro-inflammatory cytokines genes, such as *Tnfa*, *Il1b*, *Il6*. In addition, NFκB favors the activation of the NOD-like receptor family, pyrin domain containing 3 (NLRP3) inflammasome, responsible for the activation of IL1β (53).

Activated protein (AP)-1

This signaling pathway involving JNK induces the transcription of pro-inflammatory genes, that overlap with the NFκB pathway. More precisely, upon cytokine stimulation, JNK is phosphorylated which phosphorylates c-Jun. c-Jun homodimerizes or binds with c-Fos, which together form AP-1, to induce transcription (54).

Hypoxia-inducible factor (HIFs)

HIF is a family of transcription factors involved in cellular adaptations in response to low levels of oxygen. Interestingly, HIF1α and HIF2α have been association with macrophage polarization, M1 and M2 respectively. The overexpression of HIF1α enhances the transcription of several pro-inflammatory cytokines but also of glycolytic enzymes. The induction of the glycolytic pathway is an hallmark of M1 macrophages. Mechanistically, NFκB can induce HIF1α expression. In addition, HIF1α is stabilized and accumulates in M1 macrophages, due to inhibition of the prolyl hydroxylase domain (PHD) proteins (55).

Peroxisome Proliferator-Activated Receptors (PPAR)

PPARα, γ and ð/β are lipid ligand-inducible nuclear receptors involved in cellular metabolism (and particularly lipid metabolism), development, and more recently, they emerged as regulator of inflammation. The use of myeloid-specific PPARs knock-out and PPAR agonist enabled the elucidation of its function in inflammation. Indeed, pioneer studies from the groups of Glass and Seed identified that PPARγ activation limits pro-inflammatory activation of macrophages (56,57). More precisely, upon ligand binding, PPARγ is sumoylated, which blocks the release of nuclear receptor corepressor (NCoR) complexes from promoters of pro-inflammatory genes. Regarding PPARð, its activation is associated with a strong anti-inflammatory signature.

Interestingly IL4-induced STAT6 signaling favors the transcription of PPARs and its coactivator protein PGC1β. The activation of PGC1β induce an oxidative switch, which amplifies M2 polarization (58).

Liver X receptors (LXRs)

Similarly to PPARs, LXRs exist in two isoforms (α and β) and are lipid ligand-inducible transcription factors. In addition to their role in lipid and cholesterol metabolism, LXRs control

macrophage polarization, notably through repression and activation processes. They form obligate heterodimers with retinoid X receptors (RXR) to bind DNA. To repress the expression of pro-inflammatory genes, sumoylation of LXRs is required. Sumoylated LXRs inhibit the clearance of NCoR complexes at the promoters of pro-inflammatory genes, such as *inos* (59).

Krüppel like factors (KLFs)

Among the 17 members of this family of transcription factors, two have been associated with macrophage polarization : KLF2 and KLF4. Concerning KLF4, its expression is induced in M2 macrophage and decreased in M1 macrophages. Genetic knock-down of KLF4 alters macrophage function. Indeed, KLF4-depleted macrophages express more pro-inflammatory cytokines and are less able to promote wound healing. KLF4 prevents the recruitment of cofactors associated with NFκB-induced transcriptional activity (60). Similarly, KLF2 has been shown to inhibit both NFκB and AP-1 transcriptional activity. KLF2 is, therefore, a negative regulator of the pro-inflammatory M1 activation (61).

Interferon regulatory factors (IRF)

IRFs are key actors in the control of macrophage polarization. A specific part is dedicated to their signaling and roles hereafter.

The different signaling pathways are represented in Figure 5 and Figure 6 for M1 and M2 polarization respectively. The roles of these different transcription factors in macrophage polarization in the context of metabolic diseases have been reviewed in Orliaguet *et al.* 2020a and Orliaguet *et al.* 2020b (62,63), see Appendices 1 and 2.

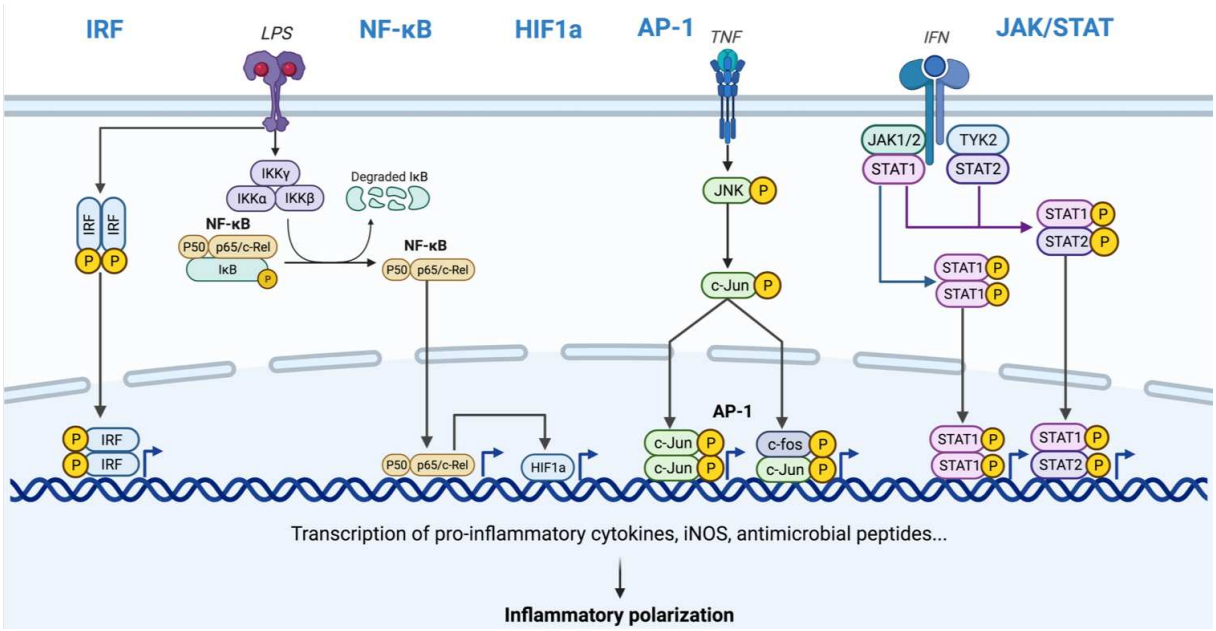

Figure 5: Transcriptional regulation of M1 polarization

Pro-inflammatory factors leads to the activation of several signaling pathways, namely IRF, NF-kB, HIF1a, AP-1 and JAK/STAT. These pathways enable the activation of specific transcription factors, favoring the transcription of a characteristic set of genes associated with a pro-inflammatory polarization of macrophages.

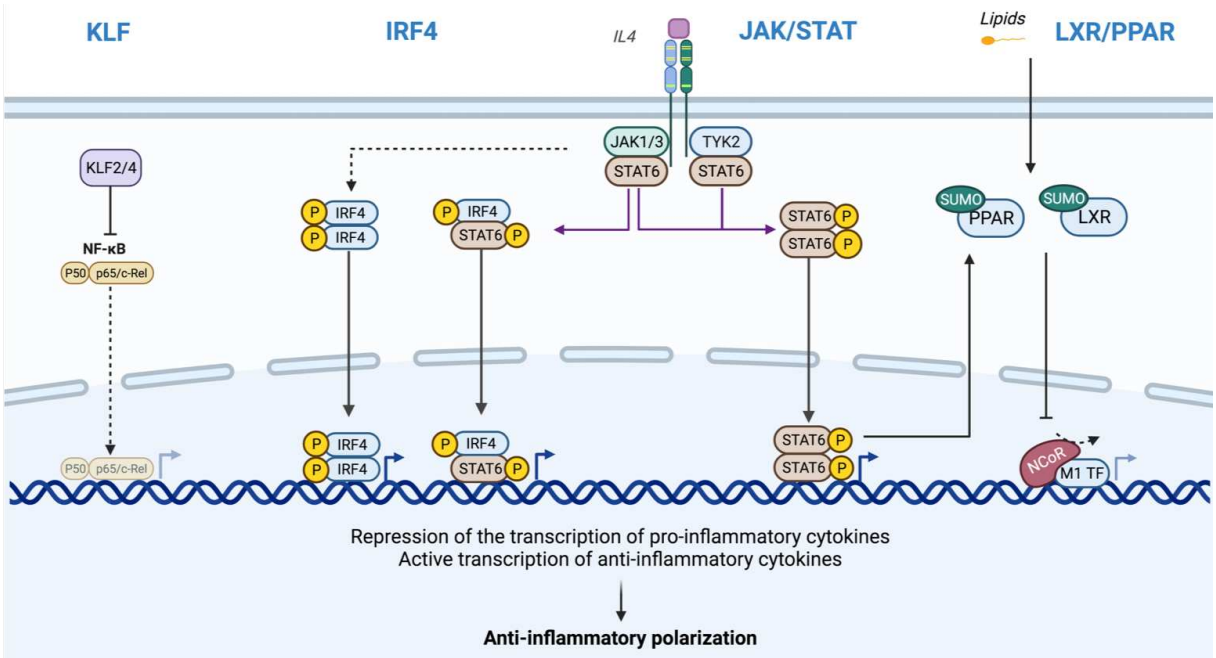

Figure 6: Transcriptional regulation of M2 polarization

Anti-inflammatory factors lead to the activation of several signaling pathways, namely KLF, IRF, LXR/PPAR and JAK/STAT. These pathways enable the activation of specific transcription factors, favoring the transcription of genes associated with an anti-inflammatory polarization. In addition, some of these pathways lead to the repression of the expression of pro-inflammatory genes, favoring overall an M2 activation.

b) Epigenetic remodeling

Another level of regulation in macrophage activation is the epigenetic remodeling which dictates the accessibility of genetic loci to transcription factors, and therefore regulates transcription factor activity. This process is mediated by transcriptional coregulators (corepressors and coactivators) and epigenetic modifying enzymes.

These epigenetic aspects and their importance in the pathogenesis of metabolic disorders are discussed in Orliaguet *et al*., 2020 (62), see Appendix 1.

c) Cellular metabolism

Macrophages adapt their cellular metabolism to meet the energetic needs associated with their activation. Metabolic pathways provide energy but also building blocks for the pro- and anti-inflammatory effector functions of macrophages. These aspects will be developed in Chapter III thereafter.

II. Interferon regulatory factors control macrophage activation

1. Overview

IRFs are a family of nine transcription factors that were first described as regulators of type I IFN signaling. They exert a wide range of functions in both innate and adaptive immunity. Three major domains are conserved among the IRFs : an N-terminal DNA binding domain which recognizes consensus DNA sequences corresponding to IFN sensitive response elements (ISRE), a C-terminal domain responsible for the regulation of the transcriptional activity of IRFs and another C-terminal domain responsible for homo- and heterodimerization of IRFs (except IRF1 and IRF2) (64).

At steady state, these transcription factors exist in the cytoplasm, in a monomeric form. Briefly, upon TLR ligation or IFN stimulation, IRFs are activated through post translational modifications on the C-terminal domain, allowing their dimerization and nuclear translocation. IRFs bind DNA and can interact with other transcription factors (STATs and NFκB), as well as transcriptional regulators (PU.1) to induce the transcription of a broad spectrum of genes associated with specific macrophage function (65).

Out of these nine IRFs, three are associated with a pro-inflammatory polarization of macrophages (IRF1, 5 and 8) whereas IRF3 and 4 control the commitment of M2 macrophages.

2. IRF5 and the pro-inflammatory activation of macrophages

Among all the IRFs, IRF5 is the most studied and the subject of this thesis. IRF5 expression is highest in monocytes and macrophages, lower in dendritic and B cells, and almost undetectable in T lymphocytes and natural killer cells.

a) Physiological functions of IRF5

Mice deficient for IRF5 are unable to produce pro-inflammatory cytokines in response to TLRs ligands. These mice are resistant to LPS-induced septic shock. IRF5 is not involve in hematopoiesis, neither in macrophage survival upon TLRs stimulation (66). Moreover, IRF5 expression is increased upon LPS stimulation and it dictates the expression of pro-inflammatory cytokines, such as *Il6*, *Tnf*, *Il12* and markers of inflammatory polarization, namely *Itgax*, encoding CD11c (67,68), both *in vivo* and *in vitro* (69). In parallel, IRF5 can repress the transcription of anti-inflammatory genes, such as *Il10* and *Tgfb1* (70). Consequently, IRF5 favors a pro-Th1 and Th17 environment (71). Interestingly, IRF5 controls the inflammatory activation of both tissue-resident macrophages and monocyte-derived macrophages (69).

b) Signaling and mechanisms of action

IRF5 is activated in response to TLR4, 7, 8 and 9 ligation. Downstream of TLRs, IRF5 interacts with MyD88 (66) and Interleukine 1 receptor associated kinase (IRAK) 1/2 and 4 (72). Then, activation of IRF5 is triggered by different post-translational modifications (poly ubiquitination and phosphorylation of serine residues) mediated by the tumor necrosis factor receptor associated factor (TRAF6) and IKKβ respectively (Figure 7).

These modifications induce conformational changes, characterized by the disruption of the intramolecular interaction between the C-terminal domain, with the N-terminal DNA binding and IRF binding domains (73). IRF5 homodimerizes, while some heterodimers IRF5/IRF7 also have been observed.

Interactome studies identified binding partners of IRF5. Notably, IRF5 binds with RelA, a NFκB subunit, to induce the transcription of a unique set of pro-inflammatory genes. More precisely, IRF5 and RelA bind to the chromatin in the 1kb region upstream of transcription start site of target genes. Their binding, which occurs in less than 30 minutes, is associated with the recruitment of RNA polymerase II (74). The specific tertiary structure of IRF5

homodimers allows the interaction with the coactivators CBP/p300 to induce transcription (73,75). Moreover, IRF5 interacts with KRAB-associated protein 1 (KAP1)/TRIM28. KAP1 is a transcriptional corepressor which acts as a scaffold protein for chromatin silencing via the recruitment of histone deacetylases and methyltransferases. Therefore, the IRF5/KAP1 complex represses the transcription of a subset of genes (76).

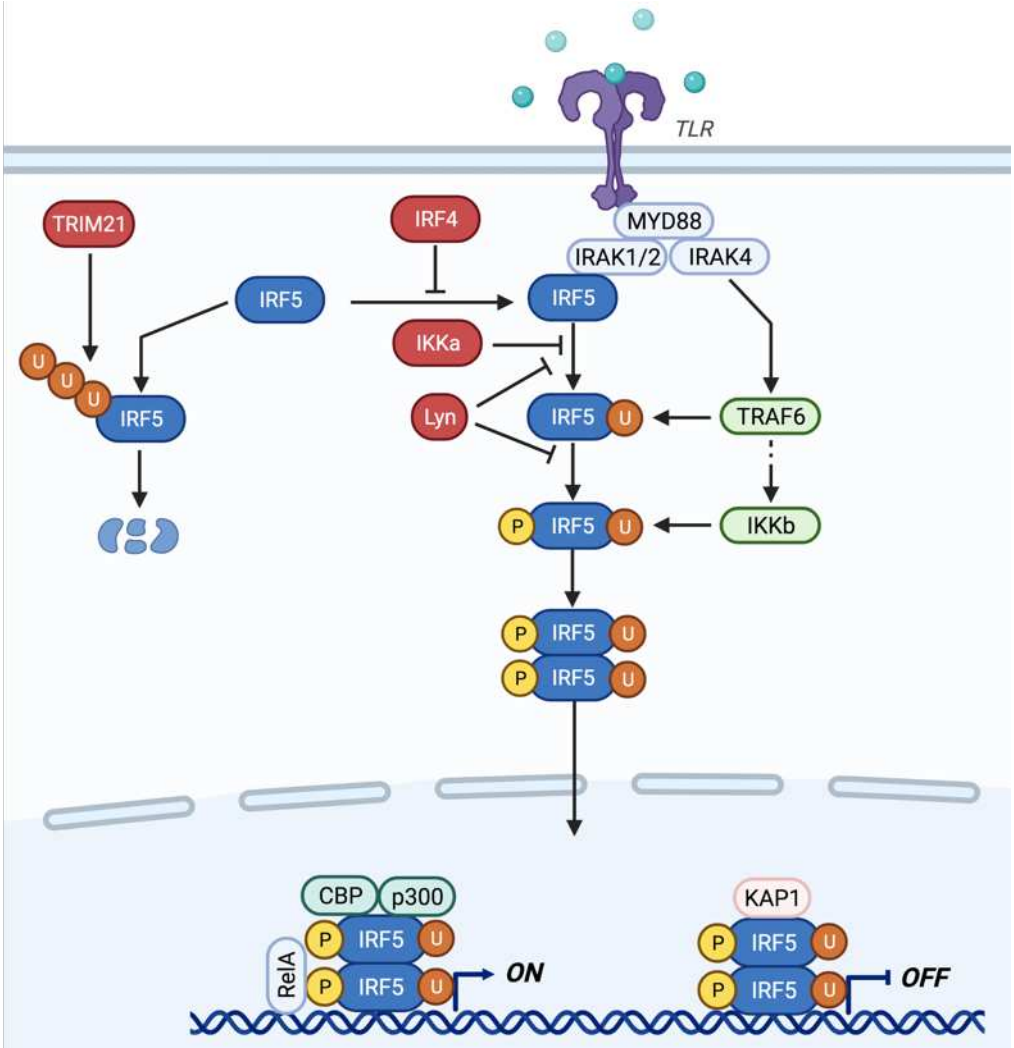

Figure 7: IRF5 signaling pathway
Upon TLR ligation, IRF5 undergoes successive phosphorylation and ubiquitination, leading to its dimerization and nuclear translocation. IRF5 induces the expression of pro-inflammatory genes and represses the expression of anti-inflammatory genes. Negative regulators of IRF5 signaling are represented in red, positive regulators in green. P: phosphorylation. U: ubiquitination

c) Positive and negative regulation of IRF5 activity

IRF5 signaling pathway can be modulated at several levels. First, IRF5 is post-transcriptionally modified by TRAF6 (ubiquitination) and IKKβ (phosphorylation). Therefore, these two enzymes are considered as positive regulators of IRF5 signaling.

On the other hand, inhibition of IKKβ or TRAF6 enzymatic activity negatively modulate IRF5 function. For example, pharmalogical inhibition of IRAK4 blocks IKKβ phosphorylation, and thus its activity. IRF5 nuclear translocation is consequently reduced (72). Moreover, IKKα-dependent phosphorylation of IRF5 inhibits its ubiquitination by TRAF6 (77).

Interestingly, in B lymphocytes and dendritic cells, the kinase Lyn has been shown to inhibit IRF5 ubiquitination and phosphorylation. This effect is dependent on the physical interaction between Lyn and IRF5, and not on Lyn kinase activity (78). In addition, IRF5 is acetylated upon viral infection, suggesting that alteration of this acetylation pattern can modulate its activity (73). IRF5 can also be degraded after poly ubiquitination mediated by E3 ubiquitin ligase tripartite motif-containing protein 21 (TRIM21). Its expression is enhanced upon TLR7 activation and represent a down-regulation pathway to limit over-activation of IRF5 (79).

Finally, other IRFs, such as IRF4, are involved in IRF5 regulation. IRF4 can specifically antagonize IRF5, by competing with IRF5 to bind MyD88 (80) (Figure 7).

d) Dysregulated expression and activity of the IRF5 pathway

Considering IRF5's key role in the control of immunity, IRF5 dysregulated expression and activity are associated with a wide range of autoimmune and inflammatory pathologies. Indeed, several studies have been performed on mice models of autoimmunity. In these settings, mice lacking IRF5 are protected from the onset and the development of these autoimmune conditions. IRF5 is thus considered as an autoimmune susceptibility gene. In humans, polymorphisms associated with higher expression and hyperactivation of IRF5 are associated with the development of autoimmune disorders such as rheumatoid arthritis (81), inflammatory bowel disease and systemic lupus erythematosus (SLE) (82). In SLE, IRF5 is found to be constitutively activated, nuclear translocated, which correlates with the high levels of pro-inflammatory cytokines in the plasma (83).

Previous work from my host laboratory has highlighted that IRF5 is also associated with the development of inflammatory diseases such as insulin-resistance and obesity associated hepatic complications (84).

Regarding obesity and insulin resistance, *Irf5* expression is induced in ATMs of obese mice (Figure 8A) and of obese patients, where it positively correlates with insulin resistance (85). Mice with a specific myeloid deletion of IRF5 (MacKO) fed with high fat diet gain more weight than WT mice, notably due to the increased expansion of subcutaneous AT (Figure 8B). They have an increased content of ATMs (Figure 8C), mostly polarized towards an M2 phenotype (Figure 8D), identified by the expression of CD206. There is an adaptive remodeling associated with a limited expansion of visceral AT, characterized by smaller adipocytes and increased collagen deposition (Figure 8E). This phenotype is specific to visceral AT as the expansion of metabolically benign subcutaneous AT is promoted. Regarding glucose homeostasis, these mice are less glucose intolerant (Figure 8F) and more sensitive to insulin (Figure 8G). Overall, the knock-out of IRF5 in myeloid cells is protective against insulin resistance (70).

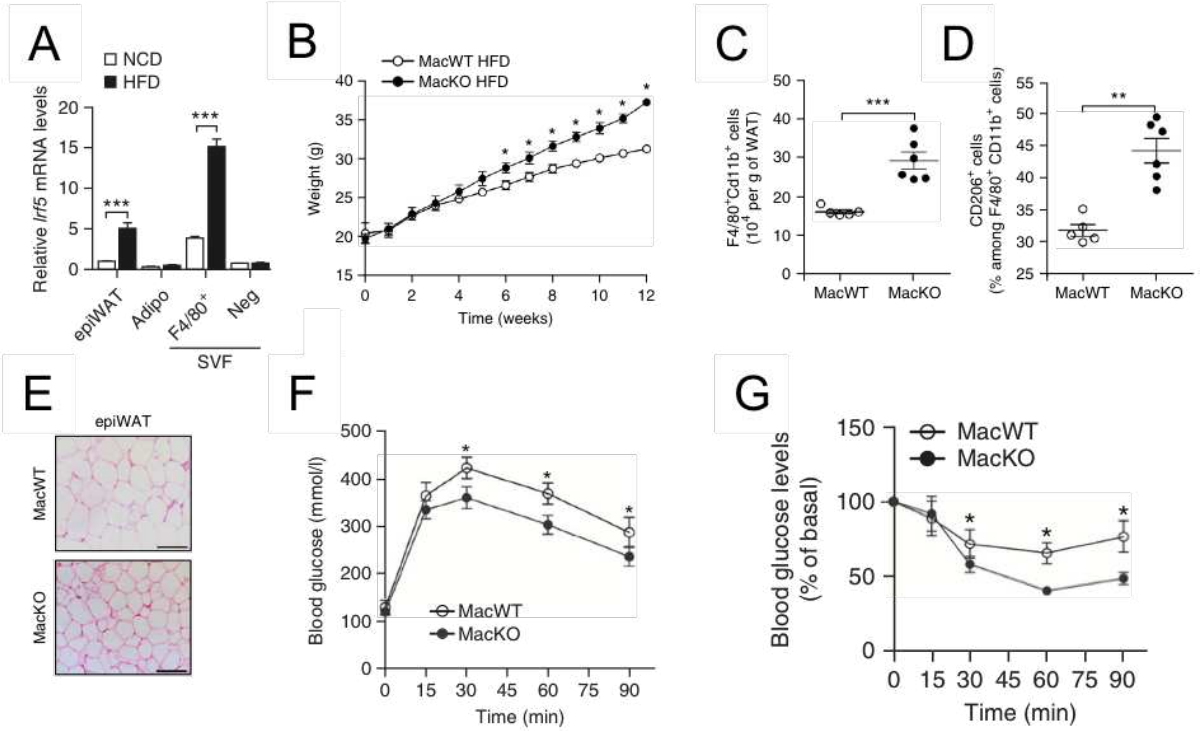

Figure 8: Irf5 deletion is protective against insulin resistance in a murine model of diet-induced obesity

A: Irf5 expression in epididymal WAT (epiWAT) and its different subpopulations (adipocytes (adipo), macrophages (F4/80+) and non-macrophage cells (Neg) composing the stromal vascular fraction (SVF)) of C57Bl6 mice with with chow diet (NCD) or high fat diet (HFD) for 12 weeks. B: Body weight of mice with a myeloid deletion of IRF5 (MacKO) and their WT littermates (MacWT) fed with HFD during 12 weeks. Macrophage (F4/80$^+$ CD11b$^+$ cells) content (C) and CD206 expression (D) in epiWAT of MacWT and MacKO mice fed with HFD. E: Collagen deposition in epiWAT of MacWT and MacKO mice fed with HFD. Glucose (F) and insulin (G) tolerance tests perfomed on MacWT and MacKO mice fed with HFD. Adapted from Dalmas et al. ***(70)***

Moreover, IRF5 is detrimental in the pathogenesis of atherosclerosis. It promotes the maintenance of pro-inflammatory $CD11c^+$ macrophages and it favors expansion of the lesions by impairing efferocytosis (67).

Surprisingly, IRF5 over-expression is protective in the context of pulmonary allergies. Mechanistically, IRF5 limits Th2 responses which are critical for airway hyper-responsiveness, mucus secretion and eosinophilic inflammation (86).

Given the crucial role of IRF5 in multiple diseases, IRF5 represents an interesting therapeutic target (87).

III. Adipose tissue macrophages and metabolic health

ATMs represent the most abundant population of leukocytes in the AT (15). Similarly to other tissue resident macrophages, they exert multiple functions to maintain AT homeostasis but also play deleterious roles upon metabolic stress.

1. Origins and heterogeneity of ATMs

Regarding ATMs origins, it appears that AT comprised a population of tissue resident macrophages and a population of monocyte-derived macrophages. Indeed, an elegant study performed in amphibians, as a model of vertebrate development, highlights the presence of a self-renewing population of ATMs, before the onset of bone marrow hematopoiesis. This population coexist with bone-marrow derived macrophages. Using a fate-mapping approach, the authors confirmed the existence of a yolk-sac derived population of ATMs in mice, before birth and during adulthood (88).

In addition to these diverse origins, the use of single cell analyses and histological techniques led to the discovery of several ATM subpopulations, with distinct transcriptome and tissue localization, namely lipid associated macrophages (LAMs) (89,90), perivascular macrophages (VAMs) (91), sympathetic neuron associated macrophages (SAMs) (92). Each of these subpopulations is involved in the maintenance of AT homeostasis and appear to be modified upon caloric excess (15,16,89,90).

2. Roles of ATMs in AT homeostasis

a) Immune function

In physiological situations, ATMs are generally identified as M2 macrophages. They are characterized by the expression of CD206 (the mannose receptor), CD301, F4/80 and CD11b as surface markers and arginase 1 (*Arg1*) and the secretion of TGFβ, IL10 and IL1R antagonist. Moreover, they express the transcription factor PPARγ which controls their lipid and oxidative metabolism to cope with the lipid-rich microenvironment.

The presence of bacterial DNA within the AT suggests that pathogens can persist in the AT environment (93). These pathogens can be phagocytized by ATMs, leading to the induction of tolerogenic immune responses. Moreover, AT can be a reservoir of virus. Therefore, as part of the AT immune system, ATMs interact with all the other immune cells found in the AT such as B and T cells, neutrophils, natural killer cells, innate lymphoid cells (ILC) and innate T cells. They form specific immune structures and exert *traditional* functions related to antimicrobial, antiviral and anti-parasitic defense (10).

b) Maintenance of tissue homeostasis

Alongside their conventional immune functions, ATM have non-immune roles, which are key for the maintenance of tissue homeostasis, expansion and innervation, upon physiological conditions. Notably, AT homeostasis is challenged daily, with periods of feeding and thus expansion, storage and then mobilization of stored-lipids during fasting or cold exposure. AT dynamics rely on different processes, either by enlarging the size of adipocytes (hypertrophy) or by increasing the number of adipocytes (hyperplasia). In relation with this plasticity, adipocytes may undergo apoptosis. M2-like ATMs remove dying adipocytes and debris of dead cell through a process named efferocytosis which enables the maintenance of an anti-inflammatory environment (94). However, in the context of adipocyte death, adipocyte size may represent a challenge for efficient efferocytosis. Therefore, it is thought that the formation of crown-like structures (CLS), which correspond to the grouping of cells around dying adipocytes, allows macrophages to phagocyte remnants of apoptotic bodies (95).

Moreover, ATMs have lipid-buffering capacities and this enables capture of all the lipids released from dead adipocytes, but also during fasting-induced lipolysis (96) or thermogenesis (97). Interestingly, this lipid-buffering function is independent of the inflammatory status of ATMs (98). Weight loss is associated with an accumulation of M2 macrophages. Surprisingly, lipid droplets were observed in ATMs from lean mice (91). These lipid droplets aggregates near the plasma membrane and are acidic, which is consistent with the fusion with lysosomes,

a hallmark of M2 macrophages (98). Lipids are stored within the macrophages and then can released in the circulation in a controlled manner (99) or they can be oxidized. This lipid-buffering process limits ectopic and pro-inflammatory accumulation of lipids, and potential tissue-level lipotoxicity. There is a specific crosstalk between ATMs and adipocytes. Indeed, inhibition of lysosome biogenesis decreases adipocytes lipolysis (98). A novel pathway of lipid release, independent of canonical lipolysis, has been recently described. Indeed, adipocytes can release exosome-sized, lipid-filled vesicles which can be uptaken and stored by ATMs (100). On the other hand, ATMs can promote the storage of lipids in adipocyte through the production of platelet-derived growth factor cc (PDGFcc)(101), favoring adipocyte hypertrophy but limiting ectopic deposition of lipids.

Controlling angiogenesis is a key factor in the maintenance of tissue homeostasis as it limits the formation of hypoxic area within the tissue and it insures a correct distribution of blood. VAMs express LYVE1 and are known to promote angiogenesis (102) through the production of PDGF, a pro-angiogenic factor (103). Moreover, these macrophages are found around capillaries and act as intermediates between blood circulation and adipocytes. They endocytose macromolecules present in the bloodstream (91). Overall, VAMs enable the maintenance of a favorable environment for adipogenesis. Moreover, ATMs form a niche for the development of adipocytes (104). They secrete osteopontin, a glycoprotein, which acts as a chemoattractant for the recruitment of pre-adipocytes. However, ATMs could also inhibit the proliferation of adipocyte progenitors through TGFβ signaling (105).

The role of adipose tissue in energy storage is largely controlled by sympathetic innervation. Interestingly, different groups have identified a subtype of macrophages (sympathetic nerves associated macrophages, SAM) that are associated with nerve bundles and regulate sympathetic tone and catecholamine metabolism. These macrophages express the Solute Carrier Family 6 Member 2 (SLC6A2), a norepinephrine transporter. By uptaking norepinephrine, SAMs are thought to modulate its availability in the microenvironment and indirectly norepinephrine-induced lipolysis (92).

Finally, M2-like ATMs favors AT insulin sensitivity thanks to the production of IL10. Indeed, acute IL10 treatment improves global insulin sensitivity in animals (106) and its expression is positively correlated with insulin sensitivity in humans (107). Furthermore, ATMs can release exosomes containing miRNA (small non coding RNA with transcriptional regulatory properties), such as miR-155 that regulates insulin sensitivity. Indeed, ATM derived exosomes

from lean mice have the capacity to improve glucose intolerance and insulin sensitivity in obese mice (108).

Altogether, in the early stages of caloric excess, their diverse roles and plasticity enable ATMs to coordinate AT metabolic adaptation.

3. Roles of ATMs in metabolic inflammation

a) Recruitment and proliferation of ATMs during obesity

Overall, obesity is associated with a complete remodeling of the AT immune populations. Monocytes and macrophages expand while immune cells associated with type-2 immunity such as regulatory T lymphocytes and ILC2 decrease (15,89). Notably, there is a massive accumulation of lipid laden macrophages (LAMs), expressing CD9 and TREM2, which represent up to 75% of the myeloid compartment after 18 weeks of high fat feeding (89). This observation was confirmed in obese patients (15,16).

The accumulation of ATMs over the course of obesity is due to *in situ* proliferation (109), circulating-monocytes recruitment and retention of ATMs within AT, mediated by netrin-1 (110). Netrin-1 is a laminin-related molecule and it inhibits ATMs migration to lymph node, contributing thus to their accumulation. Over the course of obesity, macrophages' proliferation is specific to AT, as macrophages from the liver and the spleen do not display any proliferation markers. At the molecular level, the monocyte chemoattractant protein (MCP)-1/CCL2 is a key driver in ATMs accumulation, contributing to both proliferation and monocytes recruitment. Indeed, the first phase of proliferation is driven by the IL4-STAT6 axis, and then MCP1 appears to be required (111). Several studies have demonstrated the importance of the CCR2/MCP1 axis in the recruitment of circulating monocytes (112–114), however others have shown that MCP1 might not be required in this process (115,116).

b) Phenotype and activation of ATMs during obesity

The molecular signals that drive ATMs accumulation and activation remain incompletely understood. Among them, lipids, hypoxia, cell death and stress are the most studied (96,117,118). In fat depots of genetically obese mice, 90% of ATM are surrounding dead adipocytes (119), suggesting that dead adipocytes might release danger signals (DAMPs) that promote ATMs accumulation. A hallmark of obesity is the presence of hypoxic areas within the AT, inducing the expression the pro-inflammatory transcription factor HIF1α (120).

Furthermore, lipolysis products and more generally lipids whose circulating levels are elevated in obesity, can induce an inflammatory response via binding to TLR4 (121). Similarly, VLDL potentiates an M1-like macrophage activation (122).

It has long been thought that upon obesity ATMs switch from a M2 phenotype to a pro-inflammatory M1 activation, in association with the development of insulin resistance (123). Although the M1/M2 paradigm and the "phenotypic switch" hypothesis give useful tools to understand the role of ATMs during obesity, the first observation of ATM expressing both CD11c and CD206 in obese patients reinforces the concept that these macrophages may fall within the M1/M2 continuum (124). Interestingly, a pioneer study from Kratz *et al*., revealed, with a proteomic approach, that classical markers of M1 macrophages are absent from ATMs from obese mice (125). In addition, M2 markers are suppressed or not induced. When treated with stressors that mimic the obese AT microenvironment (palmitate, glucose and insulin), macrophages express specific cell surface markers that have been associated with lipid metabolism such as ABCA1, CD36 and PLIN2. Nevertheless, considering ATMs heterogeneity, we can hypothesize that the expression of these metabolically activated markers can differ from one subpopulation to another. The development of single cell approaches could help to unravel this diversity an identify specific markers.

Metabolically activated state is a complex phenotype evolving in the spectrum of macrophage activation whose extremities are defined by M1- and M2-like phenotypes.

c) Protective and deleterious functions of ATMs during obesity

Metabolically activated macrophages (MMe) exert a myriad of functions in the AT during obesity. They have a dual role in both the adaptation of AT to metabolic stress and the pathogenesis of obesity.

First, MMe produce pro-inflammatory cytokines, such as IL6 and TNFα. These cytokines can counteract with insulin signaling, leading to the development of insulin resistance. It is interesting to note that the increase of pro-inflammatory cytokines production in MMe is modest compared to bacterial inflammation, suggesting different signaling pathways or a lower capacity to stimulate the same pathways (98,126).

Then, single cell studies highlighted that ATMs remodeling is mostly associated with a drastic increase of LAMs (15,16,89,90). These cells accumulate lipids, express PPARγ and appear to be highly oxidative. They are identified by the expression of the surface marker TREM2 which

drives the expression of a specific gene program, including phagocytosis, lipid handling, catabolism and metabolism. Interestingly, this population of LAM is also conserved in human AT upon obesity. This population is protective for the AT and metabolic homeostasis. Indeed, TREM2 deficient mice fed with HFD present hypertrophic adipocytes (89). This suggests that in absence of TREM2, LAMs are unable to cope with the excess of lipids.

LAMs also express CD9 (15,89) and localize within CLS. While the rate of adipocytes apoptosis and the number of CLS increase with obesity, the beneficial or detrimental function of these structures is currently debated. They were primarily correlated with the progression of obesity and insulin resistance (127). They are associated with a pro-inflammatory context, with the expression of CD11c. However, LAMs appear to be protective, due to their lipid-buffering capacities. Moreover, they express immunosuppressive genes (*lgals1* and *lgals3*) and thus may be involved in dampening the adipocyte death-induced inflammation (89). Hill *et al*., confirms the existence of $CD9^+$ LAMs in the CLS, but they have a pro-inflammatory transcriptional signature.

Upon obesity, SAMs accumulate in WAT and act as norepinephrine sink. They uptake and catabolize norepinephrine which inhibits adipocyte lipolysis, favoring AT expansion (92). Moreover, there is an accumulation of $Ly6c^+$ monocytes-derived macrophages, localized throughout the adipose interstitium. These cells promote tissue remodeling (90).

Finally, these beneficial and deleterious effects of MMe on AT physiology could be dependent on the time of high fat feeding. MMe appear first to induce insulin resistance due to the production of pro-inflammatory cytokines. Then, MMe dampen inflammation by clearing dead adipocytes (126).

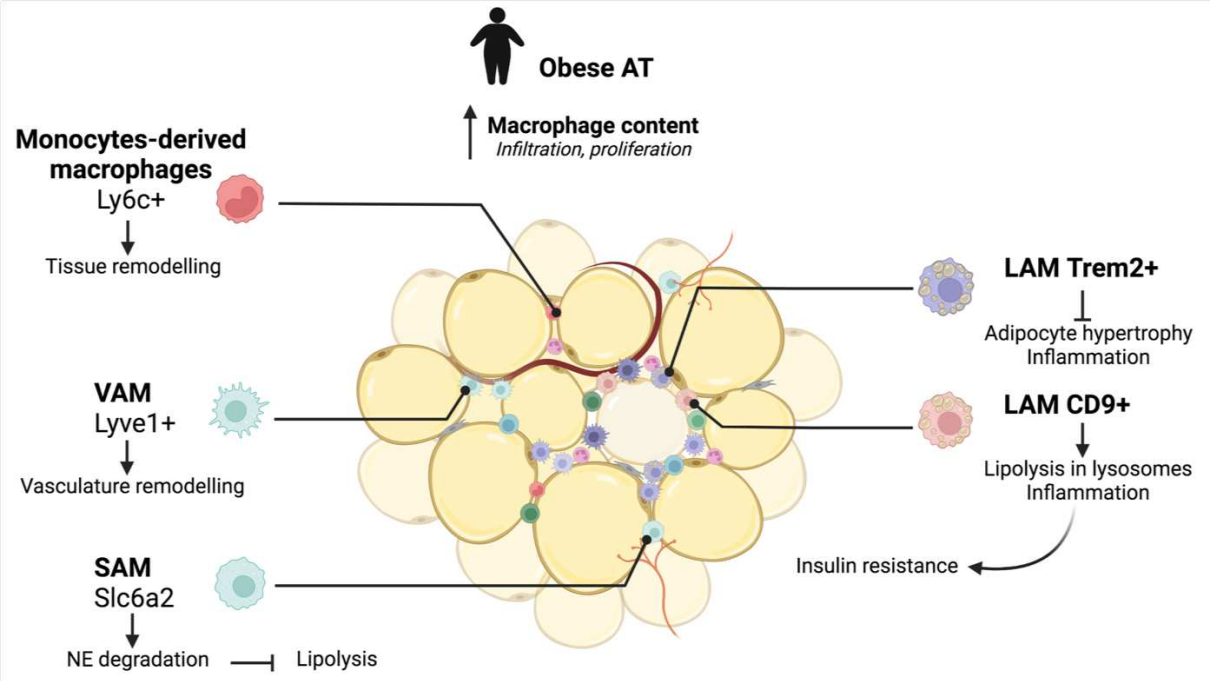

Figure 9: Subpopulations of adipose tissue macrophages upon obesity
ATMs represent an heterogenous population. Upon obesity, the proportion of these subpopulations evolves, notably with an increase of LAMs. These subpopulations of ATMs participate to both the physiological and the early response to metabolic stress and to the pathological and detrimental AT adaptation upon caloric excess, leading to adipocyte hypertrophy, vasculature defects, inflammation and insulin resistance. LAM: lipid associated macrophages. VAM: vasculature associated macrophages. SAM: sympathetic nerve associated macrophages. NE: norepinephrine. Slc6a2: NE transporter

To conclude, ATMs represent an heterogeneous, plastic and dynamic population of tissue resident macrophages (Figure 9). They are fully committed in the maintenance of tissue homeostasis and they are key actors in the pathogenesis of obesity. Their activation rely on a specific transcriptional program, an epigenetic remodeling and an adaptation of their cellular metabolism.

Chapter III : Cellular metabolism of macrophages

In addition to the remodeling of the transcriptional and epigenetic landscapes of innate immune cells, cellular metabolism plays a key role in their terminal differentiation. Metabolic pathways not solely produce energy but also dictate macrophage function (128). This chapter will focus on key metabolic pathways and how they are involved in macrophage polarization. Finally, the specific metabolic adaptations of tissue-resident macrophages will be described.

I. Cellular metabolism : overview

Cellular metabolism refers to the biochemical reactions that occur within a cell to provide energy. These pathways are crucial for the cells to metabolize nutrients to favor survival, proliferation and differentiation.

Macrophage energy production mostly relies on several metabolic pathways : glycolysis, pentose phosphate pathway (PPP), fatty acid (FA) metabolism (either oxidation (FAO) or synthesis (FAS)), amino acid (AA) metabolism and the tricarboxylic acid cycle (TCA). These pathways, which are interconnected enable the production of energy but also the generation of intermediate metabolites which can act as signaling molecules.

1. Metabolic pathways

a) Glycolysis

Glycolysis corresponds the oxidation of glucose into two molecules of pyruvate, through 10-sequential enzymatic reactions. This pathway allows the generation of two molecules of ATP per molecule of glucose and the reduction of NAD+ into NADH. First, glucose is captured from the environmental milieu through the glucose transporters (GLUT). Macrophages express the GLUT isoforms 1, 3, 5, 6 and 8 at different levels (129,130). Glucose is then phosphorylated by the hexokinases (HK) into Glucose-6-phosphate (G6P). G6P can enter either glycolysis or feed PPP. G6P is isomerized into Fructose-6-phosphate (F6P), which is phosphorylated by phosphofructose kinase 1 (PFK1) to give rise to Fructose-1,6-biphosphate (F1,6BP). Otherwise, F6P can serve as a substrate for the hexosamine biosynthesis pathway which generates uridine diphosphate N-acetylglucosamine (UDP-GlcNAc). UDP-GlcNAc is a substrate for post-translational glycosylation (131). More generally, several glycolytic intermediates can serve as biosynthetic precursors, such as 3-phosphoglycerate (serine and glycine pathway). Finally,

phosphoenolyruvate is converted into pyruvate by the pyruvate kinase (PKM1/2). Lactate dehydrogenase catalyzes the reduction of pyruvate into lactate. This process, called aerobic glycolysis, occurs upon physiologic conditions in macrophages. Otherwise, pyruvate can be converted into acetyl-CoA by a process called pyruvate decarboxylation.

b) The pentose phosphate pathway

The PPP is a metabolic pathway which plays a key role in the regulation of the redox homeostasis and in the biosynthesis of nucleotides precursors. It can be divided into two branches. First, the oxidative branch is responsible for the reduction of NADP into NADPH. On the other hand, the non-oxidative branch generates ribose-5-phosphate. NADPH promotes the synthesis of ROS through NADPH oxidase 2 (NOX2) (132). Ribose-5-phosphate is a building block for the synthesis of nucleotides and amino acids (133).

c) Amino acids metabolism

Considering the diversity of AA, they are involved in several anabolic pathways. Indeed, they serve as substrates for protein synthesis. First, glutamine, which is the most abundant AA in the organism, can enter macrophages notably through Solute Carrier 1a5 (Slc1a5) (134). Glutamine is involved in the production of UDP-GlcNAc in the hexosamine biosynthesis pathway (131) and also in the biosynthesis of nucleotides. Moreover, glutamine can be converted into glutamate in the mitochondria. Glutamate is a precursor for α-ketoglutarate (αKG), a key intermediate of the TCA cycle. Glutamate can also generate glutathione and thus acts as a keeper of the redox balance. Similarly, *de novo* synthesis of serine, from 3-phosphoglycerate, is involved in the production of glutathione (135).

Concerning tryptophan metabolism, this AA is transformed into kynurenine through the action of the enzyme indole-2,3-dioxygenase (IDO1). Kynurenine is then metabolized and this metabolic pathway is the first contributor of NAD^+ *de novo* synthesis (136).

Finally, arginine can be metabolized by NOS to generate NO. When metabolized by Arginase 1 (ARG1), arginine leads to the production of urea and ornithine.

d) Fatty acid metabolism

Fatty acid metabolism recovers both catabolic (FAO) and anabolic (FAS) processes.

FAO is the complete oxidation of fatty acids molecules. Depending on the length of their chain, FA can passively enter mitochondria or the acyl group has to be linked to a coA molecule. Then, carnitine palmitoyltransferase (CPT) I exchanges the CoA molecule with carnitine to enable the translocation of the acyl chain into the mitochondria. CPTII exchanges carnitine with CoA to generate acyl-CoA. Finally, acyl-CoA are oxidized in the mitochondria, enabling the generation of large amounts of ATP and reducing power (NADH and $FADH_2$) which feed the oxidative phosphorylation (OXPHOS). Overall, FAO is the most efficient energy producer of the cell.

FAS is a cytosolic pathway and corresponds to the synthesis of lipids required for cellular growth and proliferation, using precursors from the other metabolic pathways. For example, citrate is exported outside of the mitochondria and can be converted into acetyl-CoA by the action of ATP-citrate lyase. Acetyl-CoA is then carboxylated to generate malonyl-CoA . Next, fatty acid synthase (FASN) is responsible for the elongation of the fatty acid chain. This pathway is transcriptionally regulated by the activation of Sterol Regulatory Element-binding Protein (SREBP)(137).

e) The TCA cycle

The TCA cycle is considered as a metabolic hub as multiple metabolic intermediates, acetyl-CoA and glutamate notably, can feed into it. This metabolic pathway occurs in the mitochondrion matrix and, in a series of cycling enzymatic reactions, enables the production of reducing power (NADH, $FADH_2$) and ATP. More precisely, acetyl-CoA is added onto oxaloacetate to generate citrate, which is isomerized into isocitrate. Then two successive decarboxylations induce the production of αKG and succinyl-CoA. Succinyl-CoA is converted into succinate which is oxidized in fumarate. Notably, the enzyme driving this reaction, the succinate dehydrogenase (SDH), is also part of the mitochondrial electron transport chain (ETC). Finally, fumarate gets converted into malate and further into oxaloacetate. Interestingly, it is now well establish that TCA metabolites, notably αKG, succinate and fumarate, have functions beyond energy production. Indeed, they act as signaling molecules (138), provide substrates for protein posttranslational modifications and contribute to the epigenetic landscape.

2. Mitochondria are a metabolic hub

Mitochondria are vital organelles that are traditionally referred as the powerhouse of the cell, notably due to their central role in energy production. They are also involved in key cellular processes such as immunity, apoptosis, ROS production and calcium homeostasis (139). In the following section, only its function in cellular metabolism will be addressed. Mitochondria are a metabolic hub as they integrate metabolic fuels to provide energy to the cell, they favor the compartmentation of metabolic pathways and mitochondrial metabolites can serve as biosynthetic precursors (140).

a) Structure and function

The development of electron microscopy enabled the identification of the particular mitochondria structures. Mitochondria are organelles with a double membrane (referred as the outer and the inner mitochondrial membranes), which delimit the mitochondrial matrix and the intermembrane space. These compartments and structures favor the concentration of metabolic substrates and enzymes and the establishment of thermodynamically favorable conditions for biochemical reactions. Notably, the inner mitochondrial membrane invaginates into the mitochondrial matrix to form cristae (141). These structures are dynamic and dictate the spatial rearrangement of proteins. For example, they are the preferential docking site of the ETC (142) (Figure 10). The loss or the reorganization of these cristae structures alter the ETC function.

The mitochondrial matrix is the site of several metabolic pathways previously described, namely the TCA cycle and FAO. Both FAO and TCA cycle are tightly coordinated with OXPHOS. The generation of reducing equivalents (NADH, $FADH_2$) is required for the transfer of electron to the mitochondria ETC. The ETC is composed of a series of five main protein complexes that allow the flow of electron through redox reactions, ending in oxygen. The energy released during these chemical reactions enables the establishment of an electrochemical gradient of protons across the inner mitochondrial membrane. This gradient drives complex V function and ATP synthesis. The concomitant transfer of electrons through the ETC and the generation of ATP define OXPHOS.

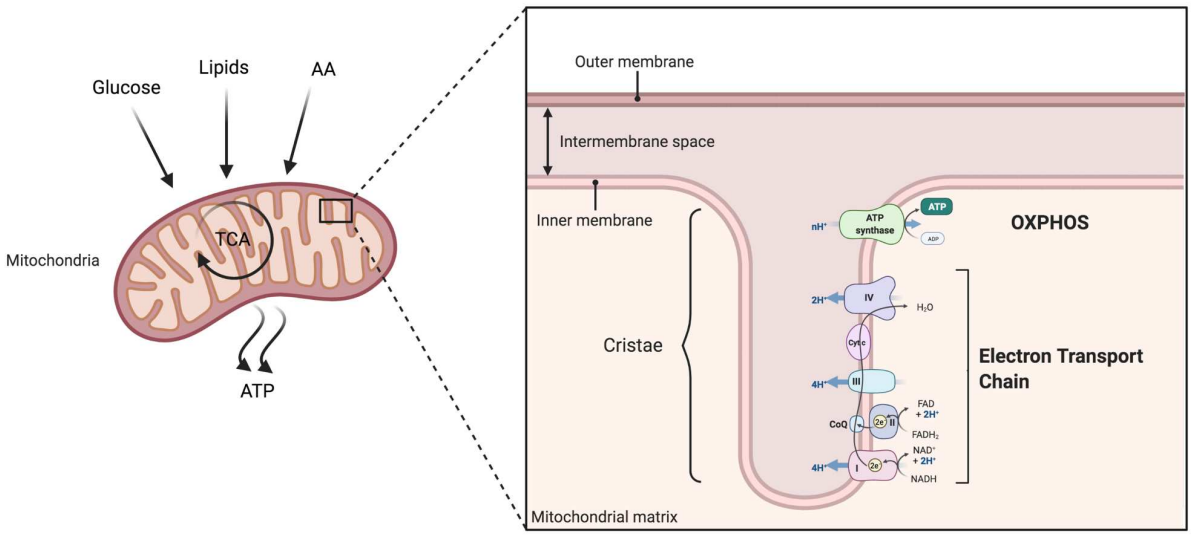

Figure 10: Mitochondria are metabolic hub

Mitochondria are organelles at the crossroad of several metabolic pathways. In particular, glucose, lipids and AA catabolic pathways feed the tricarboxylic acid cycle (TCA), which, itself, feeds the electron transport chain (ETC) and oxidative phosphorylation (OXPHOS). The different complexes of the ETC are mostly located in the cristae, which corresponds to folds of the inner mitochondrial membrane into the matrix.

b) Mitochondrial dynamics and metabolic regulation

Mitochondria form a dynamic organellar network which undergo events of fusion or fission in response to nutrient or cellular stress (Figure 11). Mitochondrial dynamics is strongly linked to its functions and activity. The morphology of mitochondria can vary over a wide spectrum from hyperfused to fragmented forms. Interestingly, there is a reciprocal crosstalk between metabolism and mitochondrial dynamics (143). Indeed, the balance between fusion and fission is sensitive to nutrient availability and metabolic demand. For example, nutrient withdrawal favors mitochondria fusion. Mitochondria fission is observed in nutrient overload conditions (144). On the other hand, mitochondrial dynamics is a driver for metabolic state. Mitochondria fusion is associated with enhanced OXPHOS, while mitochondria fragmentation is related to decrease in OXPHOS capacity. In addition, this cycle of fusion/fission is coupled with mitochondria recycling (mitophagy) and biogenesis.

At the molecular level, fusion is regulated by mitofusins and OPA1. Mitofusins 1 and 2 are GTPases and their interaction on adjacent mitochondria can induce the fusion of the outer mitochondrial membrane. Regarding the inner membrane, OPA1 is thought to interact with the mitochondrial lipid cardiolipin to induce its fusion. Fission is controlled by the cytosolic

dynamin-related protein DRP1. DRP1 can oligomerize and constrict mitochondria to induce its division (144).

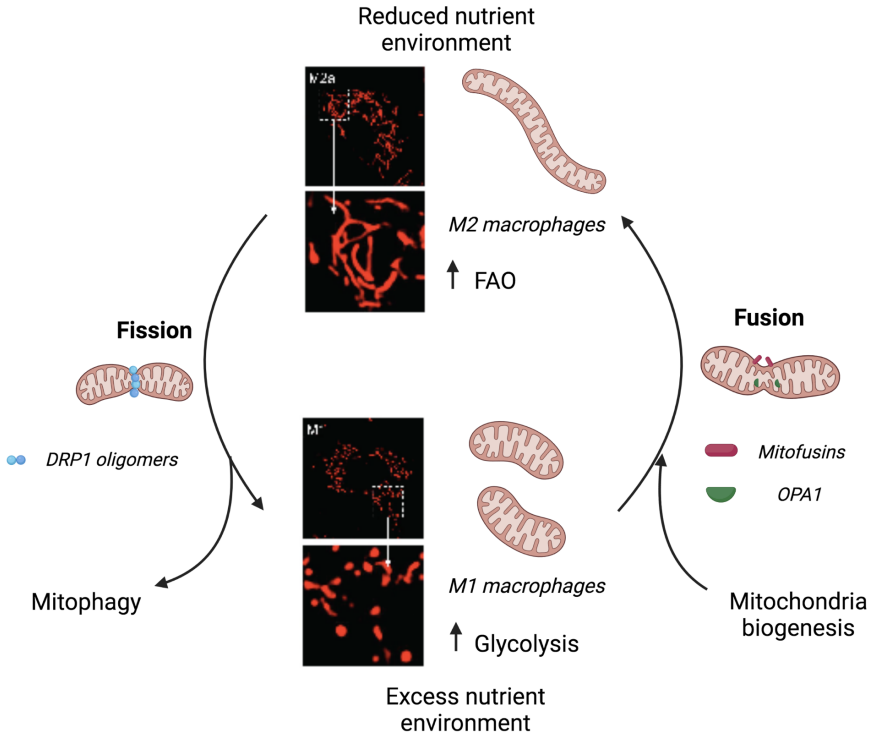

Figure 11: Mitochondrial dynamics
Mitochondria are highly dynamic organelles. They undergo cycle of fusion and fission, driven by mitofusins and OPA1 and DRP1 activity respectively. This process is tightly linked with nutrient availability and cellular metabolism. M1 macrophages have fragmented mitochondria, while M2 macrophages present fused and elongated mitochondria. FAO: fatty acid oxidation. Images adapted from Li et al., 2020 (145)

3. Experimental approaches to interrogate cellular metabolism

Due to the growing interest for cellular metabolism, and notably of immune cells, different experimental approaches have been developed to assess the bioenergetic profile of a given cell population *ex vivo* or *in vitro*. A commonly used technic, Seahorse developed by Agilent, relies on the measurement of extracellular fluxes, with oxygen consumption and extracellular acidification rates as surrogates of OXPHOS and glycolysis. This technic, used in combination with diverse inhibitory metabolic drugs can help to decipher the precise contribution of a specific metabolic pathway to the observed phenotype (146). In addition, metabolomics, and notably targeted metabolomics, can be used to accurately quantify metabolites. However, this technic only provide a snapshot of the metabolic profile at a given time-point. The use of

radio-labelled metabolic substrates in combination to targeted mass spectrometry performed at different time-points allows a more accurate assessment of metabolic fluxes. A costless cytometric-based technic to study a specific metabolic pathway or activity relies on the use of fluorescent probes, such as 2-NBDG, a fluorescent non-metabolizable analog of glucose. 2-NBDG can be used to assess glucose uptake as a read-out of glycolysis for example. All these approaches require relatively high amounts of biological material, of either cultured cells or sorted cells for *in vitro* or *ex vivo* characterizations respectively. A limit to these technics remains the *in vivo* validation. The development of single-cell approaches, notably in the field of transcriptomics can provide a first tool to overcome the cell number limitation (147).

These diverse "bulk" analysis were used to decipher the metabolic adaptations of macrophages described in the following section, and also in the following thesis in the context of metabolic stress.

II. Metabolic adaptations of pro-inflammatory (M1) macrophages

When focusing on focusing on macrophage bioenergetics, it is important to underline that pioneer studies have been performed *in vitro*, based on the M1/M2 paradigm with canonical stimulants (e.g LPS+IFNγ or IL4). Historically, the first description of M1 and M2 subsets was based on their ability to metabolize arginine (148).

1. Glycolysis and PPP

The enhanced glycolytic function is a hallmark of M1 polarization. Glycolytic metabolism facilitates pro-inflammatory differentiation to allow efficient bacterial killing (149) and the secretion of pro-inflammatory mediators. Experimentally, the inhibition of glycolysis with 2-deoxy-glucose (2-DG) reduces the pro-inflammatory response of macrophages to LPS (150).

The rapid induction of glycolysis is enhanced by the upregulation of *slc2a1* expression, encoding GLUT1 (151). Interestingly the myeloid deletion of GLUT1 completely blunts the increase of glucose and subsequent glycolysis upon M1 polarization. It highlights that, despite macrophages express other glucose transporters, GLUT1 remains the key player in LPS-induced glucose uptake (152). IL10 exerts its anti-inflammatory effects by inhibiting the translocation of GLUT1 to the membrane (153). The switch towards a glycolytic metabolism is also dependent on the transcription factor HIF1α (154). Its stabilization in hypoxic conditions

induces the transcription of glycolytic enzymes such as the hexokinase which catalyzes the first step of glycolysis, and also of the pro-inflammatory cytokine IL1β (155). Other enzymes, such as the ubiquitous isoform of phosphofructokinase-2 (uPFK2) (156) are also induced during M1 polarization to favor the glycolytic switch. More precisely, uPFK2 is a more active isoform of PFK2 and therefore its induction enhances the glycolytic flux. Indeed, uPFK2 favors the formation of fructose-2,6P2 which allosterically activates PFK1 (157). Interestingly, some glycolytic enzymes have functions outside of this metabolic pathway. Notably, pyruvate kinase isoenzyme 2 (PKM2), whose expression is increased with LPS stimulation (158), can be found as a dimer. This dimer can translocate to the nuclei and act as a coactivator for HIF1α. Consequently, PKM2 participates in a positive loop with the up-regulation of pro-inflammatory and glycolytic genes in response to HIF1α activation (159). Moreover, HK1 can be inhibited by bacterial products and then dissociate from the mitochondria, which activates NLRP3 inflammasome and therefore the production of pro-inflammatory cytokines (160).

Glucose is also a source of substrates for the PPP. PPP is also induced upon LPS stimulation and M1 polarization. The sedoheptulose kinase CARKL, which is part of PPP, is downregulated in M1 macrophages and experimentally its knock-down is sufficient to mimic the stimulatory effect of LPS on glycolysis. Thus, the downregulation of this enzyme is critical in supporting the induction of glycolysis in M1 macrophages (161).

2. TCA cycle

Alongside the enhancement of glycolysis, M1 macrophages are characterized by a decrease of oxidative respiration. Interestingly, the TCA cycle is disrupted at two key steps, due to a transcriptional downregulation of the isocitrate dehydrogenase (IDH) (162) and of the itaconate-mediated inhibition of SDH (155,163). These two breaks result in: the accumulation of (i) citrate and of (ii) succinate. The latter supporting SDH activity, subsequent production of mitochondrial ROS and expression of IL1β through stabilization of HIF1α.

Moreover, pyruvate oxidation into citrate via the pyruvate dehydrogenase in the mitochondria in maintained in M1 macrophages (164). The accumulation of citrate leads to a decrease in the levels of cis-aconitate which is the precursor of itaconate. The production of itaconate is thus inhibited. Itaconate, a key regulator of the immune response, exerts its anti-inflammatory effects by inhibiting SDH and the production of ROS, but also by inhibiting the release of pro-inflammatory cytokines such as IL6 and IL1β (155,163).

However, acute LPS treatment induces a burst of oxidative metabolism in macrophages which increases the pool of available of acetyl-CoA. This process supports histone acetylation and thus the transcription of pro-inflammatory genes such as *Il6* and *Il1b*. The shutdown of the oxidative metabolism, an hallmark of M1 macrophages, occurs afterwards with longer LPS treatments (12-24 hours) (165).

3. Fatty acid metabolism

Citrate accumulates in the cytosol (166) and favors inflammatory polarization as it is required for the production of ROS, NO and prostaglandins. Citrate is also a substrate for acetyl-CoA, which feeds fatty acid synthesis through ATP-citrate lyase (ACLY) (167). The production of fatty acids is crucial for the composition and the synthesis of the plasma membrane, and pro-inflammatory polarization. Indeed, silencing the fatty acid synthase (FAS) in myeloid cells, and thus the production of endogenous fatty acids, prevents diet-induced insulin resistance, ATM recruitment and chronic inflammation in mice (168). In parallel, FAO is repressed, in line with a decreased expression of *Cpt1* (164).

4. Amino acids metabolism

Upon LPS stimulation, glutamine uptake increases. It has been shown that glutamine is the major carbon source for αKG and TCA cycle and it can also undergo glutaminolysis to provide oxaloacetate (164). Glutamine helps to replenish the altered TCA cycle. The decrease in OXPHOS and ETC activity could be related to the altered TCA cycle. However, glutamine helps to replenish the altered TCA cycle and the production of NADH. This highlights that a decrease in ETC activity is not necessarily linked to a decrease in TCA cycle activity (164). Arginine is also metabolized into L-citrulline simultaneously to the production of NO by iNOS. NO favors the killing of bacteria. Serine supports the production of IL1β upon LPS stimulation, through glutathione synthesis (135).

Overall, pro-inflammatory macrophages are characterized by an increase of glycolytic activity and a decrease of OXPHOS, whilst altering amino acid metabolism. With regards to mitochondrial morphology, LPS induces mitochondria fragmentation (169) (Figure 11).

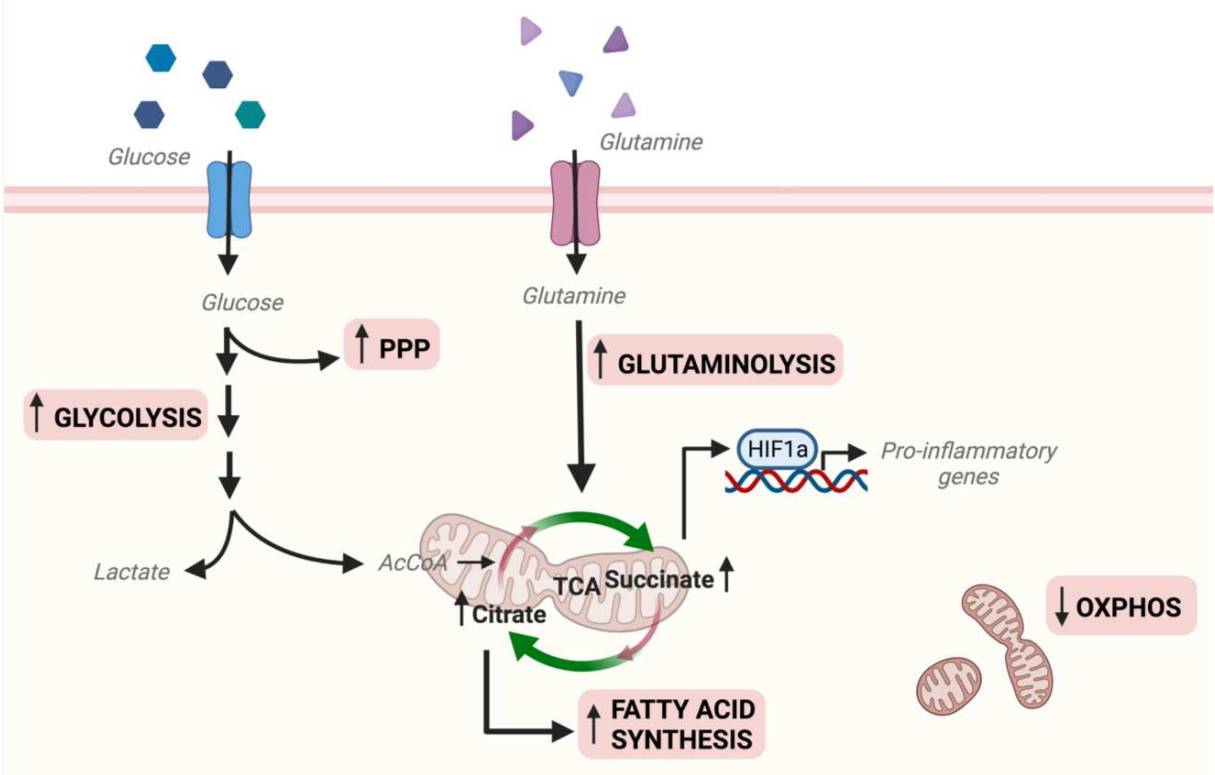

Figure 12: Metabolic adaptations of M1 macrophages
M1 macrophages are characterized by an enhanced glycolytic function, associated with an increase of glutamine uptake. Regarding mitochondria, they are mostly fragmented, which is associated with a decrease of OXPHOS. The TCA cycle is disrupted, with the accumulation of citrate and succinate. Citrate feeds fatty acid synthesis and succinate favors the transcription of pro-inflammatory genes through stabilization of HIF1a.
PPP: pentose phosphate pathway. OXPHOS: oxidative phosphorylation. TCA: tricarboxylic acid cycle

III. Metabolic adaptations of anti-inflammatory (M2) macrophages

1. TCA cycle and OXPHOS

Enhanced OXPHOS is a key feature of M2 macrophages. Unlike M1 macrophages, their TCA cycle is uninterrupted. Mitochondrial biogenesis is increased in a PGC-1β-dependent manner (170). Moreover, upon IL-4 treatment, mitochondria tend to form a hyperfused network (169). However, the different pathways contributing to the enhanced OXPHOS are still under debate.

2. Fatty acid metabolism

First, the upregulation of FAO is crucial in IL4-induced polarization. This mechanism is orchestrated in a PGC-1β manner (170). It is the main source of substrates for OXPHOS (171). Macrophages can either uptake lipids through the scavenger receptor CD36 (172) or rely on lysosomal lipolysis to support FAO and alternative activation (173). However, recent studies

highlight that FAO is dispensable for M2 polarization. Indeed, genetic knock-down of *Cpt1a* and *Cpt2* do not affect M2 activation upon IL4 treatment (174,175).

Surprisingly, lipid synthesis, mediated by LXRs, is central in M2 polarization and more generally in the resolution of inflammation. For example, SREBP1, an LXR target, has been shown to induce a reprograming of the lipid metabolism in response to pro-inflammatory signals (176). The synthesis of lipids, and in particular anti-inflammatory lipids (eicosanoids, resolvins), is first inhibited in an LXR-dependent manner before being induced by SREBP1. IL4-induced *de novo* lipogenesis also favors ROS production, by consuming NADPH (137).

3. Glycolysis

IL4 stimulation induces an increase of glycolysis in an AKT-mTORC2-IRF4 manner (177) which can fuel the TCA cycle and OXPHOS. Glucose uptake is enhanced but to a lower extent compared to M1 macrophages. The increase in glycolytic activity can feed several pathways, such as the hexosamine biosynthesis pathway which leads to the formation of UDP-GlcNAc that supports N-glycosylation, an essential process for the expression of several M2 markers (162). Glycolysis end-product, pyruvate, can be converted into acetyl-CoA a substrate for histone acetylation. This epigenetic modification enables the transcription of specific M2-genes associated with IL4 treatment (178).

Nevertheless, the importance of glycolysis contribution to the M2 phenotype is still controversial. A recent study highlights that blocking glycolysis with galactose, instead of 2-DG, does not affect oxidative phosphorylation and neither M2 polarization (171).

4. Amino acids metabolism

Interestingly, M2 macrophages were firstly identified thanks to their ability to metabolize arginine, thanks to ARG1 (148). However, the precise role of arginine metabolism in IL4-induced M2 polarization is not known.

Glutamine metabolism plays also an important role in polarization towards an M2 phenotype. The expression of *Slc1a5*, a glutamine transporter, is indeed also increased upon IL4 stimulation (179). Similarly to glucose, glutamine catabolism leads to the formation of UDP-GlcNAc. Moreover, glutaminolysis enables the production of αKG. This process fuels the TCA cycle, and OXPHOS, and αKG serves as a substrate for the epigenetic reprogramming of several M2-associated genes, through demethylation.

In regard to tryptophan, the kynurenine pathway favors M2 phenotype. Indeed, overexpression of IDO1 is associated with anti-inflammatory polarization, while its silencing induces a pro-inflammatory phenotype (180).

5. Pentose phosphate pathway

PPP is decreased in M2 macrophages. Indeed, the carbohydrate kinase-like protein CARKL is down-regulated in response to LPS treatment and is highly expressed with IL4 stimulation (181). This enzyme, a sedoheptulose kinase, inhibits the PPP.

Overall, M2 macrophages are mostly characterized by their oxidative capacity, associated with mitochondrial biogenesis (Figure 13).

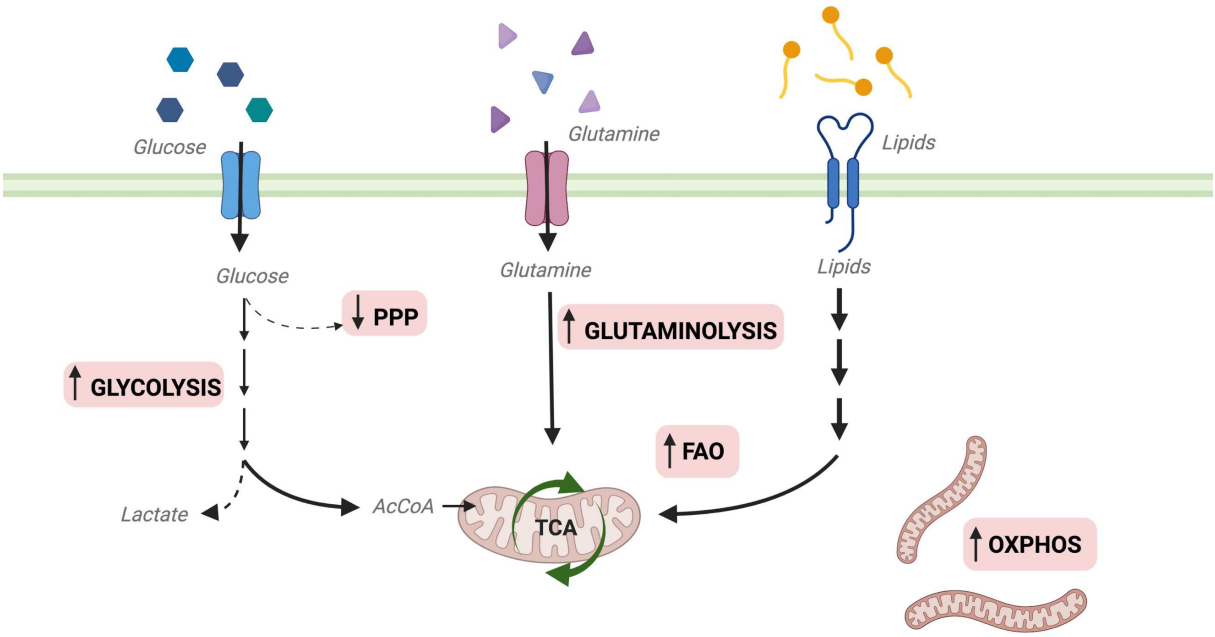

Figure 13: Metabolic adaptations of M2 macrophages
M2 macrophages are characterized by an enhanced fatty acid oxidation, associated with an increase of glutamine and glucose uptake. Regarding mitochondria, they are mostly fused, which is associated with an increase of OXPHOS. PPP: pentose phosphate pathway, FAO: fatty acid oxidation, OXPHOS: oxidative phosphorylation, TCA: tricarboxylic acid cycle

IV. Metabolic adaptations of tissue resident macrophages

While residing in specific tissues, macrophages adopt a unique transcriptional program, which reflects their adaptation to the tissue. Specific signals emerging from the micro-environment are thought to shape macrophage polarization (182). These transcriptional signatures pertain key metabolic pathways, highlighting the importance of metabolic adaptation (46).

1. Airway macrophages

For example, lung alveolar macrophages express high levels of PPARγ, a transcription factor encoding genes associated with lipid metabolism, lipolysis and cholesterol efflux notably. It subsidizes lung alveolar macrophages the ability to degrade pulmonary surfactant which is mostly composed of phospholipids and cholesterol. The expression of genes associated with lipid metabolism favors the catabolism of surfactant by FAO and the export of cholesterol, enabling macrophages to cope with the excess of fatty acids . Moreover, at steady state, the lung environment confers alveolar macrophages a specific metabolic signature as they are unable to uptake and to metabolize glucose which renders them hypo-responsive to IL4. Removal of alveolar macrophages from the lung tissue reverses this metabolic constraint. Interestingly, alveolar macrophages activation is directly linked with the availability of glucose in airways. Elevated glucose levels and metabolism are notably found in airways during asthma (183).

2. Peritoneal macrophages

The peritoneal cavity, in which visceral organs reside, is filled with several immune cells, including peritoneal macrophages. These cells can invade peritoneal organs to fulfill tissue repair, they are also key coordinators of the inflammatory response. Transcriptomic analyses reveal that peritoneal macrophages a unique transcriptional signature which is driven by the transcription factor GATA-6 (46,184). GATA-6 expression is critical for the maintenance and self-renewal of peritoneal macrophages. Interestingly, the expression of GATA-6 is tightly linked with the specificity of the peritoneal microenvironment. Indeed, Retinoic acid induces and regulates GATA-6 expression in peritoneal macrophages. Interestingly, omentum, the peritoneal associated adipose tissue, expresses high levels of the retinoic-acid converting enzymes, which suggests a high concentration of retinoic acid in the peritoneum (184).

Peritoneal macrophages display a higher mitochondrial oxidative capacity compared to bone marrow derived macrophages *in vitro*. More precisely, peritoneal fluid can increase the oxygen consumption of macrophages, suggesting a potential role for peritoneal metabolites

as mitochondrial fuel. Further studies characterized the peritoneum metabolome : higher levels of glutamate and N-acetylaspartate compared to serum were found (185). Interestingly, GATA-6 favors the expression of the gene encoding aspartoacylase, an enzyme which converses N-acetylaspartate into aspartate and acetate, favoring the synthesis of acetyl CoA (186). This metabolic axis could fuel the TCA cycle and contribute to the distinctive high mitochondrial activity of peritoneal macrophages. Moreover, glutamate can be converted into glutamine and fuel mitochondria, notably during phagocytosis to support the oxidative burst associated with the production of ROS (185). To summarize, peritoneal macrophages adapt their cellular metabolism to provide protection against pathogens while using specific metabolites present in the peritoneum.

3. Adipose tissue macrophages

a) In physiology

Metabolic adaptations of ATMs at steady-state are not extensively described. Considering the M2-like phenotype of macrophages, we could hypothesize that ATMs from lean AT display enhanced OXPHOS. Moreover, upon steady state, the efferocytic activity of ATMs could drive their cellular metabolism towards elevated FAO and OXPHOS (187) and AA metabolism. Indeed, macrophages can metabolize arginine, ornithine (188) and methionine (189) derived from the apoptotic cells.

However, metabolic flux analysis performed on ATMs isolated from lean AT highlight a specific bioenergetic profile similar to quiescent cells, with low oxygen consumption and low extracellular acidification rate, as a readout of glycolysis (190). These functional data are consistent with single cell analysis performed on lean AT where no specific transcriptional signature associated with cellular metabolism has been identified in ATMs (15,16,89).

b) During obesity

In the context of obesity, ATMs face a specific micro-environment with nutrient competition, normoxic and hypoxic areas. It is a nutrient-rich environment due do the abundance of FFA and lipolysis products. As previously mentioned, ATMs adopt a metabolically activated state in response to glucose, palmitate and insulin (125).

Recent single cell studies highlights the presence of a subpopulation of ATMs, increasing with obesity, with a transcriptional signature associated with PPARγ activity, lipid metabolism and

oxidative capacity (15,16,89). This population of lipid-laden ATMs express CD9, TREM2, CD36, ABCA1 and PLIN2. The induction of lipid catabolism signature may favor the potential of macrophages to buffer their environment from the excess of lipids (98,125).

Ex-vivo functional approaches revealed that, in the context of diet-induced obesity, ATMs have a unique bioenergetic profile with an increase of both OXPHOS and glycolysis (190–192). The enhanced OXPHOS capacity is associated with an increase in mitochondrial mass (192) and is induced by oxidized phospholipids found in AT (190). Regarding glycolysis, the role of HIF1α in its induction in the context of obesity is debated (191,192). The increase of glucose uptake and subsequent glycolysis is due to the upregulation of GLUT1 expression in CLS-associated ATMs (151). Moreover, AA metabolism could also be a field of investigation. Indeed, glutaminolysis is decreased in the AT of obese patients compared to lean subjects and glutamine levels in the serum are decreased in patients with obesity or diabetes. The contributing role of ATMs in these phenomena is yet to be determined (134).

Results

This thesis is particularly devoted to the metabolic adaptations of ATMs in the context of metabolic inflammation. A particular focus is given to IRF5 and to its role in mediating such metabolic adaptations in **Axis 1**.

Notwithstanding the considerable progress made in the field of cellular immunometabolism, the question of whether disruption of cellular metabolism *per se* can induce macrophage polarization is still unresolved. We give an insight on this question in **Axis 2** with *in vitro* experiments performed on bone-marrow derived macrophages (BMDM).

Lastly, chronic inflammation is a common feature of a wide range of pathologies. Therefore, in **Axis 3**, we investigated metabolic reprogramming of macrophages in a different context of sterile inflammation, namely gout and pseudo-gout flares.

In **Axis 1** and **Axis 2**, I have been involved in performing experiments and data analysis and I have contributed to the writing of the manuscripts. Regarding **Axis 3**, a collaborative work with Dr Ea, I have performed Seahorse experiments of BMDM treated with gout- and pseudo-gout inducing crystals.

Axis 1: IRF5 and ATMs metabolic adaptations upon metabolic stress

Hypothesis and aims of the study

A recent study highlighted that IRF5 upregulates glycolysis in response to PRR stimulation and M1 polarization. IRF5 induces AKT2 phosphorylation which in turn, activates glycolysis. Importantly IRF5 disease-associated polymorphisms in the context of autoimmunity show a similar upregulation of glycolysis. These polymorphisms result in increased IRF5 expression and activity, and consequently an activation of AKT2 (193). Moreover, IRF5 has been identified as a regulator of airway macrophages metabolic responses following influenza infection. In this context, IRF5 binding to the chromatin is enriched at metabolic genes and more precisely, IRF5 enhances glycolytic function, through an upregulation of *Hk2* expression. IRF5-deficient airway macrophages fail to metabolically activate, both glycolysis and OXPHOS in response to TLR3 activation (194). In addition, we have previously identified in liver macrophages an IRF5-dependent transcriptomic signature associated with mitochondria and lipid metabolism, in different models of liver fibrosis (84).

In line with these reports, considering the crucial role of IRF5 in the pathogenesis of metabolic disorders and the specificity of the AT microenvironment, we thus hypothesized that IRF5 may also orient ATM metabolism upon metabolic stress. More precisely, the aims of the project are:

- Determine IRF5-dependent intracellular substrate handling and metabolic adaptation of ATMs upon short-term high-fat diet,
- Determine target genes that mediate IRF5-dependent metabolic adaptations and associated molecular mechanisms,
- Assess the potential translational value of IRF5-dependent metabolic adaptations with a study on ATMs and blood monocytes from obese and/or T2D patients.

Methods

C57Bl6/J mice were fed with chow diet or HFD for 4 or 12 weeks to mimic a metabolic stress. Inflammatory profile, metabolic fluxes and cellular metabolic adaptations of ATMs were investigated by FACS analysis, bioenergetics assays (Seahorse, Agilent) and qPCR. To characterize the role of IRF5 in the cellular metabolic adaptations of ATMs, mice with a specific deletion of IRF5 in the myeloid cells (IRF5-KO) and their WT littermates were submitted to the same experimental design (4 weeks of HFD) and analysis.

Mitochondrial function of IRF5-KO bone marrow derived macrophages (BMDM) was assessed, *in vitro*, with a metabolic flux bioanalyzer and mitochondrial ultra-structure was determined by electronic microscopy. TCA metabolites were quantified by liquid chromatography coupled to high resolution mass spectrometry.

For mechanistic insight, we identified potential candidates involved in IRF5-mediated metabolic adaptations. In-house RNA-seq datasets of ATMs and BMDMs were coupled to public datasets of IRF5 ChIP-seq. BMDMs with a specific double knock-down of GHITM and IRF5 were generated using the CRISPR/Cas9 system. Mitochondrial function of these BMDMs was analyzed by Seahorse.

Characterization of metabolic adaptations in human ATM and monocytes was performed using public set of scRNA-seq and on blood samples or adipose tissue biopsies from T2D and/or obese patients, collected at Lariboisière Hospital or during bariatric surgeries at Clinique Geoffroy St Hilaire respectively.

Interferon Regulatory Factor 5 represses mitochondrial matrix protein GHITM to limit macrophage oxidative capacity in early response to obesity

Orliaguet L[1,12], Ejlalmanesh T[1,12], Humbert A[2], Ballaire R[1,3,12], Diedisheim M[1, 12], Julla JB[1,4,12], Chokr D[1,12], Cuenco J[1,12], Michieletto J[5], Charbit J[6], Linden D[7], Boucher J[7], Potier C[1,12], Hamimi A[1], Lemoine S[8], Blugeon C[8], Legoix P[9], Lameiras S[9], Baudrin LG[9], Baulande S[9], Soprani A[10], Castelli FA[5], Fenaille F[5], Riveline JP[1,4,12], Dalmas E[1,12], Rieusset J[2], Gautier JF[1,4,12], Venteclef N[1,12]** & Alzaid, F[1,11,12]*

[1] Centre de Recherche des Cordeliers, INSERM, IMMEDIAB Laboratory, Sorbonne Université, Université de Paris, Paris, France.

[2] CarMeN Laboratory, INSERM UMR-1060, Lyon 1 University, INRA U1397, F-69921, Oullins, France.

[3] Inovarion, 75005 Paris, France.

[4] Department of Diabetes, Clinical Investigation Centre (CIC-9504), Lariboisière Hospital, Assistance Publique - Hôpitaux de Paris, Paris, France.

[5] Université Paris-Saclay, CEA, INRAE, Département Médicaments et Technologies pour la Santé (DMTS), MetaboHUB, F-91191 Gif sur Yvette, France.

[6] Service d'endocrinologie, diabétologie, maladies métaboliques, Hôpital Avicenne, 127 Rte de Stalingrad, 93 009 Bobigny, France

[7] Bioscience Metabolism, Research and Early Development Cardiovascular, Renal and Metabolism, Bio-Pharmaceuticals R&D, AstraZeneca, Gothenburg, Sweden

[8] GenomiqueENS, Institut de Biologie de l'ENS (IBENS), Département de biologie, École normale supérieure, CNRS, INSERM, Université PSL, 75005 Paris, France

[9] Institut Curie Genomics of Excellence Platform, Institut Curie Research Center, PSL University, Paris, France.

[10] Centre de Recherche des Cordeliers, INSERM, University of Paris, IMMEDIAB Laboratory, F-75006, Paris, France; Department of Digestive Surgery, Générale de Santé (GDS), Geoffroy Saint Hilaire Clinic, 75005, Paris, France.

[11] Dasman Diabetes Institute, Kuwait, Kuwait

[12] Institut Necker Enfants Malades (INEM), INSERM U1151/CNRS UMRS8253, IMMEDIAB, Université de Paris Cité, 75015 Paris, France.

* Corresponding author: Alzaid F

** Co-corresponding author: Venteclef N

Competing interests

The authors declare no competing interests

Author contributions: LO, NV and FA conceived and designed the study. LO, TE, RB, JM, DC, JC, CP, AH, FC and FA performed experiments and collected data. LO, TE, AH, MD, CP, CB, SL, JR and FA analysed data. AH, MD, JM, PL, LGB, SB, SL, CB, FF and FAC contributed data or analysis tools. JBJ, DL, ED, JB, AS, JPR, JR and JFG provided key resources. LO, DL, JB, JPR, JR, JFG, NV and FA provided intellectual input. LO, NV and FA wrote the manuscript.

Acknowledgements: Image acquisitions or cytometric analysis and sorting were done at CHIC (*Centre d'Histologie, d'Imagerie Cellulaire et de Cytométrie*, Centre de Recherche des Cordeliers UMR S 1138, Paris, France). CHIC is a member of the SU Cell Imaging and Flow Cytometry network (LUMIC) and UPD cell imaging networks. Transmission electronic microscopy was performed at CIQLE platform (Centre d'Imagerie Quantitative Lyon-Est, Lyon, France) and we thank Elisabeth Errazuriz and Christel Cassin for their technical help. This

work was supported by the France Génomique national infrastructure, funded as part of the "Investissements d'Avenir" program managed by the Agence Nationale de la Recherche (contract ANR-10-INBS-09). High-throughput sequencing has been performed by the ICGex NGS platform of the Institut Curie supported by the grant ANR-10-EQPX-03 (Equipex) from the French National Research Agency (*Agence Nationale de la Recherche; ANR;* "*Investissements d'Avenir*" program), by the Canceropole Ile-de-France and by the SiRIC-Curie program - SiRIC Grant "INCa-DGOS-4654". This research was supported by the French National Research Agency (*Agence Nationale de la Recherche; ANR*) ANR-JCJC grant for the MitoFLAME Project ANR-19-CE14-0005 and by the French Society for Diabetes (*Société Francophone du Diabète; SFD*) *Allocation Exceptionnelle* to FA. Support was provided to FA and NV through a collaboration with AstraZeneca. Support was provided to FA and JFG by the European Foundation for the Study of Diabetes. Support was also provided to FC and FF by the *Commissariat à l'Energie Atomique et aux Energies Alternatives* and the MetaboHUB infrastructure (ANR-11-INBS-0010 grant). N.V. was supported by grants from the European Union H2020 framework (ERC-EpiFAT 725790), the French National Research Agency (Agence Nationale de la Recherche; ANR) ANR-PUMAs and INFLAMEX. LO was supported by *Fondation de la Recherche Médicale* (FDT202106013230).

Abstract

From transient caloric excess to diet-induced obesity (DIO), adipose tissue macrophages (ATMs) adapt to changes in their microenvironment. ATMs transition from highly oxidative and protective to highly inflammatory and metabolically deleterious. Here, we demonstrate that the Interferon Regulatory Factor (IRF)-5 is a key regulator of macrophage oxidative capacity in response to caloric excess. ATMs from mice with genetic-deficiency of IRF5 are characterised by increased oxidative respiration and mitochondrial membrane potential. This phenotype is inducible in mature macrophages and is reversible by adenoviral reconstitution of IRF5 expression. Using public ChIP-sequencing and in-house RNA-sequencing, we found that the highly oxidative nature of IRF5-deficient macrophages results from a transcriptional interaction with the *Growth Hormone Inducible Transmembrane Protein* (GHITM), that contributes to maintaining optimal mitochondrial architecture. Cas9-mediated knock-down of GHITM decreases the high oxygen consumption associated with IRF5-deficiency. Coregulated expression of IRF5 and GHITM, and associated cellular energetic phenotype, extends to ATMs and monocytes from patients with obesity and with type-2 diabetes. We shed light on a mechanism by which the inflammatory transcription factor IRF5 acts early on, and non-canonically, on GHITM to alter mitochondrial architecture in macrophages, limiting physiological adaptation to DIO.

INTRODUCTION

Macrophage metabolism is a powerful mitigating or optimising factor influencing function[1]. Generally speaking, pro-inflammatory polarisation relies on glycolysis, mediated by hypoxia inducible factor (HIF)-1α[2], with specific interruptions of the tricarboxylic acid (TCA) cycle[3]. Conversely, anti-inflammatory polarisation or regulatory function is supported by mitochondria and oxidative respiration[4]. Microenvironmental niches also impose energetic specificities on macrophages[5,6]. For example, adipose tissue macrophages (ATMs) can range from being metabolically quiescent to overall hypermetabolic[5,7,8]. In diet-induced obesity (DIO), ATMs are exposed to the same dysmetabolism as all peripheral tissues, that is glucolipotoxicity, providing a systemic abundance of metabolic substrates. It is in this context that ATMs are hypermetabolic, with highly glycolytic and highly oxidative fluxes[7,8,9]. ATMs are however a heterogenous population of cells that exhibit a range of beneficial and detrimental phenotypes over the course of obesity[10,11]. Lipid associated macrophages (LAMs) have been characterised, they are highly oxidative and have a high capacity to clear lipids and dying adipocytes[12]. Also highly responsive to lipids are the phenotypically similar $MARCO^{+}$ lipid-buffering ATMs and metabolically-activated macrophages (MMe)[13,14]. Expansion of these ATM populations, and their functional contribution to maintaining tissue homeostasis or to metabolic decline varies with duration of caloric excess[13]. Such reports indicate that macrophages are reactive beyond their inflammatory roles and their successful adaptation early in the course of DIO, may be sufficient to mitigate systemic metabolic decline.

The rise of lipid-buffering ATMs represents initial adaptation in a physiological attempt to maintain homeostasis[10]. Over prolonged caloric excess ATMs become predominantly inflammatory and contribute to insulin resistance in DIO[15,16]. The early adaptive step is marked by high oxidative capacity[14] and the later predominance of inflammatory ATMs marks their rise as critical actors in development of insulin resistance and type-2 diabetes (T2D)[13].

The Interferon Regulatory Factor (IRF)-5 is a key molecular switch mediating M1-like polarisation of ATMs[17]. ATM expression of IRF5 is increased in DIO, promoting pro-inflammatory polarisation and repressing TGFβ-signalling. This favours maladaptive white adipose tissue (WAT) expansion and insulin resistance. IRF5 is physiologically required to respond to bacterial and viral stimuli[18,19], evidence also implicates deregulated expression in conditions of chronic inflammation (e.g. auto-immune, metabolic diseases)[20,21]. Gain-of-function IRF5 variants associated with auto-immune disease have more recently been found to promote macrophage glycolytic programming[22]. Here, we reveal a non-canonical function for IRF5 in orienting macrophage energetic adaptation to caloric excess. IRF5 transcriptionally represses the *Growth Hormone Inducible Transmembrane protein* (GHITM), a key mitochondrial component required for oxidative respiration[23]. Through this interaction, IRF5 contributes to failure in maintaining normal mitochondrial cristae structures that support effective oxidative respiration. GHITM repression and failure to maintain cristae structure restrains ATM oxidative capacity in DIO. The IRF5-GHITM regulatory axis extends from short- to long-term high-fat feeding and to monocytes and ATMs in patients with obesity and T2D.

RESULTS

IRF5 is associated with ATM metabolic adaptation upon short-term high-fat diet

We started by analysing the ATM transcriptome from mice with a myeloid-deficiency of IRF5 (IRF5-KO) or wild-type (WT) mice on 4 and 12 weeks of high-fat diet (HFD). On a 12-week, long-term HFD (LT-HFD), differentially expressed genes were associated with *Inflammatory Response* and *Tissue Remodelling* (Fig. 1A, S1A). This confirms previously reported phenotypic features[17]. On a 4-week HFD, qualified short-term (ST-HFD), differentially expressed genes enriched several GO terms for *Metabolic Process*. Interestingly, terms relating to immune function (*Humoral Immune Response*, *Phagocytosis/Recognition*) were under-represented (Fig. 1B, S1B). These results indicate that IRF5 may influence ATM metabolic adaptation, in particular, in response to short-term caloric excess.

To associate ATM metabolism to IRF5, we evaluated ATM metabolic adaptation and IRF5 expression upon ST- and LT-HFD in C57BL/6J mice. Mice on ST-HFD and LT-HFD gained weight, increasing WAT mass and losing glycaemic homeostasis over time (Fig. S1C-E). IRF5 expression also increased in epididymal fat pads (EpiWAT) on ST-HFD and LT-HFD (Fig. 1C). We characterised ATM metabolic adaptation using the fluorescent lipid dye BODIPY and the JC-1 dye, a sensor for mitochondrial mass (Mt Mass) and membrane potential (mΔΨ)[24]. On ST- and LT-HFD, ATMs have a higher lipid content and Mt Mass but decreased mΔΨ and mΔΨ-to-mass ratio, relative to mice on normal chow diet (NCD) (Fig. 1D, S2A). Interestingly, effects on Mt Mass and mΔΨ upon ST-HFD are similar in magnitude to LT-HFD. These data are consistent with previous reports that ATMs become hypermetabolic in DIO[7,8], however, metabolic adaptation occurs within short-term caloric excess. This was confirmed to contribute to cellular respiration by extracellular flux analyses on F4/80^{+} ATMs (Fig. 1E, S2B).

On ST-HFD, correlations revealed that ATM Mt Mass was positively associated with IRF5 expression and ΔΨ-to-mass ratio was negatively associated (Fig. 1F), ATM lipid content was not associated (Fig. S2C). ATM numbers were positively correlated to IRF5 expression, this was observed by FACS and by qPCR analysis of F4/80 and IRF5 expression in EpiWAT (Fig. 1G, S2D). A UMAP showed that IRF5 was highly expressed in cells that also highly express F4/80 (F4/80^{Hi}; Fig. S2E), a population reported to be monocyte-derived[25]. We quantified IRF5 expression in F4/80^{Lo} and F4/80^{Hi} ATMs and found IRF5 to be upregulated in F4/80^{Hi} ATMs on ST-HFD (Fig. 1H; S2F). F4/80^{Hi} ATMs had markedly increased Mt Mass and decreased mΔΨ (Fig. 1I). These results suggest that IRF5 plays a role in ATM mitochondrial adaptation, in particular in F4/80^{Hi} ATMs.

IRF5-deficiency alters ATM oxidative respiration in response to short-term high-fat diet

We applied the same model of ST-HFD to IRF5-KO and WT mice. Weight gain and EpiWAT weight were similar between genotypes (Fig. S3A). ATMs from IRF5-KO mice had increased mΔΨ and mΔΨ-to-mass ratio relative to WT mice, lipid content and Mt Mass were not altered (Fig. 1J; Fig. S3B). Analysis by tSNE confirmed JC1-red fluorescence, indicating mΔΨ, was highest in F4/80^{Hi} ATMs and these cells had higher fluorescence in IRF5-KO (Fig. 1K). Under basal conditions, on NCD, IRF5-KO did not affect ATM metabolic phenotype (Fig. S3C) and upon LT-HFD, only a trend to increased intracellular lipid content persisted (Fig. S3D).

To link cytometric analyses to functional respiration, we analysed extracellular flux from magnetically sorted F4/80^{+} ATMs of IRF5-KO and WT mice, under NCD and following ST- and LT-HFD. ATMs from IRF5-KO mice had a higher oxygen consumption rate (OCR) following ST-HFD, but not on NCD nor LT-HFD (Fig. 2A). F4/80^{-} cells were unaffected by

IRF5-deficiency (Fig. S4A). However, higher OCR in IRF5-KO ATMs remains apparent when whole SVF is analysed under conditions testing mitochondrial, or glycolytic, respiration (Fig. 2B, 2C). OCR reflects a number of oxygen consuming processes, a major contributor to which is fatty acid oxidation (FAO)[26]. To evaluate whether the contribution of FAO to the IRF5-KO respiratory phenotype we carried out a palmitate (Palm) oxidation test on SVF, with or without etomoxir (ETO), an inhibitor of carnitine palmitoyl transferase (CPT)-1[27]. OCR was higher in Palm-loaded SVF from IRF5-KO mice upon ST-HFD. This was normalised to WT levels in the presence of ETO (Fig. 2D, S4B), indicating that FAO contributes to higher OCR in cells from IRF5-KO mice.

ATM adaptation in IRF5-deficiency alters adipose tissue phenotypic response to short-term high-fat diet

As a consequence of ATM phenotype, analysing EpiWAT sections revealed that average adipocyte diameter and frequency of large (>100 um) adipocytes was higher in EpiWAT from IRF5-KO mice (Fig. 2E, S4C). Number of crown-like structures (CLS) was higher, and number of $MAC2^+$ cells had an increasing trend (Fig. 2F, S4D). Despite CLS accumulation in IRF5-KO, we found no difference in expression of inflammatory markers in EpiWAT, (e.g., IL6, TNF, some markers were not reliably detectable). Cytokine and adipokine levels in circulation were also similar between genotypes (Fig. S4E-G). These phenotypic tissue features were concurrent to a functional increase in glucose uptake capacity in fat pads from IRF5-KO mice (Fig. 2G) and this occurs on a background of similar glycaemia and insulin levels to WT mice (Fig. S4H). Increased glucose uptake might reflect improved glucose homeostasis and insulin sensitivity at the tissue level and could also explain increased adipocyte size in IRF5-KO mice. The EpiWAT phenotype of IRF5-KO mice upon ST-HFD presents similarities with the protective EpiWAT phenotype of IRF5-KO mice upon LT-HFD[17] (i.e., increased ATM content, improved insulin sensitivity). Importantly, the IRF5-linked respiratory phenotype of ATMs occurs transiently and orchestrates tissue level adaptation at a stage when systemic metabolism is not yet impacted (Fig. S4I). Such early adaptation, underpinned by ATM mitochondrial respiration, is a key event that precedes IRF5-deficiency's protective metabolic phenotype at the stage of systemic insulin resistance (LT-HFD).

IRF5 repression of mitochondrial respiration is cell intrinsic, reversible and inducible in mature macrophages

To carry out mechanistic investigations we moved to bone marrow-derived macrophages (BMDMs). BMDMs from IRF5-KO and WT mice were differentiated and treated for 24 h with bacterial lipopolysaccharides (LPS), a canonical stimulant of the IRF5 signalling pathway, or with Palm to model lipotoxicity. Testing glycolysis, we found no genotype difference in extracellular acidification rates (ECAR) in control or treated cells (Fig. S5A). Glucose-stimulated OCR was increased IRF5-KO BMDMs following treatment with LPS or Palm (Fig. 3A, S5B). Under conditions testing mitochondrial respiration, OCR was increased in IRF5-KO BMDMs following LPS or Palm treatment, with no difference in untreated cells (Fig. 3B, S5C). The IRF5-linked respiratory phenotype is cell intrinsic and mirrors what we observed in ATMs.

To evaluate whether the respiratory phenotype is the result of genetic deficiency, or if it is inducible in mature macrophages, we applied an IRF5 inhibitory decoy peptide (IRF5-DP) to mature BMDMs from WT mice. IRF5-DP binds to IRF5, preventing its nuclear translocation[28]. LPS-induction of TNF is prevented by IRF5-DP, confirming that it blocks transcriptional activity of IRF5 (Fig. S5D). When treated with Palm, metabolic flux analyses showed that IRF5-DP increased OCR relative to vehicle, replicating the effect of genetic deficiency (Fig. 3C). This

result indicates requirement for IRF5 nuclear translocation and rules out a differentiation effect of genetic deficiency. We next used adenoviral delivery to re-introduce IRF5 expression in BMDMs from IRF5-KO mice, IRF5 adenovirus (adIRF5) resulted in a 1.4-fold increase in IRF5 expression (Fig. S5F). Following Palm treatment, OCR was decreased in cells treated with adIRF5, but not in cells treated with the control adenovirus (adGFP; Fig. 3D, S5G).

IRF5-deficiency alters concentrations of TCA cycle metabolites and structural components of mitochondria in response to palmitate treatment

To understand how IRF5 affects mitochondrial function, we quantified (TCA) cycle metabolites in IRF5-KO and WT BMDMs treated with Palm or with LPS. A PCA score plot revealed genotype-dependent difference in metabolite profile within 2 h of treatment with Palm but not with LPS, and most differences were normalised by 24 h (Fig. 4A, S6A, S6B). This was confirmed by carrying out a PCA only on 2 h Palm-treated samples (Fig. 4B). Variable ranking revealed lactate (Lac) was the biggest contributor to the IRF5-dependent response to Palm, and it had a higher concentration in IRF5-KO BMDMs (Fig. 5C). Lactate is a glycolysis end-product destined for extracellular release[29] (Fig. 4D). However, ECAR was lower in IRF5-KO BMDM under these test conditions, indicating lactate is released at a slower rate (Fig. 4E). Thus, lactate accumulation in IRF5-KO BMDM can be explained by its increased retention. Interestingly, intracellular lactate has recently been reported to be subject to oxidation in M2-like macrophages, potentially contributing to oxygen consumption [30]. Consequently, analysing mitochondrial respiration found increased OCR in IRF5-KO BMDM under these conditions.

We also applied electron microscopy to BMDMs under these same conditions to evaluate potential structural mechanisms. Mitochondrial density, form factor and aspect ratio were not altered between IRF5-KO and WT BMDM (Fig. 4G, S6C) suggesting no adaptation in mitochondrial dynamics as quantifiable by these parameters. However, we did find that mitochondrial cristae were denser and had a larger surface area in IRF5-KO BMDM (Fig. 4H). Well-developed cristae structures may provide a mechanism to increase surface area for oxidative respiration, allowing IRF5-KO BMDM to maintain their hyperoxidative phenotype.

The above analyses highlight two potential mechanisms that can contribute to increased oxidative respiration in IRF5-deficient macrophages: 1) increase in oxidisable intracellular lactate, or 2) increase in mitochondrial respiratory surface area.

IRF5 binds and regulates expression of the mitochondrial matrix protein GHITM

To resolve a transcriptional mechanism, we carried out RNA-seq on ATMs (ST- and LT-HFD) and BMDM (0h, 2h and 24h stimulation with LPS or Palm) from IRF5-KO and WT mice. Coregulated clusters were defined based on genotype-effect and on trajectory over time (Fig. 5A, S7A). A number of terms relating to lipotoxicity and mitochondrial function were enriched across all conditions (e.g., *Response to cholesterol, Mitochondrial translation*; Fig. 5B). We also acquired ChIP-seq data that maps IRF5 binding in BMDM[31]. Of 526 bound genes, 77 (14.6%) enriched the *Metabolic Process* GO term (Fig. 5C), indicating a level of transcriptional control over metabolism.

To define a list of targets, we carried out differential expression analyses of RNA-seq data between genotypes, per condition and per timepoint (Fig. 5D). Palm treatment had the highest number of differentially expressed genes, followed by LPS and HFD; 34 targets (1%) were represented in all conditions. Intersection with ChIP-seq revealed 6 genes were differentially expressed and were also bound by IRF5 at, or upstream of, transcription start sites: *ATF5, SYCE2, ABCG1, LRRC27, FNIP2 and GHITM*. GHITM has an overt function in maintaining

inner membrane cristae structures[23] (Fig. 5D), and its expression was negatively correlated with IRF5 expression in ATMs from WT mice (Fig. 5E). These data indicate that GHITM may be a mechanistic target of IRF5 that can influence mitochondrial respiration.

Single-cell sequencing data[12] from mice on HFD confirmed that IRF5 and GHITM are highly expressed in monocytes and ATMs, GHITM expression was higher than all other targets identified (Fig. 6A, 6B, S8A). IRF5 and GHITM expression were negatively correlated (R= -0.44; p<0.001), supporting our own data (Fig. 6C, 6D). IRF5 expression increased overtime and remained negatively correlated to GHITM expression in monocytes and ATMs (Fig. 6B, 6D). Data analysed from Jaitin *et al*[12], Saliba *et al*[31], together with our work, strongly suggest that the interaction between IRF5 and GHITM influences macrophage respiratory phenotype.

We chose to pursue a GHITM-mediated mechanism as a contributor to increased oxygen consumption through maintenance of cristae structures in IRF5-deficient macrophages (Fig. 4H). As for the potential contribution of lactate oxidation, none of the identified targets had a described function in lactate metabolism, and thus IRF5-dependent remodelling of the TCA cycle could be an area for future investigation beyond the scope of current work.

GHITM knockdown reverses hyperoxidative phenotype of IRF5-deficient macrophages

With guide RNAs (gRNA) targeting GHITM (gGHITM), we transduced BMDMs expressing the Clustered Regularly Interspaced Short Palindromic Repeats (CRISPR)-Associated Protein (Cas)-9 linked to EGFP and under control of the Lyz2 promoter (Fig. S8B). Transfection with gGHITM resulted in a 40 % decrease in expression (Fig. S8C). We subjected BMDM to Palm treatment, GHITM expression decreased in response to Palm and upon transfection (Fig. 6E, S8D, S8E). Transfection with gGHITM also decreased OCR measures, in particular at maximal respiration, in untreated and Palm treated cells (Fig. 6F). We then targeted IRF5 alone (gIRF5), or co-transfected with gIRF5 and gGHITM (Fig. S8F). Extracellular flux analysis after Palm treatment revealed that gIRF5 increased OCR, reproducing the IRF5-KO phenotype (Fig. 8H, S8G). Co-transfection with gGHITM normalised respiration to control levels (Fig. 6H, S8G). These results indicate GHITM contributes to increased oxidative respiration in IRF5-deficient macrophages.

IRF5-GHITM regulatory axis is conserved in patients with obesity and type-2 diabetes

RNA-seq on IRF5$^+$ and IRF5$^-$ monocytes from patients with T2D revealed 3211 upregulated and 295 downregulated genes in IRF5$^+$ monocytes (Fig. 7A). Terms for *Mitochondrial Organisation* and *Protein Localisation to Mitochondria* were under-represented amongst upregulated genes while downregulated genes enriched *Lipid Catabolism* terms (Fig. 7B). Additionally, GHITM was consistently downregulated in IRF5$^+$ relative to IRF5$^-$ cells (Fig. 7C).

ScRNA-seq on SVF from lean and obese humans[32] confirmed previous reports that IRF5 expression is increased with obesity and revealed a concurrent decrease in GHITM expression (Fig. 7D, S9A). Cell-by-cell visualisation indicated that as cells gain expression of IRF5, they lose expression of GHITM (Fig. 7D, S9B). We next binned cells by increasing levels of IRF5 expression and found that as IRF5 expression increased, the proportion of GHITM$^+$ cells decrease (Fig. 7E). Correlative analyses revealed a strong negative association between IRF5 and GHITM mean expression per bin (Fig. 7F). For further analysis, we obtained WAT biopsies from a cohort of obese patients and sorted CD14$^+$ ATMs from subcutaneous and visceral fat depots (scATMs, vATMs) for qRT-PCR analysis. Samples were designated as IRF5^{Hi} or IRF5^{Lo} expressors, in which we found similar counter-regulation of GHITM in vATMs, but not in scATMs (Fig. 7G, S9C). In functional analyses, we found negative association trends

between IRF5 expression and Mt Mass, mΔΨ and mΔΨ-to-mass ratio in vATMs, and mΔΨ-to-mass ratio in monocytes (Fig 7H, S9D). These results demonstrate that the IRF5-GHITM axis is conserved in humans and may be associated with mitochondrial adaptation of ATMs and monocytes in obesity and T2D.

To evaluate potential for transcriptional regulation we stained monocytes from patients with T2D for IRF5 and for oxidative phosphorylation (OXPHOS) enzyme complexes (Fig. 7I). These complexes are typically anchored to the cristae structures maintained by GHITM[23,33]. Monocytes with nuclear localisation of IRF5 (Nuc) had lower OXPHOS staining density relative to those with cytoplasmic staining (Cyt). Loss of OXPHOS complex density is associated with nuclear localisation of IRF5, indicating a transcriptional mechanism. Lastly, we used the University of California Santa Cruz (UCSC) genome browser to visualise IRF5 binding regions around the GHITM gene. Several IRF5 binding regions were found on and upstream of GHITM (Fig. 7J). On this same resource, expression of GHITM mRNA is decreased in LPS-treated human monocyte-derived macrophages (HMDM) and this coincides with decrease in active transcription histone mark H3K27ac. The above analyses demonstrate that IFR5 can bind to the GHITM gene in humans, IRF5 and GHITM are also reciprocally regulated, indicating that IRF5's transcriptional activity may be targeted to GHITM upon macrophage polarisation.

DISCUSSION

WAT is a key responder to caloric excess. Adaptive responses dictate disease course in metabolic syndrome, and a major determinant of tissue adaptation is the phenotype and function of ATMs. ATMs are a heterogenous population of cells ranging from regulatory to highly inflammatory, the latter contributing to systemic metabolic decline in obesity and T2D. As sentinel cells with roles in maintaining homeostasis, the molecular mechanisms of ATM adaptation to early caloric excess remain to be fully understood. Here we demonstrate that ATMs undergo extensive IRF5-dependent energetic adaptation upon short-term caloric excess. ATM oxidative capacity is limited by IRF5's transcriptional interaction with GHITM, the inner mitochondrial membrane protein that maintains mitochondrial architecture for efficient oxidative respiration. Decreased GHITM expression and loss of cristae organisation occurs at an early stage of DIO and represents an IRF5-dependent mechanism that may contribute to loss of microenvironmental homeostasis and development of insulin resistance (Fig. 8). Previous studies show that inflammation arises in WAT and is mediated by ATMs. The key implication of IRF5 in this inflammation and the development of T2D has been demonstrated[17]. IRF5 gain-of-function risk-variants have also been associated with increasing macrophage glycolytic flux[18], a cellular process that supports inflammatory effector function. A recent study also demonstrated that IRF5 regulates airway macrophage metabolic response to viral infection[34]. Here we hypothesised that this transcription factor may have a role to play in adapting ATM metabolism in response to caloric excess. We first found that metabolically relevant genes were disproportionally represented in the IRF5-deficient transcriptome upon short-term, but not long-term high-fat feeding. The latter being enriched by inflammation-related genes. In coherence with a study by Lee *et al.*[16] that demonstrated immunocompromised mice developed insulin resistance upon short-term high-fat feeding, indicating that inflammation is not required for loss of glycaemic homeostasis in short-term caloric excess. A further study by Shimobayashi *et al.*[35] confirmed this, demonstrating that WAT was disproportionately affected and that early loss of glycaemic homeostasis precedes inflammation. Our findings are supported by these studies, within 4 weeks of high-fat feeding mice develop altered glucose homeostasis, however without an overt IRF5-linked inflammatory signature. We did however demonstrate that ATMs undergo adaptation and are energetically distinct at this time point when compared to mice on a NCD.

ATMs reside in a lipid-rich environment and take on an overall hypermetabolic phenotype in DIO, increasing glycolysis as well as mitochondrial respiration[8]. More recent studies report specific LAM expansion on HFD, with LAMs being metabolically protective[12]. Similarly, $CD11c^+$, $CD206^+$ double positive macrophages were found to expand on short-term HFD and are a highly oxidative population[14]. Whilst these populations of ATMs are both highly oxidative and represent physiological adaptation to caloric excess, later engagement of glycolysis has been associated with supporting ATM inflammatory polarisation[2]. We deciphered a transcriptional mechanism that restrains cellular oxidative capacity, potentially altering microenvironmental factors and promoting greater reliance on glycolysis. IRF5-deficient macrophages have a high rate of oxygen consumption and this is linked to a transcriptional interaction with GHITM, a protein that maintains structure of OXPHOS anchoring cristae[23]. Our finding highlights an important role for IRF5 in biasing cellular metabolism by impairing mitochondrial respiration.

We also found the TCA metabolite profile to be modified in IRF5-KO relative to WT macrophages upon stimulation. And this occurs earlier and to a greater extent in response to lipotoxicity (palmitate), than in response to bacterial stimuli (LPS). Lactate was the most

important metabolite altered in IRF5-deficiency when we analysed intracellular metabolites. Its intracellular accumulation has recently been reported to be a hallmark of M2-like macrophages and supports a more tolerogenic phenotype[30]. Interestingly, increasing reports reveal intracellular lactate is itself susceptible to oxidation and can be metabolised in mitochondria[30,36,37]. We found that decreased lactate secretion leads to its accumulation in IRF5-KO macrophages, however, we do not have direct evidence of its contribution to oxygen consumption. Moreover, target genes that we identified have not been found to directly interact with pathways for lactate metabolism. This mechanism may contribute to the observed phenotype; however, it may also run in parallel to the structural mechanism we resolved in the IRF5-GHITM interaction. Whilst out of the scope of the current work, future investigations can focus on the mechanism by which IRF5 alters TCA cycle dynamics.

We were data-driven in resolving the current mechanism, in which we combined public datasets with our own RNA-seq to reveal that a transcriptional target of IRF5 impairs macrophage mitochondrial respiration at the early stage of glucose intolerance but prior to onset of insulin resistance. Interestingly, this mechanism is transient, as ATMs from IRF5-KO and WT mice do not show any difference in respiratory phenotype following 12 weeks of high-fat feeding. This may be due to the function of IRF5 being more inflammatory over time or when supported by other microenvironmental cues (e.g., hypoxia, cytokines, hyperglycaemia). Such functional specificity is clearly represented by the IRF5-deficient ATM transcriptome which is enriched by metabolism-related genes in the short-term, then enriched by inflammation-related genes on long-term high-fat feeding.

Previous studies found that GHITM knockdown causes cristae disorganisation and mitochondrial fragmentation[23]. Mitochondrial fragmentation has been associated with inflammatory polarisation, both in response to LPS and to fatty acids[38,39]. Studies in lymphocyte lines stimulated with inflammatory cytokines and from virus-exposed monocytes also report downregulation of GHITM[40,41]. These reports are in line with our current findings that loss of GHITM is associated with compromised cristae in macrophages and with increased inflammation under lipotoxic stress. We report this role for GHITM in macrophages, and in monocytes, in humans and mice in response to metabolic stress. Decreased expression of GHITM, and decreased ATM oxidative capacity, is an early and potentially key mechanism of WAT maladaptation to caloric excess.

In summary, we deciphered a mechanism by which IRF5, a well characterised pro-inflammatory transcription factor, alters cellular mitochondrial respiration. Having identified this mechanism to control cellular metabolism, a number of questions remain unanswered. For example, to elucidate how and through which regulatory elements IRF5 may be binding to such targets as GHITM. Whilst it is widely accepted that IRFs, target interferon sensitive regulatory elements (ISRE), it is unknown whether these response elements populate genes that regulate mitochondrial metabolism and structural components, such as GHITM. Furthermore, the specific functional contribution of GHITM downregulation to effective inflammation is unknown, for example consequent mitochondrial fragmentation may be a source of reactive oxygen species required for bacterial killing. Lastly, despite several lines of evidence implicating IRF5 in metabolic decline associated with diet-induced obesity, the metabolic stressors that induce IRF5 expression remain unknown. Future work on the above questions will be of important insight into how this pathway can be modulated in metabolic and inflammatory diseases.

METHODS

Human samples

Blood samples and adipose tissue biopsies were obtained from different populations admitted to the Lariboisière and Geoffroy Saint Hilaire hospitals (Paris, France). Studies were conducted in accordance with the Helsinki Declaration and were registered to a public trial registry (Clinicaltrials.gov; NCT02671864). The Ethics Committee of CPP Ile-de-France approved the clinical investigations for all individuals, and written informed consent was obtained from all individuals. The principal investigator of this clinical trial is Prof. Jean-François Gautier: jean-francois.gautier@aphp.fr. Adipose tissue biopsies were obtained from obese subjects during bariatric surgery.

Experimental animals and *In vivo* studies

Male C57BL/6J mice (5-7 weeks) were purchased from Charles River. To generate mice with a myeloid-specific deletion of IRF5, IRF5 flox/flox mice (C57BL/6-Irf5tm1Ppr/J; stock no. 017311) were crossed with LysM-Cre mice (B6.129P2-Lyz2tm1(cre)Ifo/J; stock no. 04781), purchased from The Jackson Laboratory. To generate mice with a restricted myeloid expression of the Cas9 endonuclease, Rosa26-Cas9KI mice (Gt(ROSA)26Sortm1.1(CAG-cas9*,-EGFP)Fezh/J; stock no. 024858, The Jackson Laboratory) were crossed with LysM-Cre mice.

Mice carrying mutated alleles were identified by PCR screening performed on genomic DNA (DNeasy Blood & Tissue Kit, Qiagen) with specific primers (Table S1). Mice were housed at 22°C on a 12 h light/dark cycle in the “Centre d’Explorations Fonctionnelles” of Sorbonne University (UMS-28). All mice used in the study were male and aged between 7-10 weeks old at the time of the experiment starting point. All animal experiments were approved by the French ethical board (Paris-Sorbonne University, Charles Darwin N°5, 01026.02) and conducted in accordance with the guidelines stated in the International Guiding Principles for Biomedical Research Involving Animals.

Mice were fed with High Fat Diet (HFD) (60% fat, D12492, Research Diets) or normal chow diet for 4 or 12 weeks. Mice had *ad libitum* access to food and water. Mice were weighed weekly and glycaemia measured.

For oral glucose tolerance test (GTT), mice were fasted overnight before being gavaged with glucose (2g/kg of body weight). Tail vein blood was collected to measure glycaemia with a glucometer (Verio, One touch). For insulin tolerance test (ITT), mice were fasted during 5 h before being i.p injected with insulin (0,5U/kg of body weight). Glycaemia was monitored for 120 min after insulin injection.

Organ collection and histology

Mice were sacrificed by cervical dislocation. Upon dissection, tissues were weighed. Immediately after collection, samples were either digested with collagenase, snap-frozen for further analysis or drop-fixed into 10% formalin (Sigma Aldrich) for 24 h for histological analysis. For histological analysis, tissues were processed for dehydration, clearing and paraffin embedding with an automated carousel (Leica). Sections (6µM thick) were stained with haematoxylin and eosin according to standard procedures. Images were acquired with a slide scanner (Zeiss Axio Scan Z1). Adipocyte diameter was measured (3 sections per mouse) with ImageJ® (Fiji).

Analysis of circulating plasmatic parameters

Adiponectin (Mouse Adiponectin/Acrp30 DuoSet ELISA, DY1119, R&D Systems), leptin (Mouse Leptin DuoSet ELISA, DY498-05, R&D Systems) and insulin (U-PLEX Mouse Insulin Assay, MSD) concentrations were determined by immunoassay. Plasma cytokines were quantified with LEGENDplex Mouse Inflammation kit (Biolegend) according to manufacturer's instructions.

Glucose uptake assay

EpiWAT explants were processed to measure glucose uptake with glucose analog 2-DG. After starvation and 2-DG uptake, explants were lysed in extraction buffer. Lysates were processed according to manufacturer's protocol (Glucose Uptake Fluorometric Assay Kit, MAK084, Sigma Aldrich).

Stromal vascular fraction

The stromal vascular fraction (SVF) containing mononuclear cells and preadipocytes was isolated from the adipose tissue after collagenase digestion. Briefly, adipose tissue biopsies were minced in collagenase solution (1mg/ml collagenase (C6885, Sigma Aldrich), diluted in Dulbecco's Modified Eagle Medium (DMEM) (Gibco) supplemented with 1% penicillin/streptomycin (P/S), Hepes and 2% BSA) for 20 min at 37°C. Lysate was then passed through a 200µM filter. After centrifugation, the resulting cell pellet was resuspended in red blood cell lysis buffer (155mM NH_4Cl, 12mM $NaHCO_3$, 0,1mM EDTA) and passed through a 70µM filter. Cells were centrifuged and resuspended in FACS buffer (1X PBS supplemented with 0,5% BSA and 5mM EDTA) for further analysis.

Flow cytometry and cell sorting

SVF cells were prepared as described above. Blood cells were obtained from 1 ml of venous blood after red blood cells lysis and resuspended in FACS buffer.

Cells were incubated with an Fc-blocker (120-000-422, Miltenyi Biotech) for 10 min. For metabolic analysis, cells were incubated with 200 µM JC-1 (T3168, ThermoFisher Scientific) for 30 min at 37°C. Finally, cells were stained for surface markers (Table S2) and a Live/Dead viability dye (L34957, ThermoFisher Scientific) according to manufacturer's protocol. For intracellular lipid staining, BODIPY (D3922, ThermoFisher Scientific) was added to surface markers antibodies mix. For IRF5 staining, cells were fixed with Foxp3-staining kit (00-5523-00, ThermoFisher Scientific) and then stained with an anti-IRF5 (10547-1-AP, Proteintech) for 1 h, and then with a secondary PE antibody (12-4739-81, ThermoFisher Scientific) for 30 min.

Acquisition was performed on a MACSQuant cytometer (Miltenyi Biotech). Cell sorting was performed on a FACSAria III (BD Biosciences). Cells were directly sorted in RLT lysis buffer supplemented with β-mercaptoethanol for RNA extraction (Qiagen). Data were analysed with FlowJo software (Tree Star).

Cells from the previously isolated SVF were stained for immunoselection of $F4/80^+$ or $CD14^+$ cells according to manufacturer's protocol (MACS, Miltenyi Biotec). Cells were resuspended in MACS buffer (1X PBS supplemented with 0.5% BSA and 2mM EDTA) containing the appropriate dilution of anti-F4/80 microbeads for murine samples (130-110-443, Miltenyi Biotec) or anti-CD14 microbeads for human samples (130-050-201, Miltenyi Biotec), for 10 min at 4°C. Automated magnetic cell separation was performed with the Multi-MACS Cell Separator. For RNA extraction, the $F4/80^+$ cell fraction was washed and directly resuspended

in RLT lysis buffer supplemented with β-mercaptoethanol (Qiagen). For metabolic flux measurements, F4/80$^+$ and F4/80$^-$ cells (180,000 cells per well, in XFe96 cell culture plates) were allowed to adhere overnight in RPMI medium supplemented with 10% FBS and 1% P/S.

In vitro macrophage studies

Bone marrow-derived macrophages: Murine bone marrow cells were isolated from femurs and tibias. Cells were plated in DMEM (Gibco) supplemented with 10% FBS, 1% P/S and 30% L929 conditioned-media and were allowed to differentiate for 8-10 days into bone marrow-derived macrophages.

Treatments: Cells were treated with LPS (10ng/ml) (L2630, Sigma Aldrich) or Palmitate (200µM) for the appropriate time. Palmitate stock solution was prepared by dissolving sodium palmitate (P9767, Sigma Aldrich) in 50% ethanol solution, followed by dilution in a 1% fatty acid free albumin solution (A8806, Sigma Aldrich).

Decoy peptide: Fully differentiated BMDMs were pre-treated with an IRF5 decoy peptide[28] (50µg/ml) for 30 min, before being treated for further analysis.

Transfection: Fully differentiated BMDMs were transfected with IRF5 (Mm.Cas9.IRF5.1.AB, Integrated DNA Technologies) or GHITM (Mm.Cas9.GHITM.1.AA, Integrated DNA Technologies) gRNA (30nM) complexed with lipofectamine RNAiMAX (ThermoFisher Scientific) for 48 h.

Adenoviral transduction: Fully differentiated BMDMs were incubated with adenovirus particles (AdIRF5 or AdGFP) for 48 h, at MOI 10.

Immunofluorescence

After red blood cells lysis, blood cells were cytospun onto SuperFrost Plus slides. Samples were fixed in 10% formalin (Sigma Aldrich) then stained for CD14 (13-0149-82, Invitrogen) overnight and with the appropriate secondary antibody (Streptavidin AF 647, S32357, ThermoFisher Scientifc). Samples were then permeabilized and stained for IRF5 (10547-1-AP, Proteintech) and OXPHOS (MS604, Abcam) with the appropriate secondary antibodies (goat anti-mouse FITC (A11001) and anti-rabbit AF555 (A21428), Invitrogen). Nuclei were counterstained with Hoescht 33342 (ThermoFisher Scientific). Images were acquired with a confocal microscope (Zeiss LSM 710) and analysed with ImageJ® (Fiji).

Adipose tissue sections were stained for Mac2 (CL8942AP, Cedarlanelabs) overnight and then with the appropriate secondary antibody. Nuclei were counterstained with Hoescht 33342 (ThermoFisher Scientific). Slides were scanned using Zeiss Axio Scan Z1 and Mac2 staining was quantified with Visiopharm.

Quantitative PCR with reverse transcription

RNA was extracted from cells or tissue using RNeasy Plus Mini or Micro kit (Qiagen). Complementary DNA was synthesized with M-MLV Reverse Transcriptase kit (Promega). SYBR Green qRT-PCR reactions were performed with MESA green MasterMix (Eurogentec) and sequence-specific primers (Table S3), using QuantStudio 3 Real-Time PCR Systems (ThermoFisher Scientific). 18S was used for normalization to quantify relative mRNA expression levels.

Western blotting

To extract proteins, cells were lysed in RIPA lysis buffer (Sigma), supplemented with proteases (A32955, ThermoFisher Scientific) and phosphatases inhibitors (1862495, ThermoFisher Scientific). Proteins were separated on NuPAGE 4-12% polyacrylamide gels (ThermoFisher Scientific) and then transferred onto nitrocellulose membranes. Membranes were probed with the appropriate primary (anti-GHITM, 16296-1-AP, Proteintech; anti-Actin, ab8226, Abcam) and secondary antibodies (31430 and 31460, Invitrogen) and visualized with SuperSignal West Pico Substrate (34080, ThermoFisher Scientific). Images were analysed with ImageJ® (Fiji).

Extracellular flux measurements

Real-time extracellular acidification rate (ECAR) and oxygen consumption rate (OCR) were measured using Seahorse XF24 or XFe96 extracellular flux analyser (Agilent). Briefly, cells were differentiated in XF24 or XFe96 cell culture plate (15,000 to 30,000 cells per well). Adipose stromal vascular cells (800,000 cells per well) were seeded in an XFe96 cell culture plate pretreated with CellTak (Corning). $F4/80^+$ and $F4/80^-$ cells were allowed to adhere (180,000 cells per well) overnight in RPMI medium, supplemented with 10% FBS and 1% P/S. Cells were incubated in Seahorse XF base medium supplemented with either 2 mM L-glutamine, 10mM glucose and 1mM sodium pyruvate (pH=7.4) for mitochondrial stress test or only 2 mM L-glutamine (pH=7.4) for glycolysis stress test, for 1 h at 37°C in a non-CO_2 incubator. For palmitate oxidation test, cells were placed in substrate limited medium (DMEM supplemented with 0.5 mM glucose, 1 mM GlutaMAX (Life Technologies), 0.5mM carnitine and 1% FBS) for 24 h. Assay was performed in fatty acid oxidation assay buffer (111mM NaCl, 4.7mM KCl, 1.25 mM $CaCl_2$, 2 mM $MgSO_4$, 1.2 mM NaH_2PO_4, 2.5 mM glucose, 0.5mM carnitine, 5mM Hepes, pH=7.4). Cells were pre-treated with Etomoxir (40µM) and then with palmitate (175µM) before the assay. ECAR and OCR were measured in response to injections of either glucose (10mM), oligomycin (1µM) and 2-deoxyglucose (2-DG) (50mM) for glycolysis stress test or oligomycin (1µM), carbonyl cyanide 4-(trifluoromethoxy) phenylhydrazone (FCCP) (1µM) and rotenone/antimycin A (0.5µM) for mitochondrial stress and palmitate oxidation tests. All compounds were purchased from Sigma-Aldrich. Three measurements were made under basal conditions and after each drug injection. Each measurement cycle had the following time parameters: ‘mix’ 3 min, ‘wait’ 2 min, ‘measure’ 3 min.

Electron microscopy and structural analyses

BMDMs were scraped and fixed in 2 % glutaraldehyde for 2 h at 4°C, postfixed in 1 % Osmium tetroxide for 1 h at 4°C, dehydrated, and embedded in Epon. Samples were then cut using an RMC/MTX ultramicrotome (Elexience), and ultrathin sections (60-80 nm) were mounted on copper grids, contrasted with 8% uranyl acetate and lead citrate, and observed with a Jeol 1200 EX transmission electron microscope (Jeol LTD) equipped with a MegaView II high-resolution transmission electron microscopy camera. Pictures of cells sections were taken at 45000 × magnification. Mitochondria number per section was measured to evaluate mitochondria density. For cristae analysis, mitochondria and cristae were outlined using ImageJ® (Fiji) and both the total length and number of cristae in each mitochondrion was calculated, as previously described[42]. For the analysis of mitochondria dynamics, the long and short axis of each mitochondria, as well as their perimeter and area, were measured. From these values, aspect ratio (major axis/minor axis) and form factor $(perimeter)^2/(4\pi Area)$ were calculated. TEM analyses were performed in triplicate and a minimum of 11 images per sample were taken.

Quantification of TCA metabolites by liquid chromatography coupled to high resolution mass spectrometry (LC-HRMS)

Metabolite extraction. A volume of 170 µL of ultrapure water was added to the frozen cell pellets. At this step, 20µL of each sample were withdrawn for further determining the total protein concentration (colorimetric quantification / Pierce BCA Protein Assay Kit, ThermoFisher Scientific). Then, 10 µL of 11 internal standards at 50 µg/mL were added to the remaining 150 µL of cell lysate: 13C5-alpha-hydroxyglutaric acid, 13C2-phosphoenolpyruvic acid, 13C4-fumaric acid, 13C3-pyruvic acid, 13C4-succinic acid (Merck), and D4-citric acid, 13C5-glutamine, D3-malic acid, 13C4,15N-aspartic-acid, 13C5-alpha-ketoglutaric-acid and13C5-glutamic acid (Eurisotop), followed by a volume of 350 µL of cold methanol. Resulting samples were left on ice for 90 min. After a final centrifugation step at 20,000 g for 15 min at 4°C, supernatants were recovered and dried under a stream of nitrogen using a TurboVap instrument (ThermoFisher Scientific) and stored at -80°C until analysis. Prior to LC-HRMS analysis, dried extracts were dissolved in 100 µL of 40 µL of chromatographic mobile phase A + 60 µL of mobile phase B (see below).

Preparation of calibration standards. Working solution (WS) for calibration curves and quality control solutions were prepared from two separate mother solutions (100 µg/ml in water) of each quantified compound : L-glutamic acid, L-aspartic acid , L-glutamine, succinic acid, alpha-ketoglutaric acid, trans-aconitic acid, L-(-)-malic acid, D,L-isocitric acid, D-glyceric acid, fumaric acid, citric acid, pyruvic acid, D-alpha-hydroxyglutaric acid disodium salt, D-(-)-lactic acid, D-(-)-3-phosphoglyceric acid, phosphoenolpyruvic acid and itaconic acid (all from Sigma). Several diluted solutions of calibration standard solutions (CSS) and quality control solutions (QCS) were prepared by successive two-fold dilutions of WS in ultrapure water. Then, a three-fold dilution in a BSA solution (7200 µg/mL), of each previous diluted solution (CSS1-8 and QCS1-3) was applied to prepare standards for the calibration curve (from 33.33 to 0.26 µg/mL) and quality control (from 53.33 to 1.51 µg/mL). A volume of 350µL of cold methanol was added to each calibration curve and quality control solutions and followed metabolite extraction process.

LC-HRMS analysis. Targeted LC-HRMS experiments were performed using an U3000 liquid chromatography system coupled to a Q Exactive Plus mass spectrometer (ThermoFisher Scientific). The software interface was Xcalibur (version 2.1) (ThermoFisher Scientific). The mass spectrometer was externally calibrated before each analysis in ESI- polarity using the manufacturer's predefined methods and recommended calibration mixture. The LC separation was performed on a Sequant ZIC-pHILIC 5 µm, 2.1 x 150 mm column (HILIC) maintained at 45°C (Merck, Darmstadt, Germany). Mobile phase A consisted of an aqueous buffer of 10 mM of ammonium acetate, and mobile phase B of 100% acetonitrile. Chromatographic elution was achieved with a flow rate of 200 µL/min. After injection of 10 µL of sample, elution started with an isocratic step of 2 min at 70% B, followed by a linear gradient from 70 to 40% of phase B from 2 to 7 min. The chromatographic system was then rinsed for 5 min at 0% phase B, and the run was ended with an equilibration step of 9 min. The column effluent was directly introduced into the electrospray source of the mass spectrometer, and analyses were performed in the negative ion mode. The Q Exactive Plus mass spectrometer was operated with capillary voltage set at −2.5 kV and a capillary temperature set at 350°C. The sheath gas pressure and the auxiliary gas pressure (nitrogen) were set at 60 and 10 arbitrary units, respectively. The detection was achieved from m/z 50 to 600 in the negative ion mode and at

a resolution of 70,000 at m/z 200 (full width at half maximum). All metabolites were detected as their deprotonated [M-H]- species.

Succinic acid, glyceric acid, itaconic acid, and lactic acid were detected at m/z 117.01933 (retention time (rt): 4.50 min); 105.01933 (rt 3.20 min); 129.01933 (rt 3.73 min); 89.02441 (rt 2.40 min), respectively; and quantified using 13C4-succinic acid (m/z 121.03251) as internal standard (ISTD). Malic acid and aconitic acid were monitored at m/z 133.01424 (rt 6.70 min); 173.0091 (rt 7.15 min), respectively; and quantified with D3-malic acid (m/z 136.03276). Citric acid, isocitric acid and 3-phospho glyceric acid were monitored at m/z 191.01944 (rt 7.80); 191.01952 (rt 8.35); 184.98566 (rt 7.70 min) respectively; and quantified with D4-citric acid (m/z 195.04455). Pyruvic acid (m/z 87.00876, rt 2.25 min), aspartic acid (m/z 132.03023, rt 5,20 min), glutamine (m/z 145.06186, rt 4.75 min), glutamic acid (m/z 146.04588 rt 4.80 min), alpha-hydroxyglutaric acid (m/z 147.02989, rt 6.20 min), alpha-ketoglutaric acid (m/z 152.04637, rt 6.50 min), fumaric acid (m/z 150.03072, rt 7.05 min), and phosphoenolpyruvc acid (m/z 166.97509, rt 8.20 min) were all quantified with their isotopically labeled homologues (see above).

Metabolomic data processing and quantification. Xcalibur software was used for peak detection and integration. Metabolite quantification was perform using calibration curves established from peak area ratios between metabolites and their respective internal standard. Each metabolite amount was normalised by the protein quantity measured in each sample by BCA assay.

RNA-sequencing of BMDMs and F4/80^{+} ATMs

After extraction, total RNA was analysed using Agilent RNA 6000 Pico Kit on the Agilent 2100 Bioanalyzer System. RNA quality was estimated based on capillary electrophoresis profiles using the RNA Integrity Number (RIN) and DV200 values. RNA sequencing libraries were prepared using the SMARTer Stranded Total RNA-Seq Kit v2 - Pico Input Mammalian (Clontech/Takara) from 10ng of total RNA. This protocol includes a first step of RNA fragmentation using a proprietary fragmentation mix at 94°C. The time of incubation was set up for all samples at 4 min, based on the RNA quality, and according to the manufacturer's recommendations. After fragmentation, indexed cDNA synthesis and amplification were performed followed with a ribodepletion step using probes targeting mammalian rRNAs. PCR amplification was finally achieved on ribodepleted cDNAs, using 12 cycles estimated in accordance to the input quantity of total RNA. Library quantification and quality assessment were performed using Qubit fluorometric assay (Invitrogen) with dsDNA HS (High Sensitivity) Assay Kit and LabChip GX Touch using a High Sensitivity DNA chip (Perkin Elmer). Libraries were then equimolarly pooled and quantified by qPCR using the KAPA library quantification kit (Roche). Sequencing was carried out using a pair-end 2 x 100 bp mode on the NovaSeq 6000 system (Illumina), targeting between 10 and 15M clusters per sample.

STAR v2.7.3a (Spliced Transcripts Alignment To a Reference) was used to align reads to the mouse mm10 genome and generate raw counts[43]. We processed normalization and differential expression gene analysis with DESeq2[44]. Pathway enrichment analyses were performed using clusterProfiler[45] with differentially expressed genes (abs(log2FoldChange) > 1.3 and/or adj p-value < 0.05).

RNA-sequencing of IRF5$^{+/-}$ human monocytes

Complementary DNA libraries and RNA sequencing Library preparation and Illumina sequencing were performed at the *Ecole Normale Supérieure* genomic core facility (Paris,

France). 20 ng of total RNA were amplified and converted to cDNA using SMART-Seq v4 Ultra Low Input RNA kit (Clontech). Afterwards an average of 150 pg of amplified cDNA was used to prepare library following Nextera XT DNA kit (Illumina). Libraries were multiplexed by 12 on a high-output flowcells. A 75 bp read sequencing was performed on a NextSeq 500 device (Illumina). A mean of 38,9 ± 8 million passing Illumina quality filter reads was obtained for each of the 12 samples.

The analyses were performed using the Eoulsan pipeline[46], including read filtering, mapping, alignment filtering, read quantification, normalisation and differential analysis: Before mapping, poly N read tails were trimmed, reads ≤40 bases were removed, and reads with quality mean ≤30 were discarded. Reads were then aligned against the hg19 genome from Ensembl version 91 using STAR (version 2.5.2b)[47]. Alignments from reads matching more than once on the reference genome were removed using Java version of samtools[47]. To compute gene expression, hg19 GTF genome annotation version 91 from Ensembl database was used. All overlapping regions between alignments and referenced exons were counted and aggregated by genes using HTSeq-count 0.5.3[48]. The sample counts were normalized using DESeq2 1.8.1[44]. Statistical treatments and differential analyses were also performed using DESeq2 1.8.1.

Statistics

Data analysis were performed using Microsoft Excel for Mac 16.47. Statistical analysis was performed using a two-tailed t-test for two groups, an ordinary one-way ANOVA followed by Tukey's multiple-comparisons test for multiple groups and a two-way ANOVA followed by Bonferroni's multiple comparison test on Prism 9 for macOS (GraphPad). Correlative analyses were performed on Prism 9 for macOS, computing Pearson coefficients for normally distributed data or Spearman coefficients for non-normally distributed data (GraphPad). PCA analyses were carried out on Prism 9 for macOS. Trajectory-resolved clustering was carried out on the Orange (v. 3.28.0) Python toolbox[49]. Statistical approaches per data panel are detailed in figure legends.

Public data

Single cell sequencing data: Murine single cell sequencing data from Jaitin *et al.*[12], were downloaded and treated using BioTuring BBrowser (v. 2.7.48)[50]. Data were filtered in BBrowser and exported in tabular format for subsequent treatment with Microsoft Excel for Mac and Prism9 for macOS. Human single cell sequencing data were retrieved from GSE156110 raw data[32]. Clustering was performed according to authors' instructions and IRF5 and GHITM expressions were analysed in all macrophages and monocytes, according to their lean/obese status.

UCSC genome browser: Gene tracks in Fig. 6E were visualised with the UCSC genome browser *http://genome.ucsc.edu*[51,52], using the track hubs[53]. JASPAR2020 was used to visualise transcription factor binding sites[54]. The BLUEPRINT track-set was used for RNA expression and H3K27Ac lines[55,56]. Sample lines and tracks available through this session link / live link. The Human Dec. 2013 (GRCh38/hg38) assembly was used[57,58].

Data availability: RNA-sequencing of IRF5$^{+/-}$ human monocytes: RNA-Seq gene expression data and raw fastq files will be made available on the GEO repository (www.ncbi.nlm.nih.gov/geo/) under accession number: GSE176216 (GSM5360191-4 and GSM5360167-70 not included in this study). Source data will be provided with the accepted manuscript.

REFERENCES

1. O'Neill, L. A. J., Kishton, R. J. & Rathmell, J. A guide to immunometabolism for immunologists. *Nat. Rev. Immunol.* **16**, 553–565 (2016).
2. Li, C. *et al.* HIF1α-dependent glycolysis promotes macrophage functional activities in protecting against bacterial and fungal infection. *Sci. Rep.* **8**, 3603 (2018).
3. Mills, E. L. *et al.* Succinate Dehydrogenase Supports Metabolic Repurposing of Mitochondria to Drive Inflammatory Macrophages. *Cell* **167**, 457-470.e13 (2016).
4. Van den Bossche, J. *et al.* Mitochondrial Dysfunction Prevents Repolarization of Inflammatory Macrophages. *Cell Rep.* **17**, 684–696 (2016).
5. Wculek, S. K., Dunphy, G., Heras-Murillo, I., Mastrangelo, A. & Sancho, D. Metabolism of tissue macrophages in homeostasis and pathology. *Cell. Mol. Immunol.* (2021) doi:10.1038/s41423-021-00791-9.
6. Angelin, A. *et al.* Foxp3 Reprograms T Cell Metabolism to Function in Low-Glucose, High-Lactate Environments. *Cell Metab.* **25**, 1282-1293.e7 (2017).
7. Serbulea, V. *et al.* Macrophage phenotype and bioenergetics are controlled by oxidized phospholipids identified in lean and obese adipose tissue. *Proc. Natl. Acad. Sci. U. S. A.* **115**, E6254–E6263 (2018).
8. Boutens, L. *et al.* Unique metabolic activation of adipose tissue macrophages in obesity promotes inflammatory responses. *Diabetologia* **61**, 942–953 (2018).
9. Enhanced glycolysis and HIF-1α activation in adipose tissue macrophages sustains local and systemic interleukin-1β production in obesity | Scientific Reports. https://www-nature-com.proxy.insermbiblio.inist.fr/articles/s41598-020-62272-9.
10. Hill, D. A. *et al.* Distinct macrophage populations direct inflammatory versus physiological changes in adipose tissue. *Proc. Natl. Acad. Sci. U. S. A.* **115**, E5096–E5105 (2018).
11. Sárvári, A. K. *et al.* Plasticity of Epididymal Adipose Tissue in Response to Diet-Induced Obesity at Single-Nucleus Resolution. *Cell Metab.* **33**, 437-453.e5 (2021).
12. Jaitin, D. A. *et al.* Lipid-Associated Macrophages Control Metabolic Homeostasis in a Trem2-Dependent Manner. *Cell* **178**, 686-698.e14 (2019).
13. Coats, B. R. *et al.* Metabolically Activated Adipose Tissue Macrophages Perform Detrimental and Beneficial Functions during Diet-Induced Obesity. *Cell Rep.* **20**, 3149–3161 (2017).
14. Brunner, J. S. *et al.* The PI3K pathway preserves metabolic health through MARCO-dependent lipid uptake by adipose tissue macrophages. *Nat. Metab.* **2**, 1427–1442 (2020).
15. Weisberg, S. P. *et al.* Obesity is associated with macrophage accumulation in adipose tissue. *J. Clin. Invest.* **112**, 1796–1808 (2003).
16. Lee, Y. S. *et al.* Inflammation is necessary for long-term but not short-term high-fat diet-induced insulin resistance. *Diabetes* **60**, 2474–2483 (2011).
17. Dalmas, E. *et al.* Irf5 deficiency in macrophages promotes beneficial adipose tissue expansion and insulin sensitivity during obesity. *Nat. Med.* **21**, 610–618 (2015).
18. Hedl, M., Yan, J., Witt, H. & Abraham, C. IRF5 Is Required for Bacterial Clearance in Human M1-Polarized Macrophages, and IRF5 Immune-Mediated Disease Risk Variants Modulate This Outcome. *J. Immunol. Baltim. Md 1950* **202**, 920–930 (2019).
19. Yanai, H. *et al.* Role of IFN regulatory factor 5 transcription factor in antiviral immunity and tumor suppression. *Proc. Natl. Acad. Sci. U. S. A.* **104**, 3402–3407 (2007).
20. Krausgruber, T. *et al.* IRF5 promotes inflammatory macrophage polarization and TH1-TH17 responses. *Nat. Immunol.* **12**, 231–238 (2011).
21. Weiss, M. *et al.* IRF5 controls both acute and chronic inflammation. *Proc. Natl. Acad. Sci. U. S. A.* **112**, 11001–11006 (2015).
22. Hedl, M., Yan, J. & Abraham, C. IRF5 and IRF5 Disease-Risk Variants Increase Glycolysis and Human M1 polarization By Regulating Proximal Signaling and Akt2 Activation. *Cell Rep.* **16**, 2442–2455 (2016).

23. Oka, T. *et al.* Identification of a novel protein MICS1 that is involved in maintenance of mitochondrial morphology and apoptotic release of cytochrome c. *Mol. Biol. Cell* **19**, 2597–2608 (2008).
24. Reers, M. *et al.* Mitochondrial membrane potential monitored by JC-1 dye. *Methods Enzymol.* **260**, 406–417 (1995).
25. Bassaganya-Riera, J., Misyak, S., Guri, A. J. & Hontecillas, R. PPAR gamma is highly expressed in F4/80(hi) adipose tissue macrophages and dampens adipose-tissue inflammation. *Cell. Immunol.* **258**, 138–146 (2009).
26. Nomura, M. *et al.* Fatty acid oxidation in macrophage polarization. *Nat. Immunol.* **17**, 216–217 (2016).
27. Cao, T. *et al.* Fatty Acid Oxidation Promotes Cardiomyocyte Proliferation Rate but Does Not Change Cardiomyocyte Number in Infant Mice. *Front. Cell Dev. Biol.* **7**, 42 (2019).
28. Weihrauch, D. *et al.* An IRF5 Decoy Peptide Reduces Myocardial Inflammation and Fibrosis and Improves Endothelial Cell Function in Tight-Skin Mice. *PloS One* **11**, e0151999 (2016).
29. Grist, J. T. *et al.* Extracellular Lactate: A Novel Measure of T Cell Proliferation. *J. Immunol. Baltim. Md 1950* **200**, 1220–1226 (2018).
30. Noe, J. T. *et al.* Lactate supports a metabolic-epigenetic link in macrophage polarization. *Sci. Adv.* **7**, eabi8602.
31. Saliba, D. G. *et al.* IRF5:RelA Interaction Targets Inflammatory Genes in Macrophages. *Cell Rep.* **8**, 1308–1317 (2014).
32. Hildreth, A. D. *et al.* Single-cell sequencing of human white adipose tissue identifies new cell states in health and obesity. *Nat. Immunol.* **22**, 639–653 (2021).
33. Seitaj, B. *et al.* Transmembrane BAX Inhibitor-1 Motif Containing Protein 5 (TMBIM5) Sustains Mitochondrial Structure, Shape, and Function by Impacting the Mitochondrial Protein Synthesis Machinery. *Cells* **9**, 2147 (2020).
34. Albers, G. J. *et al.* IRF5 regulates airway macrophage metabolic responses. *Clin. Exp. Immunol.* **204**, 134–143 (2021).
35. Shimobayashi, M. *et al.* Insulin resistance causes inflammation in adipose tissue. *J. Clin. Invest.* **128**, 1538–1550 (2018).
36. Young, A., Oldford, C. & Mailloux, R. J. Lactate dehydrogenase supports lactate oxidation in mitochondria isolated from different mouse tissues. *Redox Biol.* **28**, 101339 (2020).
37. Mitochondrial lactate metabolism: history and implications for exercise and disease - Glancy - 2021 - The Journal of Physiology - Wiley Online Library. https://physoc.onlinelibrary.wiley.com/doi/10.1113/JP278930.
38. Zezina, E. *et al.* Mitochondrial fragmentation in human macrophages attenuates palmitate-induced inflammatory responses. *Biochim. Biophys. Acta Mol. Cell Biol. Lipids* **1863**, 433–446 (2018).
39. Kapetanovic, R. *et al.* Lipopolysaccharide promotes Drp1-dependent mitochondrial fission and associated inflammatory responses in macrophages. *Immunol. Cell Biol.* **98**, 528–539 (2020).
40. Nagel, J. E. *et al.* Identification of genes differentially expressed in T cells following stimulation with the chemokines CXCL12 and CXCL10. *BMC Immunol.* **5**, 17 (2004).
41. Moni, M. A. & Liò, P. Network-based analysis of comorbidities risk during an infection: SARS and HIV case studies. *BMC Bioinformatics* **15**, 333 (2014).
42. Sood, A. *et al.* A Mitofusin-2-dependent inactivating cleavage of Opa1 links changes in mitochondria cristae and ER contacts in the postprandial liver. *Proc. Natl. Acad. Sci. U. S. A.* **111**, 16017–16022 (2014).
43. Dobin, A. *et al.* STAR: ultrafast universal RNA-seq aligner. *Bioinforma. Oxf. Engl.* **29**, 15–21 (2013).
44. Love, M. I., Huber, W. & Anders, S. Moderated estimation of fold change and dispersion for RNA-seq data with DESeq2. *Genome Biol.* **15**, 550 (2014).

45. Yu, G., Wang, L.-G., Han, Y. & He, Q.-Y. clusterProfiler: an R package for comparing biological themes among gene clusters. *Omics J. Integr. Biol.* **16**, 284–287 (2012).
46. Jourdren, L., Bernard, M., Dillies, M.-A. & Le Crom, S. Eoulsan: a cloud computing-based framework facilitating high throughput sequencing analyses. *Bioinforma. Oxf. Engl.* **28**, 1542–1543 (2012).
47. Li, H. *et al.* The Sequence Alignment/Map format and SAMtools. *Bioinforma. Oxf. Engl.* **25**, 2078–2079 (2009).
48. Anders, S., Pyl, P. T. & Huber, W. HTSeq--a Python framework to work with high-throughput sequencing data. *Bioinforma. Oxf. Engl.* **31**, 166–169 (2015).
49. Orange: data mining toolbox in python: The Journal of Machine Learning Research: Vol 14, No 1. https://dl.acm.org/doi/10.5555/2567709.2567736.
50. BBrowser: Making single-cell data easily accessible | bioRxiv. https://www.biorxiv.org/content/10.1101/2020.12.11.414136v1.
51. Kent, W. J. *et al.* The human genome browser at UCSC. *Genome Res.* **12**, 996–1006 (2002).
52. Navarro Gonzalez, J. *et al.* The UCSC Genome Browser database: 2021 update. *Nucleic Acids Res.* **49**, D1046–D1057 (2021).
53. Raney, B. J. *et al.* Track data hubs enable visualization of user-defined genome-wide annotations on the UCSC Genome Browser. *Bioinforma. Oxf. Engl.* **30**, 1003–1005 (2014).
54. Fornes, O. *et al.* JASPAR 2020: update of the open-access database of transcription factor binding profiles. *Nucleic Acids Res.* **48**, D87–D92 (2020).
55. Fernández, J. M. *et al.* The BLUEPRINT Data Analysis Portal. *Cell Syst.* **3**, 491-495.e5 (2016).
56. Adams, D. *et al.* BLUEPRINT to decode the epigenetic signature written in blood. *Nat. Biotechnol.* **30**, 224–226 (2012).
57. Lander, E. S. *et al.* Initial sequencing and analysis of the human genome. *Nature* **409**, 860–921 (2001).
58. Kent, W. J. & Haussler, D. Assembly of the working draft of the human genome with GigAssembler. *Genome Res.* **11**, 1541–1548 (2001).

Figure 1

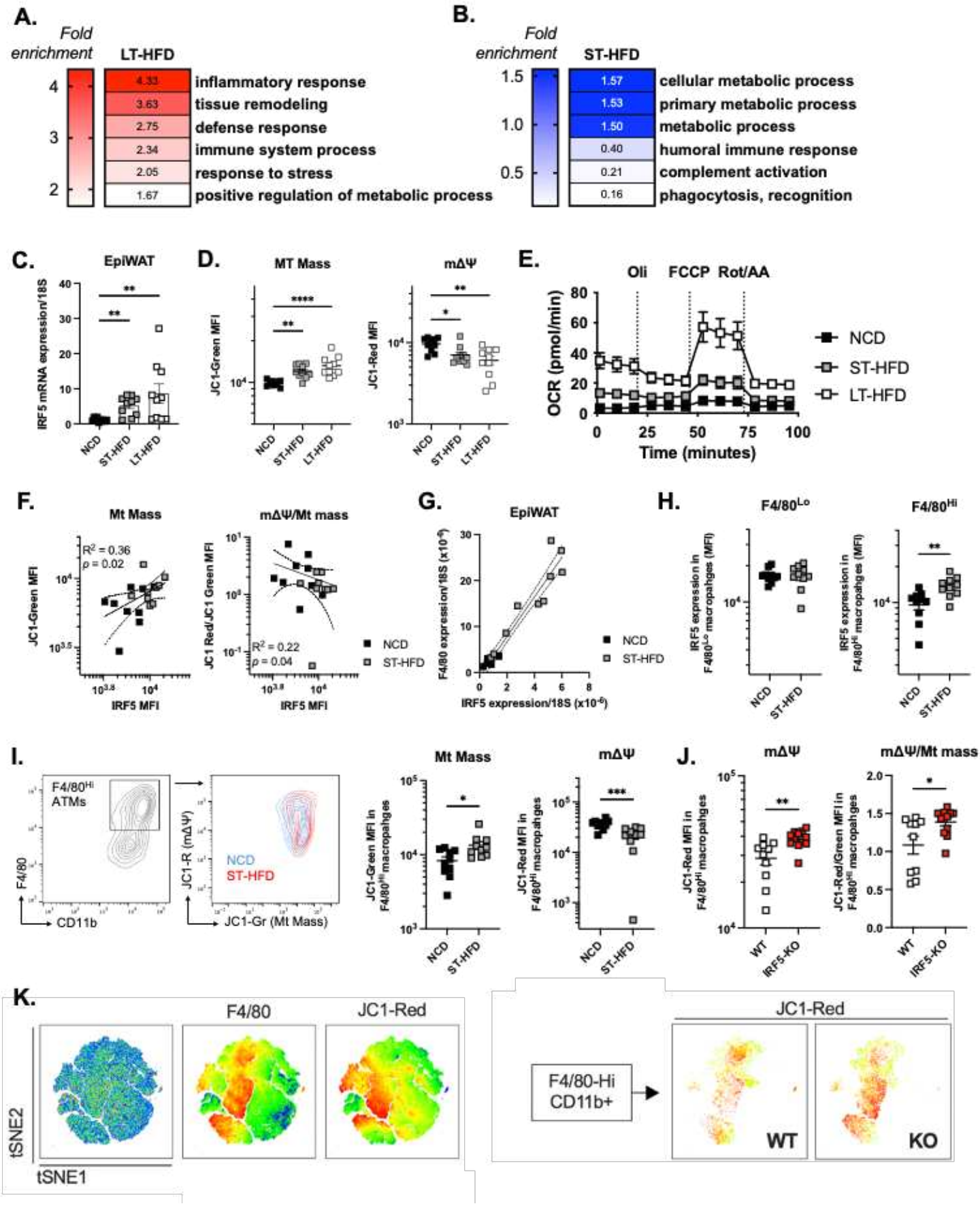
A.
Fold enrichment
LT-HFD
4.33
3.63
2.75
2.34
2.05
1.67
inflammatory response
tissue remodeling
defense response
immune system process
response to stress
positive regulation of metabolic process
B.
Fold enrichment
ST-HFD
1.57
1.53
1.50
0.40
0.21
0.16
cellular metabolic process
primary metabolic process
metabolic process
humoral immune response
complement activation
phagocytosis, recognition
C.
EpiWAT
IRF5 mRNA expression/18S
NCD
ST-HFD
LT-HFD
D.
MT Mass
JC1-Green MFI
mΔΨ
JC1-Red MFI
E.
Oli
FCCP
Rot/AA
OCR (pmol/min)
Time (minutes)
NCD
ST-HFD
LT-HFD
F.
Mt Mass
JC1-Green MFI
IRF5 MFI
R² = 0.36
p = 0.02
mΔΨ/Mt mass
JC1 Red/JC1 Green MFI
R² = 0.22
p = 0.04
G.
EpiWAT
F4/80 expression/18S (x10⁻⁶)
IRF5 expression/18S (x10⁻⁶)
H.
F4/80Lo
F4/80Hi
IRF5 expression in F4/80Lo macropahges (MFI)
IRF5 expression in F4/80Hi macropahges (MFI)
I.
F4/80Hi ATMs
F4/80
CD11b
JC1-R (mΔΨ)
JC1-Gr (Mt Mass)
Mt Mass
mΔΨ
JC1-Green MFI in F4/80Hi macropahges
JC1-Red MFI in F4/80Hi macropahges
J.
mΔΨ
mΔΨ/Mt mass
JC1-Red MFI in F4/80Hi macropahges
JC1-Red/Green MFI in F4/80Hi macropahges
WT
IRF5-KO
K.
F4/80
JC1-Red
tSNE2
tSNE1
F4/80-Hi CD11b+
JC1-Red
WT
KO

FIGURE 1. IRF5 expression is associated with ATM metabolic adaptation to short-term caloric excess.

A. Wild-type (WT) mice and mice with a myeloid-deficiency of IRF5 (IRF5-KO) were placed on a 12-week long-term (LT-) high-fat diet (HFD). F4/80^{+} adipose tissue macrophages (ATMs) were sorted from epididymal fat pads (EpiWAT) for RNA sequencing (RNA-seq). Differentially expressed genes (-log10 p > 1.3) between genotypes were used for gene ontology (GO) term enrichment. Heatmaps represent fold-enrichment (n=4 per genotype; *p* values in Fig. S1B).

B. WT and IRF5-KO mice were placed on a 4-week short-term (ST-)HFD. F4/80^{+} ATMs were sorted from EpiWAT for RNA-seq. Differentially expressed genes (-log10 *p* > 1.3) between genotypes were used for GO term enrichment. Heatmaps represent fold-enrichment (n=4 per genotype; *p* values in Fig. S1B).

C. IRF5 mRNA expression in EpiWAT from C57BL/6J mice on a normal chow diet (NCD), ST-HFD or LT-HFD (n=10 per group; Kruskal-Wallis multiple comparisons, left-to-right **p=0,0063; **p=0,0015).

D. JC1-Green and JC1-Red median fluorescence intensity (MFI) to assess mitochondrial mass (MT Mass) and mitochondrial membrane potential (mΔΨ), respectively in F4/80^{+} CD11b^{+} ATMs from EpiWAT of C57BL/6J mice on NCD, ST-HFD or LT-HFD (n=10 per group in NCD and ST-HFD; n= 7 in LT-HFD; One way ANOVA, left-to-right **p=0.0079; ****p<0.0001).

E. Oxygen consumption rate (OCR) from extracellular flux analysis performed on F4/80^{+} magnetically sorted ATMs from EpiWAT of C57BL/6J mice on NCD, ST-HFD or LT-HFD. Cells were treated with Oligomycin (Oli), carbonyl cyanide 4-(trifluoromethoxy) phenylhydrazone (FCCP) and Rotenone/Antimycin A (Rot/AA) (n=4 in NCD, n=9 in ST-HFD and n=8 in LT-HFD).

F. Correlative analyses between IRF5 MFI and JC1-Green MFI (Mt Mass) (Linear regression, Pearson correlation R^2 = 0.36; p = 0.02) and JC1-Red MFI/JC1-Green MFI (mΔΨ/Mt Mass ratio) (R^2 = 0.22; p = 0.04) in EpiWAT F4/80^{+} CD11b^{+} ATMs of C57BL/6J mice on NCD or ST-HFD (n=9 per group).

G. Correlative analysis between IRF5 and F4/80 mRNA expressions, normalized to 18S expression, in the EpiWAT of C57BL/6J mice on NCD or ST-HFD (n=10 per group)

H. IRF5 MFI in EpiWAT F4/80^{Lo} and F4/80^{Hi} macrophages of C57BL/6J mice on NCD or ST-HFD (n=10 per group, unpaired t-test, **p=0.004).

I. Overlay flow cytometry contour plot of JC1-Green and JC1-Red fluorescence in F4/80^{Hi} ATMs of C57BL/6J on NCD or ST-HFD. MFI of JC1-Green and JC1-Red fluorescence, respectively markers of Mt Mass and mΔΨ, in EpiWAT F4/80^{Hi} ATMs of C57BL/6J mice on NCD or ST-HFD (n=10 mice per group, unpaired t-tests, *p=0.01 and ***p=0.0009).

J. MFI of JC1-Red and mΔΨ/Mt Mass ratio in F4/80^{Hi} EpiWAT macrophages of WT and IRF5-KO mice on ST-HFD (n=10 for WT and 12 for IRF5-KO, unpaired t-tests, **p=0.0032 and *p=0.019).

K. tSNE plot of F4/80 and JC1-Red MFI profiles of the stromal vascular fraction of EpiWAT, tSNE plot of JC1-Red MFI on F4/80^{Hi} CD11b^{+} gated populations of WT and IRF5-KO mice on ST-HFD.

Data are presented as mean ± SEM.

909

Figure 2

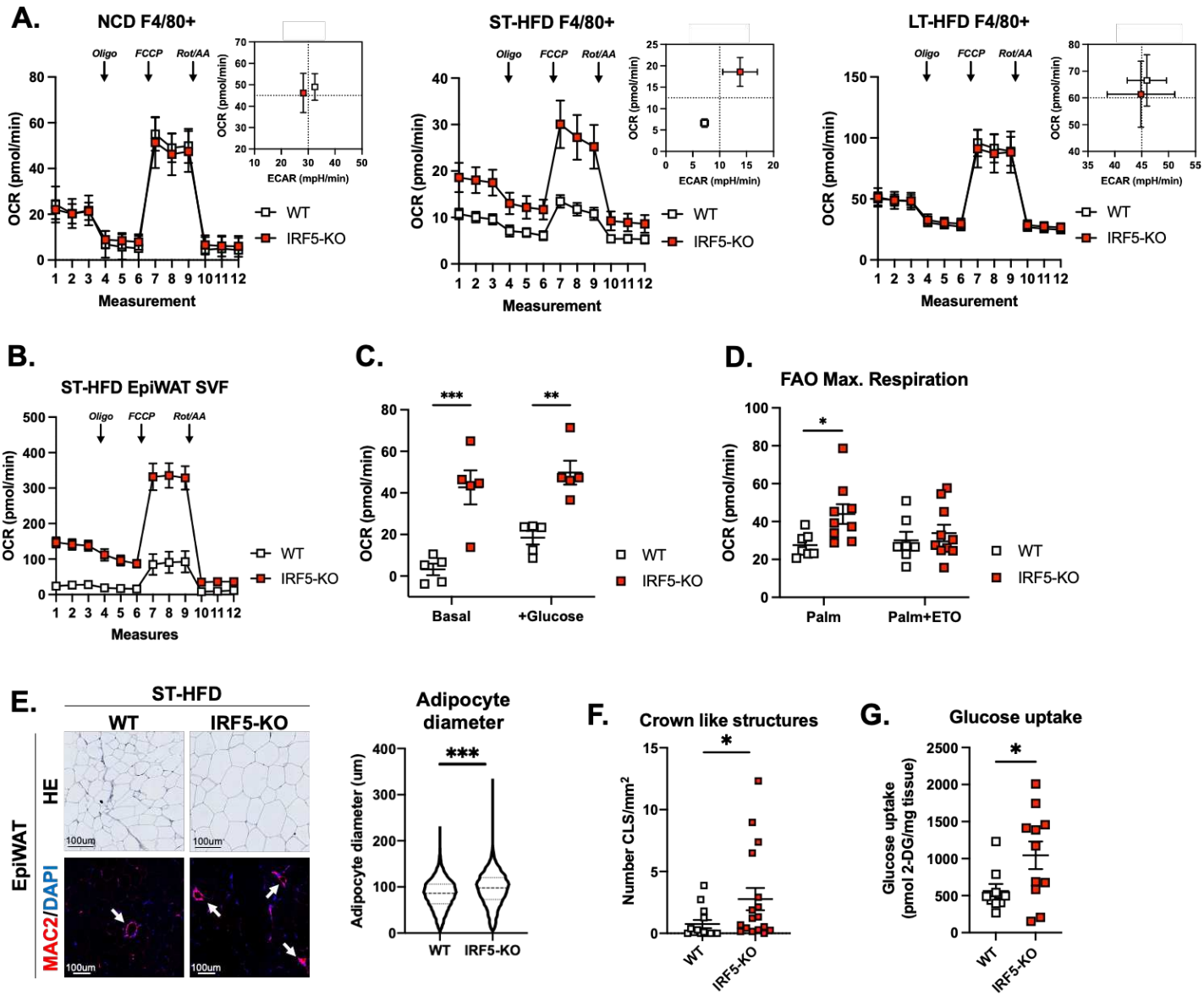
A.
NCD F4/80+
ST-HFD F4/80+
LT-HFD F4/80+
Oligo
FCCP
Rot/AA
OCR (pmol/min)
ECAR (mpH/min)
Measurement
WT
IRF5-KO
B.
ST-HFD EpiWAT SVF
Measures
C.
Basal
+Glucose
D.
FAO Max. Respiration
Palm
Palm+ETO
E.
ST-HFD
WT
IRF5-KO
EpiWAT
HE
MAC2/DAPI
100um
Adipocyte diameter
Adipocyte diameter (um)
F.
Crown like structures
Number CLS/mm2
G.
Glucose uptake
Glucose uptake (pmol 2-DG/mg tissue)

Figure 2. Increased mitochondrial respiration in IRF5-deficient macrophages alters adipose tissue phenotype and function upon short-term high-fat diet

A. Oxygen consumption rate (OCR) from extracellular flux analysis, following Oligomycin (Oli), carbonyl cyanide 4-(trifluoromethoxy) phenylhydrazone (FCCP) and Rotenone/Antimycin A (Rot/AA) treatments, from epididymal white adipose tissue (EpiWAT) magnetically sorted $F4/80^+$ cells from WT and IRF5-KO mice on normal chow diet (NCD; left), short-term (ST-) high-fat diet (HFD; middle) and long-term (LT-)HFD (right). Energetic plot with Extracellular acidification rate (ECAR) and OCR from maximal respiration (n=4 mice per genotype for NCD, n=6 WT and 8 IRF5-KO mice for ST-HFD and n=5 WT and 4 IRF5-KO mice for LT-HFD).

B. OCR from extracellular flux analysis, following Oligo, FCCP and Rot/AA treatments, from EpiWAT stromal vascular fraction (SVF) of WT and IRF5-KO mice on ST-HFD (n=5 mice per genotype).

C. OCR from extracellular flux analysis under basal conditions and following addition of glucose, performed on the EpiWAT SVF of WT and IRF5-KO mice on ST-HFD (n=5 mice per genotype, ***p= 0.0002 and **p=0.0018 two-way ANOVA).

D. Maximal OCR from Fig. S4B of fatty acid oxidation (FAO) test on EpiWAT SVF from WT (n=7) and IRF5-KO (n=9) mice on ST-HFD (*p=0.035, one-way ANOVA). Palm, palmitate; ETO, etomoxir.

E. Representative images of hematoxylin and eosin (HE) staining for adipocyte size and MAC2/DAPI immunostaining to visualize crown-like structures (white arrows), on EpiWAT sections of WT and IRF5-KO mice on ST-HFD (scale bar=100um). Right: adipocyte size quantification on the HE staining (3 sections per mouse, n=21 WT and 24 IRF5-KO mice, unpaired t-test, ***p<0.0001).

F. Crown-like structure quantification on MAC2/DAPI immunostained EpiWAT sections of WT and IRF5-KO mice on ST-HFD (n=14 WT and 17 IRF5-KO mice, unpaired t-test, *p=0.0472).

G. Glucose uptake assay performed on EpiWAT explants from WT and IRF5-KO mice on ST-HFD (n=8 WT and 11 IRF5-KO mice, unpaired t-test, p=0.0560).

Data are presented as mean ± SEM.

938

Figure 3

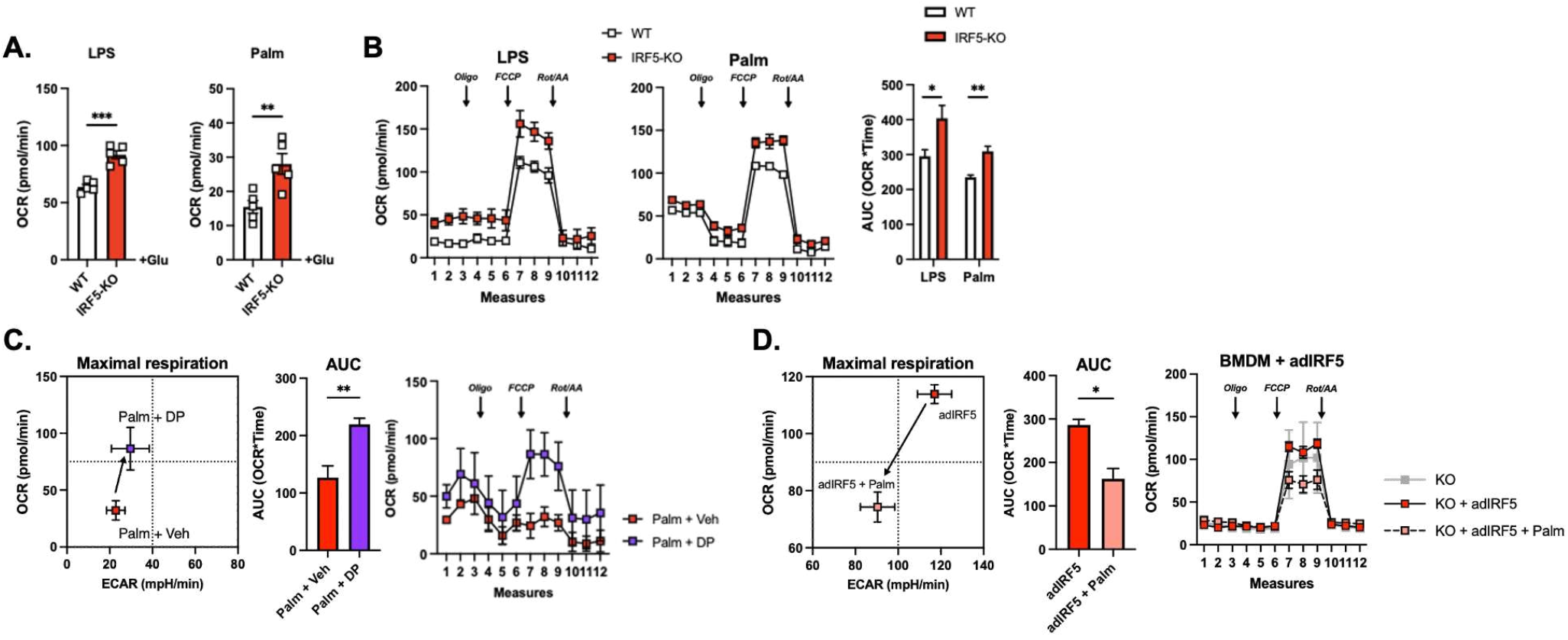
A.
LPS
Palm
OCR (pmol/min)
***
**
+Glu
WT
IRF5-KO
B
WT
IRF5-KO
LPS
Palm
Oligo
FCCP
Rot/AA
Measures
AUC (OCR *Time)
*
**
C.
Maximal respiration
Palm + DP
Palm + Veh
ECAR (mpH/min)
AUC
Palm + Veh
Palm + DP
D.
Maximal respiration
adIRF5
adIRF5 + Palm
AUC
BMDM + adIRF5
KO
KO + adIRF5
KO + adIRF5 + Palm

Figure 3. IRF5-deficient hyperoxidative phenotype is cell intrinsic, inducible and reversible in mature bone marrow-derived macrophages

BMDMs from WT and IRF5-KO mice were treated with lipopolysaccharides (LPS) or palmitate (Palm) for 24 hours.

A. Oxygen consumption rate (OCR) following addition of glucose (Glu) from extracellular flux analysis in Fig. S5A. (LPS ***p=0.0001 and Palm **p=0.008, unpaired t-tests) (n=5 per genotype).

B. OCR from extracellular flux analysis with following oligomycin (Oli), carbonyl cyanide 4-(trifluoromethoxy) phenylhydrazone (FCCP) and Rotenone/Antimycin A (Rot/AA) treatments (left) and area under the curve (AUC) (right) (n=3 per genotype; *p=0.03 and **p=0.0027 unpaired t-test).

C. BMDMs from C57BL/6J mice were treated with an IRF5-decoy peptide (DP) or a vehicle (Veh) and with palmitate (Palm). Energetic plot (left) of maximal respiration from extracellular flux analysis (right) and AUC (middle) (n=3 per condition, unpaired t-test, **p=0.0022).

D. BMDMs from IRF5-KO mice were transfected with an IRF5 adenovirus (adIRF5) and treated with palmitate. Energetic plot (left) of maximal respiration from mitochondrial stress test (right) and AUC (middle) (n=3 for KO + adIRF5 and KO + adIRF5 + Palm; n=2 for KO, unpaired t-test between KO + adIRF5 and KO + adIRF5 + Palm, *p=0.01).

Data are presented as mean ± SEM.

Figure 4

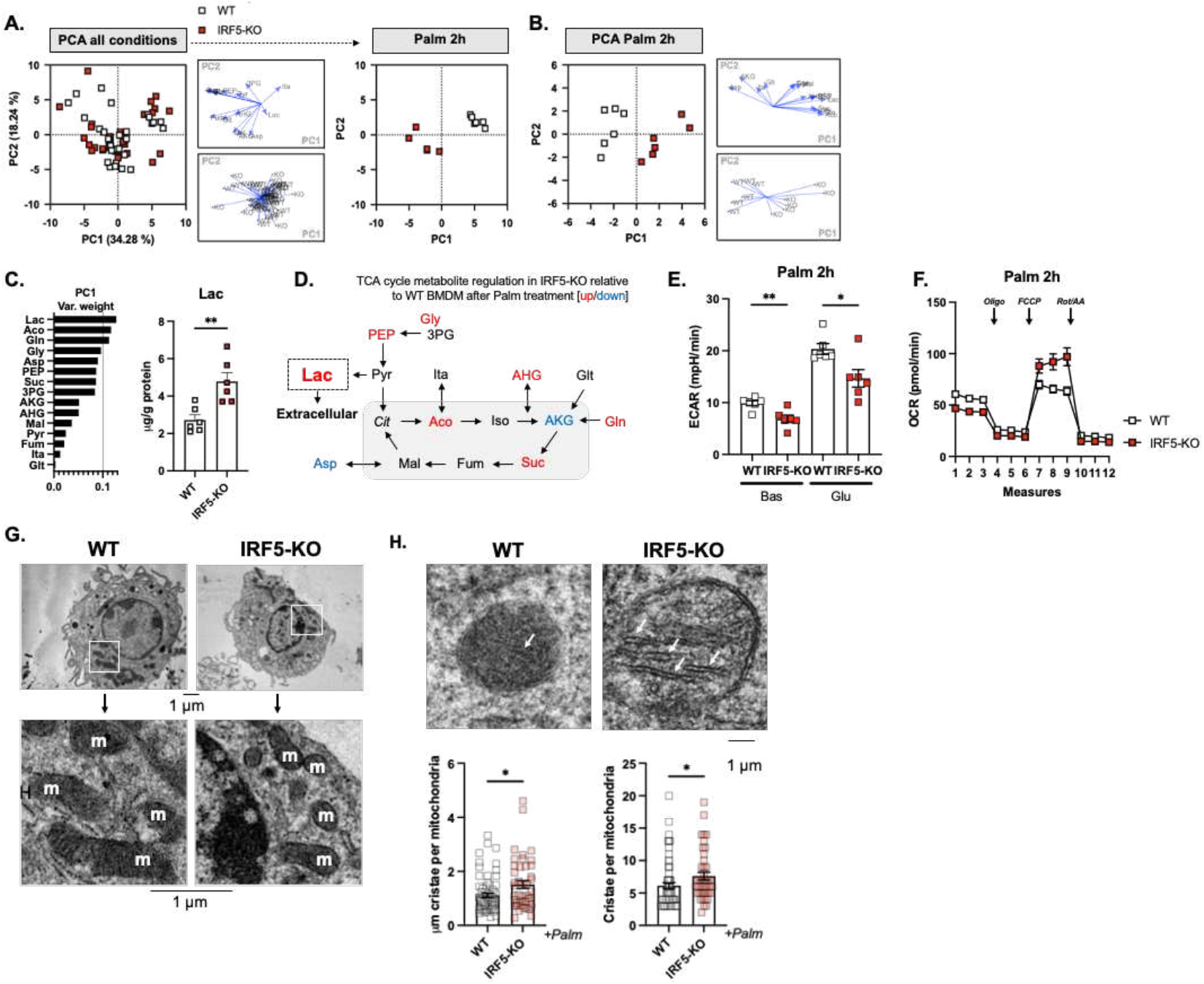
A.
WT
IRF5-KO
PCA all conditions
Palm 2h
PC2 (18.24 %)
PC1 (34.28 %)
PC2
PC1
B.
PCA Palm 2h
C.
PC1
Var. weight
Lac
Aco
Gln
Gly
Asp
PEP
Suc
3PG
AKG
AHG
Mal
Pyr
Fum
Ita
Glt
Lac
µg/g protein
WT
IRF5-KO
D.
TCA cycle metabolite regulation in IRF5-KO relative to WT BMDM after Palm treatment [up/down]
Gly
PEP
3PG
Lac
Pyr
Ita
AHG
Glt
Extracellular
Cit
Aco
Iso
AKG
Gln
Asp
Mal
Fum
Suc
E.
Palm 2h
ECAR (mpH/min)
WT IRF5-KO WT IRF5-KO
Bas
Glu
F.
Palm 2h
Oligo
FCCP
Rot/AA
OCR (pmol/min)
Measures
WT
IRF5-KO
G.
WT
IRF5-KO
1 µm
m
H.
WT
IRF5-KO
1 µm
µm cristae per mitochondria
Cristae per mitochondria
+Palm

Figure 4. IRF5-KO alters TCA cycle metabolite concentrations and mitochondrial structural components in macrophages in response to lipotoxicity

Bone marrow-derived macrophages (BMDMs) from WT and IRF5-KO mice were treated with either bacterial lipopolysaccharides (LPS) or palmitate (Palm) for 2 or 24 h. Targeted metabolomics analyses were carried out to quantify intracellular tricarboxylic acid (TCA) cycle metabolites (n=5-6 per condition) and electron microscopy was carried out to evaluate mitochondrial structural characteristics (n=3 per condition).

A. Principal component analysis (PCA) on TCA cycle metabolites in all conditions. Palm 2 h condition separated (right).

B. PCA on TCA cycle metabolites in WT and IRF5-KO BMDMs stimulated with Palm for 2 h.

C. Variable weighting from PCA, percent variance contribution to principal component (PC)1, upon 2 h of Palm treatment. Lactate (Lac) intracellular concentration in WT and IRF5-KO BMDMs treated with Palm for 2 h (n=6 per condition, $^{**}p=0.003$, unpaired t-test). Aco: aconitate; Gln: glutamine; Gly: glycerate; Asp: aspartate; PEP: phosphoenol pyruvate; Suc: succinate; 3PG: 3-phospho glycerate; AKG: a-ketoglutarate; AHG: a-hydroxyglutarate; Mal: malate; Pyr: pyruvate; Fum: fumarate; Ita: itaconate; Glt: glutamate.

D. Schematic representation of metabolites with increased (red) or decreased (blue) abundance in IRF5-KO relative to WT BMDMs following treatment with Palm. Cit: citrate; Iso: isocitrate.

E. Extracellular acidification rate (ECAR) from extracellular flux analysis under Basal (Bas) and glucose-stimulated (Glu) conditions, of WT and IRF5-KO BMDMs treated with Palm for 2h (n=5 per condition, unpaired t-tests, $^{**}p=0.006$, $^{*}p=0.01$).

F. Oxygen consumption rate (OCR) from extracellular flux analysis, with oligomycin (Oli), carbonyl cyanide 4-(trifluoromethoxy) phenylhydrazone (FCCP) and Rotenone/Antimycin A (Rot/AA) administration, performed on WT and IRF5-KO BMDMs, treated with Palm for 2 h (n=5 per condition).

G. Electron micrograph and magnified inlet of BMDMs from WT and IRF5-KO mice after 2 h Palm treatment. Mitochondria are marked by ‘m’.

H. Mitochondrial cristae (white arrows) in electron micrograph and length and number of cristae of BMDMs from IRF5-KO and WT mice following Palm treatment for 2 h ($^{*}p=0.01$, $^{*}p=0.04$ unpaired t-test).

Data are presented as mean ± SEM.

Figure 5

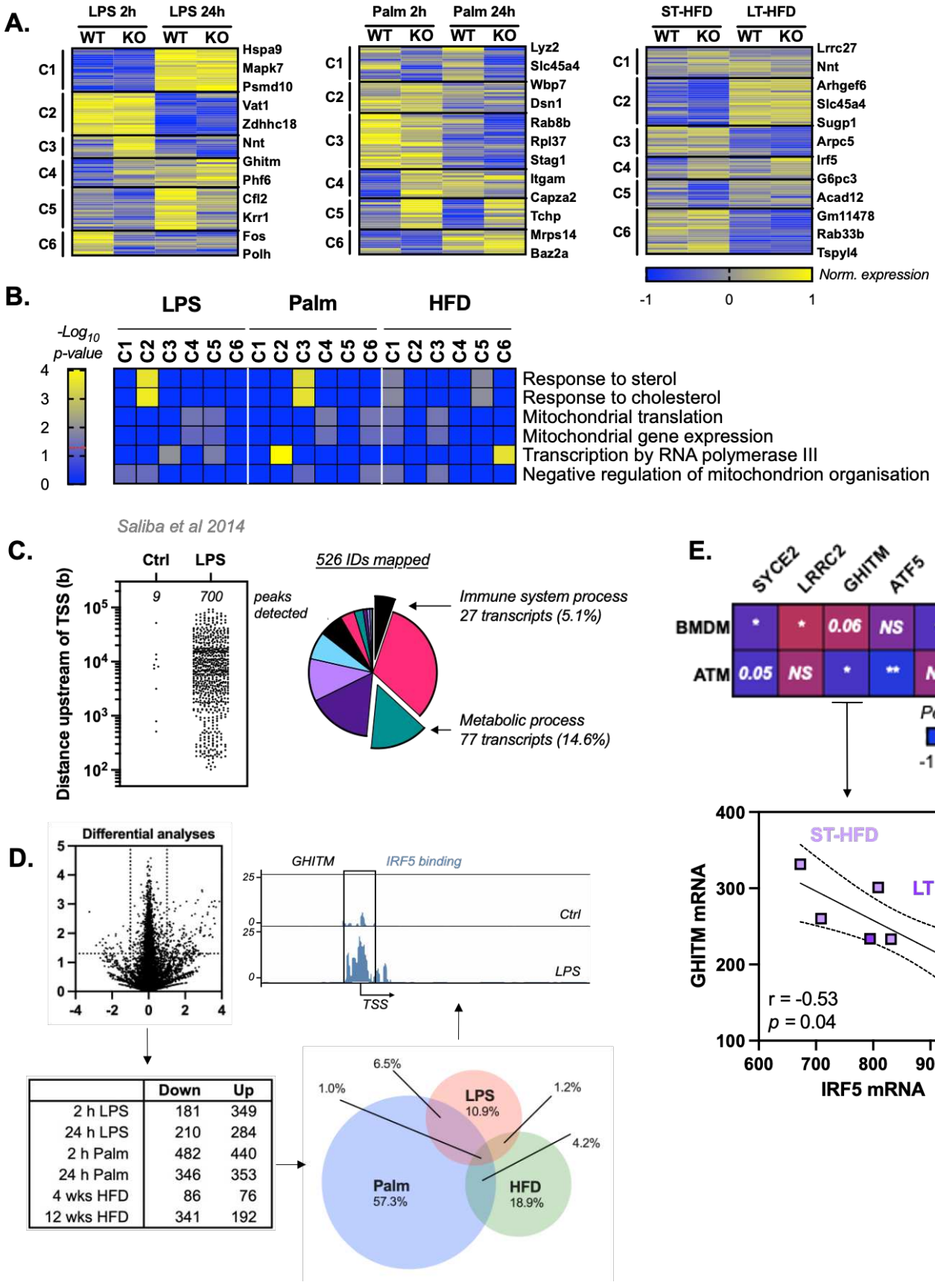
A.
LPS 2h
LPS 24h
Palm 2h
Palm 24h
ST-HFD
LT-HFD
WT KO WT KO
C1
C2
C3
C4
C5
C6
Hspa9
Mapk7
Psmd10
Vat1
Zdhhc18
Nnt
Ghitm
Phf6
Cfl2
Krr1
Fos
Polh
Lyz2
Slc45a4
Wbp7
Dsn1
Rab8b
Rpl37
Stag1
Itgam
Capza2
Tchp
Mrps14
Baz2a
Lrrc27
Nnt
Arhgef6
Slc45a4
Sugp1
Arpc5
Irf5
G6pc3
Acad12
Gm11478
Rab33b
Tspyl4
Norm. expression
-1 0 1
B.
LPS
Palm
HFD
-Log10 p-value
Response to sterol
Response to cholesterol
Mitochondrial translation
Mitochondrial gene expression
Transcription by RNA polymerase III
Negative regulation of mitochondrion organisation
Saliba et al 2014
C.
Ctrl
LPS
9
700
peaks detected
Distance upstream of TSS (b)
526 IDs mapped
Immune system process
27 transcripts (5.1%)
Metabolic process
77 transcripts (14.6%)
D.
Differential analyses
GHITM
IRF5 binding
Ctrl
LPS
TSS
Down Up
2 h LPS 181 349
24 h LPS 210 284
2 h Palm 482 440
24 h Palm 346 353
4 wks HFD 86 76
12 wks HFD 341 192
6.5%
1.0%
LPS
10.9%
1.2%
4.2%
Palm
57.3%
HFD
18.9%
E.
SYCE2
LRRC2
GHITM
ATF5
ABCG1
FNIP2
BMDM
ATM
Pearson R
-1 0 1
ST-HFD
LT HFD
GHITM mRNA
IRF5 mRNA
r = -0.53
p = 0.04

Figure 5. IRF5 binds to and regulates expression of genes that control mitochondrial structure and metabolism in bone-marrow derived macrophages and adipose tissue macrophages in response to metabolic stress

A. Clustering analysis on RNA sequencing from bone marrow-derived macrophages (BMDM) from IRF5-KO and WT mice treated for 2 or 24 h with bacterial lipopolysaccharides (LPS) or palmitate (Palm) and epididymal white adipose tissue (EpiWAT) F4/80^{+} macrophages (ATMs) from IRF5-KO and WT mice following short-term (ST-) or long-term (LT-) high-fat diet (HFD). Clustering analyses was applied to genes differentially expressed between genotypes in at least one condition.

B. Gene ontology (GO) term enrichment, related to mitochondria and lipotoxicity. Genes from differentially regulated clusters in Fig 5A and Fig S7A.

C. Publicly available chromatin immunoprecipitation (ChIP) seq of IRF5 in BMDMs treated with LPS for 120 min was procured. Peaks of interest were determined as either at or upstream of transcription start sites (TSS). Annotated genes were subjected to gene ontology (GO) enrichment analyses.

D. Differential analysis between genotypes per treatment: 2- or 24-h treatment with LPS or Palm and in EpiWAT ATMs following ST- or LT-HFD ($Log_2FC>1.0$; $-Log_{10}p>1.3$). Venn diagram of differentially expressed genes between genotypes, per treatment condition. Percentage refers to proportion of genes in overlap. Gene track from ChIP-seq in C. of GHITM gene which overlaps all conditions and also bound by IRF5.

E. Correlative analyses of IRF5 expression and the expression of previously identified overlapping genes in D; and notably GHITM expression in ATMs from IRF5-competent mice fed a ST- or LT-HFD (Pearson r=-0.83, p=0.009).

Data are presented as mean ± SEM.

Figure 6

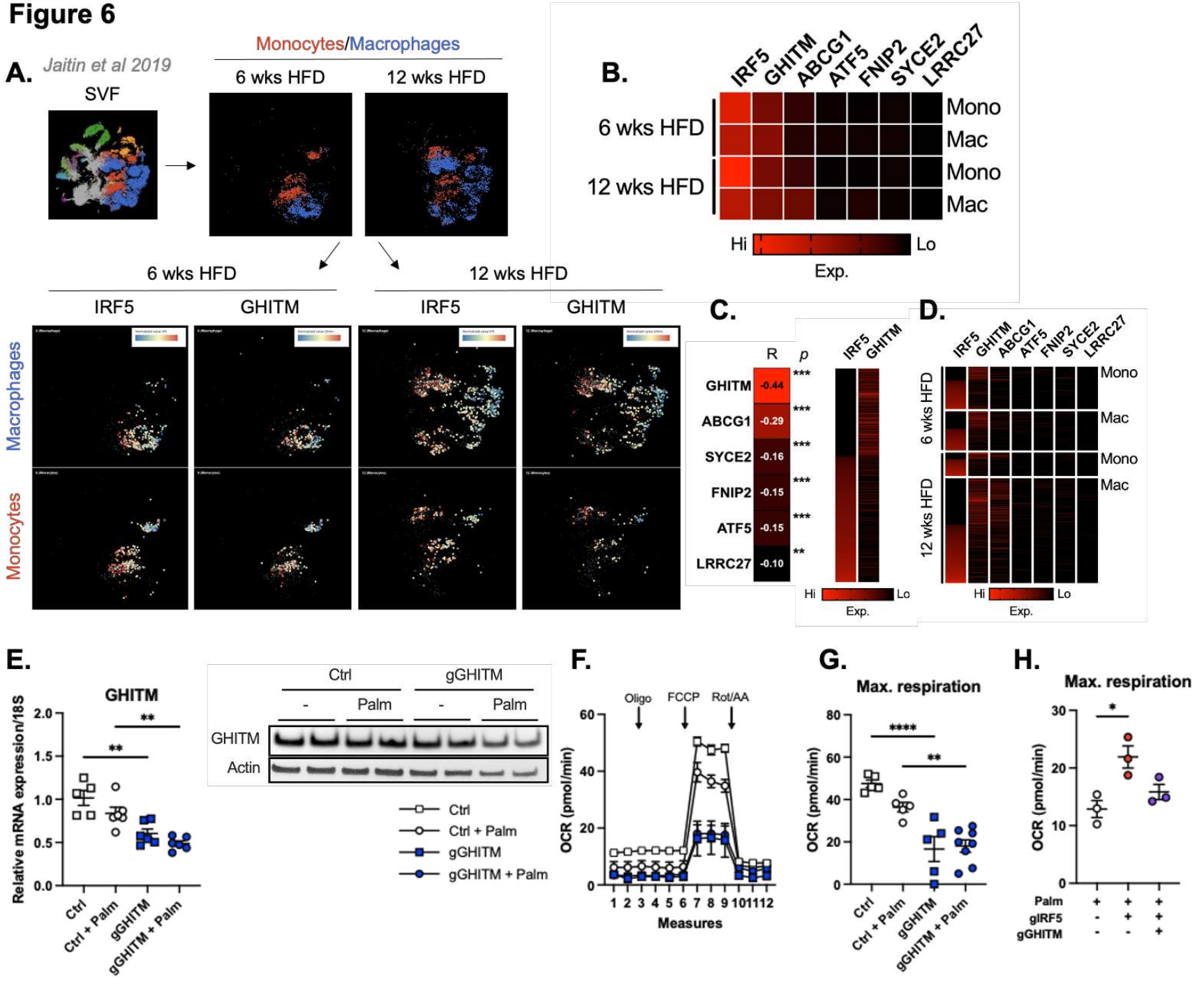
A.
Jaitin et al 2019
SVF
Monocytes/Macrophages
6 wks HFD
12 wks HFD
6 wks HFD
12 wks HFD
IRF5
GHITM
IRF5
GHITM
Macrophages
Monocytes
B.
IRF5 GHITM ABCG1 ATF5 FNIP2 SYCE2 LRRC27
6 wks HFD
12 wks HFD
Mono
Mac
Mono
Mac
Hi
Lo
Exp.
C.
R
p
GHITM -0.44 ***
ABCG1 -0.29 ***
SYCE2 -0.16 ***
FNIP2 -0.15 ***
ATF5 -0.15 ***
LRRC27 -0.10 **
IRF5 GHITM
Hi
Lo
Exp.
D.
IRF5 GHITM ABCG1 ATF5 FNIP2 SYCE2 LRRC27
6 wks HFD
12 wks HFD
Mono
Mac
Mono
Mac
Hi
Lo
Exp.
E.
GHITM
Relative mRNA expression/18S
Ctrl
Ctrl + Palm
gGHITM
gGHITM + Palm
Ctrl
gGHITM
- Palm - Palm
GHITM
Actin
Ctrl
Ctrl + Palm
gGHITM
gGHITM + Palm
F.
Oligo FCCP Rot/AA
OCR (pmol/min)
Measures
G.
Max. respiration
OCR (pmol/min)
Ctrl
Ctrl + Palm
gGHITM
gGHITM + Palm
H.
Max. respiration
OCR (pmol/min)
Palm
gIRF5
gGHITM

Figure 6. IRF5 and GHITM are highly expressed and reciprocally regulated in epididymal white adipose tissue macrophages and monocytes.

A. Single-cell RNA sequencing of the epididymal white adipose tissue (EpiWAT) stromal vascular fraction (SVF) of C57BL/6J mice following 6 or 12 weeks of high-fat feeding (Jaitin *et al*., 2019). Macrophages and monocytes were identified and expression of IRF5 and of GHITM were projected onto tSNE plots per cell type and duration of high-fat feeding.

B. Heatmap of mean expression values of IRF5, GHITM, ABCG1, SYCE2, FNIP2, ATF5 and LRRC27 over time and by cell type (monocytes (Mono) or macrophages (Mac)).

C. Correlative analyses between IRF5 expression and expression of GHITM, ABCG1, SYCE2, FNIP2, ATF5 and LRRC27 at the single cell level (Pearson R; ***p<0.0001 and **p=0.004). Heatmap of IRF5 and GHITM expression, each line represents a single cell.

D. Heatmap of single cell expression of IRF5, GHITM, ABCG1, SYCE2, FNIP2, ATF5 and LRRC27 over time and by cell type, each line represents a single cell.

E. Gene expression of GHITM in bone marrow-derived macrophages (BMDMs) from mice with myeloid-restricted Cas9-GFP expression, treated with lipofection agent (Ctrl) or with a guide RNA (gRNA) targeting GHITM (gGHITM) and with or without Palm treatment for 2 h (n=5 for Ctrl, n=6 for other conditions, one-way ANOVA. ***p=0.0003, left *p=0.0423, right *p=0.0167). Western blotting against GHITM in the same experimental design, quantification and blot in Fig. S8D, S8E (n=2 per condition).

F. Oxygen consumption rate (OCR) from extracellular flux analysis in BMDMs with or without Palm treatment following transfection with gGHITM or with lipofection agent alone (Ctrl). Oligomycin (Oli), carbonyl cyanide 4-(trifluoromethoxy) phenylhydrazone (FCCP) and Rotenone/Antimycin A (Rot/AA) were administered (n=5 for Ctrl, Ctrl + Palm and gGHITM; n=8 for gGHITM + Palm).

G. Maximal respiration from extracellular flux analysis (n=5 for Ctrl, Ctrl + Palm and gGHITM; n=8 for gGHITM + Palm; one-way ANOVA, ****p<0.0001 and **p=0.0051).

H. Maximal respiration from extracellular flux analysis on Palm treated BMDMs following transfection with a gRNA targeting IRF5 (gIRF5), double transfection with gGHITM and gIRF5 or with lipofection agent alone (Ctrl) (n=3 per condition; one-way ANOVA, *p=0.0428).

Data are presented as mean ± SEM.

Figure 7

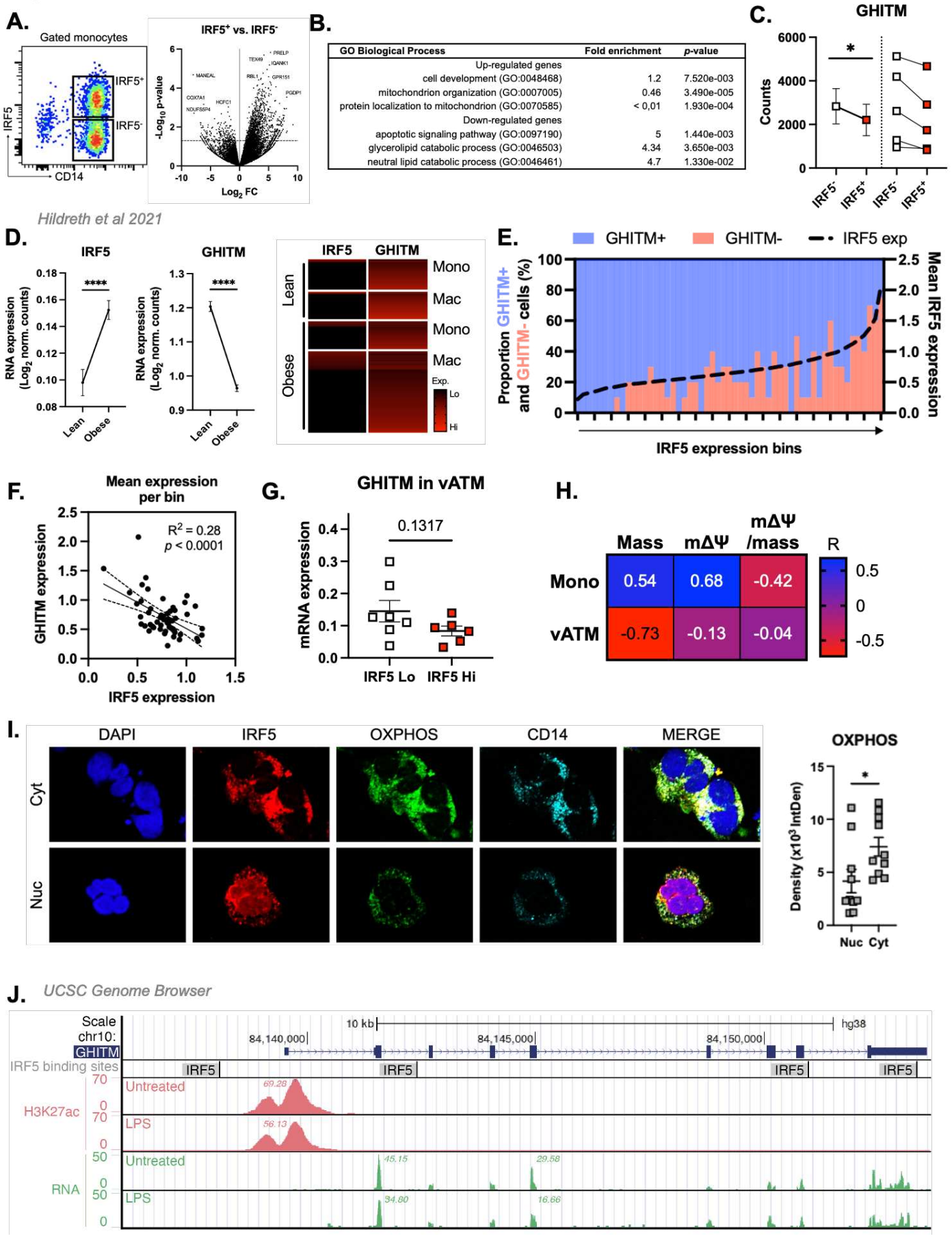
A.
Gated monocytes
IRF5
CD14
IRF5+
IRF5-
IRF5+ vs. IRF5-
-Log10 p-value
Log2 FC
B.
GO Biological Process | Fold enrichment | p-value
Up-regulated genes
cell development (GO:0048468) | 1.2 | 7.520e-003
mitochondrion organization (GO:0007005) | 0.46 | 3.490e-005
protein localization to mitochondrion (GO:0070585) | < 0,01 | 1.930e-004
Down-regulated genes
apoptotic signaling pathway (GO:0097190) | 5 | 1.440e-003
glycerolipid catabolic process (GO:0046503) | 4.34 | 3.650e-003
neutral lipid catabolic process (GO:0046461) | 4.7 | 1.330e-002
C.
GHITM
Counts
IRF5- IRF5+ IRF5- IRF5+
Hildreth et al 2021
D.
IRF5
GHITM
RNA expression (Log2 norm. counts)
Lean
Obese
Mono
Mac
Exp.
Lo
Hi
E.
GHITM+
GHITM-
IRF5 exp
Proportion GHITM+ and GHITM- cells (%)
Mean IRF5 expression
IRF5 expression bins
F.
Mean expression per bin
R2 = 0.28
p < 0.0001
GHITM expression
IRF5 expression
G.
GHITM in vATM
0.1317
mRNA expression
IRF5 Lo
IRF5 Hi
H.
Mass
mΔΨ
mΔΨ /mass
R
Mono
vATM
0.54
0.68
-0.42
-0.73
-0.13
-0.04
I.
DAPI
IRF5
OXPHOS
CD14
MERGE
Cyt
Nuc
OXPHOS
Density (x10³ IntDen)
Nuc Cyt
J.
UCSC Genome Browser
Scale
chr10:
GHITM
10 kb
hg38
84,140,000
84,145,000
84,150,000
IRF5 binding sites
IRF5
H3K27ac
Untreated
LPS
RNA
69.26
56.13
45.15
29.58
34.80
16.66

Figure 7. IRF5 binds to GHITM and regulates mitochondrial activity in human monocytes and adipose tissue macrophages.

A. $CD14^+$ Monocytes from patients with type-2 diabetes (T2D; n=5) were sorted based on their expression of IRF5 and subjected to RNA sequencing analyses. Differential analyses were paired by patient and carried out on $IRF5^+$ versus $IRF5^-$ monocytes (n=5, $-\log_{10}p>1.3$).

B. Gene ontology (GO) term enrichment analyses on up-regulated and down-regulated genes in $IRF5^+$ versus $IRF5^-$ monocytes.

C. Expression of GHITM mRNA in $IRF5^-$ and $IRF5^+$ monocytes (**p*=0.039, paired t-test).

D. IRF5 and GHITM RNA counts in white adipose tissue (WAT) macrophages and monocytes, from public dataset of single-cell RNA sequencing of the stromal vascular fraction (SVF) of lean and obese patients[32] (unpaired t-test, *****p*<0.0001). Heatmap of single cell expression of IRF5 and GHITM from monocytes (Mon) and macrophages (Mac) from WAT of lean and obese patients, each line represents a single cell.

E. Proportion of GHITM+ (blue) and GHITM- (red) cells in 10-cell bins by increasing IRF5 expression.

F. Correlative analysis of GHITM and IRF5 mean expression per bin (Pearson, R^2=0.28, p<0.0001).

G. RNA expression of GHITM normalized to actin in $CD14^+$ human visceral adipose tissue macrophages (vATMs). Samples were stratified based on their expression level of IRF5 into $IRF5^{Lo}$ versus $IRF5^{Hi}$ expressors ($IRF5^{Lo}$ n=7 and $IRF5^{Hi}$ n=6, unpaired t-test, *p*=0.13).

H. Correlative analyses of MFI of IRF5, JC1-Green (mitochondrial mass, Mt Mass), JC1-Red (mΔΨ), and JC1-Red-to-Green ratio (mΔΨ/mass) in human visceral ATMs (vATM) from obese patients and in monocytes from patients with T2D (Mono) analysed by FACS (n=11 for monocytes, n=9 for ATMs, Pearson r, *p*-values in Fig S9D).

I. Immunofluorescence staining of IRF5, oxidative phosphorylation (OXPHOS) enzyme complexes and CD14 in cytospin prepared human monocytes from patients with T2D. Samples were separated based on IRF5 localization being either nuclear (Nuc) or cytoplasmic (Cyt). Quantification of OXPHOS staining in IRF5 Nuc and Cyt samples (n=10 per condition, unpaired t-test, **p*=0.0335).

J. University of California Santa Cruz (UCSC) genome browser[51–53] (http://genome.ucsc.edu) tracks at the GHITM locus with tracks from JASPAR2020[54] to visualize transcription factor binding sites for IRF5 and from BLUEPRINT[56,] to visualise RNA expression and H3K27 acetylation marks in LPS treated and untreated human monocyte-derived macrophages (session link).

Data are presented as mean ± SEM.

1060

Figure 8

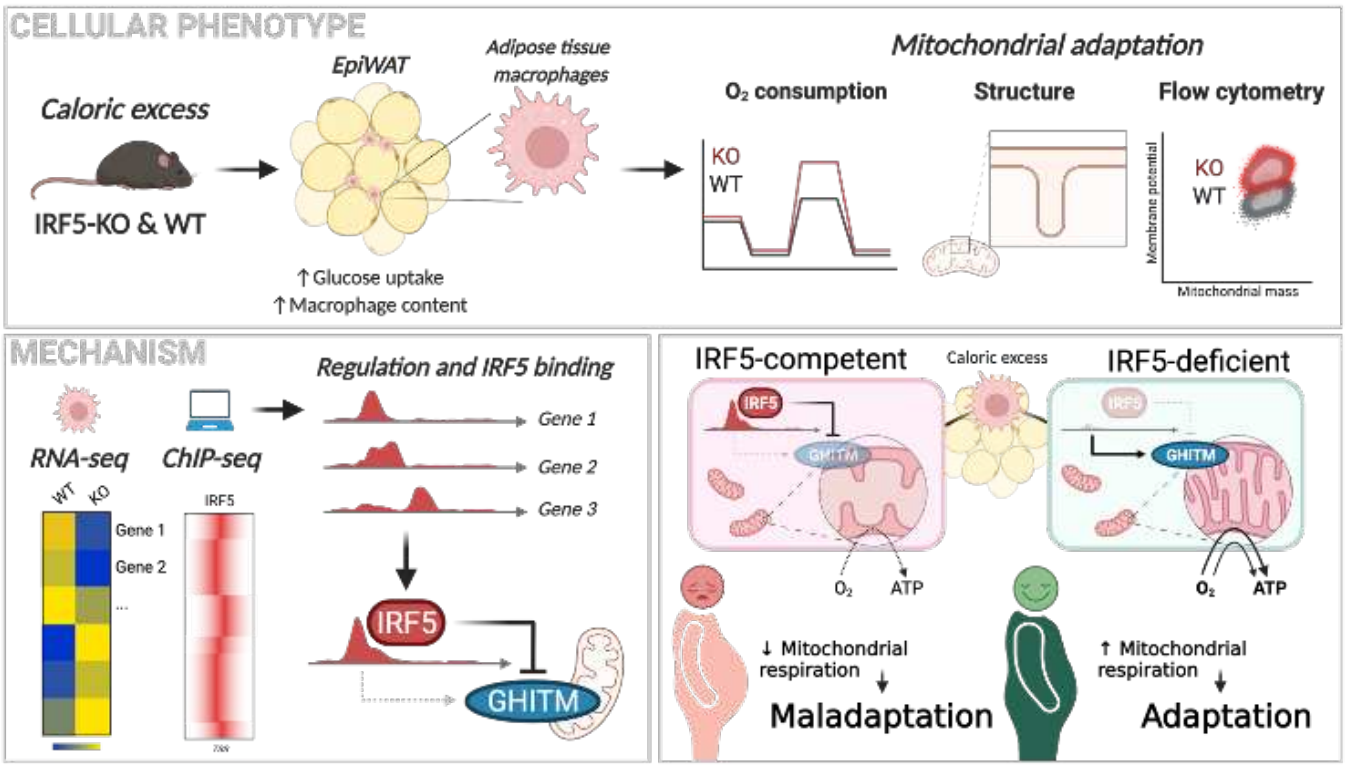

Figure 8. IRF5 transcriptional interaction with the mitochondrial structural protein GHITM limits adipose tissue macrophage oxidative capacity. This mechanism alters mitochondrial cristae structures in adipose tissue macrophages to influence tissue adaptation in diet-induced obesity.

Figure S1

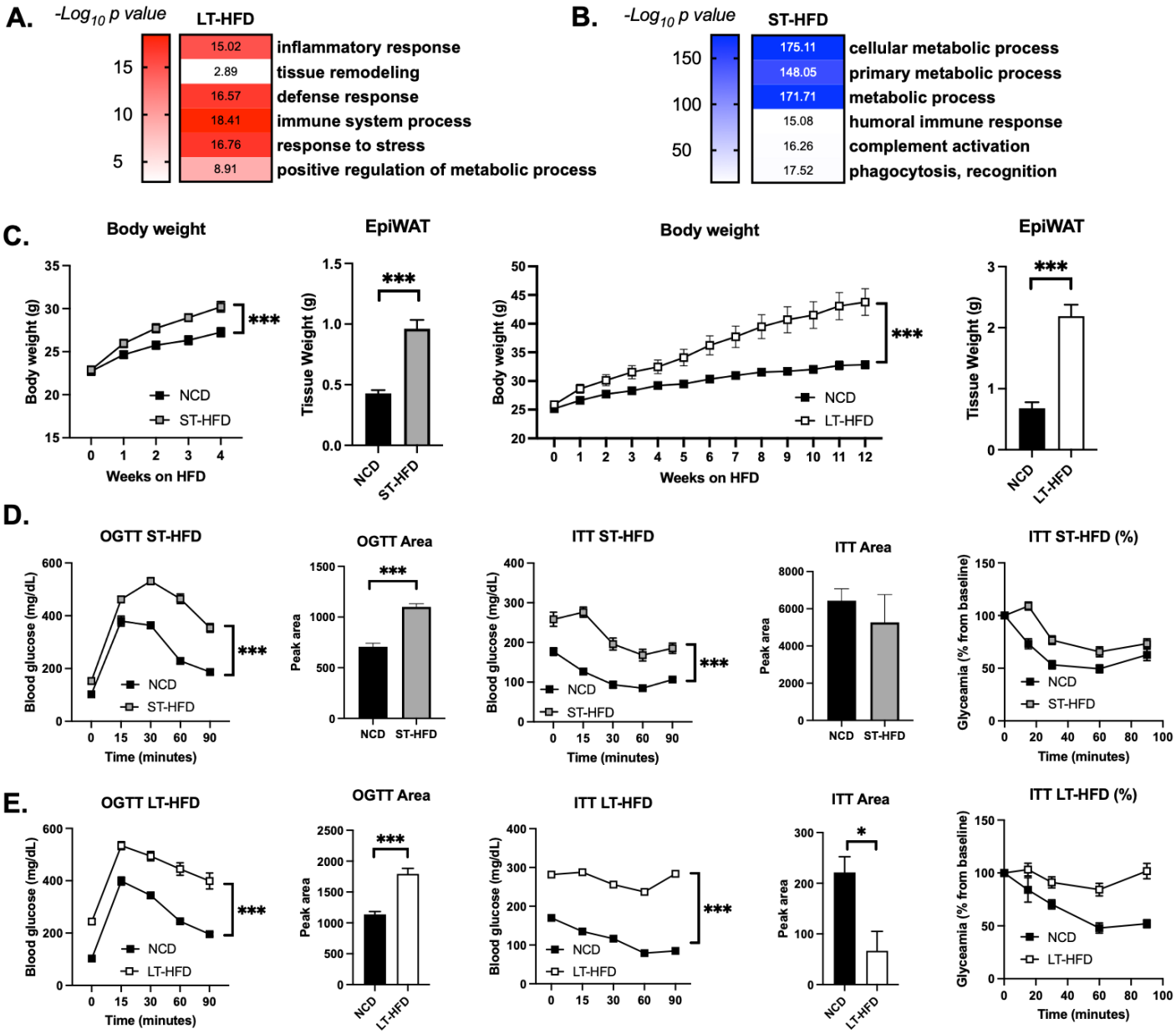
A.
-Log10 p value
LT-HFD
15.02
2.89
16.57
18.41
16.76
8.91
inflammatory response
tissue remodeling
defense response
immune system process
response to stress
positive regulation of metabolic process
B.
-Log10 p value
ST-HFD
175.11
148.05
171.71
15.08
16.26
17.52
cellular metabolic process
primary metabolic process
metabolic process
humoral immune response
complement activation
phagocytosis, recognition
C.
Body weight
Body weight (g)
Weeks on HFD
NCD
ST-HFD
EpiWAT
Tissue Weight (g)
Body weight
Body weight (g)
Weeks on HFD
NCD
LT-HFD
EpiWAT
Tissue Weight (g)
D.
OGTT ST-HFD
Blood glucose (mg/dL)
Time (minutes)
OGTT Area
Peak area
ITT ST-HFD
Blood glucose (mg/dL)
Time (minutes)
ITT Area
Peak area
ITT ST-HFD (%)
Glycaemia (% from baseline)
Time (minutes)
E.
OGTT LT-HFD
Blood glucose (mg/dL)
Time (minutes)
OGTT Area
Peak area
ITT LT-HFD
Blood glucose (mg/dL)
Time (minutes)
ITT Area
Peak area
ITT LT-HFD (%)
Glycaemia (% from baseline)
Time (minutes)

Figure S1. IRF5-transcriptome is associated with altered cellular metabolic adaptation and mice on short-term high-fat diet lose glycaemic homeostasis over time

A. & B. WT and IRF5-KO mice were placed on a long-term (LT-) high-fat diet (HFD) (**A**) or a short-term (ST-HFD) (**B**). F4/80^{+} adipose tissue macrophages (ATMs) were sorted from epididymal fat pads (EpiWAT) for RNA sequencing (RNA-seq). Differentially expressed genes (-log10 p > 1.3) between genotypes were used for gene ontology (GO) term enrichment. Heatmaps represent p values (n=4 per genotype).

C. Body weight and EpiWAT weight of C57BL/6J mice on NCD, ST-HFD (left) or LT-HFD (right) (n=10 per group, ANOVA weight curves and unpaired t-test for tissue weight p<0.0001).

D. & **E.** Oral glucose tolerance test (OGTT) and insulin tolerance test (ITT) performed on mice following NCD, ST-HFD (**D.**) or LT-HFD (**E.**), and peak area of the corresponding curves (n=10 for NCD and ST-HFD, n=4 for NCD and n=6 for LT-HFD; ANOVA for curves and unpaired t-test for area p<0.0001).

Data are presented as mean ± SEM.

Figure S2

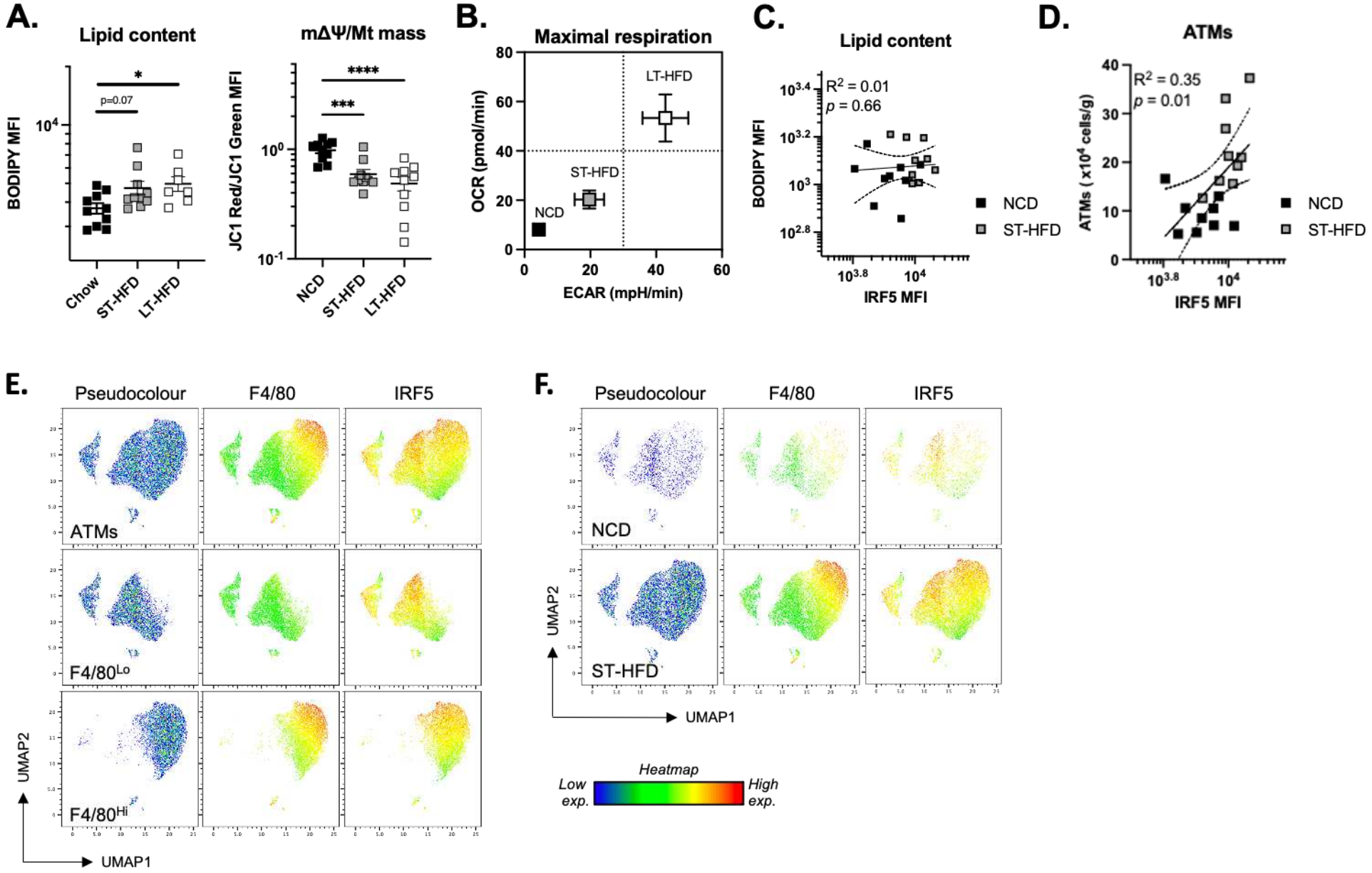
A.
Lipid content
BODIPY MFI
p=0.07
*
Chow
ST-HFD
LT-HFD
mΔΨ/Mt mass
JC1 Red/JC1 Green MFI
****
***
NCD
ST-HFD
LT-HFD
B.
Maximal respiration
OCR (pmol/min)
ECAR (mpH/min)
LT-HFD
ST-HFD
NCD
C.
Lipid content
BODIPY MFI
R² = 0.01
p = 0.66
IRF5 MFI
NCD
ST-HFD
D.
ATMs
ATMs (x10⁴ cells/g)
R² = 0.35
p = 0.01
IRF5 MFI
NCD
ST-HFD
E.
Pseudocolour
F4/80
IRF5
ATMs
F4/80Lo
F4/80Hi
UMAP2
UMAP1
F.
Pseudocolour
F4/80
IRF5
NCD
ST-HFD
UMAP2
UMAP1
Heatmap
Low exp.
High exp.

Figure S2. Adipose tissue macrophages undergo metabolic adaptation on high-fat diet and IRF5 is highly expressed in F4/80^{Hi} cells

A. Median fluorescence intensity (MFI) of BODIPY and JC1-Red/JC1-Green ratio to assess lipid content and mΔΨ/Mt mass respectively, in epididymal white adipose tissue (EpiWAT) F4/80^{+} CD11b^{+} macrophages (ATMs) of C57BL/6J mice on a normal chow diet (NCD), short-term (ST-) high-fat diet (HFD) or a long-term (LT-)HFD (n=10 per group in NCD and ST-HFD; n= 7 in LT-HFD; ANOVA, *p=0.042).

B. Energetic plot with extracellular acidification rate (ECAR) and oxygen consumption rate (OCR) from maximal respiration of extracellular flux analysis (Fig. 1E.). Assay performed on F4/80^{+} magnetically sorted from the EpiWAT of C57BL/6J mice on NCD (n=4), ST-HFD (n=9) or LT-HFD (n=8).

C. Correlative analysis between IRF5 and BODIPY MFI (Linear regression, Pearson correlation, R^2 = 0.01; p = 0.66) in EpiWAT F4/80^{+} CD11b^{+} ATMs of C57BL/6J mice on NCD or ST-HFD (n=9 per group).

D. Correlative analysis between IRF5 MFI in EpiWAT F4/80^{+} CD11b^{+} ATMs and EpiWAT ATM content (Linear regression, Pearson correlation, R^2 = 0.35; p = 0.0104) of C57BL/6J mice on NCD or ST-HFD (n=9 per group).

E. UMAP projection of IRF5 expression across ATMs, F4/80^{Lo} and F4/80^{Hi} cells from the EpiWAT of mice upon NCD or ST-HFD.

F. UMAP projection of IRF5 expression in ATMs across on NCD or ST-HFD.

Data are presented as mean ± SEM.

Figure S3

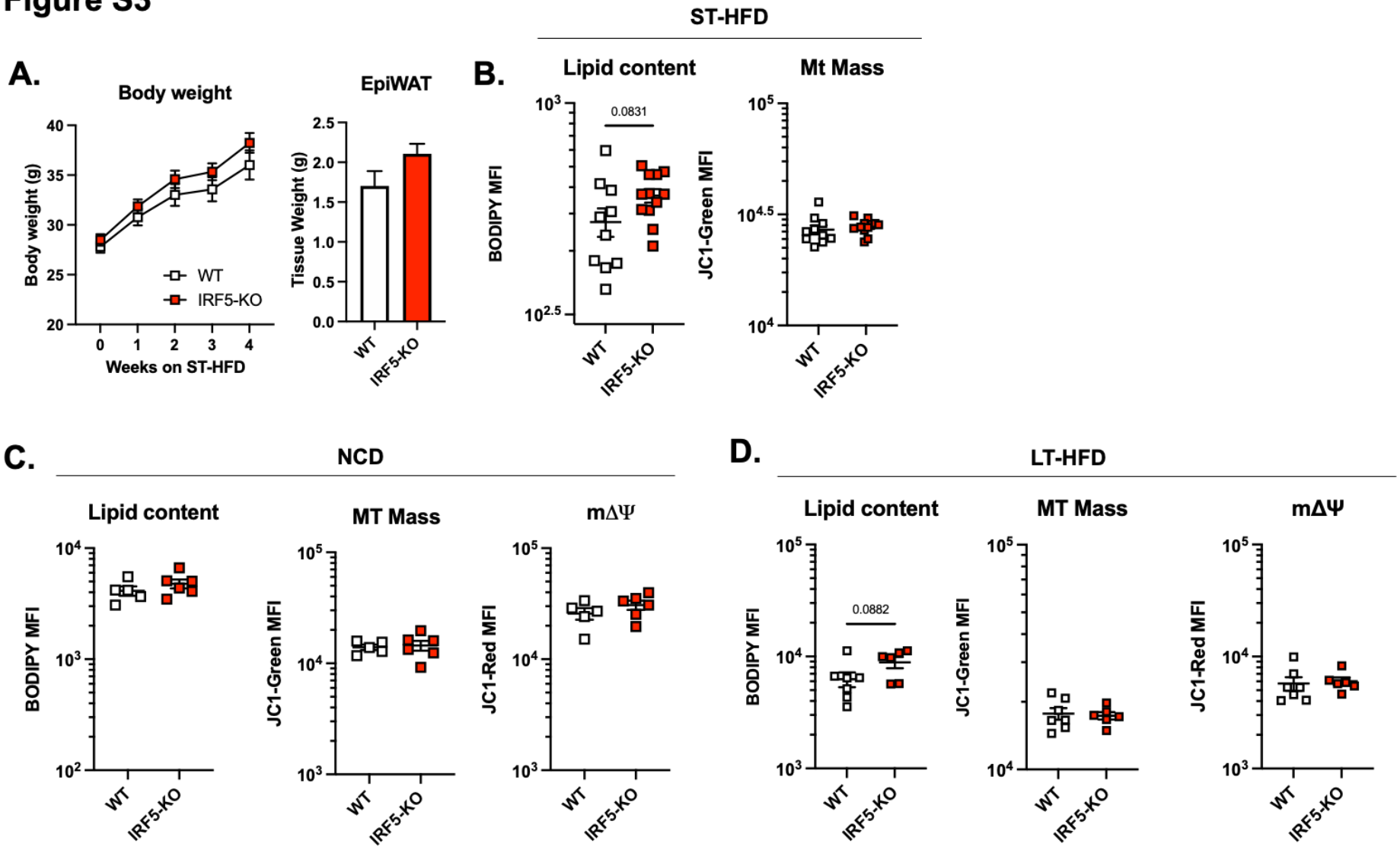

1096

Figure S3. Normal chow and long-term high-fat diet are not associated with adaptive cellular metabolism in IRF5-deficiency.

A. Body weight and epididymal white adipose tissue (EpiWAT) weight of WT and IRF5-KO mice on short-term (ST-) high-fat diet (HFD) (n=10 for WT and n=12 for IRF5-KO)

B. MFI of BODIPY and JC1-Green in EpiWAT F4/80^{+} CD11b^{+} macrophages of WT and IRF5-KO mice on ST-HFD (n=10 for WT and 12 for IRF5-KO, unpaired t-test, p=0.0831).

C. & D. MFI of BODIPY, JC1-Green and JC1-Red in EpiWAT F4/80^{Hi} macrophages of WT and IRF5-KO mice on normal chow diet (NCD) (**C**) or long term (LT-) HFD (**D**) (n=5 WT and 6 IRF5-KO mice on NCD, n=7 WT and n=6 IRF5-KO on LT-HFD, unpaired t-test, p=0.0882).

Data are presented as mean ± SEM.

Figure S4

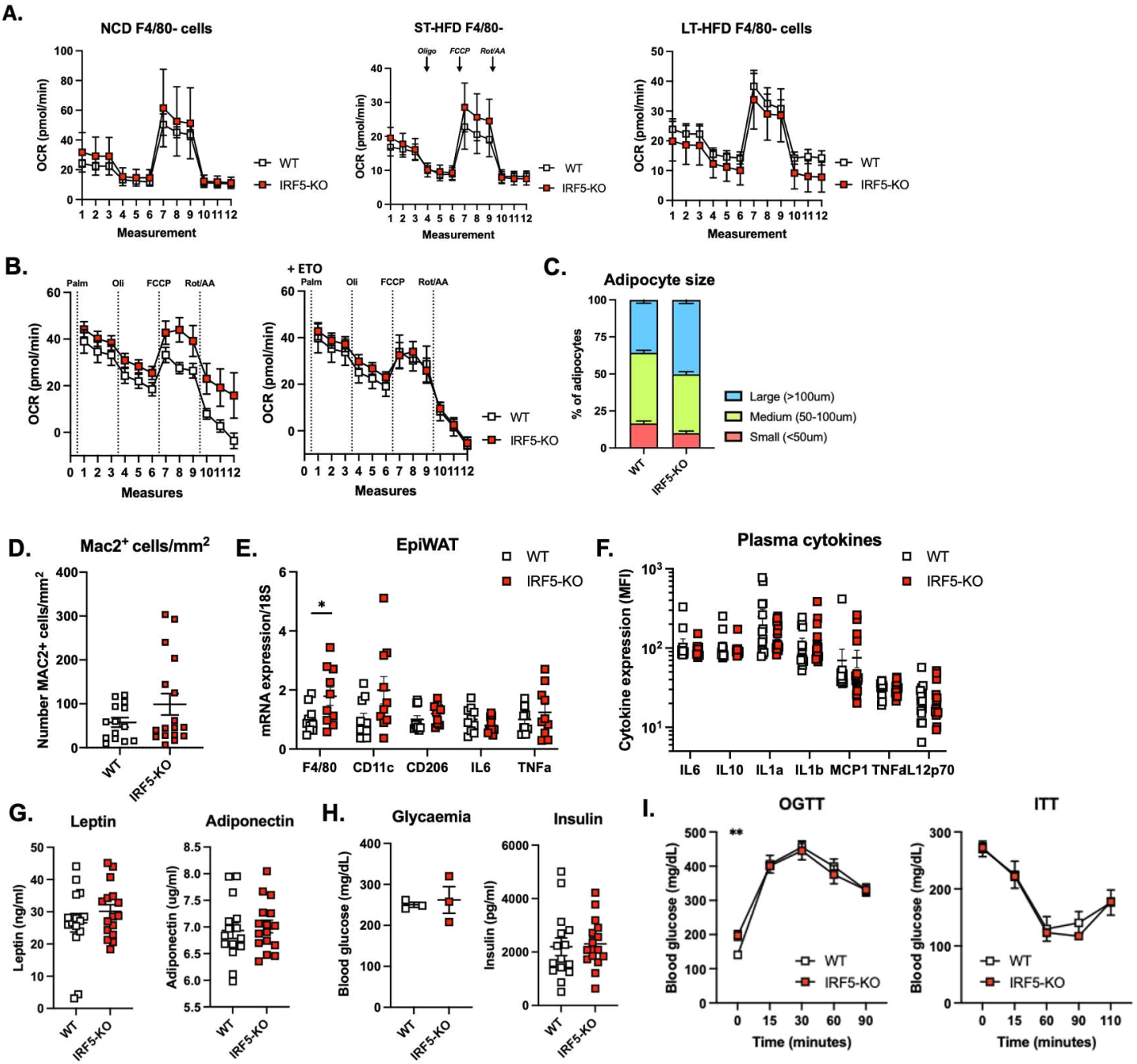
A.
NCD F4/80- cells
ST-HFD F4/80-
LT-HFD F4/80- cells
Oligo
FCCP
Rot/AA
OCR (pmol/min)
Measurement
WT
IRF5-KO
B.
Palm
Oli
FCCP
Rot/AA
+ ETO
Measures
C.
Adipocyte size
% of adipocytes
Large (>100um)
Medium (50-100um)
Small (<50um)
D.
Mac2+ cells/mm2
Number MAC2+ cells/mm2
E.
EpiWAT
mRNA expression/18S
F4/80
CD11c
CD206
IL6
TNFa
F.
Plasma cytokines
Cytokine expression (MFI)
IL6
IL10
IL1a
IL1b
MCP1
TNFa
IL12p70
G.
Leptin
Adiponectin
Leptin (ng/ml)
Adiponectin (ug/ml)
H.
Glycaemia
Insulin
Blood glucose (mg/dL)
Insulin (pg/ml)
I.
OGTT
ITT
Time (minutes)

Figure S4. F4/80- cells and inflammatory status of adipose tissue are not affected by IRF5-deficiency upon short-term high-fat diet

A. Oxygen consumption rate (OCR) from extracellular flux analysis with oligomycin (Oli), carbonyl cyanide 4-(trifluoromethoxy) phenylhydrazone (FCCP) and Rotenone/Antimycin A (Rot/AA) administration. Analysis on F4/80- cells of the stromal vascular fraction (SVF) of epididymal white adipose tissue (EpiWAT) from WT and IRF5-KO mice on a normal chow diet (NCD; left), short-term (ST-) high-fat diet (HFD; middle) and long-term (LT-) HFD (right) (n=4 mice per genotype for NCD, n=6 WT and 9 IRF5-KO mice for ST-HFD and n=6 WT and 5 IRF5-KO mice for LT-HFD).

B. OCR from extracellular flux analysis, following palmitate with or without etomoxir, Oligo, FCCP and Rot/AA were administered. Cells were from SVF of EpiWAT of WT and IRF5-KO mice on ST-HFD (n=7 WT and 9 IRF5-KO mice).

C. Proportions of small (<50 um), medium (50-100 um) or large (>100 um) adipocytes in EpiWAT of WT and IRF5-KO mice on ST-HFD (Related to Fig 2E).

D. Number of Mac2+ cells on EpiWAT sections of WT and IRF5-KO mice on ST-HFD (n=14 WT and 17 IRF5-KO mice) (Related to Fig 2E, F).

E. F4/80, CD11c, CD206, IL6 and TNFa mRNA expression normalized to 18S, in EpiWAT of WT and IRF5-KO mice on ST-HFD (n=10 mice per genotype, unpaired t-test **p*= 0.027)

F. Plasma cytokine quantification from WT and IRF5-KO mice on ST-HFD (n=14 WT and n=16 IRF5-KO mice). Median fluorescence intensity (MFI) of IL6, IL10, IL1a, IL1b, MCP1, TNFa or IL12p70 coated beads.

G. Plasma levels of leptin and adiponectin from WT and IRF5-KO mice on ST-HFD (n=15 WT and n=16 IRF5-KO mice).

H. Glycaemia (n=3 per genotype) and plasma insulin levels (n=15 WT and n=16 IRF5-KO mice) from WT and IRF5-KO mice on ST-HFD.

I. Oral glucose tolerance test (OGTT) and insulin tolerance test (ITT) performed on WT and IRF5-KO mice following ST-HFD (n=8 for WT and n=5 for IRF5-KO).

Data are presented as mean ± SEM.

1135

Figure S5

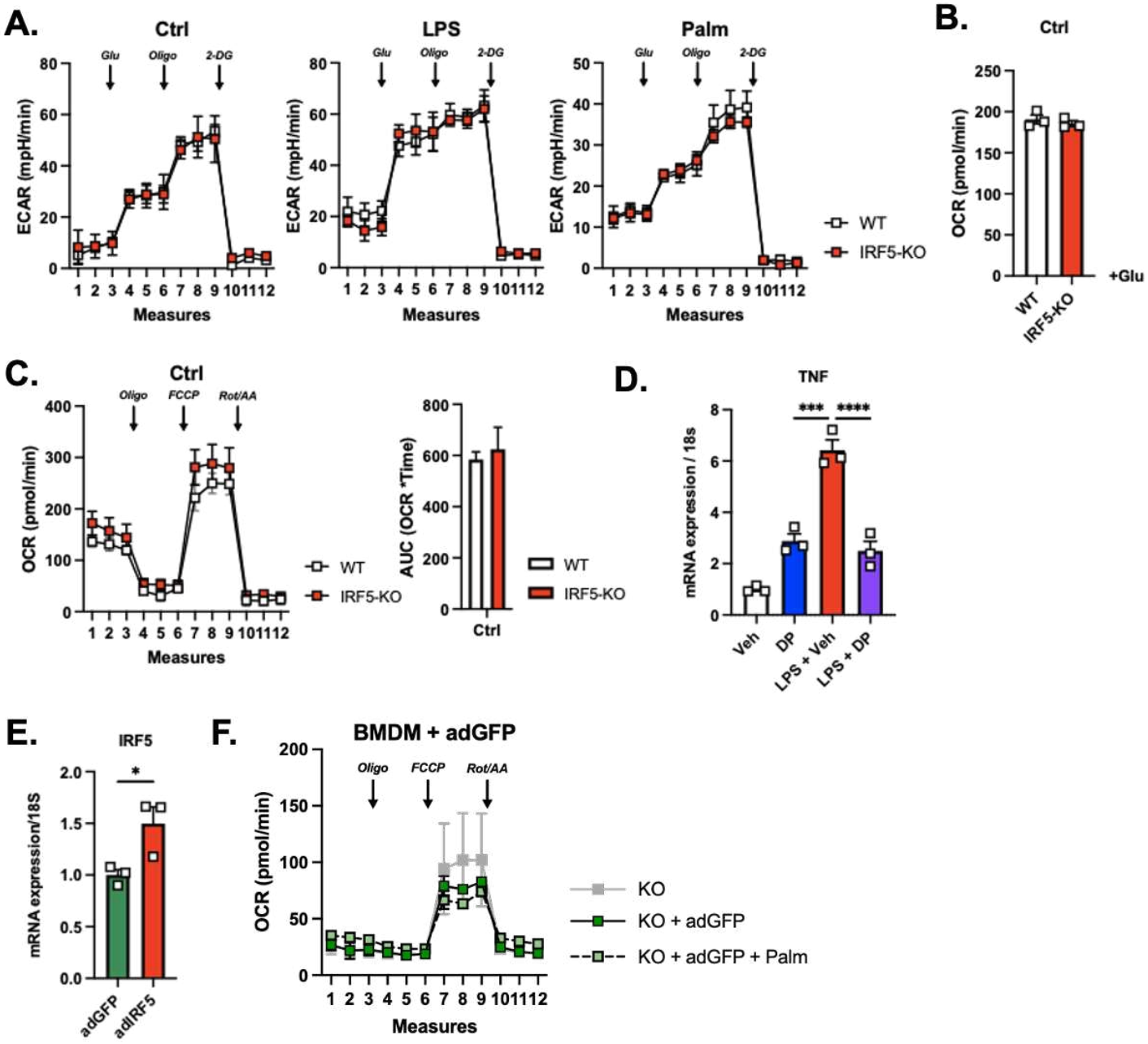

Figure S5. IRF5-deficiency does not alter mitochondrial respiration under basal conditions nor glycolysis under basal and treated conditions

A. Bone marrow-derived macrophages (BMDM) from WT and IRF5-KO mice were treated with lipopolysaccharides (LPS) or palmitate (Palm) for 24 hours. Extracellular acidification rate (ECAR) was measured in extracellular flow analysis following addition of glucose (Glu), oligomycin (Oligo) and 2-deoxyglucose (2-DG) (n=5 per genotype for treated conditions and n=3 per genotype for control).

B. Oxygen consumption rate (OCR) following glucose administration in extracellular flux analysis of untreated WT and IRF5-KO BMDMs, in Fig S5A (n=5 per genotype).

C. OCR measurements during extracellular flux analysis, with Oligo, carbonyl cyanide 4-(trifluoromethoxy) phenylhydrazone (FCCP) and Rotenone/Antimycin A (Rot/AA) administration (left) and area under the curve (right) of untreated WT and IRF5-KO BMDMs (n=3 per genotype).

D. BMDMs from C57BL/6J mice were treated with an IRF5-decoy peptide (DP) or a vehicle (Veh) and with LPS. RNA expression of TNF was quantified, and normalized to 18S (***p=0.0002 and ****p<0.0001, one-way ANOVA).

E. BMDMs from IRF5-KO mice were treated with an IRF5 adenovirus (adIRF5) or a control adenovirus (adGFP). IRF5 RNA expression was quantified (n=3 per group; *p=0.04, unpaired t-test).

F. Metabolic flux analysis of BMDMs from IRF5-KO mice were treated with an adGFP and with Palm (n=3 per group). Cells were treated with Oligo, FCCP and Rot/AA.

Data are presented as mean ± SEM.

1158

Figure S6

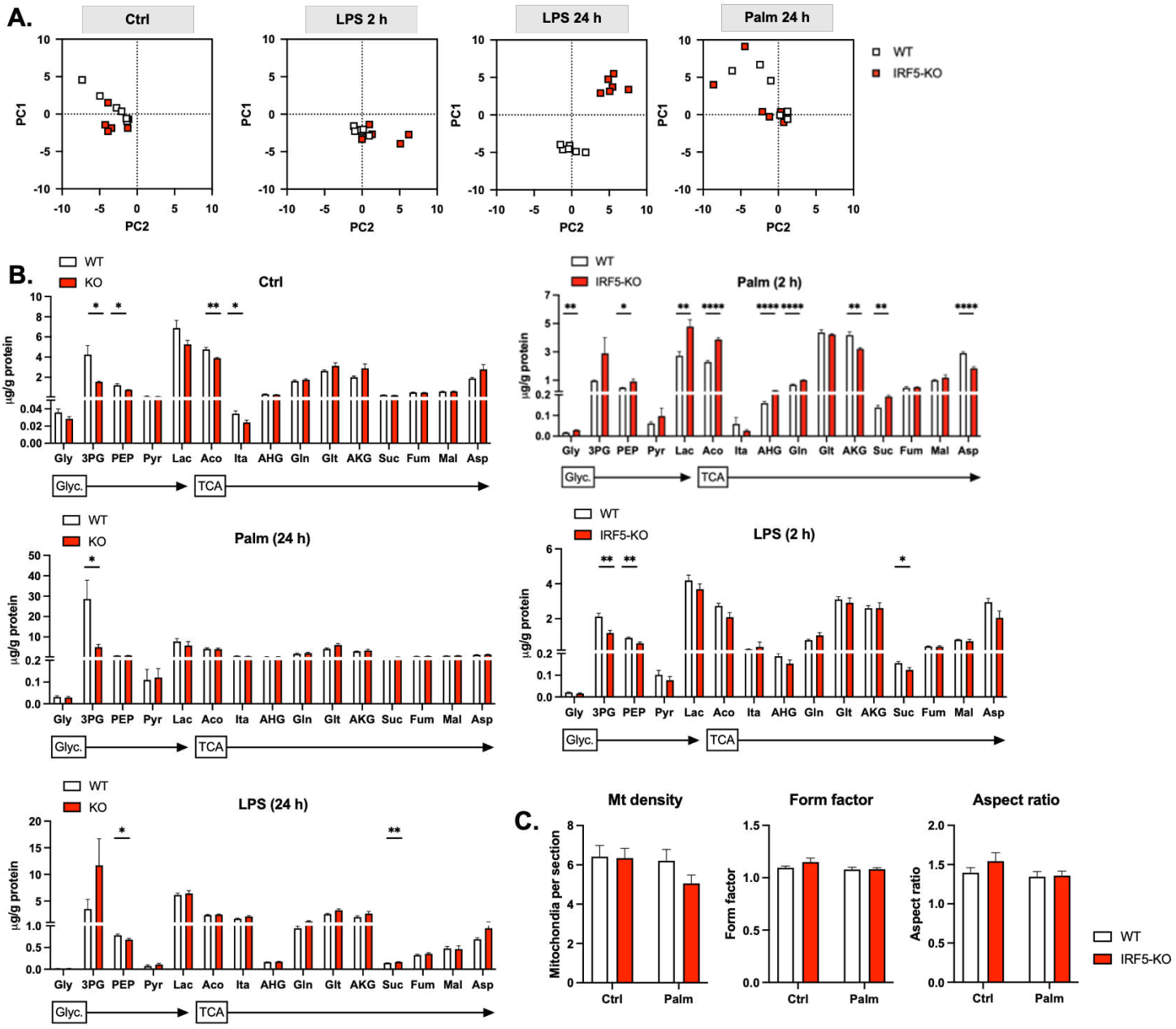

Figure S6. TCA metabolite quantification and mitochondrial dynamics in bone marrow-derived macrophages from IRF5-KO and WT mice following treatment with LPS and palmitate

A. Principal component analysis (PCA) on TCA cycle metabolites in WT and IRF5-KO bone marrow-derived macrophages (BMDMs) left untreated, or stimulated with bacterial lipopolysaccharides (LPS) for 2 or 24 h or with palmitate (Palm) for 24 h.

B. Absolute quantification of TCA metabolites in BMDMs from WT and IRF5-KO mice, left untreated, stimulated with LPS or Palm for 2 or 24 h (left to right, Ctrl: *p=0.013, *p=0.013, **p=0.002, *p=0.04; LPS 2h: **p=0.0041, **p=0.0068, *p=0.038; LPS 24h: *p=0.02 **p=0.002; Palm 2h: **p=0.001, *p=0.03, **p=0.004, ****p<0.0001, ****p=0.000005, ****p=0.00006, **p=0.002, **p=0.002 ****p=0.000015; Palm 24h: *p= 0.02).

D. Analysis of mitochondrial density, form factor and aspect ratio from electron micrographs in WT and IRF5-KO BMDMs treated with Palm for 2 h or in untreated controls (Ctrl).

Data are presented as mean ± SEM.

Figure S7

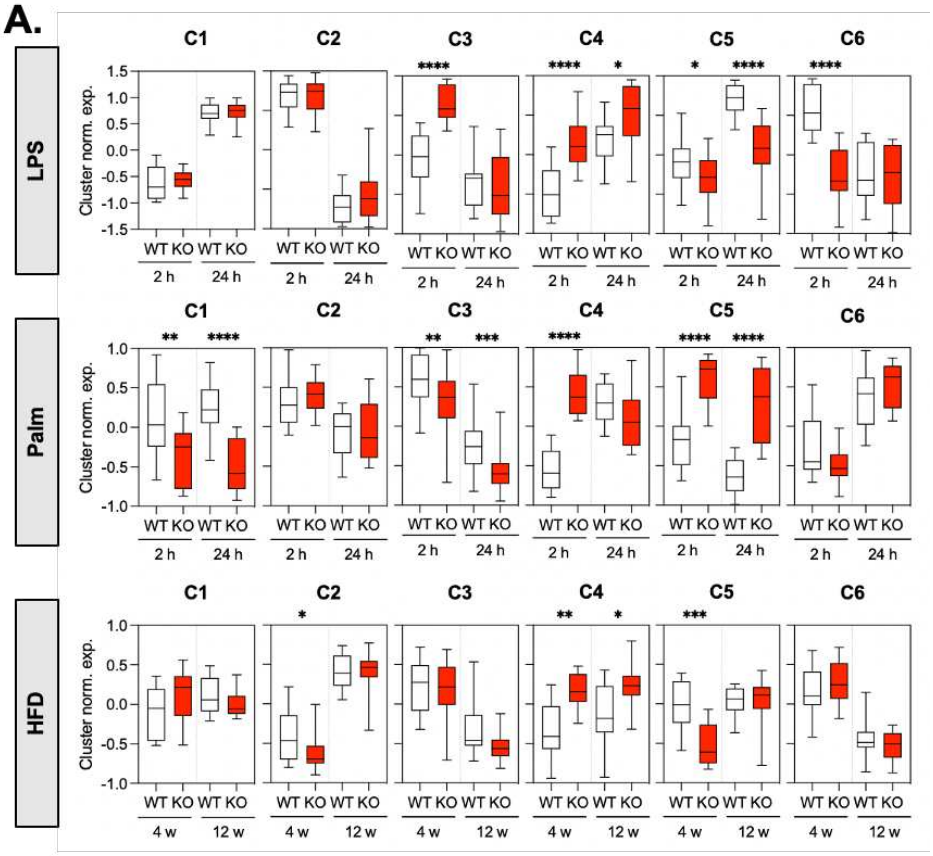

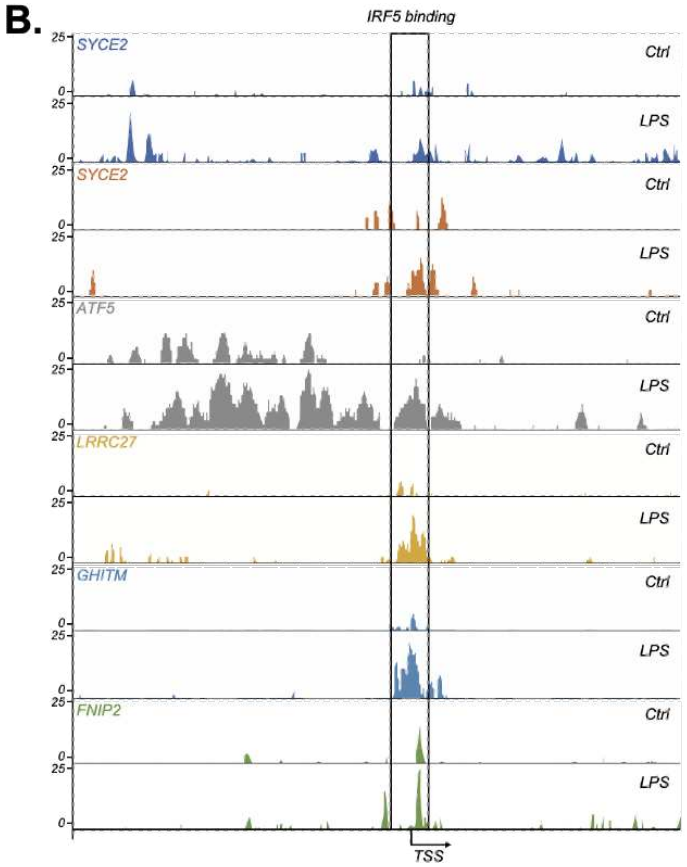

1173

Figure S7. IRF5-cistrome and transcriptomic analysis in IRF5-KO and WT bone-marrow derived and adipose tissue macrophages upon stimulation.

A. Normalized mRNA expression per cluster identified in Fig 5A (left to right: LPS ****p<0.0001, ****p<0.0001, *p=0.028, *p=0.031, ****p<0.0001, ****p<0.0001; Palm **p=0.016, ****p<0.0001, **p=0.0038, ***p=0.0003, ****p<0.0001, ****p<0.0001; HFD *p=0.013, **p=0.0017, *p=0.0156, ***p=0.0001; one-way ANOVA).

B. Gene track from ChIP-seq in Fig 5C. of overlapping genes in all conditions with IRF5 binding, in control (Ctrl) condition or upon lipopolysaccharide (LPS) stimulation.

Data are presented as mean ± SEM.

Figure S8

Jaitin et al 2019

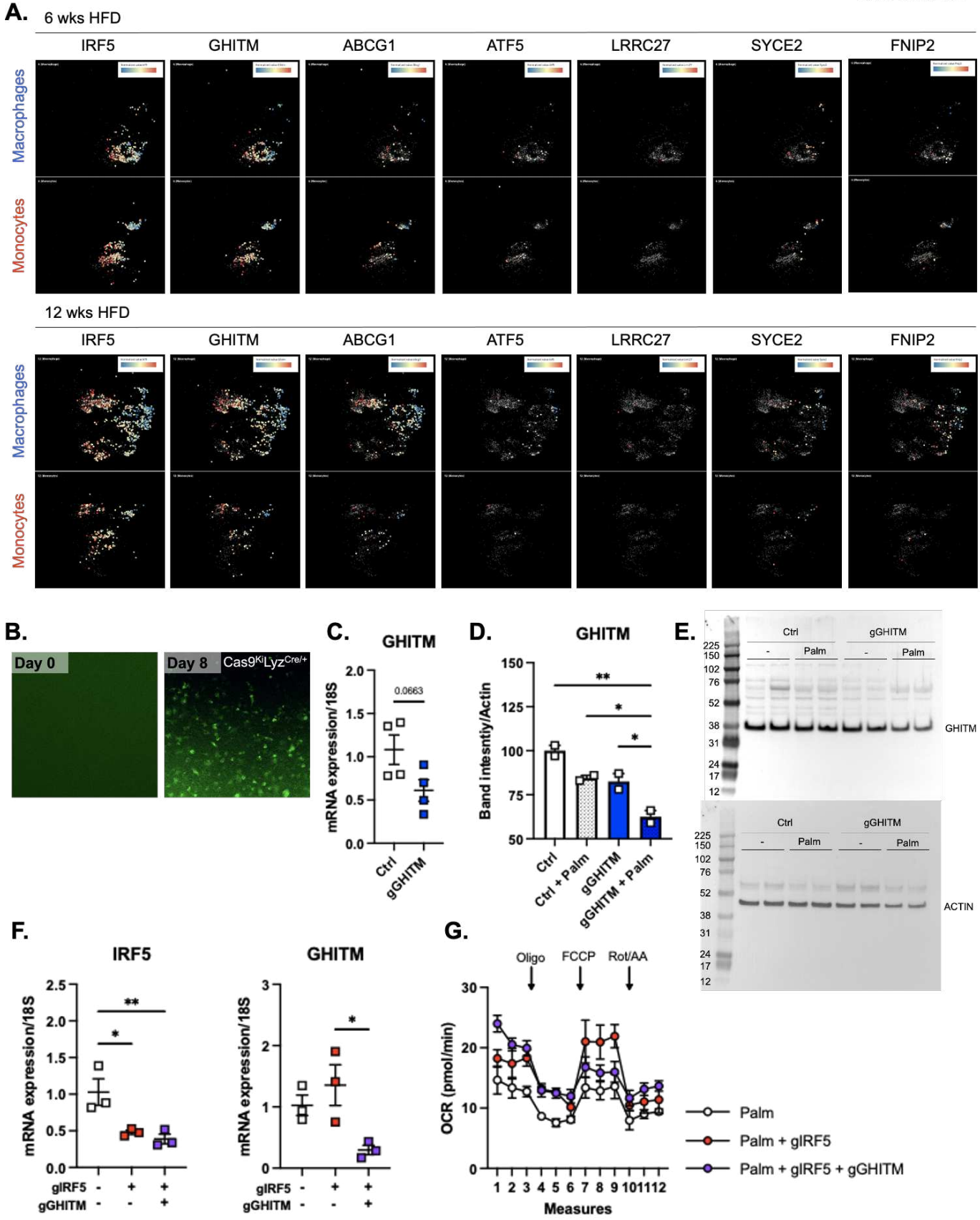

Figure S8: GHITM is highly expressed in epididymal visceral white adipose tissue macrophages and monocytes relative to other IRF5 targets.

A. Public dataset of single-cell RNA sequencing of the epididymal white adipose tissue stromal vascular fraction of C57BL/6J mice following 6 or 12 weeks of high-fat feeding. Macrophages and monocytes were identified and expression of IRF5, of GHITM and of ABCG1, SYCE2, FNIP2, ATF5 and LRRC27 were projected onto tSNE plots per cell type and duration of high-fat feeding.

B. Fluorescent image of bone marrow-derived macrophages (BMDMs) from mice with myeloid-restricted Cas9-GFP at day 0 and day 8 of differentiation (20 x magnification).

C. Gene expression of GHITM in Cas9-expressing BMDMs treated with lipofection agent (Ctrl) or with a gRNA targeting GHITM (gGHITM) (n=4 per condition, unpaired t-test p=0.0663).

D. Quantification of western blotting against GHITM in the same experiment as Fig. 6E (n=2 per condition, one-way ANOVA. **p=0.0046, *p=0.031, *p=0.043).

E. Full membranes of Fig. 6E western blotting.

F. IRF5 and GHITM expression (normalized to 18S), in Cas9-expressing BMDMs following transfection with a gRNA targeting IRF5 (gIRF5), double transfection with gGHITM and gIRF5 or with lipofection agent alone (Ctrl) (n=3 per condition, one-way ANOVA, *p=0.022, **p=0.009 for IRF5; and *p=0.019 for GHITM).

G. Oxygen consumption rate and maximal respiration from extracellular flux analysis on Palm-treated BMDMs following transfection with a gRNA targeting IRF5 (gIRF5), double transfection with gGHITM and gIRF5 or with lipofection agent alone (Ctrl). Cells were treated with oligomycin (Oli), carbonyl cyanide 4-(trifluoromethoxy) phenylhydrazone (FCCP) and Rotenone/Antimycin A (Rot/AA) administration (n=3 per condition).

Data are presented as mean ± SEM.

1208

Figure S9

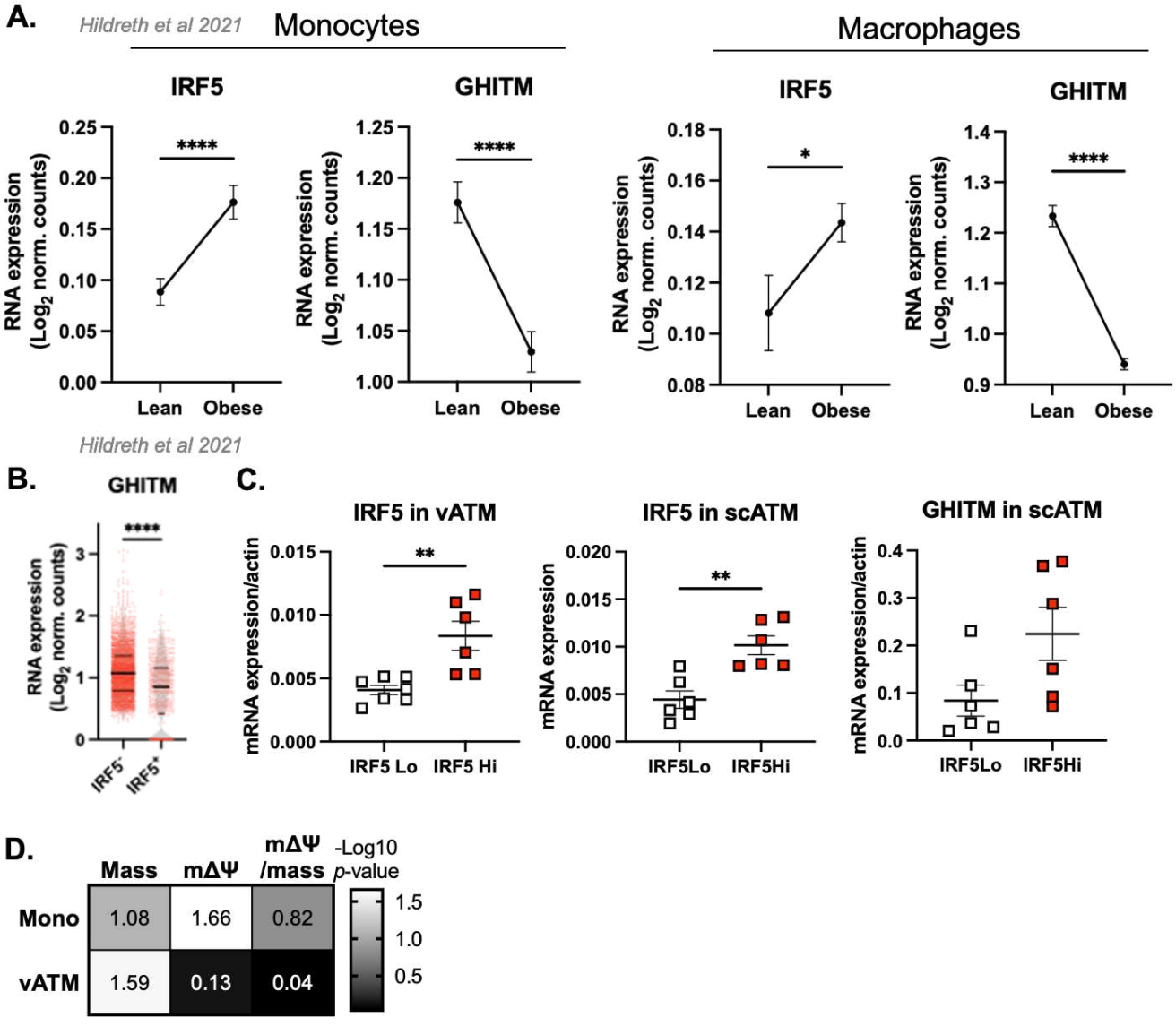

Figure S9

A. IRF5 and GHITM RNA counts in visceral AT (WAT) macrophages (top) and monocytes (bottom), from single-cell RNA sequencing of the stromal vascular fraction of healthy lean and obese human WAT (Hildreth *et al* 2021) (left-to-right, unpaired t-test ****p<0.0001, **** p<0.0001, *p=0.02, ****p<0.0001).

B. GHITM RNA expression in $IRF5^-$ and $IRF5^+$ expressing cells (Hildreth *et al* 2021) (unpaired t-test ****p<0.0001).

C. RNA expression of IRF5 normalized to actin in $CD14^+$ human visceral (vATMs) and subcutaneous adipose tissue macrophages (scATMs). GHITM RNA expression normalised to actin in $CD14^+$ scATMs. Samples were stratified based on their expression level of IRF5 into $IRF5^{Lo}$ versus $IRF5^{Hi}$ expressors (n=7-8 per group).

D. Correlative analyses of MFI of IRF5, JC1-Green (mitochondrial mass, Mt Mass), JC1-Red (mΔΨ), and JC1-Red-to-Green ratio (mΔΨ/mass) in human visceral ATMs (vATM) from obese patients and in monocytes from patients with T2D (Mono) analysed by FACS (n=11 for monocytes, n=9 for ATMs, Pearson r in Fig 7H).

SUPPLEMENTARY TABLES

Table S1. Genotyping primers

Genotyping		
IRF5 WT	F	CGT GTA GCA CTC CAT GCT CT
	R	AGG GCC TGT CCA GAA TTAGG
IRF5 Mut	F	CTT CGT ATA GCA TAC ATT ATACG
	R	AGG GCC TGT CCA GAA TTAGG
LyzM WT	F	TTA CAG TCG GCC AGG CTG AC
	R	CTT GGG CTG CCA GAA TTTCTC
LyzM Mut	F	CCC AGA AAT GCC AGA TTA CG
	R	CTT GGG CTG CCA GAA TTTCTC
Cas9 cre std WT	F	AAGGGAGCTGCAGTGGAGTA
	R	CAGGACAACGCCCACACA
Cas9 cre std MUT	F	CTTCTTCTTTGGGGCCATCT
	R	TCCCCATCAAGCTGATCC

Table S2. Surface markers for FACS analyses

Antibody	**Dye**	**Clone**	**Reference**
Human			
HLA-DR	Vioblue	AC122	Miltenyi ; 130-095-293
CD19	BV510	HIB19	BioLegend ; 302242
CD14	PE-Cy7	M5E2	BioLegend ; 301814
CD16	APC	3G8	BioLegend ; 302012
CD45	APC-eFluor780	HI30	eBioscience ; 47-0459-42
CD31	BV510	M89D3	BD ; 744463
CD11c	PerCP-Cy5.5	Bu15	Biolegend ; 337209
CD206	APC	15-2	BioLegend ; 321110
Mouse			
Antibody	Dye	Clone	Reference
CD206	BV421	C068C2	Biolegend ; 141717
CD19	BV510	6D5	Biolegend ; 115546
CD3	BV510	17A2	Biolegend ; 100234
CD45	PE-eF610	30-F11	Invitrogen ; 61-0451-82
F4/80	PE-Cy7	BM8	Invitrogen ; 25-4801-82
CD11c	APC	N418	Invitrogen ; 17-0114-81
CD11b	APC-Cy7	M1/70	Biolegend ; 101226

Table S3. Sequence-specific primers for quantitative RT-PCR

Murine primers		
Irf5	F	GATGGGGACAACACCATCTT
	R	GGCTTTTGTTAAGGGCACAG
TNF	F	CCACCACGCTCTTCTGTCTA
	R	CACTTGGTGGTTTGCTACGA
IL6	F	TACCACTTCACAAGTCGGAGGC
	R	CTGCAAGTGCATCATCGTTGTTC
GHITM	F	CTGCATTCTGGTGTGATGGG
	R	TGAGTACAGAGTGGCACCAG
F4/80	F	CCTTGGGAGCCTTCTGGATC
	R	CATCTGTGGCTGCCTCCCT
MCP1	F	GGGCCTGCTGTTCACAGTT
	R	CCAGCCTACTCATTGGGAT
18S	F	GGGAGCCTGAGAAACGGC
	R	GGGTCGGGAGTGGGTAATTT
Actin	F	GGCTGTATTCCCCTCCATCG
	R	CCAGTTGGTAACAATGCCATGT
CD206	F	TGTGGTGAGCTGAAAGGTGA
	R	CAGGTGTGGGCTCAGGTAGT
CD11c	F	CCATTTGCTTCCTCCAACAT
	R	GAGAGCCCAGACGAAGACAG
Human primers		
GHITM	F	TTCCATCACGAAGAATCAATGGC
	R	CCATAGTAGCACAATGCTCCAA
IRF5	F	CTCTTGTTAAGGGCACAGC
	R	AACACCATCTTCAAGGCCT
Actin	F	GGACTTCGAGCAAGAGATGG
	R	AGCACTGTGTTGGCGTACAG

Discussion and perspectives

The aim of the study was to characterize IRF5's role in the early metabolic adaptation of macrophages. This project highlights a novel role for IRF5, alongside its canonical function of promoting type-1 immunity, it also mediates cellular metabolic adaptations.

Based on our results, ATM undergo extensive IRF5-dependent remodeling of their cellular metabolism upon caloric excess. We used several *in vitro* approaches to modulate IRF5 expression and activity to assess its role in macrophage mitochondrial function. More precisely, IRF5 inhibits transcription of growth hormone inducible transmembrane protein (GHITM), which thus, represses mitochondrial function, potentially through a disruption of cristae structures.

To date, IRF5-dependent metabolic adaptations in macrophages were associated with glycolytic function, notably in the context of bacterial and viral infections (193,194). This study reveals a unique role for IRF5 in mitochondrial function in obesogenic conditions, underlying the specificity of the tissue micro-environment.

Nevertheless, additional evidences are required to fully support the mechanisms. Cristae structures need to be assessed in ATMs of IRF5-KO mice, and the potential role for GHITM in these cells requires to be addressed.

Macrophage mitochondrial function upon obesity and T2D

In this project, we confirmed the hypermetabolic state of ATMs upon obesity, and notably the increase in oxidative capacity and mitochondrial mass (190–192). We highlight that the hyperoxidative phenotype of IRF5-KO ATMs is protective, consistent with other studies (195,196). Interestingly, in our laboratory, current investigations performed on circulating monocytes from T2D patients underline that mitochondrial dysfunction is associated with a higher risk to develop a cardiovascular complication (Julla & Girard *et al*., in preparation). Monocytes treated with palmitate, *in vitro*, which levels are found to be elevated in obesity, undergo mitochondrial fragmentation. This process is protective as it attenuates inflammatory responses (197). Therefore, mitochondria appear to play a central role in macrophages/monocytes activation upon obesity and T2D and add a new axis of immunometabolic regulation. In this context, targeting macrophage mitochondrial function could represent an interesting therapeutic approach.

IRF5 activity upon metabolic stress : which signaling pathways ?

IRF5 expression and the IRF5-dependent metabolic adaptations are observed both with LPS and palmitate stimulation *in vitro*, and metabolic stressors *in vivo*. IRF5 appears to be a metabolic-responsive transcription factor and a sensor of lipotoxicity. However, lipotoxic signaling pathways mediating IRF5 activation remain unknown. TLR2/4-signaling can be activated by nutritional fatty acids, and notably palmitate (121) and IRF5 is one of the downstream targets of TLR4-signaling pathway, upon its ligation by bacterial LPS (66). However, a recent study demonstrated that palmitate is not a TLR4 agonist. TLR4 is yet required for palmitate-induced inflammation. TLR4 priming alters cellular metabolism and gene expression and palmitate metabolism are necessary for palmitate-mediated JNK pro-inflammatory signaling (198).

A priority in the field will be to further characterize the signaling pathways which induce IRF5 activation upon lipotoxicity. To answer this question, it would be interesting to assess IRF5 expression and activation upon metabolic stress in BMDMs deleted for TLR2, TLR4 and also the lipid scavenger receptor CD36.

Role of GHITM in immune cell polarization ?

To reveal IRF5-dependent mechanism that impairs macrophage mitochondrial respiration, we combined public datasets with our sets of RNA sequencing. We identified GHITM as a potential target. GHITM is an inner mitochondrial membrane protein which is required for the maintenance of cristae structures, where ETC complexes anchor (199). In our study, GHITM expression is maintained in IRF5-KO macrophages upon stimulation. Modification of cristae structure in IRF5-KO macrophages can explain the hyperoxidative phenotype and could be mediated by GHITM.

Interestingly, previous reports have reported a downregulation of GHITM in lymphocytes stimulated with pro-inflammatory cytokines and in monocytes exposed to viruses (200,201). Here, we highlight a novel mechanism in which IRF5 appears to repress GHITM expression upon metabolic stress and LPS stimulation, *in vitro*. However, the specific functional contribution of GHITM downregulation to effective inflammation remains unknown.

GHITM downregulation has been associated with mitochondria fragmentation and could be a source of ROS for bacteria killing. M1 macrophages have a smaller mitochondrial network which is fragmented. M2 macrophages have larger interconnected mitochondria where

OXPHOS can be maximized by remodeling of cristae shape (142). The fragmentation of the mitochondrial network and ROS production when IRF5 and/or GHITM are knocked-down remain yet to be explored.

In addition, IRF5 is expressed in several immune cell types, such as dendritic cells. It could be interesting to validate if this macrophage IRF5-GHITM axis can extend to other immune cells and contexts, and notably viral or bacterial infections.

Understanding IRF5 binding decisions and GHITM repression

Moreover, ChIP-seq analysis of IRF5 indicate that IRF5 could control transcription of inflammatory pathways (as previously described) and of metabolic pathways. This observation is consistent with other studies (194) and gives insight into novel roles for IRF5 as a transcription factor controlling cellular metabolism and adaptation to microenvironmental metabolic cues. It would be interesting to elucidate how and through which regulatory elements IRF5 may be binding to such non-inflammatory targets as GHITM. Whilst it is widely accepted that IRF5, and other IRFs, target ISRE, the presence and significance of ISREs on metabolically relevant genes remains to be investigated. Furthermore, it appears that after long-term (LT)-HFD, IRF5 mostly controls the transcription of genes associated with the inflammatory response. This suggests that the binding decision induced by ST- and LT-HFD and the associated signaling pathways might be different.

First, it would be interesting to understand how IRF5 represses the expression of GHITM, whether this repression is direct or not. In this study, we use different public data-sets to highlight that IRF5 binds on or upstream of GHITM transcription start site. Nevertheless, we should confirm IRF5 binding in the context of metabolic stress, notably on ATMs using CUT&Tag approaches. RNA polymerase II recruitment of the promoter of GHITM upon metabolic stress needs to be assessed. Finally, IRF5-mediated repression of genes requires interaction with KAP1 (76), a transcriptional co-repressor. KAP1 contributes to the recruitment of complexes involved in chromatin silencing. Further analysis to characterize IRF5 interactome, chromatin opening and epigenetic marks would be required to understand by which mechanism IRF5 represses GHITM expression.

Linking cellular metabolic adaptations with AT phenotype ?

In this study, IRF5-KO ATMs are hyperoxidative during short-term caloric excess. This

hyperoxidative phenotype is associated with a protective AT phenotype, characterized by a better insulin sensitivity. One area of further investigation will be to integrate cellular metabolism with the beneficial adaptation of AT. Two different studies have linked macrophage oxidative phenotype with systemic insulin sensitivity and metabolic health. First Jung *et al*. developed a murine model with decreased macrophage oxidative respiration. These mice, when subjected to obesity, are more insulin resistant (195). Moreover, the decrease in mitochondrial function is associated with a pro-inflammatory phenotype, due to an altered secretion of GDF15. Then, Wang *et al*. developed an anti-inflammatory agent that targets ATMs mitochondria. This peptide accumulates in the mitochondria, promotes an hyperoxidative phenotype and inhibits pro-inflammatory polarization of macrophages. Obese mice treated with this compound exhibit a better insulin sensitivity and a lower body gain compared to mice treated with vehicle. This treatment also reverses hepatic steatosis (196). In these two studies, the authors link the beneficial effects of ATMs hyperoxidative phenotype with a decrease in the pro-inflammatory polarization. However, in our study, IRF5-KO and WT ATMs do not differ in terms of inflammatory polarization. To further characterize the mechanisms by which IRF5-KO ATMs affect AT phenotype, it would be interesting to assess the secretome of these hyperoxidative macrophages, upon metabolic stress. Indeed, this phenotype could be related to non-inflammatory mediators, similarly to liver macrophages that regulate systemic metabolism independently of inflammation (202). Moreover, macrophages excretes metabolites that can act on a paracrine manner on adipocytes. Macrophages produce lactate (203), which is known to inhibit lipolysis in the AT through the G-coupled receptor GPR81 (204). Extracellular succinate, potentially released by macrophages (205) can bind to GPR91 and affect adipocyte function by inhibiting lipolysis (206). Therefore, analysis of macrophage secretome coupled with intracellular metabolome could give insights on a potential metabolite-related macrophage-adipocyte crosstalk to understand how IRF5-KO hyperoxidative phenotype promotes beneficial adaptation of the AT.

Therapeutic strategies to target IRF5 ?

This study highlights the role of IRF5 in the early metabolic adaptations to caloric stress, before the establishment of a frank insulin resistance status. IRF5 dysregulated activity has been associated with the development of metabolic disorders (67,70,84) and as well as autoimmune pathologies (82). Given its deleterious role in these conditions, and notably in

obesity and T2D, IRF5 represents an interesting therapeutic target. Inhibiting IRF5 activity during metabolic surplus could favor a beneficial AT adaptation in the early stages of caloric excess, and later on, promote AT remodeling and protect from insulin resistance and T2D.

Strategies to modulate its activity involve silencing its expression, interfering with the post-translational modifications and with its binding partners. Kinases inhibitors could represent an attractive alternative to downregulate its activation. To silence its expression, small interfering RNA (siRNA) approaches have been developed. One challenge consists in efficient delivery to the target cells, notably with lipid cationic nanoparticles. In the context of obesity and metabolic disorders, glucan-encapsulated particles have been shown to target specifically ATMs (207). In the present study, we used a cell-penetrating IRF5-decoy peptide to inhibit IRF5 dimerization and nuclear translocation, *in vitro*. This peptide represent a potent tool to target IRF5 activity in a therapeutic approach. More precisely, this peptide could be used in combination of glucan-encapsulated particles-based approaches to specifically target ATMs (208,209).

Axis 2: Cellular metabolism and macrophage polarization

Hypothesis and aims of the study

Macrophages are innate immune cells with high phenotypic plasticity. Upon environmental stressors, they polarize on a large spectrum from anti-inflammatory (M2) to pro-inflammatory (M1) phenotype. While the different pathways involved in macrophage polarization at the transcriptional, epigenetic and more particularly metabolic levels are well described, the directionality between cellular metabolism and macrophage polarization is not clearly established.

The aim of the project is to study whether the disruption of cellular metabolism influences *per se* macrophage polarization and cytokine production *in vitro*. To answer this question, we applied metabolic inhibitors to BMDMs and assessed their polarization by gene expression and cytokine production.

Perspective on Direction of control: Cellular metabolism and macrophage polarization

Ronan Thibaut[1*], Lucie Orliaguet[1*], Tina Ejlalmanesh[1], Nicolas Venteclef[1], Fawaz Alzaid[1,2*]

[1]Institut Necker Enfants Malades (INEM), INSERM U1151/CNRS UMRS8253, IMMEDIAB, Université de Paris Cité, 75015 Paris, France

[2]Dasman Diabetes Institute, Kuwait, Kuwait

[*]Equal contribution

[*]Correspondence: Dr Fawaz Alzaid
fawaz.alzaid@dasmaninstitute.org; fawaz.alzaid@inserm.fr

Keywords: **Macrophages, Polarization, Metabolism**

Abstract

Macrophages are innate immune cells with high phenotypic plasticity. Depending on the microenvironmental cues they receive, they polarize on a spectrum with extremes being pro- or anti-inflammatory. As well as responses to microenvironmental cues, cellular metabolism is increasingly recognized as a key factor influencing macrophage function. While pro-inflammatory macrophages mostly use glycolysis to meet their energetic needs, anti-inflammatory macrophages heavily rely on mitochondrial respiration. The relationship between macrophage phenotype and macrophage metabolism is well established, however its precise directionality is still under question. Indeed, whether cellular metabolism *per se* influences macrophage phenotype or whether macrophage polarization dictates metabolic activity is an area of active research. In this short perspective article, we sought to shed light on this area. By modulating several metabolic pathways in bone marrow-derived macrophages, we show that disruption of cellular metabolism does *per se* influence cytokine secretion profile and expression of key pro-inflammatory genes. Only some pathways seem to be involved in these processes, highlighting macrophage need for specific metabolic functions in regulation of their phenotype. We thus demonstrate that the intact nature of cell metabolism influences macrophage phenotype and function, addressing the directionality between these two aspects of macrophage biology.

Introduction

Macrophages are innate immune cells that populate all tissues and have a number of homeostatic roles (removing dead cells and cellular debris, recycling iron…). One of their main immune functions is to recognize and phagocytose pathogens (Murray 2011). Following recognition, they also produce cytokines that can recruit and induce differentiation of monocytes and T cells. Additionally, they play an important role in tissue repair once the immune response has been terminated (Murray 2011).

Macrophages can respond to a variety of molecular cues through activation of Toll-Like Receptors (TLRs), and will secrete cytokines accordingly. Following activation, they will transition from a quiescent state to an activated one. Depending on the cues

they receive, they can adopt different activated phenotypes. Based on *in vitro* experiments, activated macrophages have been historically divided into M1 pro-inflammatory or M2 anti-inflammatory macrophages (Mantovani 2002). Stimulating macrophages with lipopolysaccharide (LPS) and interferon-γ (IFN-γ) triggers their differentiation into M1 macrophages whereas interleukin 4 (IL4) and IL13 promote M2 phenotype (Stein 1992, Biswas 2010).

M1 and M2 macrophages display different metabolic properties. M1 macrophages have increased glucose uptake through the Hypoxia Inducible Factor 1α (HIF1α)-dependent upregulation of glucose transporters. This increased glucose uptake is essential to fuel glycolysis and thus produce ATP. M1 macrophages scarcely use mitochondrial respiration as they have a defective tricarboxylic acid (TCA) cycle (**Figure 1A**) (Tannahil 2013, Meiser 2016, Wculek 2022).

M2 macrophages, on the other hand, produce ATP mostly through mitochondrial respiration and have only limited glycolytic activity. Fueling the TCA cycle, M2 macrophages enhance their uptake of fatty acids. Fatty acid oxidation (FAO) provides Acetyl-coA to a fully functional TCA cycle (Huang 2014). TCA cycle-derived NADH is then used by the electron transport chain (ETC) to generate ATP through ATP synthase (**Figure 1A**) (Orliaguet 2020, Wculek 2022).

In vivo, environmental factors that vary between different tissues or between homeostasis and disease are increasingly recognized as powerful dictators of macrophage metabolism. Macrophages in inflammatory conditions and inflammatory diseases are predominantly glycolytic. For example, macrophages in rheumatoid arthritis (RA) up-regulate the enolase enzyme, which stimulates production of pro-inflammatory cytokines, and show elevated succinate levels (Bae 2011, Kim 2014). In diet-induced obesity, adipose tissue macrophages are hypermetabolic, up-regulating both glycolytic activity and mitochondrial respiration (Boutens 2018). Yet, these macrophages were long considered M1-like and are known to promote insulin resistance and metabolic syndrome (Orliaguet 2020). Such environmentally adapted profiles raise the question of precise directionality between macrophage metabolism and inflammatory profile.

Here, we use bone marrow-derived macrophages (BMDMs), with inhibitors of specific metabolic pathways to shed light on the direction of control between cellular metabolism and capacity to mount an inflammatory response. Using cytokine production as a functional read-out for macrophage phenotype, we show that impairing metabolic pathways drastically impacts macrophage phenotype. Some metabolic pathways have differential effects on cytokine secretion profile, suggesting that additional factors may directly influence macrophage phenotype in synergy with metabolic parameters.

Results

Biasing cellular metabolism alters inflammatory marker expression in quiescent macrophages

We first wondered whether biasing macrophage metabolism could *per se* influence macrophages in their quiescent state. Following treatment with inhibitors of glycolysis, mitochondrial respiration or both, we quantified transcription of inflammatory markers

Tnfα, Il6, Il1β and *Mcp1* (**Figure 1B**). When treated with 2-deoxyglucose (2DG), a non-metabolizable glucose analog which inhibits glycolysis, BMDMs showed decreased *Tnfα and Mcp1* transcription compared to untreated cells, but no change for *Il6* and *Il1β* (**Figure 1C**). Inhibiting the mitochondrial ETC with Rotenone and antimycin A (Rot/AA) resulted in similar decrease in *Tnfα* transcription. Oligomycin (Oligo, inhibitor of ATP synthase) and Etomoxir, which inhibits carnitine palmitoyl transferase 1a (Cpt1a), a rate-limiting enzyme for FAO, did not show any significant effect on cytokine transcription. The combination of Etomoxir and 2DG did not display any additive effect compared with the single inhibitor setting. These results suggest that cellular metabolism, in particular intact activity of glycolysis and mitochondrial ETC, is important to maintain macrophages in a quiescent state. However, the lack of impact of the different aforementioned metabolic inhibitors on *Il6* and *Il1β* transcription suggests that metabolism could impact specific pathways.

Conversely, inhibiting some metabolic pathways also resulted in increased transcription of inflammatory markers. For example, oligomycin results in increased *Il6* expression in quiescent BMDMs.

Cellular metabolism influences macrophage response to an inflammatory challenge

We next wondered what was the impact of cellular metabolism on macrophage capacity to polarize. BMDMs were pretreated with metabolic inhibitors then stimulated with bacterial LPS, the main TLR4 ligand known to induce M1-like polarization. In cells pre-treated with 2DG, LPS-induced expression of *Il6* was attenuated (**Figure 2A**). This effect was also observed in cells pre-treated with oligomycin. No major effect was observed when the cells were treated with Rot/AA or with Etomoxir. Interestingly, inhibition of metabolic pathways did not affect LPS-induced *Tnfα* transcription. This indicates a functionally specific requirement for glycolysis and ATP synthase activity in LPS-induced expression of *Il6* and *Tnfα*. *Il6* expression, but not *Tnfα*, requires intact glycolytic flux and ATP synthase activity.

We next measured cytokine secretion into the extracellular medium. Inhibiting any of the aforementioned metabolic pathways resulted in decreased IL6 and MCP1 secretion. Metabolic inhibition, with the exception of FAO inhibition alone, also had a dramatic effect on TNFα secretion, while it did not induce significant changes in IL1β and IL10 secretion. Inhibiting glycolysis had the most dramatic and consistent effect across measured cytokines. Inhibiting mitochondrial ETC at multiple levels, NADH:ubiquinone oxidoreductase, coenzyme Q-cytochrome c reductase or ATP synthase (Complexes I, III or V), comparably attenuated cytokine secretion. Inhibiting FAO had the least pronounced effect cytokine secretion except for IL10 (**Figure 2B**). These results suggest that targeted metabolic pathways alter macrophage capacity to secrete inflammatory cytokines in response to LPS. Glycolysis and the mitochondrial ETC are instrumental in cytokine secretion in response to TLR4 ligation while FAO contributes in a more limited extent. Overall, these findings show that metabolism is important for macrophage secretory profile. However, only specific metabolic pathways are capable of influencing transcriptional profile.

We next evaluated transcriptional response to IL4, a canonical M2-like inducer. Following IL4 stimulation, few cytokines showed an increase in their transcription (**Figure 2C**). Inhibiting any metabolic pathway other than FAO strongly decreased *Mcp1* transcription in response to IL4. Strikingly, while glycolysis did not seem to play any role in *Mcp1* up-regulation following LPS stimulation, it was pivotal in response to IL4. However, metabolic inhibition did not modulate transcription of the other measured

cytokines. These results show that macrophage cellular metabolism greatly impacts macrophage capacity to polarize and that specific metabolic pathways have differential roles in promoting M1 or M2 phenotype.

Discussion

Metabolism is tightly linked to macrophage polarization as M1 macrophages are predominantly glycolytic while M2 macrophages rely heavily on mitochondria. Here, we studied the impact of macrophage cellular metabolism on macrophage phenotype. We show that macrophage polarization depends on cellular metabolic activities and more particularly on some pivotal metabolic pathways like glycolysis. Interestingly, this dependency is functionally specific with respect to the cytokines affected and alters secretory capacity to a greater extent than transcription.

Additionally, we show that transcription of some cytokines was unexpectedly boosted by metabolic inhibition. It is possible that, following inhibition of a given pathway, metabolites used by this pathway are redirected towards other pathways in which activity is increased. This could be a mechanism of adaptation to the metabolically challenging environment. Such compensatory mechanisms have already been described in monocytes, in which IL6 production is quickly restored after depriving monocytes of ATP and glucose (Krauss 2021).

The impact of cellular metabolism on quiescent macrophage polarization differs between M1 and M2 macrophages. The impact of metabolic inhibition on M2 differentiation seems to be more limited than on M1 differentiation. This is of particular interest in some contexts like metabolic syndrome. In this disease, macrophages face changes in metabolic substrate availability, such as lipid overload. Moreover, in treated individuals, macrophages are also exposed to metabolically active therapeutic agents. Macrophages can accumulate in metabolic organs, adipose tissue and the liver, and exhibit an M1-like phenotype which is central to metabolic decline and the development of insulin resistance (Prieur 2011, Han 2013, Orliaguet 2020). Thus, our data suggest that changes in the metabolic environment of the cells could lead to changes in macrophage metabolic status and subsequently in macrophage phenotype. Alternatively, in therapeutic perspectives, altering availability of substrates or functioning of metabolic pathways can profoundly impact macrophage secretory profile. The question remains in defining at-risk groups and controlling cell-specific delivery of metabolically acting drugs. Future preclinical work will shed light on the feasibility of such approaches.

The M1/M2 classification has been challenged since it was first proposed. It poorly recapitulates the diversity of macrophage subpopulations found *in vivo.* Macrophages display great phenotypic and functional diversity depending on the tissues they populate, their ontogeny, or their states in health and disease (Blériot 2020). Such specificity could also arise in macrophage reliance on metabolic pathways or on adaptability of cellular metabolism. Additionally, recent studies have uncovered diversity in macrophage populations of a given tissue. For instance, Chakarov *et al* showed the existence of two subpopulations of macrophages that are conserved across several tissues and are localized in distinct tissular niches (Chakarov 2019). Whether such subpopulations share common metabolic features or whether their different localizations also translate into different metabolic activities largely remains

unknown. Differences in metabolic status between tissue-resident and monocyte-derived macrophages are still under investigation.

Future work could decipher the metabolic diversity of macrophages *in vivo*, adding mechanistic insight and rationale for redeployment of metabolically active therapeutics. Until recently, such investigations were considered technically challenging. However, techniques allowing single-cell resolution in analysis, e.g. SCENITH (Argüello 2020), are gaining accessibility and bring us closer to overcoming the technical challenges encountered when studying cellular heterogeneity across tissues, both in health and disease.

Methods

BMDMs production and stimulation

Tibias and femurs from C57BL/6J mice were collected. Bone marrow cells were recovered by flushing the bones with PBS. After red blood cell lysis, cells were plated in 12- or 24-well plates at a concentration of $1x10^6$/mL in BMDM medium (DMEM with GlutaMAX supplemented with 10% FCS, 30% L929-conditioned medium and 100U/mL Penicilin, 100µg/mL streptomycin). Culture medium was renewed every two days.
After 6 to 7 days of differentiation, BMDMs were pre-treated for 30 min with either 10mM 2-DG (D8375), 10µM rotenone (R8875), 5µM antimycin A (A8674), 10µM oligomycin (O4876), 10µM etomoxir (E1905) or a combination of several of these drugs for 30min. The cells were then stimulated with LPS (10ng/ml) (L2630) or IL4 (10ng/mL) (130-094-061, Miltenyi Biotech) for 2h in continued presence of metabolic inhibitors. Unless otherwise stated, all compounds were purchased from Sigma Aldrich.

Quantification of cytokine transcription

mRNAs were purified using either Qiagen RNeasy or Macherey-Nagel Nucleospin RNA kits, according to manufacturer's instruction.
mRNAs were retrotranscribed into cDNAs using M-MLV Reverse Transcriptase kit (Promega). Quantitative RT-PCRs were performed with MESA green mastermix (Eurogentec) and target-specific primers using QuantStudio 3 Real-Time PCR Systems (ThermoFisher Scientific). *18S* RNA was used for normalization of mRNA levels. The DNA sequences of primers used for qPCR are listed in **Table 1**.

	Forward	Reverse
18S	GGGAGCCTGAGAAACGGC	GGGTCGGGAGTGGGTAATTT
Il6	TACCACTTCACAAGTCGGAGGC	CTGCAAGTGCATCATCGTTGTTC
Tnfa	CCACCACGCTCTTCTGTCTA	CACTTGGTGGTTTGCTACGA
Mcp1	GGGCCTGCTGTTCACAGTT	CCAGCCTACTCATTGGGAT
Il10	GCTGGACAACATACTGCTAACC	ATTTCCGATAAGGCTTGGCAA
Il1b	GCAACTGTTCCTGAACTCAACT	ATCTTTTGGGGTCCGTCAACT

Table 1. Sequences of DNA primers used in RT-qPCR reactions.

Quantification of cytokine secretion

Culture medium from stimulated BMDMs was recovered and cytokine quantification was performed using BioLegend LegendPlex kit according to manufacturer's instructions. Data were analyzed using Qognit software.

Statistical analysis

Statistical analysis was performed with GraphPad Prism (La Jolla, CA, USA). Data are presented as mean ± SEM. Comparison between groups was performed with either one-way ANOVA followed by Tukey's test or two-way ANOVA followed by Dunnett's multiple comparison test.

Conflict of interest

The authors declare that the research was conducted in the absence of any commercial or financial relationships that could be construed as a potential conflict of interest.

Author contributions

RT, LO and FA designed the study. RT, LO and TE produced and analyzed experimental data. RT and FA wrote the manuscript. LO, TE and NV contributed in manuscript writing.

Funding

This work was supported by the French National Research Agency (*Agence Nationale de la Recherche*; ANR) ANR-JCJC grant for the MitoFLAME Project ANR-19-CE14-0005 to FA. RT was supported by a grant from the European Foundation for the Study of Diabetes (EFSD). LO was supported by *Fondation de la Recherche Médicale* (FDT202106013230).

Bibliography

Argüello RJ, Combes AJ, Char R, Gigan J-P, Baaziz AI, Bousiquot E, Camosseto V, Samad B, Tsui J, Yan P, et al. SCENITH: A Flow Cytometry-Based Method to Functionally Profile Energy Metabolism with Single-Cell Resolution. *Cell Metab* (2020) **32**:1063-1075.e7. doi: 10.1016/j.cmet.2020.11.007

Bae S, Kim H, Lee N, Won C, Kim H-R, Hwang Y, Song YW, Kang JS, Lee WJ. α-Enolase expressed on the surfaces of monocytes and macrophages induces robust synovial inflammation in rheumatoid arthritis. *J Immunol* (2012) **189**:365–372. doi: 10.4049/jimmunol.1102073

Biswas SK, Mantovani A. Macrophage plasticity and interaction with lymphocyte subsets: cancer as a paradigm. *Nat Immunol* (2010) **11**:889–896. doi: 10.1038/ni.1937

Blériot C, Chakarov S, Ginhoux F. Determinants of Resident Tissue Macrophage

293 Identity and Function. *Immunity* (2020) **52**:957–970. doi:
294 10.1016/j.immuni.2020.05.014

295 Boutens L, Hooiveld GJ, Dhingra S, Cramer RA, Netea MG, Stienstra R. Unique
296 metabolic activation of adipose tissue macrophages in obesity promotes
297 inflammatory responses. *Diabetologia* (2018) **61**:942–953. doi: 10.1007/s00125-
298 017-4526-6

299 Chakarov S, Lim HY, Tan L, Lim SY, See P, Lum J, Zhang X-M, Foo S, Nakamizo S,
300 Duan K, et al. Two distinct interstitial macrophage populations coexist across
301 tissues in specific subtissular niches. *Science* (2019) **363**:eaau0964. doi:
302 10.1126/science.aau0964

303 Han MS, Jung DY, Morel C, Lakhani SA, Kim JK, Flavell RA, Davis RJ. JNK
304 expression by macrophages promotes obesity-induced insulin resistance and
305 inflammation. *Science* (2013) **339**:218–222. doi: 10.1126/science.1227568

306 Huang SC-C, Everts B, Ivanova Y, O'Sullivan D, Nascimento M, Smith AM, Beatty W,
307 Love-Gregory L, Lam WY, O'Neill CM, et al. Cell-intrinsic lysosomal lipolysis is
308 essential for alternative activation of macrophages. *Nat Immunol* (2014) **15**:846–
309 855. doi: 10.1038/ni.2956

310 Kim S, Hwang J, Xuan J, Jung YH, Cha H-S, Kim KH. Global Metabolite Profiling of
311 Synovial Fluid for the Specific Diagnosis of Rheumatoid Arthritis from Other
312 Inflammatory Arthritis. *PLoS ONE* (2014) **9**:e97501. doi:
313 10.1371/journal.pone.0097501

314 Krauss P-L, Pfeiffenberger M, Damerau A, Buttgereit T, Chen Y, Gaber T, Buttgereit
315 F. Production of IL-6 and Phagocytosis Are the Most Resilient Immune
316 Functions in Metabolically Compromised Human Monocytes. *Front Immunol*
317 (2021) **12**:730672. doi: 10.3389/fimmu.2021.730672

318 Mantovani A, Sozzani S, Locati M, Allavena P, Sica A. Macrophage polarization:
319 tumor-associated macrophages as a paradigm for polarized M2 mononuclear
320 phagocytes. *Trends Immunol* (2002) **23**:549–555. doi: 10.1016/s1471-
321 4906(02)02302-5

322 Meiser J, Krämer L, Sapcariu SC, Battello N, Ghelfi J, D'Herouel AF, Skupin A, Hiller
323 K. Pro-inflammatory Macrophages Sustain Pyruvate Oxidation through Pyruvate
324 Dehydrogenase for the Synthesis of Itaconate and to Enable Cytokine
325 Expression. *J Biol Chem* (2016) **291**:3932–3946. doi: 10.1074/jbc.M115.676817

326 Murray PJ, Wynn TA. Protective and pathogenic functions of macrophage subsets.
327 *Nat Rev Immunol* (2011) **11**:723–737. doi: 10.1038/nri3073

328 Orliaguet L, Dalmas E, Drareni K, Venteclef N, Alzaid F. Mechanisms of Macrophage
329 Polarization in Insulin Signaling and Sensitivity. *Front Endocrinol (Lausanne)*
330 (2020) **11**:62. doi: 10.3389/fendo.2020.00062

331 Prieur X, Mok CYL, Velagapudi VR, Núñez V, Fuentes L, Montaner D, Ishikawa K,
332 Camacho A, Barbarroja N, O'Rahilly S, et al. Differential lipid partitioning
333 between adipocytes and tissue macrophages modulates macrophage lipotoxicity

and M2/M1 polarization in obese mice. *Diabetes* (2011) **60**:797–809. doi: 10.2337/db10-0705

Stein M, Keshav S, Harris N, Gordon S. Interleukin 4 potently enhances murine macrophage mannose receptor activity: a marker of alternative immunologic macrophage activation. *J Exp Med* (1992) **176**:287–292. doi: 10.1084/jem.176.1.287

Tannahill GM, Curtis AM, Adamik J, Palsson-McDermott EM, McGettrick AF, Goel G, Frezza C, Bernard NJ, Kelly B, Foley NH, et al. Succinate is an inflammatory signal that induces IL-1β through HIF-1α. *Nature* (2013) **496**:238–242. doi: 10.1038/nature11986

Wculek SK, Dunphy G, Heras-Murillo I, Mastrangelo A, Sancho D. Metabolism of tissue macrophages in homeostasis and pathology. *Cell Mol Immunol* (2022) **19**:384–408. doi: 10.1038/s41423-021-00791-9

Data availability statement

The raw data supporting the conclusions of this article will be made available by the authors upon request.

Figure legends

Figure 1: Impact of macrophage metabolism on quiescent macrophage phenotype. (A) Representation of M1 and M2 macrophage metabolism. FAO: fatty acid oxidation. ETC: Electron transport chain. TCA cycle: tricarboxylic acid cycle. (B) Experimental design: bone marrow-derived macrophages (BMDMs) were treated with metabolic inhibitors for 30 min before being stimulated with M1/M2 stimulus or left untreated for 2 h. Macrophage response was then assessed by quantifying cytokine concentration in the extracellular medium or through mRNA quantification by qPCR. (C) Relative mRNA expression for *Tnfα*, *Il6*, *Il1β*, *Mcp1* and *Il10* in quiescent BMDMs either left untreated or treated with 2-deoxyglucose (2-DG), oligomycin (Oligo), rotenone/antimycin A (Rot/AA), Etomoxir (Eto) or a combination of 2-DG and Etomoxir (Eto+2-DG). Data are expressed as mean ± SEM. ns: non significant. * p<0.05, *** p<0,001, **** p<0,0001. Unless otherwise stated, comparison between groups are non significant.

Figure 2: Impact of macrophage metabolism on activated macrophage polarization. Bone marrow-derived macrophages (BMDMs) were treated with metabolic inhibitors for 30 min before being stimulated with M1/M2 stimulus or left untreated for 2 h. Macrophage response was then assessed by quantifying cytokine concentration in the extracellular medium or through mRNA quantification by qPCR. (A) Relative mRNA expression for *Tnfα*, *Il6*, *Il1β*, *Mcp1* and *Il10* in BMDMs pre-treated with 2-deoxyglucose (2-DG), oligomycin (Oligo), rotenone/antimycin A (Rot/AA), Etomoxir (Eto) or a combination of 2-DG and Etomoxir (Eto+2-DG) and then stimulated with LPS for 2h. (B) Concentration of TNFα, IL6, IL1β, MCP1 and IL10 in extracellular

medium of BMDMs. (C) Relative mRNA expression for *Tnfα*, *Il6*, *Il1β*, *Mcp1* and *Il10* in BMDMs pre-treated with 2-DG, Oligo, Rot/AA, Eto or Eto+2-DG, and then stimulated with IL4 for 2h. ns: non significant, *p<0.05, **** p<0.0001. Unless otherwise stated, comparison between groups are non-significant.

381 **Figure 1**

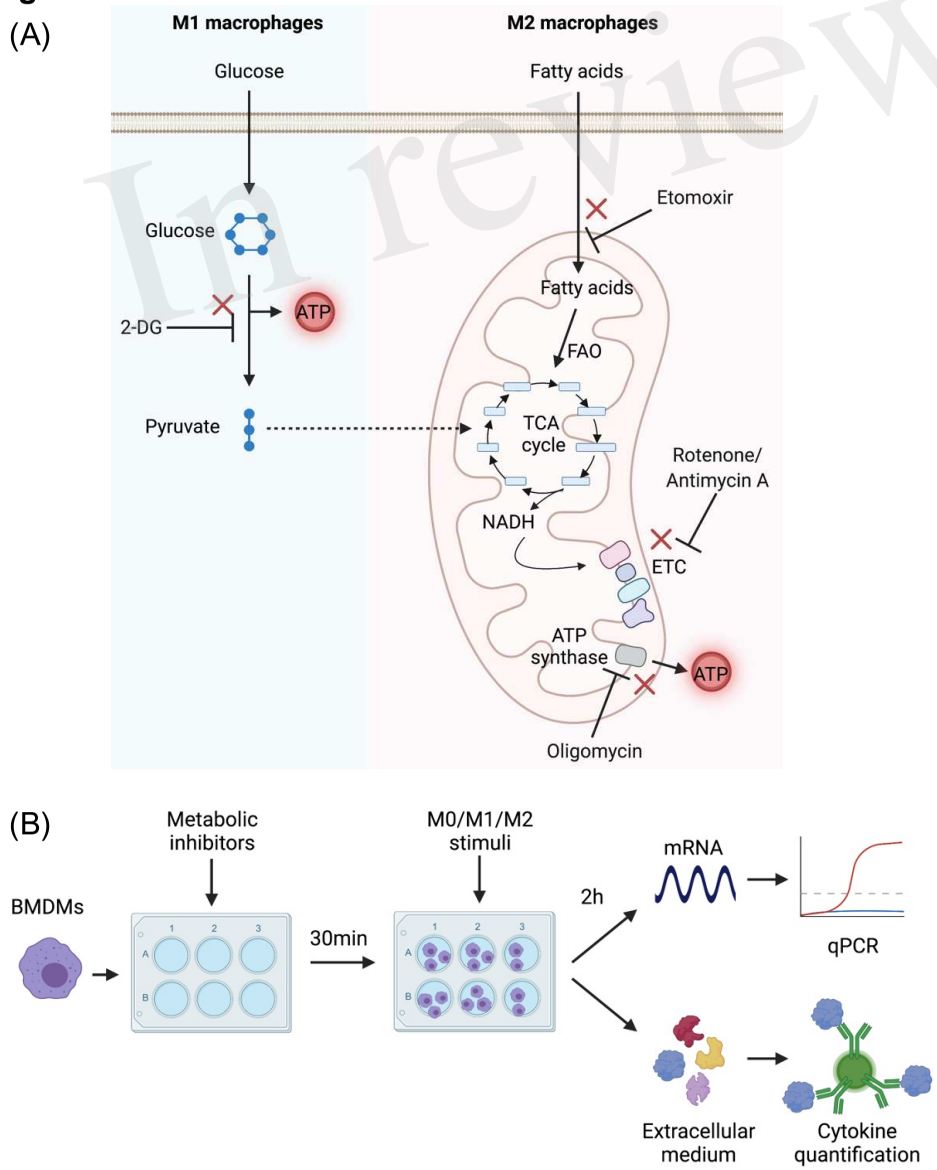

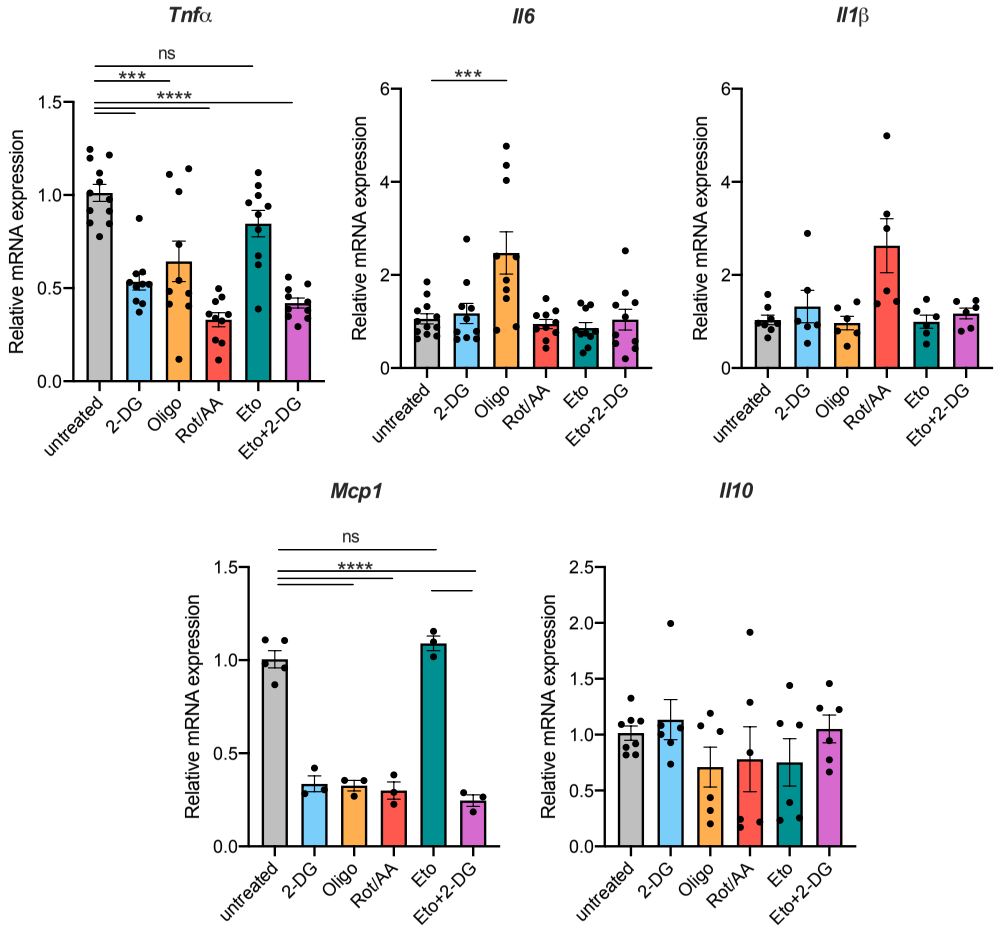

382 **Figure 2**

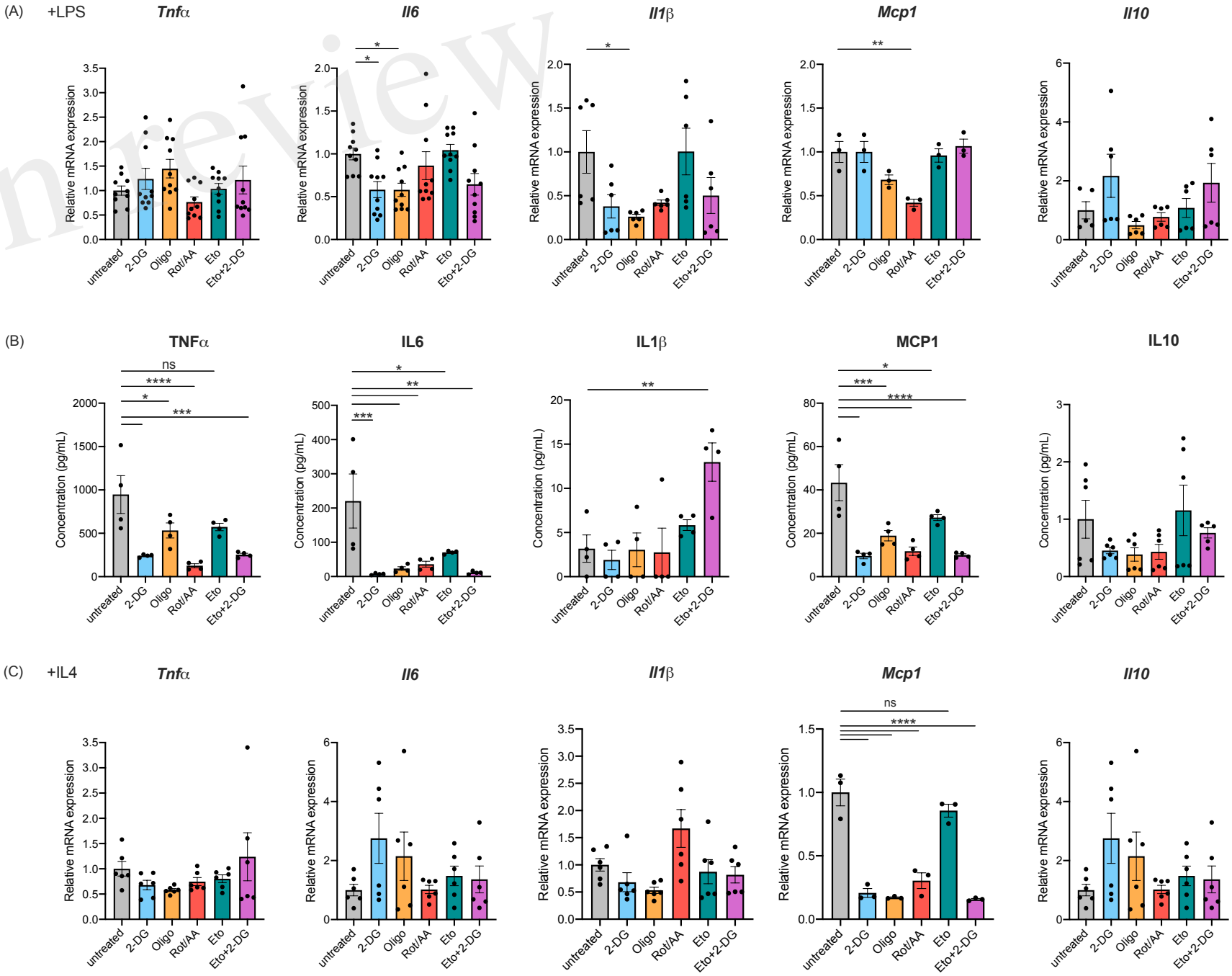

Discussion and perspectives

This short report underlies the importance of cellular metabolism in the polarization of macrophages. Inhibition of metabolic pathways alters cytokine transcription and secretion, and thus macrophage polarization. Metabolic pathways provide energy and building blocks for cytokine production and act as a potent regulator of macrophage polarization. For a mechanistic insight, it would be interesting to understand the precise contribution of each pathway to cytokine production.

As a perspective, integrating these *in vitro* data with the specificity of tissue-resident macrophages and their microenvironment would provide interesting insight to understand macrophage activation *in vivo*. Indeed, as mentioned earlier, the environment in which macrophages reside shape their metabolism and their activation, notably due to nutrient availability (182).

In this study, we used metabolic inhibitors, which can reflect specific nutritional status. For example, ketogenic diet (low carbohydrate and high fat diet) favors FAO and reduces glucose availability, which can be mimicked *in vitro* with glucose inhibitors. In addition, caloric restriction, where calories and nutrients are reduced but provided in sufficient quantities, also results in decreased glucose availability. These two diets have been shown to promote overall immune fitness (210). The metabolic adaptations of immune cells induced by these specific nutritional status may provide an explanation for the improvement of the immune response.

Axis 3: Metabolic reprogramming of macrophages during gout and pseudo-gout flares

Hypothesis and aims of the study

Macrophages play a pivotal role in inflammation, being involved in both the initiation and the resolution of the process. Therefore, macrophages are associated with the pathogenesis of a wide range of inflammatory conditions. In the field of arthritis, gout and pseudo-gout flares are the most common and studied disorders. Gout occurs more frequently in men and has a prevalence between 1 and 6.8%. Aging and obesity are risk factors for gout (211). Chronic and elevated serum levels of urate (hyperuricaemia) leads to the deposition of monosodium urate crystals (MSU) in joints, toe and knee mostly. Crystal deposition triggers painful acute inflammatory responses known as gout flares. Calcium pyrophosphate dihydrate deposition (m-CPPD crystals) leads to similar symptoms, also known as pseudo-gout flares. Both obesity and gout are pathologies characterized by a sterile activation of the inflammatory response.

Mechanistically, macrophages and monocytes in the joint microenvironment are activated by the crystals. Activated macrophages uptake crystals by phagocytosis which leads to NLRP3 activation. NLRP3 is a multiprotein complex involved in the processing of IL1β and IL18 into their active forms. IL1β and IL18 production are critical to the upregulation of the pro-inflammatory environment. Neutrophils are recruited in the joint, favoring the establishment of a pro-inflammatory environment (211) (Figure 14).

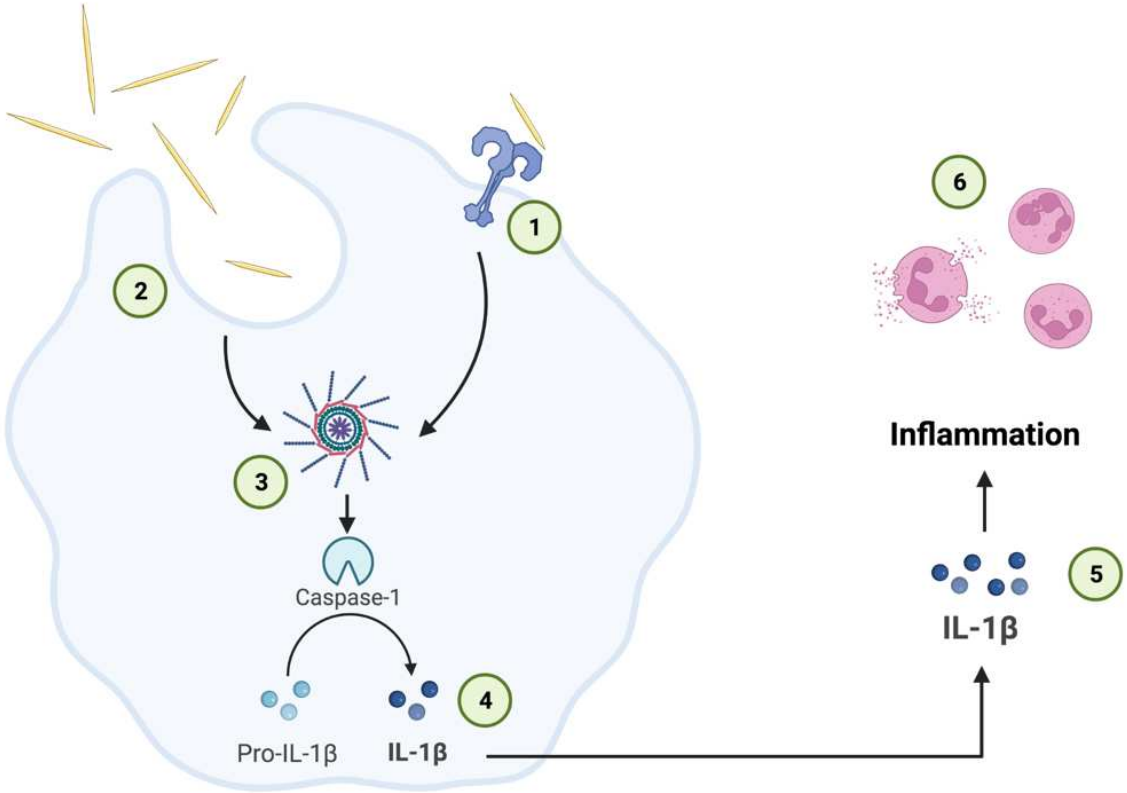

Figure 14: Initiation of the inflammatory process during gout and pseudo-gout flares
1: crystals recognition by TLR. 2: crystals phagocytosis. 3: inflammasome activation. 4: processing of pro-IL1β into IL1β by Caspase-1. 5: secretion of IL1β in the joint microenvironment. 6: inflammatory response and neutrophils recruitment.

It is now well described that macrophages undergo metabolic adaptations during inflammatory polarization. Moreover, TCA cycle disruption and accumulation of succinate induce IL1β expression. Gout and pseudo-gout flares are associated with an increase of glucose uptake in joint microenvironment (212,213). We wondered whether macrophages specifically adapt their cellular metabolism in response to gout- and pseudo-gout inducing crystals.

TRANSLATIONAL SCIENCE

Gout and pseudo-gout-related crystals promote GLUT1-mediated glycolysis that governs NLRP3 and interleukin-1β activation on macrophages

Felix Renaudin,[1,2] Lucie Orliaguet ,[1,3] Florence Castelli,[4] François Fenaille,[4] Aurelie Prignon,[5] Fawaz Alzaid,[1,3] Christele Combes,[6] Aurélie Delvaux,[4] Yasmina Adimy,[4] Martine Cohen-Solal ,[1,7] Pascal Richette ,[1,2] Thomas Bardin ,[1,2] Jean-Pierre Riveline,[1,3] Nicolas Venteclef,[1,3] Frédéric Lioté,[1,2] Laure Campillo-Gimenez,[1,2] Hang-Korng Ea [1,2]

Handling editor Josef S Smolen

► Additional material is published online only. To view, please visit the journal online (http://dx.doi.org/10.1136/annrheumdis-2020-217342).

For numbered affiliations see end of article.

Correspondence to
Pr Hang-Korng Ea, Rheumatology, Lariboisiere Hospital, Paris 75010, France; korngea@yahoo.fr

This work was presented as a poster communication in the Annual European Congress of Rheumatology (ARD, June 2019, Volume: 78, Supplement: 2, Pages 233-233) and in the American Congress of Rheumatology (Arthritis and Rheumatology, October 2019, Volume: 71, Supplement: 10, Meeting Abstract: 1238).

Received 14 March 2020
Revised 25 May 2020
Accepted 25 June 2020
Published Online First 22 July 2020

To cite: Renaudin F, Orliaguet L, Castelli F, *et al*. *Ann Rheum Dis* 2020;**79**:1506–1514.

ABSTRACT

Objective Macrophage activation by monosodium urate (MSU) and calcium pyrophosphate (CPP) crystals mediates an interleukin (IL)-1β-dependent inflammation during gout and pseudo-gout flare, respectively. Since metabolic reprogramming of macrophages goes along with inflammatory responses dependently on stimuli and tissue environment, we aimed to decipher the role of glycolysis and oxidative phosphorylation in the IL-1β-induced microcrystal response.

Methods Briefly, an in vitro study (metabolomics and real-time extracellular flux analysis) on MSU and CPP crystal-stimulated macrophages was performed to demonstrate the metabolic phenotype of macrophages. Then, the role of aerobic glycolysis in IL-1β production was evaluated, as well in vitro as in vivo using ^{18}F-fluorodeoxyglucose positron emission tomography imaging and glucose uptake assay, and molecular approach of glucose transporter 1 (GLUT1) inhibition.

Results We observed that MSU and CPP crystals led to a metabolic rewiring toward the aerobic glycolysis pathway explained by an increase in GLUT1 plasma membrane expression and glucose uptake on macrophages. Also, neutrophils isolated from human synovial fluid during gout flare expressed GLUT1 at their plasma membrane more frequently than neutrophils isolated from bloodstream. Both glucose deprivation and treatment with either 2-deoxyglucose or GLUT1 inhibitor suppressed crystal-induced NLRP3 activation and IL-1β production, and microcrystal inflammation in vivo.

Conclusion In conclusion, we demonstrated that GLUT1-mediated glucose uptake is instrumental during the inflammatory IL-1β response induced by MSU and CPP crystals. These findings open new therapeutic paths to modulate crystal-related inflammation.

Key messages

What is already known about this subject?

- A switch of cell metabolism from oxidative phosphorylation to aerobic glycolysis in order to support energy demand is a hallmark of inflammatory phenotype of macrophages and multiple immune-mediated inflammatory diseases such as cancer or autoimmune diseases.
- Gout and pseudo-gout flare depend on monosodium urate (MSU) and calcium pyrophosphate crystal-induced interleukin (IL)-1β production, respectively, by macrophages.

What does this study add?

- MSU and monoclinic calcium pyrophosphate dihydrate (m-CPPD) crystal stimulation leads to a metabolic reprogramming of macrophages in favour of aerobic glycolysis.
- MSU and m-CPPD crystal-induced NLRP3 inflammasome activation and IL-1β production by macrophages, as well as microcrystal-mediated inflammation in vivo, rely on a de novo glucose uptake through glucose transporter 1.

How might this impact on clinical practice or future developments?

- This study demonstrated the key role of inflammatory cell metabolism and glucose availability in the inflammatory process of microcrystal-related pathology. It thus highlights a potential new therapeutic path for acute and chronic patients' arthritis care.

INTRODUCTION

Monosodium urate (MSU) and monoclinic calcium pyrophosphate dihydrate (m-CPPD) crystals are responsible for gout and m-CPPD deposition diseases, respectively. Both crystals activate the innate immune system and induce recurrent and painful flares, which are interleukin (IL)-1β-driven inflammations caused by macrophage-mediated neutrophil infiltration and activation in joints.[1 2] IL-1β production is a two-step process which can both be activated by MSU and m-CPPD crystals. The first step involves nuclear factor-κB and mitogen-activated protein kinase pathways,[3] leading to pro-IL-1β synthesis, and the second one relies on the nucleotide-binding oligomerisation domain (NOD)-like receptor family, pyrin (NLRP) domain-containing 3 inflammasome complex and

gives rise to the secretion of active IL-1β.[1] Activated NLRP3 stimulates speck formation of the adaptor protein apoptosis-associated speck-like containing a CARD (ASC) and recruits pro-caspase-1 into the NLRP3/ASC complex through homotypic domain–domain interactions.[4 5] Assembly of pro-caspase-1 within the NLRP3 inflammasome allows its autoproteolysis and the release of active caspase-1, which cleaves its substrates pro-IL-1β and pro-IL-18 into their mature forms.[4] NLRP3-deficient macrophages are unable to produce mature IL-1β under MSU and m-CPPD crystal stimulation.[1 3] Blocking IL-1β abrogates MSU-induced and m-CPPD-induced inflammation and constitutes an efficient therapeutic option in gout flare.[6 7] However, long-term inhibition of IL-1β may increase infection risk. Thus, understanding mechanisms of NLRP3 activation by MSU and m-CPPD crystals might offer a safer way to modulate IL-1β effects.

NLRP3 can be activated through several mechanisms, including reprogramming of cell metabolism.[8–11] First described in cancer cells, the so-called Warburg effect characterised by an increase in glucose uptake and aerobic glycolysis, along with a reduction of the mitochondrial respiration (oxidative phosphorylation (OXPHOS)), and an inhibition of tricarboxylic acid (TCA) cycle plays a critical role in host defence and inflammation and is a metabolic hallmark of activated immune cells and proinflammatory macrophages.[8–10] Thus, high concentrations of glucose increase IL-1β production through the NLRP3-dependent pathway, while inhibition of glycolysis with 2-deoxyglucose (2-DG) suppresses IL-1β production by macrophages stimulated with the TLR-4 agonist lipopolysaccharide (LPS) or ATP.[12 13] LPS-induced glycolysis stimulates IL-1β production through hexokinase (HK) 1, hypoxia-inducible factor 1α (HIF-1α) and pyruvate kinase muscle (PKM) 2 activation, three molecules of the glycolysis pathway directly involved in NLRP3 activation and IL-1β production.[14–16] In parallel, TLR4 activation induces TCA cycle alteration stimulating IL-1β production through cytosolic accumulation of succinate, which prevents degradation of HIF-1α by prolylhydroxylase enzyme.[12] Stabilised HIF-1α then enhances the expression of genes encoding IL-1β and proteins involved in glycolysis pathways, such as glucose transporter 1 (GLUT1) and HK, which further amplify glucose uptake and glycolysis.[12 15 17] Interestingly, glucose uptake quantified with ^{18}F-fluorodeoxyglucose ([^{18}F]-FDG) positron emission tomography (PET) is increased in joints with gout flare and in soft-tissue surrounding MSU or m-CPPD crystal deposition, suggesting that glucose consumption plays an important role in crystal-induced inflammation.[18 19] Moreover, the ketone body β-hydroxybutyrate produced during starvation or low-carbohydrate ketogenic diet inhibits IL-1β production

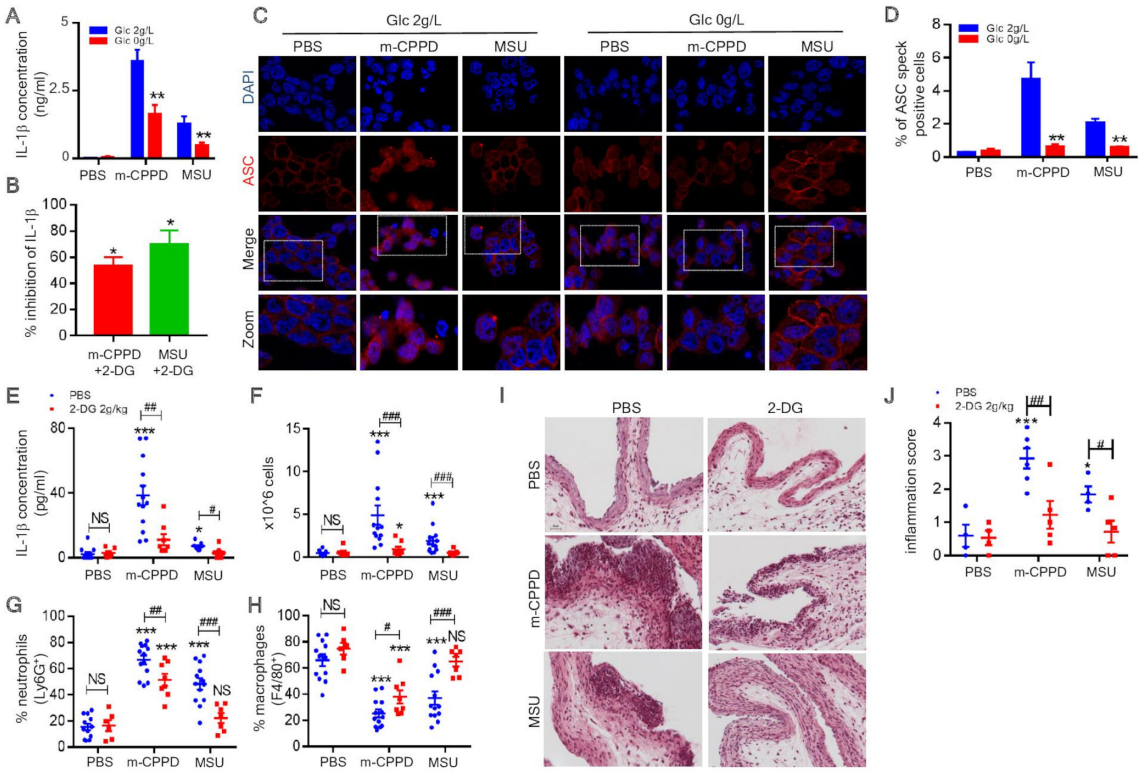

Figure 1 Crystal-induced inflammation depends on glucose availability. Primed THP-1 cells were stimulated with either PBS or MSU or m-CPPD crystals. (A,B) IL-1β production was quantified by ELISA in supernatants of cell culture in the (A) absence or presence of glucose (n=9). Multiple t-test with false discovery rate (FDR) correction between +glucose and –glucose (*): $^{\#}$p<0.05, $^{\#\#}$p<0.01, $^{\#\#\#}$p<0.001. (B) In the absence (PBS) or presence of 2-DG (20 mM, n=4). Data are presented in % of inhibition of IL-1β production compared with PBS (100%). Kruskal-Wallis test with FDR correction (*): *p<0.05, **p<0.01, ***p<0.001. (C,D) ASC speck formation was observed with confocal microscopy and quantified in cells cultured with medium containing or not containing glucose. (C) Imaging representative of three independent experiments and (D) quantification of cells expressing at least one speck complex (n=3). Multiple t-test with FDR correction between +glucose and –glucose ($^{\#}$): $^{\#}$p<0.05, $^{\#\#}$p<0.01, $^{\#\#\#}$p<0.001. (E–J) Mouse air pouch model of microcrystal inflammation: IL-1β concentration (E), cell infiltration (F), proportion of neutrophils and macrophages (F,G) in the air pouch lavages of mice injected by either PBS, MSU or m-CPPD crystals and treated with 2-DG or PBS (n=12/group); H&E staining of air pouch membranes (I) and scoring of the inflammation (J) (n=5). Two-way analysis of variance test with FDR correction ($^{\#}$): $^{\#}$p<0.05, $^{\#\#}$p<0.01, $^{\#\#\#}$p<0.001. 2-DG, 2-deoxyglucose; ASC, apoptosis-associated speck-like containing a CARD; IL, interleukin; m-CPPD, monoclinic calcium pyrophosphate dihydrate; MSU, monosodium urate; NS, not significant.

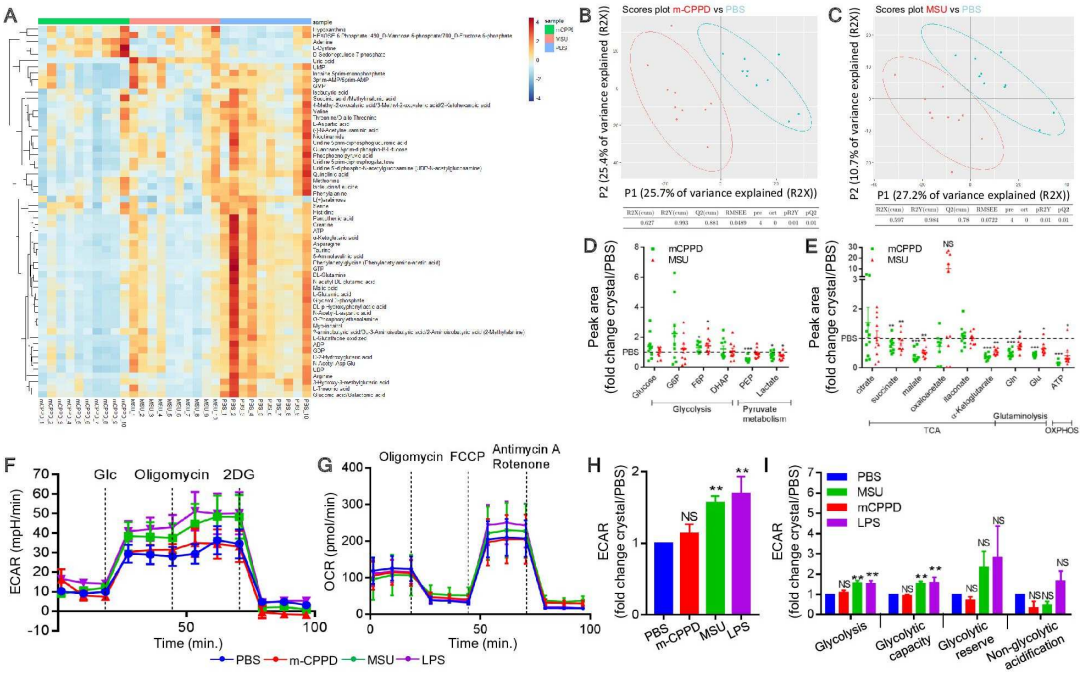

Figure 2 MSU and m-CPPD crystals induce metabolic changes in the glycolysis pathway and the TCA cycle. (A–E) Metabolomics analysis was performed by mass spectrometry in primed THP-1 cells treated by either PBS, MSU or m-CPPD crystals. (A) Heatmap analysis and (B,C) principal component analysis of MSU and m-CPPD crystals versus PBS (n=10). Relative quantification (ratio of MSU or m-CPPD to PBS) of the different metabolites related to glycolysis (D) and Krebs cycle or OXPHOS (E). Kruskal-Wallis test with FDR correction (*): *p<0.05, **p<0.01, ***p<0.001. (F–H) Real-time extracellular flux analysis on LPS-primed BMDMs stimulated with either MSU or m-CPPD. (F) Time course of real-time changes in the ECAR after Glycolysis Stress Assay (n=6). (G) Time course of real-time changes in the OCR after Cell Mito Stress Assay (n=4). (H) Mean of basal ECAR (ratio of crystals over PBS). (I) Glycolysis Stress Assay (n=6): each rate was determined according to the SeaHorse Agilent Guide and described in the Materials and methods section. Kruskal-Wallis test with FDR correction (*): *p<0.05, **p<0.01, ***p<0.001. 2-DG, 2-deoxyglucose; BMDM, bone marrow-derived macrophage; DHAP, dihydroxyacetone phosphate; ECAR, extracellular acidification rate; FCPP, carbonyl cyanide-4-(trifluoromethoxy) phenylhydrazone; LPS, lipopolysaccharide; m-CPPD, monoclinic calcium pyrophosphate dihydrate; MSU, monosodium urate; NS, not significant; OCR, oxygen consumption rate; OXPHOS, oxidative phosphorylation; PEP, phosphoenolpyruvate; TCA, tricarboxylic acid.

by macrophages and inflammation in a mouse gout model.[20 21] Nevertheless, whether macrophage metabolism reprogramming is involved in MSU and m-CPPD crystal-induced IL-1β production remains unknown.

In this study, we aimed to assess the metabolic phenotype of macrophages and the role of glucose uptake in the NLRP3-dependent IL-1β production in response to MSU and m-CPPD crystals. We observed that MSU and m-CPPD crystals induced metabolic modifications in macrophages towards an increase in glycolytic activity. Upregulation of glycolysis corroborated with a de novo glucose uptake mediated by the glucose transporter (GLUT) GLUT1, in response to microcrystals. Interestingly, glucose deprivation or glycolysis inhibition by knock-down of GLUT1 prevented ASC oligomerisation (NLRP3 activation) and IL-1β secretion induced by both crystals. Moreover, both inhibition of GLUT1 and glycolysis inhibition by 2-DG decreased MSU and m-CPPD crystal-induced inflammation in an in vivo mouse model. Finally, in patients with gout flare, neutrophils isolated from the inflamed joint expressed more frequently GLUT1 at their surface membrane than circulating neutrophils, which highlights a promising specific approach for GLUT1 targeting as a gout flare therapy.

RESULTS

MSU and m-CPPD crystal-induced inflammation depends on glucose metabolism

To assess the role of glucose metabolism in crystal-induced inflammation, we stimulated cells with media containing increasing concentrations of glucose (0–4 g/L) or supplemented with the glucose analogue 2-DG, an inhibitor of glycolysis. Both glucose deprivation and glycolysis inhibition drastically decreased IL-1β production by primed THP-1 cells or mouse bone marrow-derived macrophages (BMDMs) stimulated by either MSU or m-CPPD crystals (glucose deprivation decreased by more than 90% the crystal-induced IL-1β production by BMDMs) (figure 1A,B; online supplementary figure S1A,B). In contrary, increasing concentrations of glucose-enhanced IL-1β production (see online supplementary figure 1C). Nevertheless, prostaglandin E2 and CXCL1 production, two proinflammatory mediators involved in crystal inflammation, did not depend on glucose availability (see online supplementary figure S1E–F). Suppression of IL-1β production is secondary to the inhibition of NLRP3 inflammasome.[1 3] Here, we demonstrated that glucose deprivation suppressed ASC oligomerisation and speck formation induced by either MSU or m-CPPD crystals (figure 1C,D). We confirmed, in vivo, the central role of glycolysis and observed that mice treated with 2-DG displayed mild inflammatory response compared to untreated mice 6 hours after MSU or m-CPPD crystal stimulation. Indeed, 2-DG abrogated crystal-induced IL-1β production and prevented crystal-induced neutrophil infiltration assessed in the air pouch lavages (figure 1E–H). Histology analysis of air pouch membranes after H&E staining further evidenced that glycolysis inhibition suppressed neutrophil infiltration with a major decrease in inflammation score in mice treated by 2-DG (figure 1I,J).

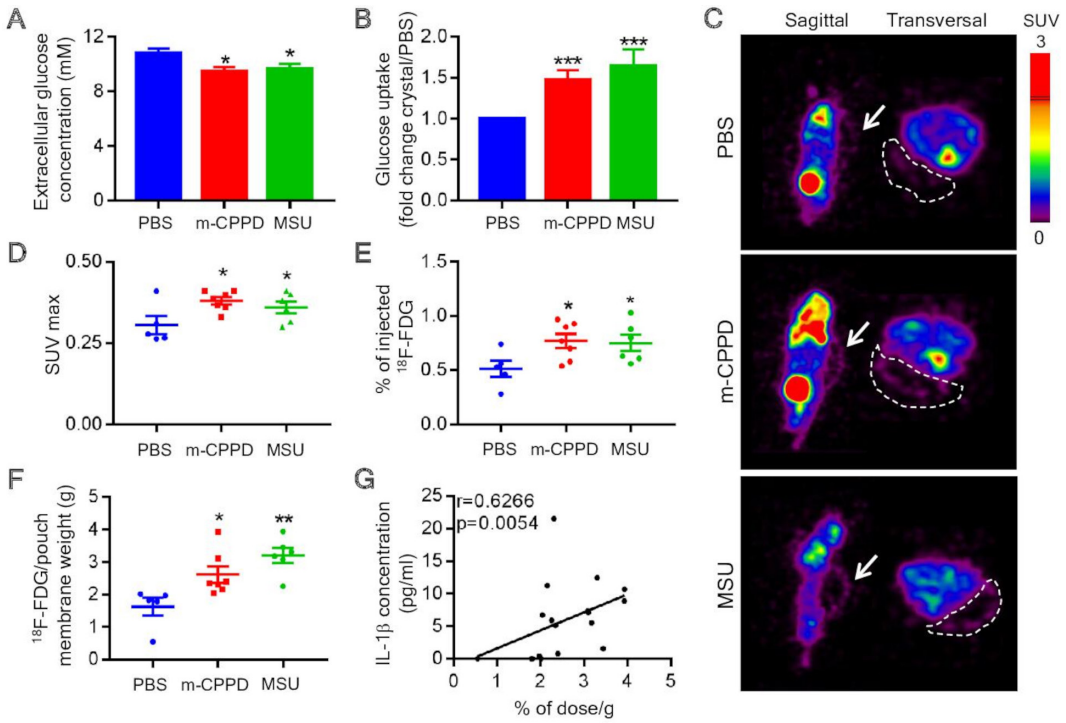

Figure 3 Crystal-induced inflammation is associated with an increase in glucose uptake. (A) Extracellular glucose concentration in cell culture media was quantified 6 hours after crystal stimulation (n=5). (B) [^{18}F]-fluorodeoxyglucose ([^{18}F]-FDG) was quantified in cell pellets to assess glucose uptake after 1 hour of stimulation by either MSU or m-CPPD crystals (n=8). (C–E) Glucose uptake was quantified in air pouch (arrow) model using [^{18}F]-FDG PET/CT. (C) Imaging representative of 6 mice; (D) SUV_{max} of air pouch; and (E) proportion of injected [^{18}F]-FDG dose detected in the air pouch (n=6 mice per group). (F) Ratio of [^{18}F]-FDG per weight (g) of ex vivo isolated air pouch membranes. Kruskal-Wallis test with FDR correction (*): *p<0.05, **p<0.01, ***p<0.001. (G) Correlation between IL-1β concentration (pg/mL) in the air pouch and the [^{18}F]-FDG quantification (% dose/g) in the cell infiltrate, Spearman test. [^{18}F]-FDG, ^{18}F-fluorodeoxyglucose; IL, interleukin; m-CPPD, monoclinic calcium pyrophosphate dihydrate; MSU, monosodium urate; SUV_{max}, maximum standardised uptake value.

MSU and m-CPPD crystals induce modifications in the glycolysis and TCA cycle pathways

To better understand the involvement of glucose and cell metabolism in the microcrystal inflammatory response, we performed a metabolomics study and observed in partial least squares discriminant analysis that cells stimulated by either MSU or m-CPPD crystals had robust distinct metabolic profiles without overlap components compared with unstimulated cells. Metabolomics data are available in online supplementary table S1. Specifically, we observed modifications of the abundance of multiple metabolites (figure 2A–C). Crystals induced perturbation of multiple metabolic pathways, including amino acids and glucose metabolism (see online supplementary figure S2). We observed modifications in both glycolysis pathway and TCA cycle with a slight increase of fructose-6 phosphate and a strong decrease of phosphoenolpyruvate, α-ketoglutarate and malate (figure 2D,E). Beside glycolysis and TCA cycle components, there was also a decrease of glutamate and glutamine, two amino acids able to refuel the Krebs cycle in the absence of pyruvate.[22 23] Interestingly, the intracellular ATP was very low in crystal-stimulated cells, suggesting either an alteration of its production or an increased turnover. Then, we evaluated whether these crystals also modulated the expression of genes encoding enzymes or transporters involved in the glycolysis pathway and Krebs cycle. We did observe variations in expression of genes encoding HK-2, mitochondrial pyruvate carrier 1 and 2, monocarboxylate transporter 4, pyruvate dehydrogenase phosphatase 2, isocitrate dehydrogenase 1 and 2, and pyruvate dehydrogenase kinase 2 and 3 (see online supplementary figure S3A–D). Altogether, these results suggested that crystals altered glycolytic activity and mitochondrial function. We assessed this hypothesis with Seahorse experiments that permit analysis of real-time changes in the extracellular acidification rate (ECAR) (figure 2F) and oxygen consumption rate (OCR) (figure 2G), as surrogates of glycolysis and mitochondrial respiration, respectively. We observed that only MSU crystals increased macrophage basal glycolysis (figure 2H), glycolytic rate and glycolytic activity (figure 2I) while both MSU and m-CPPD crystals did not affect the OXPHOS (figure 2G; online supplementary figure S3E,F). Analysis of OCR suggested that MSU crystals increased only non-mitochondrial oxygen consumption (see online supplementary figure S3F).

MSU and m-CPPD crystals increase glucose uptake associated with GLUT1 expression at the cell surface

As crystal-induced IL-1β production relied on glucose availability, we quantified the variation of glucose concentrations in cell culture media. By doing this, we observed that glucose concentrations were significantly lower in culture media of macrophages stimulated by either MSU or m-CPPD crystals than in culture media of unstimulated cells (figure 3A). Then, we confirmed the de novo glucose uptake by showing that MSU and m-CPPD crystals enhanced the intracellular level of radiolabelled [^{18}F]-FDG by 152% and 148%, respectively (figure 3B). Glucose uptake has been reported in gouty joint flare in patients[18 19]; we reproduced this observation in the air pouch model using

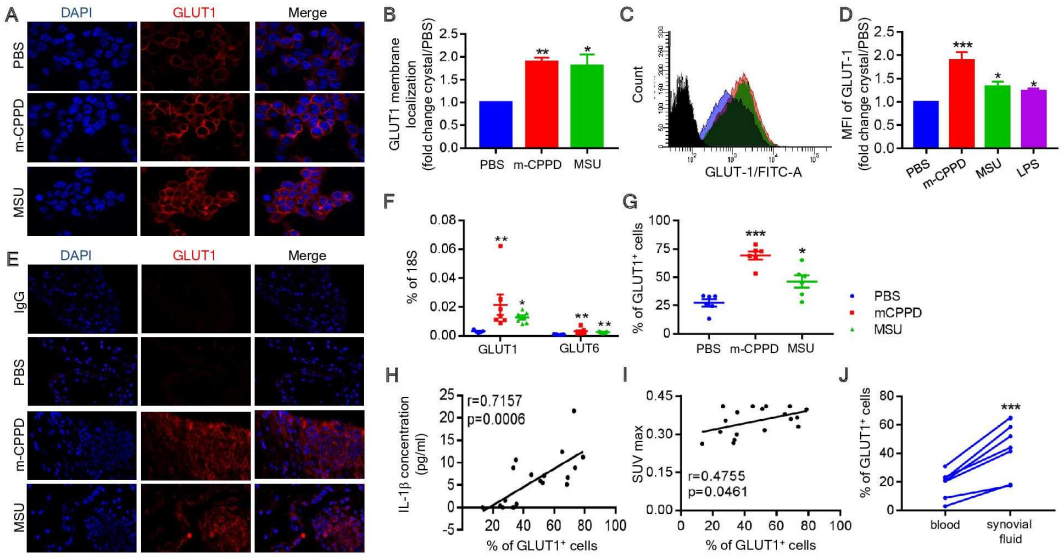

Figure 4 MSU and m-CPPD crystals increase GLUT1 expression at the cell plasma membrane. (A–C) GLUT1 membrane localisation in primed-THP-1 cells stimulated by PBS, MSU or m-CPPD was assessed by immunofluorescence confocal microscopy. (A) Imaging representative of five experiments and (B) quantification of GLUT1 membrane expression. (C) Representative overlay (MFI) by FACS of GLUT1 cell surface expression, (D) quantification of the ratio of GLUT1 MFI (crystal over PBS, LPS used as a positive control of stimulation) (n=5). Kruskal-Wallis test with FDR correction (*): *p<0.05, **p<0.01, ***p<0.001. (E–I) GLUT1 expression was evaluated in mouse air pouch model of microcrystal inflammation. After PBS, MSU or m-CPPD injection (E) GLUT1 expression in the air pouch membranes was assessed by immunofluorescence confocal microscopy (representative images (n=5), (F) expression of GLUT1 gene was assessed by RT-qPCR using RNA isolated from infiltrated cells collected in air pouch lavages. Data are represented as a % of GLUT1 or GLUT6 mRNA expression compared with 18S mRNA expression in each condition of stimulation. (n=6). (G) Percentage of GLUT1-expressing cells was assessed by FACS using infiltrated cells collected in air pouch lavages (n=6). Kruskal-Wallis test with FDR correction (*): *p<0.05, **p<0.01, ***p<0.001. Correlation between GLUT1-positive cells in the air pouch lavages and (H) IL-1β production or (I) glucose uptake, Spearman test. (J) Plasma membrane expression of GLUT1 was evaluated FACS comparing neutrophils isolated from flaring joint and circulating neutrophils isolated from peripheral blood of the same patient at the same moment (n=7). Two-tailed paired t test (*): *p<0.05, **p<0.01, ***p<0.001. FACS, fluorescence activated cell sorting; GLUT1, glucose transporter 1; IL, interleukin; LPS, lipopolysaccharide; m-CPPD, monoclinic calcium pyrophosphate dihydrate; MFI, mean fluorescence intensity; mRNA, messenger RNA; MSU, monosodium urate; SUV_{max}, maximum standardised uptake value.

[^{18}F]-FDG. By PET/CT imaging, glucose uptake in response to MSU and m-CPPD crystals was evidenced by a higher labelling of the air pouch where crystals were injected, as well as higher maximum standardised uptake value (SUV_{max}) and ratio of radio-labelled tracer found in air pouch compared with air pouch injected by saline solution (figure 3C–E). Moreover, after in vivo acquisition, quantification of the radiotracer showed that the level of [^{18}F]-FDG was higher in air pouch membranes isolated from crystal-stimulated mice than from saline-stimulated mice (figure 3F), which was strongly correlated with IL-1β production in the air pouch (figure 3G).

Glucose enters the cells through GLUTs that belong to solute carrier family 2 (SCL2A), which encompasses 14 members. SLC2A proteins are overexpressed in tumour cells, and SLC2A1 (GLUT1) is rapidly upregulated in inflammatory macrophages and contributes to glycolytic phenotype.[24] GLUT6 has been previously reported as not being involved in glucose uptake and glycolysis[25]; therefore, we focused on GLUT1 expression. We first showed that both MSU and m-CPPD crystal stimulation in vitro upregulated the GLUT1 gene expression on BMDMs (see online supplementary figure S4B) and the GLUT1 protein expression on THP-1 cells (figure 4A–D; see also figure 5A). By confocal microscopy, we observed that microcrystals induced a higher expression of GLUT1 at the cell plasma membrane compared with unstimulated cells (figure 4A,B). Moreover, the analysis by flow cytometry showed that both crystals, as well as the NLRP3 activator LPS, induced an increase in mean of GLUT1 expression intensity at the cell surface (figure 4C,D). The increased GLUT1 expression in response to crystals was confirmed in vivo (figure 4E–G). First, we observed by immunofluorescence an increased expression of GLUT1 in the air pouch membrane (figure 4E). Second, the infiltrated cells into the air pouch expressed a higher level of GLUT1 messenger RNA (mRNA) (figure 4F) after crystal injection compared with saline injection, and between 50% and 70% of the recruited cells were positive for GLUT1 (figure 4G). The percentage of GLUT1-positive cells was also correlated with the inflammatory response and glucose uptake measured by IL-1β concentration and SUV_{max}, respectively, in the air pouch (figure 4H1). Finally, we validated these in vivo data by GLUT1 expression analysis on inflammatory cells isolated from gout flare patients. We observed that the ratio of GLUT1-expressing cells among the neutrophils was higher in the synovial fluid than in blood (figure 4J), suggesting that cells increased their GLUT1 expression at the site of inflammation where MSU crystals are present (MSU crystals were observed in 100% of the synovial fluid samples).

Altogether, these results suggested that MSU and m-CPPD crystal inflammation is supported by a de novo increase in GLUT1 expression and its relocalisation to the plasma membrane, required for glucose uptake and metabolic reprogramming.

GLUT1 regulates crystal-induced inflammation

To assess the role of GLUT1 in MSU and m-CPPD crystal-induced inflammation, we adopted pharmacological (STF-31: iGLUT1) and genetic knock-down approaches (SLC2A1 small interfering RNA: siGLUT1; see validation in figure 5A) of GLUT1 inhibition. First, iGLUT1 suppressed the glucose

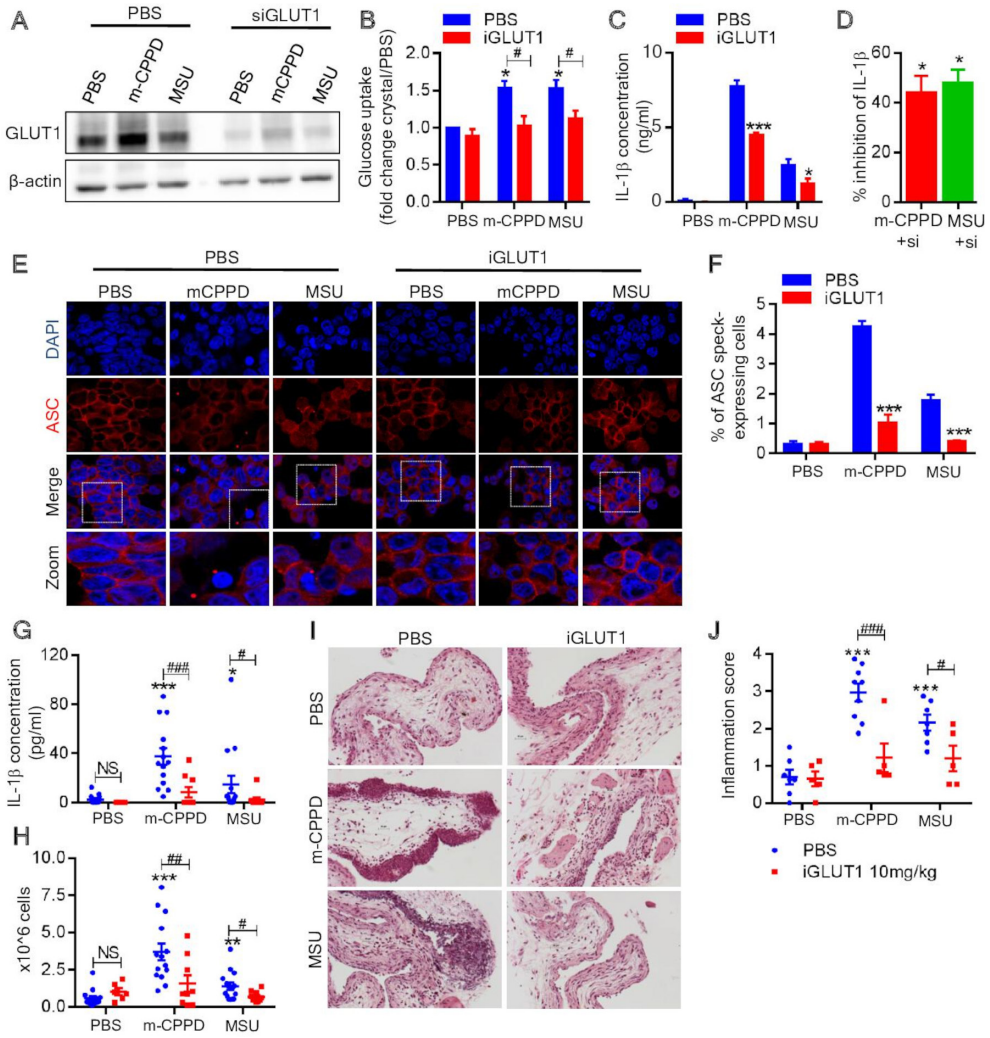

Figure 5 GLUT1 drives crystal-induced inflammation. (A–F) PBS, MSU or m-CPPD crystal stimulation of primed THP-1 cells pretreated or not (PBS) with STF-31 (20 µM, iGLUT1) or transfected with GLUT1 siRNA (si). (A) Validation of GLUT1 expression knock-down by western blot, (B) Quantification of [^{18}F]-FDG in the cell pellets. Data shown as fold change after crystal stimulation compared with PBS. (C,D) IL-1β concentration measured by ELISA in the supernatants of cell culture (n=3). (D) Data are presented as % of inhibition compared with wild type THP-1 cells (n=3). (E,F) ASC speck formation was assessed by immunofluorescence confocal microscopy. (E) Imaging representative of four experiments. (F) Quantification of cells showing at least one ASC speck formation. Kruskal-Wallis test with FDR correction (*): *p<0.05, **p<0.01, ***p<0.001. (G–J) On air pouch model of crystal inflammation in mice treated or not with GLUT1 inhibitor STF-31 (iGLUT1, 10 mg/kg). (G) IL-1β concentration quantified by ELISA and (H) number of infiltrate cells in air pouch lavages (n=15 per group). H&E staining (PBS: n=8 mice per group, iGLUT1: n=5 mice per group) realised on air pouch membrane sections. (I) Representative images and (J) scoring of inflammation. Two-way analysis of variance test with FDR correction (*): *p<0.05, **p<0.01, ***p<0.001. [^{18}F]-FDG, ^{18}F-fluorodeoxyglucose; ASC, apoptosis-associated speck-like containing a CARD; GLUT1, glucose transporter 1; IL, interleukin; m-CPPD, monoclinic calcium pyrophosphate dihydrate; MSU, monosodium urate; NS, not significant.

uptake induced by MSU and m-CPPD crystals (figure 5B), positioning GLUT1 as the main GLUT involved in the microcrystal response. Then, we demonstrated that GLUT1 inhibition by either of the two technical approaches led to a 50% inhibition of IL-1β production in response to MSU and m-CPPD (figure 5C,D). This IL-1β reduction under iGLUT1 was due to an inhibition of the NLRP3 inflammasome activation as GLUT1 inhibition prevented by 75% the ASC speck formation (figure 5E). Partial inhibition of NLRP3 activation and subsequently IL-1β production by iGLUT1 suggested that GLUT1 was involved in an amplification loop but not an initial signal of IL-1β production. Nevertheless, we observed that glucose depletion and GLUT1 inhibition decreased both NLRP3 and IL-1β gene expression and pro-IL-1β synthesis induced by phorbol myristate acetate (PMA) priming, suggesting that glucose also played a role in the first signal (see online supplementary figure S5A,B).

Finally, we evaluated the iGLUT1 efficiency on microcrystal inflammation in vivo. iGLUT1 delivered by intraperitoneal injection allowed to drastically inhibit all signs of local inflammation induced by MSU and m-CPPD into the air pouch, namely, a decrease in IL-1β production (figure 5G), a reduction of cell infiltration (figure 5H) associated with neutrophil recruitment (see online supplementary figure S5C,D) and a global alleviation of the inflammatory score observed from HE staining of air pouch membrane (figure 5I).

DISCUSSION

We found that MSU and m-CPPD crystal-induced macrophage production of IL-1β, which orchestrated the recurrent

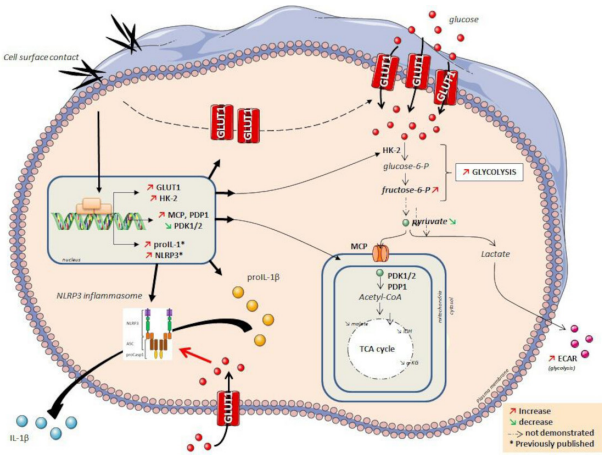

Figure 6 GLUT1 and glycolysis regulate NLRP3 inflammasome activation and IL-1β production induced by MSU and m-CPPD crystals. Crystals induced *GLUT1* gene expression, GLUT1 production and its localisation in plasma membrane. NLRP3 activation and IL-1β production in response to MSU and m-CPPD crystals rely on glucose uptake through GLUT1 and glycolysis. In parallel, MSU and m-CPPD crystals induce gene expression of pro-IL-1β and NLRP3, along with enzymes involved in glycolysis and TCA pathways, including GLUT1, HK-2, MCT, PDP1 and PDK1/2. ECAR, extracellular acidification rate; GLUT1, glucose transporter 1; HK, hexokinase; IL, interleukin; m-CPPD, monoclinic calcium pyrophosphate dihydrate; MCP, mitochondrial carrier proteins; MCT, monocarboxylate transporter; PDP, pyruvate dehydrogenase phosphatase; PDK, pyruvate dehydrogenase kinase. TCA, tricarboxylic acid.

inflammatory flares in gout and m-CPPD deposition disease, respectively, relied on glucose uptake through GLUT1 (figure 6). Glucose deprivation and glycolysis inhibition decreased NLRP3 and IL-1β gene expression and suppressed ASC speck formation (ie, NLRP3 activation), IL-1β production and neutrophil infiltration induced by MSU and m-CPPD crystals. Crystals induced GLUT1 de novo expression and its localisation to plasma membrane, along with gene expression of enzymes involved in glycolysis such as HK-2. Increase glucose uptake during MSU and m-CPPD crystal-induced inflammation has been reported in patients using [^{18}F]-FDG PET/CT.[18 19] We reproduced these observations in a mouse model, and we identified for the first time the key role of GLUT1 in both MSU and m-CPPD crystal-induced inflammation in mice and in human samples harvested during gout flare. Interestingly, we discovered that MSU crystal-induced glucose uptake favoured glycolytic activity, while m-CPPD crystals induced glucose uptake without modulation of glycolytic activity. Surprisingly, both microcrystals did not modulate OXPHOS. These results were distinct from the Warburg effect described in cancer cells and LPS-stimulated macrophages, where metabolic switch enhanced aerobic glycolysis at the expense of mitochondrial respiration.[8–10 12 26] Also reported, MSU crystals increased both OXPHOS and glycolytic activity on human neutrophils.[27] These findings further supported the complexity of cellular metabolic programmes and responses, which varied with the type and concentration of stimuli, cell type and cell species and tissue environment.[13 28–30] For example, LPS stimulated Warburg-like metabolic reprogramming in human monocytes at concentrations between 1 and 100 ng/mL but increased OXPHOS at a low dose of 0.1 ng/mL.[29] Likewise, monocytes stimulated with TLR2 agonist Pam3CysSK4 (P3C) or by whole microorganisms activated both glycolysis pathway and OXPHOS.[29] Finally, analysis of monocyte transcriptomic responses under 28 different stimuli identified 10 clusters that represented distinct activation states with distinct metabolic responses.[30] These data suggested that a specific stimulus would trigger metabolic responses corresponding to a specific and functional requirement of the cells. For instance, MSU and m-CPPD crystal-induced metabolic reprogramming might increase either the phagocytosis capacity (as shown in monocytes stimulated by P3C) or the reactive oxygen species (ROS) production (as shown in neutrophils stimulated by MSU crystals),[27 29] two well-known mechanisms of crystal-induced NLRP3 activation.[1 31] In parallel, we found that MSU crystals activated macrophage glycolysis pathway to produce IL-1β as well described in macrophages stimulated by LPS, in activated T cells and cancer cells.[8–10 12 17 26 28] However, how MSU-induced and m-CPPD crystal-induced glucose uptake activates the NLRP3 inflammasome remained unknown. One explanation could come from the induction of HK-2 by MSU and m-CPPD. Indeed, in LPS-stimulated macrophages, IL-1β production can be modulated by metabolites and enzymes involved in the glycolysis pathway, including HK-1 and HK-2, which can both interact with mitochondrial voltage-dependent anion channel to activate NRLP3,[32] glyceraldehyde 3-phosphate dehydrogenase[33] and inactive PKM2.[14 34] Cancer cells and LPS-stimulated macrophages overexpress inactive dimer PKM2, which promotes HIF-1α activation and transcription of HIF-1α-dependent genes, including IL-1β and glycolytic enzymes.[14 34] Alternatively, MSU and m-CPPD crystal-induced glucose uptake might stimulate IL-1β production through Akt pathway and ROS production.[27 35 36] PI3K (phosphatidylinositol-3 kinase)/Akt pathway is commonly activated by MSU and m-CPPD crystals.[27 36 37] Akt activation enhanced IL-1β production through induction of ROS and glucose metabolism. Akt promoted glycolysis through stimulation of HK-2 and glucose uptake via translocation of GLUT1 to cell surface membrane and activation of its downstream mTORC1. This later stimulated HIF-1α, which enhanced expression of genes involved in glycolytic reprogramming, such as *SLC2A1* (GLUT1).[38]

Glucose is a critical nutrient component for inflammatory macrophages, and GLUT1 is the main GLUT expressed in LPS-stimulated macrophages.[24] Elevated GLUT1 expression increased glucose metabolism and glycolysis, ROS production and expression of proinflammatory mediators, including IL-1β.[24] Here, we found that MSU and m-CPPD crystals triggered plasma membrane localisation of GLUT1, which drove glucose uptake, NLRP3 activation and IL-1β production. Furthermore, we observed in gouty patients that GLUT1 was more frequently expressed at the surface of neutrophils isolated from flaring joint than neutrophils isolated from peripheral blood of the same patient. These results added crystal-induced IL-1β production to the list of inflammatory conditions regulated by GLUT1-induced glucose uptake in macrophages, such as cancer, infection, autoimmune disease, diabetes and obesity.[14 24 28 35 39 40] Interestingly GLUT1 also governed postprandial glucose uptake by peritoneal macrophages, leading to IL-1β production and, subsequently, insulin secretion.[35] This might explain why gout flare frequently occurred after a feast. MSU and m-CPPD crystals enhanced both GLUT1 mRNA expression and GLUT1 plasma membrane localisation by unknown mechanisms. GLUT1 activity is regulated by its membrane localisation and activation, kinetic of its internalisation, endosomal sorting and recycling back to the cell membrane, which depends on retromer cargo complex.[41 42] Cancer cells favour aerobic glycolysis by promoting GLUT1 plasma membrane localisation through the PI3K/Akt/mTORC

pathway.[43–45] Akt activation promotes cell surface membrane recycling of GLUT1 and reduces its internalisation.[43] Inversely, Akt inhibition by phosphatase TENsin homologue deleted on chromosome 10 (PTEN) prevented GLUT1 plasma membrane localisation[45–47] Whether MSU and m-CPPD crystals regulated GLUT1 membrane expression through the Akt pathway needs to be studied. Alternatively, MSU and m-CPPD crystals might induce GLUT1 membrane localisation through thioredoxin-interacting protein, which facilitated GLUT1 endocytosis via clathrin-coated pits, modulated PTEN activity and was involved in crystal-induced inflammation.[31 48] Lastly, crystal-induced glucose uptake might be due to an increase in GLUT1 transport activity. Indeed, the drastic decrease of cytosolic ATP observed after MSU and m-CPPD crystal stimulation might stimulate GLUT1 transport activity, as previously reported.[49 50]

Although *SLC2A6* (GLUT6) gene expression in THP-1 cells was highly enhanced by either MSU or m-CPPD crystal stimulation, its exact role in crystal-induced inflammation and glucose uptake is currently unknown. Recent data suggested that GLUT6 was involved in neither glucose uptake nor glycolysis nor OXPHOS.[25 51 52] GLUT6-deficient mice had normal glucose metabolism[51] and GLUT6-deficient BMDMs had similar ECAR and OCR than wild-type cells.[25 52] Moreover, expression of proinflammatory mediators such as IL-1β and TNF-α was unchanged in the absence of GLUT6.[52] Further studies are needed to understand how GLUT6 participates to crystal-induced inflammation.

How MSU and m-CPPD crystals induced GLUT1 membrane localisation constituted the main limitation of our study. Although we did not identify the exact mechanisms involved in crystal effects, our results suggested that MSU and m-CPPD crystals increased, in THP-1 and mouse BMDM cells, GLUT1 gene expression, GLUT1 protein production and membrane location and GLUT1 activity. Whether crystals induced IL-1β production by primary human monocytes does also depend on glucose uptake need specific studies. Similarly, we did not assess in this study how hyperglycaemic modulated crystal-induced inflammation in vivo. We planned to address this question in type 2 and type 1 diabetes using Ob/Ob mice and streptozotocin mouse models, respectively. Interestingly, recent report supported our findings by showing that patients treated with metformin had less gout flare.[53] Finally, metabolic reprogramming during gout flare needed also to be confirmed in patients by doing metabolomics analysis in neutrophils isolated from inflamed joint.

Overall, metabolic changes characterised by GLUT1-mediated glucose uptake and increase in glycolysis governed MSU and m-CPPD crystal-activated IL-1β production. These findings open new therapeutic paths to modulate crystal-related inflammation.

MATERIALS AND METHODS

See a fully detailed Materials and methods in the online supplementary file.

Author affiliations
[1]Universite de Paris, Paris, France
[2]INSERM, UMR-S 1132, F-75010, Paris, France
[3]INSERM, Immunity and Metabolism in Diabetes Laboratory, Centre de Recherche des Cordelier, Paris, France
[4]Service de Pharmacologie et immunoanalyse (SPI), Laboratoire d'Etude du Métabolisme des Médicaments, CEA, INRAE, Université Paris Saclay, Gif-Sur-Yvette, France
[5]UMS28 Phénotypage du Petit Animal, Laboratoire d'Imagerie Moléculaire Positonique (LIMP), F-75020, Sorbonne Université, Paris, France
[6]UMR 5085 INPT-UPS-CNRS, Université de Toulouse, ENSIACET, F-31000, Toulouse, France
[7]Bone and Joint Laboratory, INSERM U1132, Paris, France

Twitter Fawaz Alzaid @DrFAlzaid

Acknowledgements We thank Mylène Zarka Prost-Dumont, Morgane Bourmaud, Yohan Jouan and Yetki Aslan (UMRS-1132) for their precious help during the in vivo experiments.

Contributors H-KE conceived the study. FR, LC-G and H-KE contributed to its design and coordination, participated in data interpretation and cowrote the manuscript. LC-G and FR performed the laboratory experiments. CC synthesised calcium pyrophosphate crystals, characterised their physicochemical structure and contributed to writing the manuscript. LO, FA and NV performed the Seahorse experiments. FC and FF realised the metabolomics study. AP performed PET study. PR, TB, FR and H-KE collected the patient samples. H-KE, CC, PR, MC-S and FL secured the funding. All authors participated in the final approval of the manuscript.

Funding The study was funded by ANR (ANR-126BS08-0022-01), ART Viggo, the 'Prevention et Traitement des Décalcifications (PTD)' Association, Arthritis Courtin foundation (Arthritis R&D 2018-2019) and the French Society of Rheumatology (SFR 2017-2018, SFR 2018-2019). LC-G was financially supported by grants from ANR and ART Viggo, and FR by Paris Diderot University and ART Viggo, PTD.

Competing interests None declared.

Patient and public involvement Patients and/or the public were not involved in the design, conduct, reporting or dissemination plans of this research.

Patient consent for publication Not required.

Provenance and peer review Not commissioned; externally peer reviewed.

Data availability statement No data are available. All data relevant to the study are included in the article or uploaded as supplementary information. All data are included in the article.

ORCID iDs
Lucie Orliaguet http://orcid.org/0000-0002-3209-457X
Martine Cohen-Solal http://orcid.org/0000-0002-8582-8258
Pascal Richette http://orcid.org/0000-0003-2132-4074
Thomas Bardin http://orcid.org/0000-0002-5080-4790
Hang-Korng Ea http://orcid.org/0000-0002-2393-7475

REFERENCES

1 Martinon F, Pétrilli V, Mayor A, *et al*. Gout-associated uric acid crystals activate the NALP3 inflammasome. *Nature* 2006;440:237–41.
2 Martin WJ, Walton M, Harper J. Resident macrophages initiating and driving inflammation in a monosodium urate monohydrate crystal-induced murine peritoneal model of acute gout. *Arthritis Rheum* 2009;60:281–9.
3 Campillo-Gimenez L, Renaudin F, Jalabert M, *et al*. Inflammatory potential of four different phases of calcium pyrophosphate relies on NF-κB activation and MAPK pathways. *Front Immunol* 2018;9:2248.
4 Martinon F, Burns K, Tschopp J. The inflammasome: a molecular platform triggering activation of inflammatory caspases and processing of proIL-beta. *Mol Cell* 2002;10:417–26.
5 Lu A, Magupalli VG, Ruan J, *et al*. Unified polymerization mechanism for the assembly of ASC-dependent inflammasomes. *Cell* 2014;156:1193–206.
6 Sivera F, Andrés M, Pascual E. Current advances in therapies for calcium pyrophosphate crystal arthritis. *Curr Opin Rheumatol* 2016;28:140–4.
7 Richette P, Doherty M, Pascual E, *et al*. 2018 Updated European League against rheumatism evidence-based recommendations for the diagnosis of gout. *Ann Rheum Dis* 2020;79:31–8.
8 Warburg O, Wind F, Negelein E. The metabolism of tumors in the body. *J Gen Physiol* 1927;8:519–30.
9 Jha AK, Huang SC-C, Sergushichev A, *et al*. Network integration of parallel metabolic and transcriptional data reveals metabolic modules that regulate macrophage polarization. *Immunity* 2015;42:419–30.
10 Próchnicki T, Latz E. Inflammasomes on the crossroads of innate immune recognition and metabolic control. *Cell Metab* 2017;26:71–93.
11 Andrejeva G, Rathmell JC. Similarities and distinctions of cancer and immune metabolism in inflammation and tumors. *Cell Metab* 2017;26:49–70.
12 Tannahill GM, Curtis AM, Adamik J, *et al*. Succinate is an inflammatory signal that induces IL-1β through HIF-1α. *Nature* 2013;496:238–42.
13 Everts B, Amiel E, Huang SC-C, *et al*. TLR-driven early glycolytic reprogramming via the kinases TBK1-IKKε supports the anabolic demands of dendritic cell activation. *Nat Immunol* 2014;15:323–32.
14 Palsson-McDermott EM, Curtis AM, Goel G, *et al*. Pyruvate kinase M2 regulates HIF-1α activity and IL-1β induction and is a critical determinant of the Warburg effect in LPS-activated macrophages. *Cell Metab* 2015;21:65–80.

15 Moon J-S, Hisata S, Park M-A, *et al*. mTORC1-Induced HK1-Dependent glycolysis regulates NLRP3 inflammasome activation. *Cell Rep* 2015;12:102–15.
16 Hughes MM, O'Neill LAJ. Metabolic regulation of NLRP3. *Immunol Rev* 2018;281:88–98.
17 Mills EL, Kelly B, Logan A, *et al*. Succinate dehydrogenase supports metabolic repurposing of mitochondria to drive inflammatory macrophages. *Cell* 2016;167:457–70.
18 Steiner M, Vijayakumar V. Widespread tophaceous gout demonstrating avid F-18 fluorodeoxyglucose uptake. *Clin Nucl Med* 2009;34:433–4.
19 Shen G, Su M, Liu B, *et al*. A case of tophaceous pseudogout on 18F-FDG PET/CT imaging. *Clin Nucl Med* 2019;44:e98–100.
20 Youm Y-H, Nguyen KY, Grant RW, *et al*. The ketone metabolite β-hydroxybutyrate blocks NLRP3 inflammasome-mediated inflammatory disease. *Nat Med* 2015;21:263–9.
21 Goldberg EL, Asher JL, Molony RD, *et al*. β-Hydroxybutyrate Deactivates Neutrophil NLRP3 Inflammasome to Relieve Gout Flares. *Cell Rep* 2017;18:2077–87.
22 Yang C, Ko B, Hensley CT, *et al*. Glutamine oxidation maintains the TCA cycle and cell survival during impaired mitochondrial pyruvate transport. *Mol Cell* 2014;56:414–24.
23 Palmieri EM, Menga A, Martín-Pérez R, *et al*. Pharmacologic or genetic targeting of glutamine synthetase skews macrophages toward an M1-like phenotype and inhibits tumor metastasis. *Cell Rep* 2017;20:1654–66.
24 Freemerman AJ, Johnson AR, Sacks GN, *et al*. Metabolic reprogramming of macrophages: glucose transporter 1 (GLUT1)-mediated glucose metabolism drives a proinflammatory phenotype. *J Biol Chem* 2014;289:7884–96.
25 Caruana BT, Byrne FL, Knights AJ, *et al*. Characterization of glucose transporter 6 in lipopolysaccharide-induced bone marrow-derived macrophage function. *J Immunol* 2019;202:ji1801063.
26 O'Neill LAJ, Kishton RJ, Rathmell J. A guide to immunometabolism for immunologists. *Nat Rev Immunol* 2016;16:553–65.
27 Rousseau L-S, Paré G, Lachhab A, *et al*. S100A9 potentiates the activation of neutrophils by the etiological agent of gout, monosodium urate crystals. *J Leukoc Biol* 2017;102:805–13.
28 Stienstra R, Netea-Maier RT, Riksen NP, *et al*. Specific and complex reprogramming of cellular metabolism in myeloid cells during innate immune responses. *Cell Metab* 2017;26:142–56.
29 Lachmandas E, Boutens L, Ratter JM, *et al*. Microbial stimulation of different Toll-like receptor signalling pathways induces diverse metabolic programmes in human monocytes. *Nat Microbiol* 2016;2:16246.
30 Xue J, Schmidt SV, Sander J, *et al*. Transcriptome-based network analysis reveals a spectrum model of human macrophage activation. *Immunity* 2014;40:274–88.
31 Zhou R, Tardivel A, Thorens B, *et al*. Thioredoxin-interacting protein links oxidative stress to inflammasome activation. *Nat Immunol* 2010;11:136–40.
32 Moon HY, van Praag H. Muscle over mind. *Cell Metab* 2014;20:560–2.
33 Kornberg MD, Bhargava P, Kim PM, *et al*. Dimethyl fumarate targets GAPDH and aerobic glycolysis to modulate immunity. *Science* 2018;360:449–53.
34 Luo W, Hu H, Chang R, *et al*. Pyruvate kinase M2 is a PHD3-stimulated coactivator for hypoxia-inducible factor 1. *Cell* 2011;145:732–44.
35 Dror E, Dalmas E, Meier DT, *et al*. Postprandial macrophage-derived IL-1β stimulates insulin, and both synergistically promote glucose disposal and inflammation. *Nat Immunol* 2017;18:283–92.
36 Tavares LD, Galvão I, Costa VV, *et al*. Phosphoinositide-3 kinase gamma regulates caspase-1 activation and leukocyte recruitment in acute murine gout. *J Leukoc Biol* 2019;106:619–29.
37 Liu-Bryan R, Pritzker K, Firestein GS, *et al*. TLR2 signaling in chondrocytes drives calcium pyrophosphate dihydrate and monosodium urate crystal-induced nitric oxide generation. *J Immunol* 2005;174:5016–23.
38 Lee KY, Gesta S, Boucher J, *et al*. The differential role of Hif1β/Arnt and the hypoxic response in adipose function, fibrosis, and inflammation. *Cell Metab* 2011;14:491–503.
39 Meireles P, Sales-Dias J, Andrade CM, *et al*. GLUT1-mediated glucose uptake plays a crucial role during Plasmodium hepatic infection. *Cell Microbiol* 2017;19. doi:10.1111/cmi.12646. [Epub ahead of print: 02 Aug 2016].
40 Loisel-Meyer S, Swainson L, Craveiro M, *et al*. Glut1-mediated glucose transport regulates HIV infection. *Proc Natl Acad Sci U S A* 2012;109:2549–54.
41 Roy S, Leidal AM, Ye J, *et al*. Autophagy-Dependent shuttling of TBC1D5 controls plasma membrane translocation of GLUT1 and glucose uptake. *Mol Cell* 2017;67:84–95.
42 Steinberg F, Gallon M, Winfield M, *et al*. A global analysis of SNX27-retromer assembly and cargo specificity reveals a function in glucose and metal ion transport. *Nat Cell Biol* 2013;15:461–71.
43 Wieman HL, Wofford JA, Rathmell JC. Cytokine stimulation promotes glucose uptake via phosphatidylinositol-3 kinase/Akt regulation of GLUT1 activity and trafficking. *Mol Biol Cell* 2007;18:1437–46.
44 Beg M, Abdullah N, Thowfeik FS, *et al*. Distinct Akt phosphorylation states are required for insulin regulated GLUT4 and GLUT1-mediated glucose uptake. *Elife* 2017;6:e26896.
45 Phadngam S, Castiglioni A, Ferraresi A, *et al*. Pten dephosphorylates Akt to prevent the expression of GLUT1 on plasmamembrane and to limit glucose consumption in cancer cells. *Oncotarget* 2016;7:84999–5020.
46 Morani F, Phadngam S, Follo C, *et al*. PTEN regulates plasma membrane expression of glucose transporter 1 and glucose uptake in thyroid cancer cells. *J Mol Endocrinol* 2014;53:247–58.
47 Shinde SR, Maddika S. PTEN regulates glucose transporter recycling by impairing SNX27 retromer assembly. *Cell Rep* 2017;21:1655–66.
48 Wu N, Zheng B, Shaywitz A, *et al*. AMPK-dependent degradation of TXNIP upon energy stress leads to enhanced glucose uptake via GLUT1. *Mol Cell* 2013;49:1167–75.
49 Ives A, Nomura J, Martinon F, *et al*. Xanthine oxidoreductase regulates macrophage IL1β secretion upon NLRP3 inflammasome activation. *Nat Commun* 2015;6:6555.
50 Blodgett DM, De Zutter JK, Levine KB, *et al*. Structural basis of GLUT1 inhibition by cytoplasmic ATP. *J Gen Physiol* 2007;130:157–68.
51 Byrne FL, Olzomer EM, Brink R, *et al*. Knockout of glucose transporter GLUT6 has minimal effects on whole body metabolic physiology in mice. *Am J Physiol Endocrinol Metab* 2018;315:E286–93.
52 Maedera S, Mizuno T, Ishiguro H, *et al*. GLUT6 is a lysosomal transporter that is regulated by inflammatory stimuli and modulates glycolysis in macrophages. *FEBS Lett* 2019;593:195–208.
53 Vazirpanah N, Ottria A, van der Linden M, *et al*. mTOR inhibition by metformin impacts monosodium urate crystal-induced inflammation and cell death in gout: a prelude to a new add-on therapy? *Ann Rheum Dis* 2019;78:663–71.

Discussion and perspectives

This study focuses on macrophage metabolism in another context of sterile inflammation, gout and pseudo-gout flares induced by MSU and m-CPPD crystals. We unravel the contribution of metabolic pathways to the inflammatory process associated with IL1β production in this context.

Interestingly, both crystals induce GLUT1 translocation and consequent glucose uptake. Surprisingly, only MSU upregulates glycolysis. Despite changes in the TCA cycle, OXPHOS was not modulated with crystals stimulation. Interestingly, these metabolic adaptations are different from those typically described for M1 macrophages stimulated with LPS, and also different from those observed in other contexts of sterile inflammation, such as obesity. These differences highlight that macrophages specifically adapt their cellular metabolism in response to specific stressors and micro-environment. A precise description of the receptors and signaling pathways involved in these diverse contexts of macrophage polarization could provide a mechanistic insight.

In vivo, inhibition of glucose uptake with 2-DG limits the inflammatory response. Prior to considering 2-DG as a potent novel therapeutic strategy, it is crucial to fully understand the role of glucose metabolism in the pathogenesis of gout and pseudo-gout flares. The importance of glucose metabolism extends to neutrophils. Indeed, neutrophils found in the joint express higher levels of GLUT1 compared to circulating neutrophils.

Neutrophils, which are the predominant cell type in the synovial fluid during gouty inflammation, are key actors in gout and pseudo-gout development. IL1β production by macrophages triggers neutrophils recruitment and activation, with degranulation, cytokines production (214). Neutrophils appear to be also involved in the rapid resolution of inflammation (215), the precise mechanism is still controversial (216). Neutrophils undergo NETosis, a specific form of cell death associated with the release of DNA that can trap and degrade cytokines and chemokines (215). Regarding metabolic requirements of NETosis, it appears that neutrophils rely on glycolysis, PPP and glutaminolysis. 2-DG utilization can inhibit NETosis (217), and hypothetically the resolution of gouty inflammation. Therefore, glucose metabolism could to be critical for both the initiation and the resolution of inflammation.

Conclusion

This thesis mostly focused on the metabolic adaptations of ATMs during metabolic stress (**Axis 1**). More precisely, we shed the light on a novel function for the pro-inflammatory transcription factor IRF5 in regulating cellular metabolism of macrophages during the early adaptations to caloric excess. The repression of mitochondrial function induced by the activation of IRF5 is associated with AT maladaptation upon metabolic stress. We propose that IRF5 transcriptionally represses GHITM expression, inducing mitochondrial cristae disruption and subsequent decrease of the mitochondrial function of ATMs. In addition, this project highlights the major role of IRF5 in the pathogenesis of obesity and T2D, controlling both metabolic and inflammatory processes in a time-dependent manner. To date, this study highlights for the first time a role for IRF5 in controlling mitochondrial function.

Moreover, **Axis 2** underlies the importance of cellular metabolism in macrophage polarization *in vitro*. Finally, in **Axis 3**, we highlighted the potent role of glucose metabolism in the initiation of inflammation mediated by macrophages in the context of gout and pseudo-gout flares.

In this thesis, we confirmed the hyperoxidative phenotype of ATMs upon obesity. While not investigated in this thesis, ATMs are also hyperglycolytic in response to high fat feeding, notably due to GLUT1 translocation. This metabolic adaptation of macrophages is similarly observed in gouty inflammation, with the upregulation of GLUT1 translocation and subsequent glucose uptake and glycolysis. Nevertheless, the macrophage hyperoxidative phenotype appears to be a specific feature of the inflammatory contexts associated with metabolic disorders. This observation could be related to the fact that macrophages evolves in an environment that is metabolically rich in these pathological conditions.

As suggested in Axis 2, several metabolic pathways are involved in cytokine expression and secretion. Therefore, the diversity of the metabolic adaptations observed across the myriad of disorders and conditions associated with sterile inflammation can mirror the diversity of the macrophage functions and phenotypes that have been described in all these conditions.

In the context of obesity, considering ATMs heterogeneity and their pleiotropic functions, it could be interesting to focus on certain subpopulations of ATMs. Moreover, macrophage metabolic adaptations are stimulus-driven and location-specific. There is, therefore, a specific need to determine precise markers to study the different subpopulations of tissue-resident

macrophages and to develop experimental tools to assess their metabolic adaptations taking into account the influence of the micro-environment. Current approaches require cell sorting, which can affect cellular metabolism, or important quantity of biological material, which might be limiting in the context of tissue resident macrophages. Efforts have notably been made to integrate the spatial dimension of tissue organization with metabolomics approaches (147). Interestingly, a novel flow-cytometry based technology, SCENITH technology, has been developed to focus *ex vivo* on rare subpopulations of immune cells. This technic uses protein translation as a read-out of cellular metabolism. This approach could be applied to the different subpopulations of tissue resident macrophages, and in particular ATMs, in the context of metabolic stress (218,219).

Understanding metabolic adaptations of macrophages could provide powerful tools to harness inflammatory responses in a wide range of disorders, notably obesity, T2D and the associated comorbidities whose progressions are tightly linked with metainflammation. While clinical trials testing the therapeutic value of anti-inflammatory drugs in metabolic disorders are ongoing, targeting macrophage bioenergetics represents an interesting alternative. For example, IRF5 represents a potential therapeutic target to tackle AT maladaptation in early caloric excess, by enhancing mitochondrial function. Glycolysis could also be targeted to prevent the initiation of gouty inflammation. Therapeutic strategies could involve nutritional and dietary interventions to modulate nutrient availability (210) or drugs that mimic certain endogenous metabolites with immunomodulatory capacities, namely itaconate or fumarate or metabolic inhibitors, such as 2-DG (220). Nevertheless, one challenge remains to specifically target tissue-resident macrophages.

Overall, this thesis provides novel elements in the comprehension of immunometabolic processes related to macrophage activation, notably in different contexts of sterile inflammation. Cellular metabolism appears to be a determinant of macrophage phenotype, and more generally of immune cells activation.

Publications and presentations

Publications

This work is in the process of publication in peer-reviewed journals (Axis 1 and 2). The collaborative work presented in axis 3 has been published in Annals of the Rheumatic Diseases in 2020. Moreover, I have contributed to the writing of three reviews, two of them are presented in Appendix A and B.

1. **Orliaguet L**, Ejlalmanesh T, Humbert A, Ballaire R, Diedisheim M, Julla JB, Chokr D, Cuenco J, Michieletto J, Charbit J, Linden D, Boucher J, Potier C, Hamimi A, Lemoine S, Blugeon C, Legoix P, Lameiras S, Baudrin LG, Baulande S, Soprani A, Castelli FA, Fenaille F, Riveline JP, Dalmas E, Rieusset J, Gautier JF, Venteclef N, Alzaid, F. Interferon Regulatory Factor 5 represses mitochondrial matrix protein GHITM to limit macrophage oxidative capacity in early response to obesity. *Under consideration*
2. Thibaut R*, **Orliaguet L***, Ejlalmanesh T, Venteclef N, Alzaid F. Perspectives on Direction of control : Cellular metabolism and macrophage polarization. *Under consideration*
3. Renaudin F, **Orliaguet L**, Castelli F, Fenaille F, Prignon A, Alzaid F, Combes C, Delvaux A, Adimy Y, Cohen-Solal M, Richette P, Bardin T, Riveline JP, Venteclef N, Lioté F, Campillo-Gimenez L, Ea K. Gout and pseudo-gout-related crystals promote GLUT1-mediated glycolysis that governs NLRP3 and interleukin-1β activation on macrophages. Ann Rheum Dis. 2020 Nov;79(11):1506-1514. doi: 10.1136/annrheumdis-2020- 217342
4. **Orliaguet L**, Ejlalmanesh T, Alzaid F. Metabolic and Molecular Mechanisms of Macrophage Polarisation and Adipose Tissue Insulin Resistance. Int J Mol Sci. 2020, 21, 5731. doi: 10.3390/ijms21165731
5. **Orliaguet L**, Ejlalmanesh T, Venteclef N, Alzaid F. Inflammation métabolique : importance des macrophages et de leur métabolisme. Médecine des Maladies Métaboliques. 2020 Sept;14(5):429-436. doi: 10.1016/j.mmm.2020.06.017
6. **Orliaguet L**, Dalmas E, Drareni K, Venteclef N, Alzaid F. Mechanisms of Macrophage Polarization in Insulin Signaling and Sensitivity. Front Endocrinol. 2020 Feb 19;11:62doi: 10.3389/fendo.2020.00062

Presentations

This work focusing on IRF5 has been presented during several conferences.

Oral communications

2022: Annual congress of the French Society of Diabetes (SFD), Nice (France)
2021: Annual congress of the SFD, virtual
2020: Annual congress of the SFD, virtual
2019: Annual congress of the SFD, Marseille (France)

Posters

2022: Translational Immunometabolism, Cell Symposium, Basel (Switzerland)
2021: Annual congress of the French Society of Immunology, Paris (France)
2019: 4th International Conference on Immunometabolism, Rhodes (Greece)
2018: 6th DZD Diabetes Research School, Berlin (Germany)
2018: Translational Immunometabolism, Cell Symposium, Basel (Switzerland)

Bibliography

1. Blüher M. Obesity: global epidemiology and pathogenesis. Nat Rev Endocrinol. 2019;15(5):288–98.
2. Cameron NA, Petito LC, McCabe M, Allen NB, O'Brien MJ, Carnethon MR, et al. Quantifying the Sex-Race/Ethnicity-Specific Burden of Obesity on Incident Diabetes Mellitus in the United States, 2001 to 2016: MESA and NHANES. Journal of the American Heart Association. 2021 Feb 16;10(4):e018799.
3. Lange SJ. Longitudinal Trends in Body Mass Index Before and During the COVID-19 Pandemic Among Persons Aged 2–19 Years — United States, 2018–2020. MMWR Morb Mortal Wkly Rep [Internet]. 2021 [cited 2022 May 15];70. Available from: https://www.cdc.gov/mmwr/volumes/70/wr/mm7037a3.htm
4. Yeo GSH, Chao DHM, Siegert AM, Koerperich ZM, Ericson MD, Simonds SE, et al. The melanocortin pathway and energy homeostasis: From discovery to obesity therapy. Molecular Metabolism. 2021 Jun 1;48:101206.
5. Suriano F, Vieira-Silva S, Falony G, Roumain M, Paquot A, Pelicaen R, et al. Novel insights into the genetically obese (ob/ob) and diabetic (db/db) mice: two sides of the same coin. Microbiome. 2021 Jun 28;9(1):147.
6. Lutz TA, Woods SC. Overview of Animal Models of Obesity. Curr Protoc Pharmacol. 2012 Sep;CHAPTER:Unit5.61.
7. Bastías-Pérez M, Serra D, Herrero L. Dietary Options for Rodents in the Study of Obesity. Nutrients. 2020 Oct 22;12(11):3234.
8. Porter SA, Massaro JM, Hoffmann U, Vasan RS, O'Donnel CJ, Fox CS. Abdominal subcutaneous adipose tissue: a protective fat depot? Diabetes Care. 2009 Jun;32(6):1068–75.
9. Acosta JR, Douagi I, Andersson DP, Bäckdahl J, Rydén M, Arner P, et al. Increased fat cell size: a major phenotype of subcutaneous white adipose tissue in non-obese individuals with type 2 diabetes. Diabetologia. 2016 Mar 1;59(3):560–70.
10. Kane H, Lynch L. Innate Immune Control of Adipose Tissue Homeostasis. Trends Immunol. 2019 Sep;40(9):857–72.
11. Song Z, Xiaoli AM, Yang F. Regulation and Metabolic Significance of De Novo Lipogenesis in Adipose Tissues. Nutrients. 2018 Sep 29;10(10):1383.
12. Czech MP, Tencerova M, Pedersen DJ, Aouadi M. Insulin signalling mechanisms for triacylglycerol storage. Diabetologia. 2013 May;56(5):949–64.
13. Coelho M, Oliveira T, Fernandes R. Biochemistry of adipose tissue: an endocrine organ. Arch Med Sci. 2013 Apr 20;9(2):191–200.
14. Jo J, Gavrilova O, Pack S, Jou W, Mullen S, Sumner AE, et al. Hypertrophy and/or Hyperplasia: Dynamics of Adipose Tissue Growth. PLoS Comput Biol. 2009 Mar 27;5(3):e1000324.
15. Emont MP, Jacobs C, Essene AL, Pant D, Tenen D, Colleluori G, et al. A single-cell atlas of human and mouse white adipose tissue. Nature. 2022 Mar;603(7903):926–33.
16. Sárvári AK, Hauwaert ELV, Markussen LK, Gammelmark E, Marcher AB, Ebbesen MF, et

al. Plasticity of Epididymal Adipose Tissue in Response to Diet-Induced Obesity at Single-Nucleus Resolution. Cell Metabolism. 2021 Feb 2;33(2):437-453.e5.
17. Engin A. Adipose Tissue Hypoxia in Obesity and Its Impact on Preadipocytes and Macrophages: Hypoxia Hypothesis. In: Engin AB, Engin A, editors. Obesity and Lipotoxicity [Internet]. Cham: Springer International Publishing; 2017 [cited 2022 May 23]. p. 305–26. (Advances in Experimental Medicine and Biology). Available from: https://doi.org/10.1007/978-3-319-48382-5_13
18. Datta R, Podolsky MJ, Atabai K. Fat fibrosis: friend or foe? JCI Insight. 3(19):e122289.
19. Drareni K, Ballaire R, Alzaid F, Goncalves A, Chollet C, Barilla S, et al. Adipocyte Reprogramming by the Transcriptional Coregulator GPS2 Impacts Beta Cell Insulin Secretion. Cell Rep. 2020 Sep 15;32(11):108141.
20. Cao H, Sekiya M, Ertunc ME, Burak MF, Mayers JR, White A, et al. Adipocyte lipid chaperone AP2 is a secreted adipokine regulating hepatic glucose production. Cell Metab. 2013 May 7;17(5):768–78.
21. Hausberger FX. Pathological changes in adipose tissue of obese mice. The Anatomical Record. 1966;154(3):651–60.
22. Pekala P, Kawakami M, Vine W, Lane MD, Cerami A. Studies of insulin resistance in adipocytes induced by macrophage mediator. J Exp Med. 1983 Apr 1;157(4):1360–5.
23. Hotamisligil GS, Shargill NS, Spiegelman BM. Adipose expression of tumor necrosis factor-alpha: direct role in obesity-linked insulin resistance. Science. 1993 Jan 1;259(5091):87–91.
24. Calle MC, Fernandez ML. Inflammation and type 2 diabetes. Diabetes Metab. 2012 Jun;38(3):183–91.
25. Hotamisligil GS. Inflammation, metaflammation and immunometabolic disorders. Nature. 2017 Feb 8;542(7640):177–85.
26. Medzhitov R. Origin and physiological roles of inflammation. Nature. 2008 Jul 24;454(7203):428–35.
27. Rohm TV, Meier DT, Olefsky JM, Donath MY. Inflammation in obesity, diabetes, and related disorders. Immunity. 2022 Jan 11;55(1):31–55.
28. Weisberg SP, McCann D, Desai M, Rosenbaum M, Leibel RL, Ferrante AW. Obesity is associated with macrophage accumulation in adipose tissue. J Clin Invest. 2003 Dec;112(12):1796–808.
29. Hotamisligil GS, Peraldi P, Budavari A, Ellis R, White MF, Spiegelman BM. IRS-1-mediated inhibition of insulin receptor tyrosine kinase activity in TNF-alpha- and obesity-induced insulin resistance. Science. 1996 Feb 2;271(5249):665–8.
30. Haeusler RA, McGraw TE, Accili D. Biochemical and cellular properties of insulin receptor signalling. Nat Rev Mol Cell Biol. 2018 Jan;19(1):31–44.
31. Kanety H, Feinstein R, Papa MZ, Hemi R, Karasik A. Tumor necrosis factor alpha-induced phosphorylation of insulin receptor substrate-1 (IRS-1). Possible mechanism for suppression of insulin-stimulated tyrosine phosphorylation of IRS-1. J Biol Chem. 1995 Oct 6;270(40):23780–4.

32. Jager J, Grémeaux T, Cormont M, Le Marchand-Brustel Y, Tanti JF. Interleukin-1beta-induced insulin resistance in adipocytes through down-regulation of insulin receptor substrate-1 expression. Endocrinology. 2007 Jan;148(1):241–51.
33. Wunderlich CM, Hövelmeyer N, Wunderlich FT. Mechanisms of chronic JAK-STAT3-SOCS3 signaling in obesity. JAKSTAT. 2013 Apr 1;2(2):e23878.
34. Shimobayashi M, Albert V, Woelnerhanssen B, Frei IC, Weissenberger D, Meyer-Gerspach AC, et al. Insulin resistance causes inflammation in adipose tissue. J Clin Invest. 2018 Apr 2;128(4):1538–50.
35. Teh YC, Ding JL, Ng LG, Chong SZ. Capturing the Fantastic Voyage of Monocytes Through Time and Space. Frontiers in Immunology [Internet]. 2019 [cited 2022 May 8];10. Available from: https://www.frontiersin.org/article/10.3389/fimmu.2019.00834
36. Geissmann F, Manz MG, Jung S, Sieweke MH, Merad M, Ley K. Development of monocytes, macrophages and dendritic cells. Science. 2010 Feb 5;327(5966):656–61.
37. Ginhoux F, Greter M, Leboeuf M, Nandi S, See P, Gokhan S, et al. Fate mapping analysis reveals that adult microglia derive from primitive macrophages. Science. 2010 Nov 5;330(6005):841–5.
38. Yona S, Kim KW, Wolf Y, Mildner A, Varol D, Breker M, et al. Fate mapping reveals origins and dynamics of monocytes and tissue macrophages under homeostasis. Immunity. 2013 Jan 24;38(1):79–91.
39. Hashimoto D, Chow A, Noizat C, Teo P, Beasley MB, Leboeuf M, et al. Tissue resident macrophages self-maintain locally throughout adult life with minimal contribution from circulating monocytes. Immunity. 2013 Apr 18;38(4):10.1016/j.immuni.2013.04.004.
40. Epelman S, Lavine KJ, Beaudin AE, Sojka DK, Carrero JA, Calderon B, et al. Embryonic and adult-derived resident cardiac macrophages are maintained through distinct mechanisms at steady state and during inflammation. Immunity. 2014 Jan 16;40(1):91–104.
41. Guilliams M, De Kleer I, Henri S, Post S, Vanhoutte L, De Prijck S, et al. Alveolar macrophages develop from fetal monocytes that differentiate into long-lived cells in the first week of life via GM-CSF. J Exp Med. 2013 Sep 23;210(10):1977–92.
42. Ginhoux F, Guilliams M. Tissue-Resident Macrophage Ontogeny and Homeostasis. Immunity. 2016 Mar 15;44(3):439–49.
43. Martinez FO, Gordon S. The M1 and M2 paradigm of macrophage activation: time for reassessment. F1000Prime Rep. 2014;6:13.
44. Mantovani A, Sica A, Sozzani S, Allavena P, Vecchi A, Locati M. The chemokine system in diverse forms of macrophage activation and polarization. Trends Immunol. 2004 Dec;25(12):677–86.
45. Remmerie A, Martens L, Scott CL. Macrophage Subsets in Obesity, Aligning the Liver and Adipose Tissue. Front Endocrinol [Internet]. 2020 [cited 2020 May 29];11. Available from: https://www.frontiersin.org/articles/10.3389/fendo.2020.00259/full#h10
46. Gautier EL, Shay T, Miller J, Greter M, Jakubzick C, Ivanov S, et al. Gene expression profiles and transcriptional regulatory pathways underlying mouse tissue macrophage identity and diversity. Nat Immunol. 2012 Nov;13(11):1118–28.

47. Davies LC, Jenkins SJ, Allen JE, Taylor PR. Tissue-resident macrophages. Nat Immunol. 2013 Oct;14(10):986–95.
48. Blériot C, Chakarov S, Ginhoux F. Determinants of Resident Tissue Macrophage Identity and Function. Immunity. 2020 Jun 16;52(6):957–70.
49. Tugal D, Liao X, Jain MK. Transcriptional Control of Macrophage Polarization. Arteriosclerosis, Thrombosis, and Vascular Biology. 2013 Jun;33(6):1135–44.
50. Aaronson DS, Horvath CM. A Road Map for Those Who Don't Know JAK-STAT. Science. 2002 May 31;296(5573):1653–5.
51. Park C, Li S, Cha E, Schindler C. Immune Response in Stat2 Knockout Mice. Immunity. 2000 Dec 1;13(6):795–804.
52. Ohmori Y, Hamilton TA. STAT6 is required for the anti-inflammatory activity of interleukin-4 in mouse peritoneal macrophages. J Biol Chem. 1998 Oct 30;273(44):29202–9.
53. Liu T, Zhang L, Joo D, Sun SC. NF-κB signaling in inflammation. Sig Transduct Target Ther. 2017 Jul 14;2(1):1–9.
54. Fujioka S, Niu J, Schmidt C, Sclabas GM, Peng B, Uwagawa T, et al. NF-kappaB and AP-1 connection: mechanism of NF-kappaB-dependent regulation of AP-1 activity. Mol Cell Biol. 2004 Sep;24(17):7806–19.
55. McGettrick AF, O'Neill LAJ. The Role of HIF in Immunity and Inflammation. Cell Metabolism. 2020 Oct 6;32(4):524–36.
56. Ricote M, Li AC, Willson TM, Kelly CJ, Glass CK. The peroxisome proliferator-activated receptor-γ is a negative regulator of macrophage activation. Nature. 1998 Jan;391(6662):79–82.
57. Jiang C, Ting AT, Seed B. PPAR-gamma agonists inhibit production of monocyte inflammatory cytokines. Nature. 1998 Jan 1;391(6662):82–6.
58. Chawla A. Control of macrophage activation and function by PPARs. Circ Res. 2010 May 28;106(10):1559–69.
59. Ghisletti S, Huang W, Ogawa S, Pascual G, Lin ME, Willson TM, et al. Parallel SUMOylation-dependent pathways mediate gene- and signal-specific transrepression by LXRs and PPARgamma. Mol Cell. 2007 Jan 12;25(1):57–70.
60. Liao X, Sharma N, Kapadia F, Zhou G, Lu Y, Hong H, et al. Krüppel-like factor 4 regulates macrophage polarization. J Clin Invest. 2011 Jul 1;121(7):2736–49.
61. Das H, Kumar A, Lin Z, Patino WD, Hwang PM, Feinberg MW, et al. Kruppel-like factor 2 (KLF2) regulates proinflammatory activation of monocytes. Proceedings of the National Academy of Sciences. 2006 Apr 25;103(17):6653–8.
62. Orliaguet L, Dalmas E, Drareni K, Venteclef N, Alzaid F. Mechanisms of Macrophage Polarization in Insulin Signaling and Sensitivity. Front Endocrinol (Lausanne). 2020;11:62.
63. Orliaguet L, Ejlalmanesh T, Alzaid F. Metabolic and Molecular Mechanisms of Macrophage Polarisation and Adipose Tissue Insulin Resistance. Int J Mol Sci. 2020 Aug 10;21(16):E5731.
64. Thompson CD, Matta B, Barnes BJ. Therapeutic Targeting of IRFs: Pathway-Dependence or Structure-Based? Frontiers in Immunology [Internet]. 2018 [cited 2022 Apr

4];9. Available from: https://www.frontiersin.org/article/10.3389/fimmu.2018.02622
65. Antonczyk A, Krist B, Sajek M, Michalska A, Piaszyk-Borychowska A, Plens-Galaska M, et al. Direct Inhibition of IRF-Dependent Transcriptional Regulatory Mechanisms Associated With Disease. Frontiers in Immunology [Internet]. 2019 [cited 2022 May 11];10. Available from: https://www.frontiersin.org/article/10.3389/fimmu.2019.01176
66. Takaoka A, Yanai H, Kondo S, Duncan G, Negishi H, Mizutani T, et al. Integral role of IRF-5 in the gene induction programme activated by Toll-like receptors. Nature. 2005 Mar 10;434(7030):243–9.
67. Seneviratne AN, Edsfeldt A, Cole JE, Kassiteridi C, Swart M, Park I, et al. Interferon Regulatory Factor 5 Controls Necrotic Core Formation in Atherosclerotic Lesions by Impairing Efferocytosis. Circulation. 2017 Sep 19;136(12):1140–54.
68. Corbin AL, Gomez-Vazquez M, Berthold DL, Attar M, Arnold IC, Powrie FM, et al. IRF5 guides monocytes toward an inflammatory CD11c+ macrophage phenotype and promotes intestinal inflammation. Science Immunology. 2020 May 22;5(47):eaax6085.
69. Weiss M, Byrne AJ, Blazek K, Saliba DG, Pease JE, Perocheau D, et al. IRF5 controls both acute and chronic inflammation. Proc Natl Acad Sci USA. 2015 Sep 1;112(35):11001–6.
70. Dalmas E, Toubal A, Alzaid F, Blazek K, Eames HL, Lebozec K, et al. Irf5 deficiency in macrophages promotes beneficial adipose tissue expansion and insulin sensitivity during obesity. Nat Med. 2015 Jun;21(6):610–8.
71. Krausgruber T, Blazek K, Smallie T, Alzabin S, Lockstone H, Sahgal N, et al. IRF5 promotes inflammatory macrophage polarization and TH1-TH17 responses. Nat Immunol. 2011 Mar;12(3):231–8.
72. Cushing L, Winkler A, Jelinsky SA, Lee K, Korver W, Hawtin R, et al. IRAK4 kinase activity controls Toll-like receptor-induced inflammation through the transcription factor IRF5 in primary human monocytes. J Biol Chem. 2017 Nov 10;292(45):18689–98.
73. Chen W, Lam SS, Srinath H, Jiang Z, Correia JJ, Schiffer CA, et al. Insights into interferon regulatory factor activation from the crystal structure of dimeric IRF5. Nat Struct Mol Biol. 2008 Nov;15(11):1213–20.
74. Saliba DG, Heger A, Eames HL, Oikonomopoulos S, Teixeira A, Blazek K, et al. IRF5:RelA interaction targets inflammatory genes in macrophages. Cell Rep. 2014 Sep 11;8(5):1308–17.
75. Feng D, Sangster-Guity N, Stone R, Korczeniewska J, Mancl ME, Fitzgerald-Bocarsly P, et al. Differential Requirement of Histone Acetylase and Deacetylase Activities for IRF5-Mediated Proinflammatory Cytokine Expression. The Journal of Immunology. 2010 Nov 15;185(10):6003–12.
76. Eames HL, Saliba DG, Krausgruber T, Lanfrancotti A, Ryzhakov G, Udalova IA. KAP1/TRIM28: an inhibitor of IRF5 function in inflammatory macrophages. Immunobiology. 2012 Dec;217(12):1315–24.
77. Balkhi MY, Fitzgerald KA, Pitha PM. IKKalpha negatively regulates IRF-5 function in a MyD88-TRAF6 pathway. Cell Signal. 2010 Jan;22(1):117–27.
78. Ban T, Sato GR, Nishiyama A, Akiyama A, Takasuna M, Umehara M, et al. Lyn Kinase Suppresses the Transcriptional Activity of IRF5 in the TLR-MyD88 Pathway to Restrain the

Development of Autoimmunity. Immunity. 2016 Aug 16;45(2):319–32.
79. Lazzari E, Korczeniewska J, Ní Gabhann J, Smith S, Barnes BJ, Jefferies CA. TRIpartite motif 21 (TRIM21) differentially regulates the stability of interferon regulatory factor 5 (IRF5) isoforms. PLoS One. 2014;9(8):e103609.
80. Negishi H, Ohba Y, Yanai H, Takaoka A, Honma K, Yui K, et al. Negative regulation of Toll-like-receptor signaling by IRF-4. Proceedings of the National Academy of Sciences. 2005 Nov;102(44):15989–94.
81. Sigurdsson S, Padyukov L, Kurreeman FAS, Liljedahl U, Wiman AC, Alfredsson L, et al. Association of a haplotype in the promoter region of the interferon regulatory factor 5 gene with rheumatoid arthritis. Arthritis Rheum. 2007 Jul;56(7):2202–10.
82. Tang L, Chen B, Ma B, Nie S. Association between IRF5 polymorphisms and autoimmune diseases: a meta-analysis. Genet Mol Res. 2014 Jun 16;13(2):4473–85.
83. Song S, De S, Nelson V, Chopra S, LaPan M, Kampta K, et al. Inhibition of IRF5 hyperactivation protects from lupus onset and severity. J Clin Invest. 2020 Dec 1;130(12):6700–17.
84. Alzaid F, Lagadec F, Albuquerque M, Ballaire R, Orliaguet L, Hainault I, et al. IRF5 governs liver macrophage activation that promotes hepatic fibrosis in mice and humans. JCI Insight [Internet]. 2016 Dec 8 [cited 2020 May 29];1(20). Available from: https://insight.jci.org/articles/view/88689
85. Sindhu S, Kochumon S, Thomas R, Bennakhi A, Al-Mulla F, Ahmad R. Enhanced Adipose Expression of Interferon Regulatory Factor (IRF)-5 Associates with the Signatures of Metabolic Inflammation in Diabetic Obese Patients. Cells. 2020 Mar 16;9(3):E730.
86. Byrne AJ, Weiss M, Mathie SA, Walker SA, Eames HL, Saliba D, et al. A critical role for IRF5 in regulating allergic airway inflammation. Mucosal Immunol. 2017 May;10(3):716–26.
87. Almuttaqi H, Udalova IA. Advances and challenges in targeting IRF5, a key regulator of inflammation. The FEBS Journal. 2019;286(9):1624–37.
88. Hassnain Waqas SF, Noble A, Hoang AC, Ampem G, Popp M, Strauß S, et al. Adipose tissue macrophages develop from bone marrow–independent progenitors in Xenopus laevis and mouse. J Leukoc Biol. 2017 Sep;102(3):845–55.
89. Jaitin DA, Adlung L, Thaiss CA, Weiner A, Li B, Descamps H, et al. Lipid-Associated Macrophages Control Metabolic Homeostasis in a Trem2-Dependent Manner. Cell. 2019 25;178(3):686-698.e14.
90. Hill DA, Lim HW, Kim YH, Ho WY, Foong YH, Nelson VL, et al. Distinct macrophage populations direct inflammatory versus physiological changes in adipose tissue. Proc Natl Acad Sci USA. 2018 29;115(22):E5096–105.
91. Silva HM, Báfica A, Rodrigues-Luiz GF, Chi J, Santos P d'Emery A, Reis BS, et al. Vasculature-associated fat macrophages readily adapt to inflammatory and metabolic challenges. J Exp Med. 2019 01;216(4):786–806.
92. Pirzgalska RM, Seixas E, Seidman JS, Link VM, Sánchez NM, Mahú I, et al. Sympathetic neuron–associated macrophages contribute to obesity by importing and metabolizing norepinephrine. Nat Med. 2017 Nov;23(11):1309–18.

93. Burcelin R, Serino M, Chabo C, Garidou L, Pomié C, Courtney M, et al. Metagenome and metabolism: the tissue microbiota hypothesis. Diabetes Obes Metab. 2013 Sep;15 Suppl 3:61–70.
94. Fischer-Posovszky P, Wang QA, Asterholm IW, Rutkowski JM, Scherer PE. Targeted deletion of adipocytes by apoptosis leads to adipose tissue recruitment of alternatively activated M2 macrophages. Endocrinology. 2011 Aug;152(8):3074–81.
95. Lindhorst A, Raulien N, Wieghofer P, Eilers J, Rossi FMV, Bechmann I, et al. Adipocyte death triggers a pro-inflammatory response and induces metabolic activation of resident macrophages. Cell Death Dis. 2021 Jun 5;12(6):1–15.
96. Kosteli A, Sugaru E, Haemmerle G, Martin JF, Lei J, Zechner R, et al. Weight loss and lipolysis promote a dynamic immune response in murine adipose tissue. J Clin Invest. 2010 Oct;120(10):3466–79.
97. Nguyen KD, Qiu Y, Cui X, Goh YPS, Mwangi J, David T, et al. Alternatively activated macrophages produce catecholamines to sustain adaptive thermogenesis. Nature. 2011 Nov 20;480(7375):104–8.
98. Xu X, Grijalva A, Skowronski A, van Eijk M, Serlie MJ, Ferrante AW. Obesity activates a program of lysosomal-dependent lipid metabolism in adipose tissue macrophages independently of classic activation. Cell Metab. 2013 Dec 3;18(6):816–30.
99. Aouadi M, Vangala P, Yawe JC, Tencerova M, Nicoloro SM, Cohen JL, et al. Lipid storage by adipose tissue macrophages regulates systemic glucose tolerance. Am J Physiol Endocrinol Metab. 2014 Aug 15;307(4):E374-383.
100. Flaherty SE, Grijalva A, Xu X, Ables E, Nomani A, Ferrante AW. A lipase-independent pathway of lipid release and immune modulation by adipocytes. Science. 2019 01;363(6430):989–93.
101. Cox N, Crozet L, Holtman IR, Loyher PL, Lazarov T, White JB, et al. Diet-regulated production of PDGFcc by macrophages controls energy storage. Science. 2021 Jul 2;373(6550):eabe9383.
102. Cho CH, Jun Koh Y, Han J, Sung HK, Jong Lee H, Morisada T, et al. Angiogenic Role of LYVE-1–Positive Macrophages in Adipose Tissue. Circulation Research. 2007 Mar 2;100(4):e47–57.
103. Pang C, Gao Z, Yin J, Zhang J, Jia W, Ye J. Macrophage infiltration into adipose tissue may promote angiogenesis for adipose tissue remodeling in obesity. Am J Physiol Endocrinol Metab. 2008 Aug;295(2):E313-322.
104. Lee YH, Petkova AP, Granneman JG. Identification of an adipogenic niche for adipose tissue remodeling and restoration. Cell Metab. 2013 Sep 3;18(3):355–67.
105. Nawaz A, Aminuddin A, Kado T, Takikawa A, Yamamoto S, Tsuneyama K, et al. CD206+ M2-like macrophages regulate systemic glucose metabolism by inhibiting proliferation of adipocyte progenitors. Nat Commun. 2017 18;8(1):286.
106. Kim HJ, Higashimori T, Park SY, Choi H, Dong J, Kim YJ, et al. Differential effects of interleukin-6 and -10 on skeletal muscle and liver insulin action in vivo. Diabetes. 2004 Apr;53(4):1060–7.

107. Blüher M, Fasshauer M, Tönjes A, Kratzsch J, Schön MR, Paschke R. Association of interleukin-6, C-reactive protein, interleukin-10 and adiponectin plasma concentrations with measures of obesity, insulin sensitivity and glucose metabolism. Exp Clin Endocrinol Diabetes. 2005 Oct;113(9):534–7.
108. Ying W, Riopel M, Bandyopadhyay G, Dong Y, Birmingham A, Seo JB, et al. Adipose Tissue Macrophage-Derived Exosomal miRNAs Can Modulate In Vivo and In Vitro Insulin Sensitivity. Cell. 2017 Oct 5;171(2):372-384.e12.
109. Zheng C, Yang Q, Cao J, Xie N, Liu K, Shou P, et al. Local proliferation initiates macrophage accumulation in adipose tissue during obesity. Cell Death Dis. 2016 Mar 31;7:e2167.
110. Ramkhelawon B, Hennessy EJ, Ménager M, Ray TD, Sheedy FJ, Hutchison S, et al. Netrin-1 promotes adipose tissue macrophage retention and insulin resistance in obesity. Nat Med. 2014 Apr;20(4):377–84.
111. Amano SU, Cohen JL, Vangala P, Tencerova M, Nicoloro SM, Yawe JC, et al. Local proliferation of macrophages contributes to obesity-associated adipose tissue inflammation. Cell Metab. 2014 Jan 7;19(1):162–71.
112. Weisberg SP, Hunter D, Huber R, Lemieux J, Slaymaker S, Vaddi K, et al. CCR2 modulates inflammatory and metabolic effects of high-fat feeding. J Clin Invest. 2006 Jan;116(1):115–24.
113. Kamei N, Tobe K, Suzuki R, Ohsugi M, Watanabe T, Kubota N, et al. Overexpression of monocyte chemoattractant protein-1 in adipose tissues causes macrophage recruitment and insulin resistance. J Biol Chem. 2006 Sep 8;281(36):26602–14.
114. Kanda H, Tateya S, Tamori Y, Kotani K, Hiasa K ichi, Kitazawa R, et al. MCP-1 contributes to macrophage infiltration into adipose tissue, insulin resistance, and hepatic steatosis in obesity. J Clin Invest. 2006 Jun;116(6):1494–505.
115. Inouye KE, Shi H, Howard JK, Daly CH, Lord GM, Rollins BJ, et al. Absence of CC chemokine ligand 2 does not limit obesity-associated infiltration of macrophages into adipose tissue. Diabetes. 2007 Sep;56(9):2242–50.
116. Kirk EA, Sagawa ZK, McDonald TO, O'Brien KD, Heinecke JW. Monocyte chemoattractant protein deficiency fails to restrain macrophage infiltration into adipose tissue [corrected]. Diabetes. 2008 May;57(5):1254–61.
117. Cinti S, Mitchell G, Barbatelli G, Murano I, Ceresi E, Faloia E, et al. Adipocyte death defines macrophage localization and function in adipose tissue of obese mice and humans. J Lipid Res. 2005 Nov;46(11):2347–55.
118. Rausch ME, Weisberg S, Vardhana P, Tortoriello DV. Obesity in C57BL/6J mice is characterized by adipose tissue hypoxia and cytotoxic T-cell infiltration. Int J Obes (Lond). 2008 Mar;32(3):451–63.
119. Murano I, Barbatelli G, Parisani V, Latini C, Muzzonigro G, Castellucci M, et al. Dead adipocytes, detected as crown-like structures, are prevalent in visceral fat depots of genetically obese mice. J Lipid Res. 2008 Jul;49(7):1562–8.
120. Boutens L, Stienstra R. Adipose tissue macrophages: going off track during obesity.

Diabetologia. 2016 May;59(5):879–94.
121. Shi H, Kokoeva MV, Inouye K, Tzameli I, Yin H, Flier JS. TLR4 links innate immunity and fatty acid-induced insulin resistance. J Clin Invest. 2006 Nov;116(11):3015–25.
122. Shin KC, Hwang I, Choe SS, Park J, Ji Y, Kim JI, et al. Macrophage VLDLR mediates obesity-induced insulin resistance with adipose tissue inflammation. Nat Commun. 2017 20;8(1):1087.
123. Lumeng CN, Bodzin JL, Saltiel AR. Obesity induces a phenotypic switch in adipose tissue macrophage polarization. J Clin Invest. 2007 Jan;117(1):175–84.
124. Wentworth JM, Naselli G, Brown WA, Doyle L, Phipson B, Smyth GK, et al. Pro-Inflammatory CD11c+CD206+ Adipose Tissue Macrophages Are Associated With Insulin Resistance in Human Obesity. Diabetes. 2010 Jul;59(7):1648–56.
125. Kratz M, Coats BR, Hisert KB, Hagman D, Mutskov V, Peris E, et al. Metabolic dysfunction drives a mechanistically distinct proinflammatory phenotype in adipose tissue macrophages. Cell Metab. 2014 Oct 7;20(4):614–25.
126. Coats BR, Schoenfelt KQ, Barbosa-Lorenzi VC, Peris E, Cui C, Hoffman A, et al. Metabolically Activated Adipose Tissue Macrophages Perform Detrimental and Beneficial Functions during Diet-Induced Obesity. Cell Reports. 2017 Sep 26;20(13):3149–61.
127. Apovian CM, Bigornia S, Mott M, Meyers MR, Ulloor J, Gagua M, et al. Adipose Macrophage Infiltration Is Associated With Insulin Resistance and Vascular Endothelial Dysfunction in Obese Subjects. Arteriosclerosis, Thrombosis, and Vascular Biology. 2008 Sep;28(9):1654–9.
128. O'Neill LAJ, Kishton RJ, Rathmell J. A guide to immunometabolism for immunologists. Nat Rev Immunol. 2016;16(9):553–65.
129. Fu Y, Maianu L, Melbert BR, Garvey WT. Facilitative glucose transporter gene expression in human lymphocytes, monocytes, and macrophages: a role for GLUT isoforms 1, 3, and 5 in the immune response and foam cell formation. Blood Cells Mol Dis. 2004 Feb;32(1):182–90.
130. Caruana BT, Byrne FL, Knights AJ, Quinlan KGR, Hoehn KL. Characterization of Glucose Transporter 6 in Lipopolysaccharide-Induced Bone Marrow–Derived Macrophage Function. The Journal of Immunology. 2019 Mar 15;202(6):1826–32.
131. Olson AK, Bouchard B, Zhu WZ, Chatham JC, Rosiers CD. First characterization of glucose flux through the hexosamine biosynthesis pathway (HBP) in ex vivo mouse heart. Journal of Biological Chemistry. 2020 Feb 14;295(7):2018–33.
132. Panday A, Sahoo MK, Osorio D, Batra S. NADPH oxidases: an overview from structure to innate immunity-associated pathologies. Cell Mol Immunol. 2015 Jan;12(1):5–23.
133. Ge T, Yang J, Zhou S, Wang Y, Li Y, Tong X. The Role of the Pentose Phosphate Pathway in Diabetes and Cancer. Frontiers in Endocrinology [Internet]. 2020 [cited 2022 May 3];11. Available from: https://www.frontiersin.org/article/10.3389/fendo.2020.00365
134. Ren W, Xia Y, Chen S, Wu G, Bazer FW, Zhou B, et al. Glutamine Metabolism in Macrophages: A Novel Target for Obesity/Type 2 Diabetes. Adv Nutr. 2019 01;10(2):321–30.
135. Rodriguez AE, Ducker GS, Billingham LK, Martinez CA, Mainolfi N, Suri V, et al. Serine

Metabolism Supports Macrophage IL-1β Production. Cell Metab. 2019 02;29(4):1003-1011.e4.
136. Minhas PS, Liu L, Moon PK, Joshi AU, Dove C, Mhatre S, et al. Macrophage de novo NAD+ synthesis specifies immune function in aging and inflammation. Nat Immunol. 2019 Jan;20(1):50–63.
137. Bidault G, Virtue S, Petkevicius K, Jolin HE, Dugourd A, Guénantin AC, et al. SREBP1-induced fatty acid synthesis depletes macrophages antioxidant defences to promote their alternative activation. Nat Metab. 2021 Sep 1;3(9):1150–62.
138. Martínez-Reyes I, Chandel NS. Mitochondrial TCA cycle metabolites control physiology and disease. Nat Commun. 2020 Jan 3;11(1):102.
139. Anderson AJ, Jackson TD, Stroud DA, Stojanovski D. Mitochondria—hubs for regulating cellular biochemistry: emerging concepts and networks. Open Biology. 9(8):190126.
140. Spinelli JB, Haigis MC. The multifaceted contributions of mitochondria to cellular metabolism. Nat Cell Biol. 2018 Jul;20(7):745–54.
141. Palade GE. An electron microscope study of the mitochondrial structure. J Histochem Cytochem. 1953 Jul;1(4):188–211.
142. Cogliati S, Frezza C, Soriano ME, Varanita T, Quintana-Cabrera R, Corrado M, et al. Mitochondrial cristae shape determines respiratory chain supercomplexes assembly and respiratory efficiency. Cell. 2013 Sep 26;155(1):160–71.
143. Rambold AS, Pearce EL. Mitochondrial Dynamics at the Interface of Immune Cell Metabolism and Function. Trends in Immunology. 2018 Jan 1;39(1):6–18.
144. Wai T, Langer T. Mitochondrial Dynamics and Metabolic Regulation. Trends in Endocrinology & Metabolism. 2016 Feb 1;27(2):105–17.
145. Li Y, He Y, Miao K, Zheng Y, Deng C, Liu TM. Imaging of macrophage mitochondria dynamics in vivo reveals cellular activation phenotype for diagnosis. Theranostics. 2020 Feb 3;10(7):2897–917.
146. Van den Bossche J, Baardman J, de Winther MPJ. Metabolic Characterization of Polarized M1 and M2 Bone Marrow-derived Macrophages Using Real-time Extracellular Flux Analysis. J Vis Exp. 2015 Nov 28;(105):53424.
147. Artyomov MN, den Bossche JV. Immunometabolism in the single-cell era. Cell Metab. 2020 Nov 3;32(5):710–25.
148. Munder M, Eichmann K, Modolell M. Alternative metabolic states in murine macrophages reflected by the nitric oxide synthase/arginase balance: competitive regulation by CD4+ T cells correlates with Th1/Th2 phenotype. J Immunol. 1998 Jun 1;160(11):5347–54.
149. Pavlou S, Wang L, Xu H, Chen M. Higher phagocytic activity of thioglycollate-elicited peritoneal macrophages is related to metabolic status of the cells. J Inflamm (Lond). 2017;14:4.
150. Kellett DN. 2-Deoxyglucose and inflammation. J Pharm Pharmacol. 1966 Mar;18(3):199–200.
151. Freemerman AJ, Johnson AR, Sacks GN, Milner JJ, Kirk EL, Troester MA, et al. Metabolic reprogramming of macrophages: glucose transporter 1 (GLUT1)-mediated glucose metabolism drives a proinflammatory phenotype. J Biol Chem. 2014 Mar 14;289(11):7884–

96.
152. Freemerman AJ, Zhao L, Pingili AK, Teng B, Cozzo AJ, Fuller AM, et al. Myeloid Slc2a1-Deficient Murine Model Revealed Macrophage Activation and Metabolic Phenotype Are Fueled by GLUT1. J Immunol. 2019 Feb 15;202(4):1265–86.
153. Ip WKE, Hoshi N, Shouval DS, Snapper S, Medzhitov R. Anti-inflammatory effect of IL-10 mediated by metabolic reprogramming of macrophages. Science. 2017 05;356(6337):513–9.
154. Blouin CC, Pagé EL, Soucy GM, Richard DE. Hypoxic gene activation by lipopolysaccharide in macrophages: implication of hypoxia-inducible factor 1alpha. Blood. 2004 Feb 1;103(3):1124–30.
155. Tannahill GM, Curtis AM, Adamik J, Palsson-McDermott EM, McGettrick AF, Goel G, et al. Succinate is an inflammatory signal that induces IL-1β through HIF-1α. Nature. 2013 Apr 11;496(7444):238–42.
156. Rodríguez-Prados JC, Través PG, Cuenca J, Rico D, Aragonés J, Martín-Sanz P, et al. Substrate fate in activated macrophages: a comparison between innate, classic, and alternative activation. J Immunol. 2010 Jul 1;185(1):605–14.
157. Rodríguez-Prados JC, Través PG, Cuenca J, Rico D, Aragonés J, Martín-Sanz P, et al. Substrate Fate in Activated Macrophages: A Comparison between Innate, Classic, and Alternative Activation. The Journal of Immunology. 2010 Jul 1;185(1):605–14.
158. Palsson-McDermott EM, Curtis AM, Goel G, Lauterbach MA, Sheedy FJ, Gleeson LE, et al. Pyruvate Kinase M2 regulates Hif-1α activity and IL-1β induction, and is a critical determinant of the Warburg Effect in LPS-activated macrophages. Cell Metab. 2015 Jan 6;21(1):65–80.
159. Luo W, Hu H, Chang R, Zhong J, Knabel M, O'Meally R, et al. Pyruvate kinase M2 is a PHD3-stimulated coactivator for hypoxia-inducible factor 1. Cell. 2011 May 27;145(5):732–44.
160. Wolf AJ, Reyes CN, Liang W, Becker C, Shimada K, Wheeler ML, et al. Hexokinase Is an Innate Immune Receptor for the Detection of Bacterial Peptidoglycan. Cell. 2016 Jul 28;166(3):624–36.
161. Baardman J, Verberk SGS, Prange KHM, van Weeghel M, van der Velden S, Ryan DG, et al. A Defective Pentose Phosphate Pathway Reduces Inflammatory Macrophage Responses during Hypercholesterolemia. Cell Rep. 2018 20;25(8):2044-2052.e5.
162. Jha AK, Huang SCC, Sergushichev A, Lampropoulou V, Ivanova Y, Loginicheva E, et al. Network integration of parallel metabolic and transcriptional data reveals metabolic modules that regulate macrophage polarization. Immunity. 2015 Mar 17;42(3):419–30.
163. Lampropoulou V, Sergushichev A, Bambouskova M, Nair S, Vincent EE, Loginicheva E, et al. Itaconate Links Inhibition of Succinate Dehydrogenase with Macrophage Metabolic Remodeling and Regulation of Inflammation. Cell Metab. 2016 12;24(1):158–66.
164. Meiser J, Krämer L, Sapcariu SC, Battello N, Ghelfi J, D'Herouel AF, et al. Pro-inflammatory Macrophages Sustain Pyruvate Oxidation through Pyruvate Dehydrogenase for the Synthesis of Itaconate and to Enable Cytokine Expression. J Biol Chem. 2016 Feb 19;291(8):3932–46.

165. Langston PK, Nambu A, Jung J, Shibata M, Aksoylar HI, Lei J, et al. Glycerol phosphate shuttle enzyme GPD2 regulates macrophage inflammatory responses. Nat Immunol. 2019;20(9):1186–95.
166. Infantino V, Convertini P, Cucci L, Panaro MA, Di Noia MA, Calvello R, et al. The mitochondrial citrate carrier: a new player in inflammation. Biochemical Journal. 2011 Aug;438(3):433–6.
167. Infantino V, Iacobazzi V, Palmieri F, Menga A. ATP-citrate lyase is essential for macrophage inflammatory response. Biochem Biophys Res Commun. 2013 Oct 11;440(1):105–11.
168. Wei X, Song H, Yin L, Rizzo MG, Sidhu R, Covey DF, et al. Fatty acid synthesis configures the plasma membrane for inflammation in diabetes. Nature. 2016 10;539(7628):294–8.
169. Cervantes-Silva MP, Cox SL, Curtis AM. Alterations in mitochondrial morphology as a key driver of immunity and host defence. EMBO Rep. 2021 Sep 6;22(9):e53086.
170. Vats D, Mukundan L, Odegaard JI, Zhang L, Smith KL, Morel CR, et al. Oxidative metabolism and PGC-1beta attenuate macrophage-mediated inflammation. Cell Metab. 2006 Jul;4(1):13–24.
171. Wang F, Zhang S, Vuckovic I, Jeon R, Lerman A, Folmes CD, et al. Glycolytic Stimulation Is Not a Requirement for M2 Macrophage Differentiation. Cell Metab. 2018 04;28(3):463-475.e4.
172. Feingold KR, Shigenaga JK, Kazemi MR, McDonald CM, Patzek SM, Cross AS, et al. Mechanisms of triglyceride accumulation in activated macrophages. J Leukoc Biol. 2012 Oct;92(4):829–39.
173. Huang SCC, Everts B, Ivanova Y, O'Sullivan D, Nascimento M, Smith AM, et al. Cell-intrinsic lysosomal lipolysis is essential for alternative activation of macrophages. Nat Immunol. 2014 Sep;15(9):846–55.
174. Nomura M, Liu J, Rovira II, Gonzalez-Hurtado E, Lee J, Wolfgang MJ, et al. Fatty acid oxidation in macrophage polarization. Nat Immunol. 2016 Mar;17(3):216–7.
175. Divakaruni AS, Hsieh WY, Minarrieta L, Duong TN, Kim KKO, Desousa BR, et al. Etomoxir Inhibits Macrophage Polarization by Disrupting CoA Homeostasis. Cell Metab. 2018 Sep 4;28(3):490-503.e7.
176. Oishi Y, Spann NJ, Link VM, Muse ED, Strid T, Edillor C, et al. SREBP1 Contributes to Resolution of Pro-inflammatory TLR4 Signaling by Reprogramming Fatty Acid Metabolism. Cell Metab. 2017 07;25(2):412–27.
177. Huang SCC, Smith AM, Everts B, Colonna M, Pearce EL, Schilling JD, et al. Metabolic Reprogramming Mediated by the mTORC2-IRF4 Signaling Axis Is Essential for Macrophage Alternative Activation. Immunity. 2016 Oct 18;45(4):817–30.
178. Covarrubias AJ, Aksoylar HI, Yu J, Snyder NW, Worth AJ, Iyer SS, et al. Akt-mTORC1 signaling regulates Acly to integrate metabolic input to control of macrophage activation. Elife. 2016 Feb 19;5.
179. Tavakoli S, Downs K, Short JD, Nguyen HN, Lai Y, Jerabek PA, et al. Characterization of Macrophage Polarization States Using Combined Measurement of 2-Deoxyglucose and

Glutamine Accumulation: Implications for Imaging of Atherosclerosis. Arterioscler Thromb Vasc Biol. 2017;37(10):1840–8.
180. Wang XF, Wang HS, Wang H, Zhang F, Wang KF, Guo Q, et al. The role of indoleamine 2,3-dioxygenase (IDO) in immune tolerance: focus on macrophage polarization of THP-1 cells. Cell Immunol. 2014 Jun;289(1–2):42–8.
181. Haschemi A, Kosma P, Gille L, Evans CR, Burant CF, Starkl P, et al. The sedoheptulose kinase CARKL directs macrophage polarization through control of glucose metabolism. Cell Metab. 2012 Jun 6;15(6):813–26.
182. Caputa G, Castoldi A, Pearce EJ. Metabolic adaptations of tissue-resident immune cells. Nat Immunol. 2019 Jul;20(7):793–801.
183. Svedberg FR, Brown SL, Krauss MZ, Campbell L, Sharpe C, Clausen M, et al. The lung environment controls alveolar macrophage metabolism and responsiveness in type 2 inflammation. Nat Immunol. 2019 May;20(5):571–80.
184. Okabe Y, Medzhitov R. Tissue-Specific Signals Control Reversible Program of Localization and Functional Polarization of Macrophages. Cell. 2014 May 8;157(4):832–44.
185. Davies LC, Rice CM, Palmieri EM, Taylor PR, Kuhns DB, McVicar DW. Peritoneal tissue-resident macrophages are metabolically poised to engage microbes using tissue-niche fuels. Nat Commun. 2017 Dec 12;8(1):2074.
186. Gautier EL, Ivanov S, Williams JW, Huang SCC, Marcelin G, Fairfax K, et al. Gata6 regulates aspartoacylase expression in resident peritoneal macrophages and controls their survival. J Exp Med. 2014 Jul 28;211(8):1525–31.
187. Zhang S, Weinberg S, DeBerge M, Gainullina A, Schipma M, Kinchen JM, et al. Efferocytosis Fuels Requirements of Fatty Acid Oxidation and the Electron Transport Chain to Polarize Macrophages for Tissue Repair. Cell Metab. 2019 Feb 5;29(2):443-456.e5.
188. Yurdagul A, Subramanian M, Wang X, Crown SB, Ilkayeva OR, Darville L, et al. Macrophage Metabolism of Apoptotic Cell-Derived Arginine Promotes Continual Efferocytosis and Resolution of Injury. Cell Metabolism. 2020 Mar 3;31(3):518-533.e10.
189. Ampomah PB, Cai B, Sukka SR, Gerlach BD, Yurdagul A, Wang X, et al. Macrophages use apoptotic cell-derived methionine and DNMT3A during efferocytosis to promote tissue resolution. Nat Metab. 2022 Apr;4(4):444–57.
190. Serbulea V, Upchurch CM, Schappe MS, Voigt P, DeWeese DE, Desai BN, et al. Macrophage phenotype and bioenergetics are controlled by oxidized phospholipids identified in lean and obese adipose tissue. Proc Natl Acad Sci U S A. 2018 Jul 3;115(27):E6254–63.
191. Boutens L, Hooiveld GJ, Dhingra S, Cramer RA, Netea MG, Stienstra R. Unique metabolic activation of adipose tissue macrophages in obesity promotes inflammatory responses. Diabetologia. 2018;61(4):942–53.
192. Sharma M, Boytard L, Hadi T, Koelwyn G, Simon R, Ouimet M, et al. Enhanced glycolysis and HIF-1α activation in adipose tissue macrophages sustains local and systemic interleukin-1β production in obesity. Sci Rep. 2020 Mar 27;10(1):5555.
193. Hedl M, Yan J, Abraham C. IRF5 and IRF5 Disease-Risk Variants Increase Glycolysis and Human M1 Macrophage Polarization by Regulating Proximal Signaling and Akt2 Activation.

Cell Rep. 2016 30;16(9):2442–55.
194. Albers GJ, Iwasaki J, McErlean P, Ogger PP, Ghai P, Khoyratty TE, et al. IRF5 regulates airway macrophage metabolic responses. Clin Exp Immunol. 2021 Apr;204(1):134–43.
195. Jung SB, Choi MJ, Ryu D, Yi HS, Lee SE, Chang JY, et al. Reduced oxidative capacity in macrophages results in systemic insulin resistance. Nat Commun. 2018 Apr 19;9(1):1551.
196. Wang Y, Tang B, Long L, Luo P, Xiang W, Li X, et al. Improvement of obesity-associated disorders by a small-molecule drug targeting mitochondria of adipose tissue macrophages. Nat Commun. 2021 Jan 4;12(1):102.
197. Zezina E, Snodgrass RG, Schreiber Y, Zukunft S, Schürmann C, Heringdorf DMZ, et al. Mitochondrial fragmentation in human macrophages attenuates palmitate-induced inflammatory responses. Biochim Biophys Acta Mol Cell Biol Lipids. 2018 Apr;1863(4):433–46.
198. Lancaster GI, Langley KG, Berglund NA, Kammoun HL, Reibe S, Estevez E, et al. Evidence that TLR4 Is Not a Receptor for Saturated Fatty Acids but Mediates Lipid-Induced Inflammation by Reprogramming Macrophage Metabolism. Cell Metab. 2018 May 1;27(5):1096-1110.e5.
199. Oka T, Sayano T, Tamai S, Yokota S, Kato H, Fujii G, et al. Identification of a Novel Protein MICS1 that is Involved in Maintenance of Mitochondrial Morphology and Apoptotic Release of Cytochrome c. Mol Biol Cell. 2008 Jun;19(6):2597–608.
200. Nagel J, Smith R, Shaw L, Bertak D, Dixit V, Schaffer E, et al. Identification of genes differentially expressed in T cells following stimulation with the chemokines CXCL12 and CXCL10. BMC Immunology. 2004 Aug 5;5(1):17.
201. Moni MA, Liò P. Network-based analysis of comorbidities risk during an infection: SARS and HIV case studies. BMC Bioinformatics. 2014 Oct 24;15(1):333.
202. Morgantini C, Jager J, Li X, Levi L, Azzimato V, Sulen A, et al. Liver macrophages regulate systemic metabolism through non-inflammatory factors. Nature Metabolism. 2019 Apr;1(4):445–59.
203. López-Villegas D, Lenkinski Robert E, Wehrli SL, Ho WZ, Douglas SD. Lactate production by human monocytes/macrophages determined by proton mr spectroscopy. Magnetic Resonance in Medicine. 1995;34(1):32–8.
204. Liu C, Wu J, Zhu J, Kuei C, Yu J, Shelton J, et al. Lactate inhibits lipolysis in fat cells through activation of an orphan G-protein-coupled receptor, GPR81. J Biol Chem. 2009 Jan 30;284(5):2811–22.
205. Littlewood-Evans A, Sarret S, Apfel V, Loesle P, Dawson J, Zhang J, et al. GPR91 senses extracellular succinate released from inflammatory macrophages and exacerbates rheumatoid arthritis. Journal of Experimental Medicine. 2016 Aug 1;213(9):1655–62.
206. Regard JB, Sato IT, Coughlin SR. Anatomical Profiling of G Protein-Coupled Receptor Expression. Cell. 2008 Oct 31;135(3):561–71.
207. Aouadi M, Tencerova M, Vangala P, Yawe JC, Nicoloro SM, Amano SU, et al. Gene silencing in adipose tissue macrophages regulates whole-body metabolism in obese mice. Proc Natl Acad Sci U S A. 2013 May 14;110(20):8278–83.
208. Banga J, Srinivasan D, Sun CC, Thompson CD, Milletti F, Huang KS, et al. Inhibition of IRF5 cellular activity with cell-penetrating peptides that target homodimerization. Science

Advances. 2020 May 15;6(20):eaay1057.
209. Weihrauch D, Krolikowski JG, Jones DW, Zaman T, Bamkole O, Struve J, et al. An IRF5 Decoy Peptide Reduces Myocardial Inflammation and Fibrosis and Improves Endothelial Cell Function in Tight-Skin Mice. PLoS One. 2016;11(4):e0151999.
210. Collins N, Belkaid Y. Control of immunity via nutritional interventions. Immunity. 2022 Feb 8;55(2):210–23.
211. Dehlin M, Jacobsson L, Roddy E. Global epidemiology of gout: prevalence, incidence, treatment patterns and risk factors. Nat Rev Rheumatol. 2020 Jul;16(7):380–90.
212. Shen G, Su M, Liu B, Kuang A. A Case of Tophaceous Pseudogout on 18F-FDG PET/CT Imaging. Clinical Nuclear Medicine. 2019 Feb;44(2):e98.
213. Steiner M, Vijayakumar V. Widespread Tophaceous Gout Demonstrating AvidF-18 Fluorodeoxyglucose Uptake. Clinical Nuclear Medicine. 2009 Jul;34(7):433–4.
214. Mitroulis I, Kambas K, Ritis K. Neutrophils, IL-1β, and gout: is there a link? Semin Immunopathol. 2013 Jul 1;35(4):501–12.
215. Schauer C, Janko C, Munoz LE, Zhao Y, Kienhöfer D, Frey B, et al. Aggregated neutrophil extracellular traps limit inflammation by degrading cytokines and chemokines. Nat Med. 2014 May;20(5):511–7.
216. Reber LL, Gaudenzio N, Starkl P, Galli SJ. Neutrophils are not required for resolution of acute gouty arthritis in mice. Nat Med. 2016 Dec;22(12):1382–4.
217. Morán G, Uberti B, Quiroga J. Role of Cellular Metabolism in the Formation of Neutrophil Extracellular Traps in Airway Diseases. Front Immunol. 2022 Apr 12;13:850416.
218. Argüello RJ, Combes AJ, Char R, Gigan JP, Baaziz AI, Bousiquot E, et al. SCENITH: A Flow Cytometry-Based Method to Functionally Profile Energy Metabolism with Single-Cell Resolution. Cell Metab. 2020 Dec 1;32(6):1063-1075.e7.
219. Verberk SGS, de Goede KE, Gorki FS, van Dierendonck XAMH, Argüello RJ, Van den Bossche J. An integrated toolbox to profile macrophage immunometabolism. Cell Reports Methods. 2022 Apr 25;2(4):100192.
220. Pålsson-McDermott EM, O'Neill LAJ. Targeting immunometabolism as an anti-inflammatory strategy. Cell Res. 2020 Apr;30(4):300–14.

Appendix 1

Review published in February 2020, in Frontiers in Endocrinology.

frontiers in Endocrinology

REVIEW
published: 19 February 2020
doi: 10.3389/fendo.2020.00062

Mechanisms of Macrophage Polarization in Insulin Signaling and Sensitivity

Lucie Orliaguet[1], *Elise Dalmas*[1], *Karima Drareni*[1,2], *Nicolas Venteclef*[1] *and Fawaz Alzaid*[1]*

[1] Centre de Recherche des Cordeliers, INSERM, Sorbonne Université, USPC, Université Paris Descartes, Université Paris Diderot, Paris, France, [2] Institute for Diabetes, Obesity and Metabolism, University of Pennsylvania, Philadelphia, PA, United States

Type-2 diabetes (T2D) is a disease of two etiologies: metabolic and inflammatory. At the cross-section of these etiologies lays the phenomenon of metabolic inflammation. Whilst metabolic inflammation is characterized as systemic, a common starting point is the tissue-resident macrophage, who's successful physiological or aberrant pathological adaptation to its microenvironment determines disease course and severity. This review will highlight the key mechanisms in macrophage polarization, inflammatory and non-inflammatory signaling that dictates the development and progression of insulin resistance and T2D. We first describe the known homeostatic functions of tissue macrophages in insulin secreting and major insulin sensitive tissues. Importantly we highlight the known mechanisms of aberrant macrophage activation in these tissues and the ways in which this leads to impairment of insulin sensitivity/secretion and the development of T2D. We next describe the cellular mechanisms that are known to dictate macrophage polarization. We review recent progress in macrophage bio-energetics, an emerging field of research that places cellular metabolism at the center of immune-effector function. Importantly, following the advent of the metabolically-activated macrophage, we cover the known transcriptional and epigenetic factors that canonically and non-canonically dictate macrophage differentiation and inflammatory polarization. In closing perspectives, we discuss emerging research themes and highlight novel non-inflammatory or non-immune roles that tissue macrophages have in maintaining microenvironmental and systemic homeostasis.

Keywords: macrophage, inflammation, type-2 diabetes, adipose tissue, liver, pancreas, immunometabolism

OPEN ACCESS

Edited by:
Rinke Stienstra, Radboud University Nijmegen Medical Centre, Netherlands

Reviewed by:
Anne-Francoise Burnol, INSERM U1016 Institut Cochin, France
Xavier Prieur, INSERM U1087 L'unité de recherche de l'institut du thorax, France

***Correspondence:**
Fawaz Alzaid
fawaz.alzaid@gmail.com;
fawaz.alzaid@inserm.fr

Specialty section:
This article was submitted to Diabetes: Molecular Mechanisms, a section of the journal Frontiers in Endocrinology

Received: *03 December 2019*
Accepted: *30 January 2020*
Published: *19 February 2020*

Citation:
Orliaguet L, Dalmas E, Drareni K, Venteclef N and Alzaid F (2020) Mechanisms of Macrophage Polarization in Insulin Signaling and Sensitivity. Front. Endocrinol. 11:62. doi: 10.3389/fendo.2020.00062

INTRODUCTION: INFLAMMATION IN INSULIN SECRETION, SENSITIVITY AND RESISTANCE

Type-2 diabetes (T2D) is a disease with dual etiologies, inflammatory, and metabolic. Over the past 20 years, inflammation has gained increasing recognition for the important role it plays in increasing risk of insulin resistance and can be seen as an aetiological starting point for metabolic decline. Several studies have attempted to define the kinetics between inflammation and insulin resistance, where some report local insulin resistance preceding inflammation (1) and others reporting inflammation prior to insulin resistance (2). However, blunting inflammatory responses has consistently been reported as metabolically protective, mitigating the development of insulin resistance and T2D. Thus, inflammation is seen decisive factor in losing tolerance to metabolic

dysregulation. Insulin resistance in the liver, adipose tissue and skeletal muscle is initially met with a burst of activity from the pancreas that maintains normal levels of glycaemia (the pre-diabetic stage) (3–5). When this stage is prolonged and insulin production can no longer meet demands, frank T2D develops and predisposes individuals to a variety of complications and comorbidities (**Figure 1**). These complications and comorbidities are broadly hepatic and cardiovascular in nature and are directly related to increasing inflammation, hyperglycaemia, and dyslipidemia. The following review addresses the various mechanisms and roles of inflammation in the development of T2D with a particular focus on the liver, adipose tissue and the pancreas.

Inflammation and Metabolic Health

The first evidence linking inflammation to metabolic health dates back to 1993 when Gokhan Hotamisligil and Bruce Spiegelman discovered the increasing expression of pro-inflammatory cytokine tumor necrosis factor (TNF)-α in adipose tissue (AT) of rodent models of obesity (6). Neutralizing TNF-α in obese rats led to a significant increase in glucose uptake in response to insulin. Their study showed that blocking a single cytokine can restore insulin sensitivity. A decade later, macrophages were identified as the main source of TNF-α and other pro-inflammatory molecules (IL-6 and iNOS) in obesity (7). Moreover, macrophages drastically accumulate in adipose tissue during obesity and at the onset of insulin resistance. These early studies brought-to-light the contribution of inflammation to metabolic decline associated with insulin resistance and T2D.

Since these findings, the immune system has gained considerable attention as a major regulator of metabolic homeostasis. Innate immune cells, namely macrophages, reside in all the metabolic tissues that coordinate glycemic homeostasis, namely AT, liver, and pancreas. Tissue-resident innate immune cells form a *bona fide* tissue-specific immune niche, with each niche having its particularities to cope with microenvironmental cues. Macrophages are by far the most studied and proportionally numerous innate immune cell type [25% of AT innate immune cells (8), 20–35% of the non-parenchymal hepatic cells in the liver (9), up to 90% of immune cells in pancreatic islets (10)].

Macrophage Polarization: Regulation of Acute and Chronic Inflammation

Macrophages were firstly identified by Ellie Metchnikoff as phagocytic cells. They form part of the myeloid lineage and are capable of rapidly mounting non-specific responses to a wide range of pathogens. Phagocytosis is a cellular process associated with innate immune responses to pathogens, is critical in the clearance of cellular debris, tissue repair, and maintaining tissue homeostasis throughout the organism. Tissue-resident macrophages develop from progenitors in the yolk sac, fetal liver, and from circulating monocytes that originate in bone marrow (11). Under physiological conditions, tissue-resident macrophages play a key role in the maintenance of the integrity and homeostasis of their respective tissues.

Macrophages quickly respond to environmental cues and consequently adapt their function, they sense changes in their microenvironment through cell surface receptor engagement. The main receptors relaying environmental signals are toll-like receptors (TLRs), which form part of the larger family of pattern recognition receptors (PRRs). Ligation of TLRs/PRRs by damage- or pathogen-associated molecular patterns (DAMP/PAMPs) present in the microenvironment activates transcriptional programs in macrophages to mount an adapted functional phenotype (12). Whilst these transcriptional mechanisms have been well-described (and are addressed in this review), macrophages also extensively adapt their cellular metabolism to meet the bioenergetic needs and optimize effector function (13). The latter has gained much attention in recent research.

A dichotomy is currently used to describe macrophage polarization states: M1 as pro-inflammatory or classically activated vs. M2 as anti-inflammatory or alternatively activated (**Figure 2**). The nomenclature of these subsets derives from

Abbreviations: 2-DG, 2-deoxyglucose; ABCA/G1, ATP-binding cassette transporter; ACLY, ATP citrate lyase; AMPK, AMP-activated protein kinase; AP-1, Activator protein 1; APOA1, Apolipoprotein A1; ARG1, Arginase 1; AT, Adipose tissue; ATM, Adipose tissue macrophage; ATP, Adenosine triphosphate; CARKL, carbohydrate kinase like (sedoheptulose kinase); CCL2, Chemokine (C-C motif) ligand 2/monocyte chemoattractant protein 1; CCR2, C-C chemokine receptor 2; CD, Cluster of differentiation; Clec4F, C-type lectin domain family 4 member F; CLS, Crown-like structure; COX2, Cyclooxygenase 2; DAMP, Damage-associated molecular pattern; ETC, Electron transfer chain; EZH2, Enhancer of zeste homolog 2; FA, Fatty acid; FAS, Fatty acid synthase; FATP, Fatty acid transporter protein; FOXO, Forkhead box protein O; GC, Glucocorticoids; GLUT1, Glucose transporter 1; GPS2, G Protein Pathway Suppressor 2; GR, Glucocorticoid receptor; GRIP1, Glutamate receptor interacting protein 1; HDAC, Histone deacetylase; HFD, High-fat diet; HIF1, Hypoxia inducible factor 1; HK, Hexokinase; HRE, Hypoxia response element; HSC, Hepatic stellate cell; IFN, Interferon; IGFBP-7, Insulin-like growth factor binding protein 7; IKK, IκB Kinase; IL, Interleukin; iNOS, inducible nitrous oxide synthase; IRAK, Interleukin-1 receptor associated kinase; IRF, Interferon regulatory factor; IRS, Insulin receptor substrate; JAK, Janus Kinase; JNK, c-Jun N-terminal kinase; KC, Kupffer cell; KDM6B, Lysine demethylase 6B; KLF4, Kruppel-like factor 4; LPL, Lipoprotein lipase; LPS, Lipopolysaccharides; LXR, Liver-X-receptor; Ly6c/g, Lymphocyte antigen 6 c/g; MAPK, Mitogen activated protein kinase; miRNA/miR, Micro RNA; Mme, metabolically activated macrophage; MSR, Macrophage scavenger receptor; MyD88, Myeloid differentiation primary response 88; NADH, Nicotinamide adenine dinucleotide + hydrogen; NADPH, Nicotinamide adenine dinucleotide phosphate; NAFLD, Non-alcoholic fatty liver disease; NASH, Non-alcoholic steatohepatitis; NCoR, Nuclear receptor corepressor; NFκB, Nuclear factor-kB; NLRP3, NACHT, LRR and PYD domains-containing protein 3; NO, Nitrous oxide; NR, Nuclear receptor; OPN, Osteopontin; OXPHOS, Oxidative phosphorylation; PAMP, Pathogen associated molecular pattern; PD1, programmed cell death protein 1; PDGF-R, Platelet-derived growth factor receptor; PDH, Pyruvate dehydrogenase; PFK/uPFK, Phosphofructokinase/ubiquitous Phosphofructokinase; PGC-1a, Peroxisome proliferator-activated receptor gamma coactivator 1-alpha; PKM2, Pyruvate kinase isozyme M2; PPAR, Peroxisome proliferator-activated receptor; PPP, Pentose phosphate pathway; PRR, Pattern recognition receptor; ROS, Reactive oxygen species; SDH, Succinate dehydrogenase; SLC1A5, Solute carrier family 1 member 5; SMRT, Silencing mediator for retinoid or thyroid-hormone receptor; SOCS, Suppressor of cytokine signaling; SREBP, Sterol regulatory element binding protein; STAT, Signal transducer and activator of transcription; T2D, Type-2 diabetes; TCA, Tricarboxylic acid; TGF, Transforming growth factor; Th, T-helper; TIRAP, Till-interleukin 1 receptor domain containing adaptor protein; TLR, Toll-like receptor; TNF, Tumor necrosis factor; TRAM, TRIF-related adaptor molecule; Treg, Regulatory T-cell; TREM2, Triggering receptor expressed on myeloid cells 2; TRIF, Toll-interleukin receptor adaptor inducing interferon-B; UDP-GlcNac, Uridine diphosphate N-acetylglucosamine; VASP, Vasodilator-stimulated phosphoprotein; VLDL, Very-low density lipoproteins.

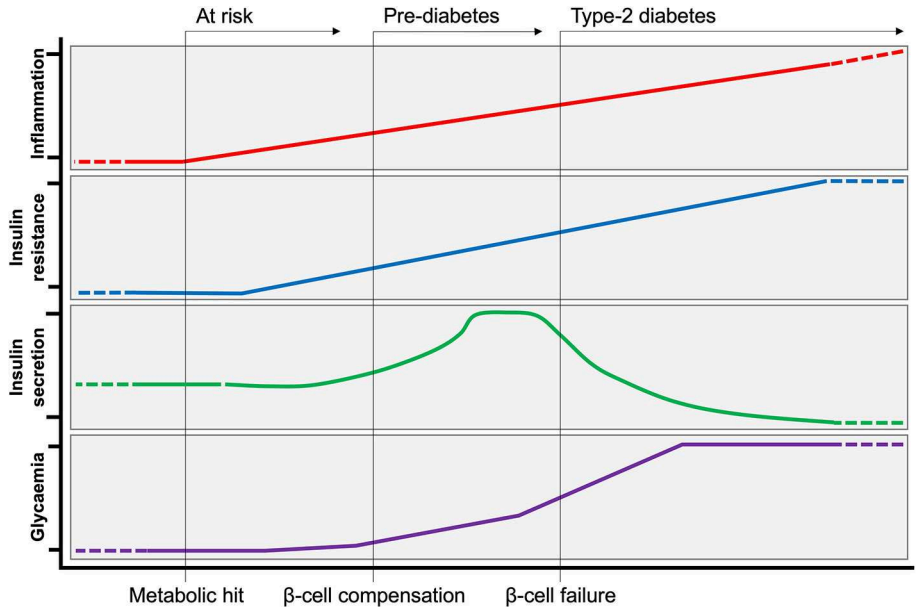

FIGURE 1 | Evolution of Type-2 Diabetes. Following a metabolic hit, inflammation is at the initial steps of developing type-2 diabetes (T2D). Peripheral insulin resistance develops in tandem with increasing inflammation. Insulin resistance is initially met by a compensatory response from the pancreas, producing more insulin to maintain normoglycemia (pre-diabetes). Over time, insulin producing β-cells can no longer cope with increased demand, and insulin production ceases (β-cell failure). At this stage of persistent hyperglycaemia T2D is established.

the type-1 or type-2 immune responses canonically associated with signaling molecules released upon polarization. Macrophage signaling also polarizes the adaptive immune compartment to maintain a chronic T helper (Th)1/17 or Th2 response. The M1 polarization state is associated with a type-1 response (Th1/17) and the production of pro-inflammatory mediators associated with bacterial or viral responses. M1 macrophages have strong microbicidal and antigen presenting capacities. They produce powerful pro-inflammatory cytokines such as TNF-α, IL-6, IL-1β, and reactive oxygen species (ROS). M2 macrophages elicit type-2 signaling, typically in response to extracellular pathogens (helminths, parasites), producing anti-inflammatory mediators such as IL-10 and TGF-β. M2 polarization is also considered a pro-resolution response, associated with later stages of resolving inflammation. The adaptive immune system appropriately undergoes Th2 polarization producing regulatory and remodeling cytokines such as IL-4, IL-5, and IL-13. Accordingly, the immunoregulatory response has been attributed to the specialized regulatory T-cells (T_{Reg}) subpopulation. The pro-resolution response can manifest as scarring or tissue remodeling, which when aberrant causes tissue fibrosis, type-2 effector molecules also exacerbate allergic responses (14). Whilst the discrete M1 and M2 classification remains in use today, underlying this dichotomy exists a continuum of diverse responses and intermediate macrophage phenotypes. Novel functional classifications represent polarized macrophages along a sliding scale between M1 and M2 depending on chemokine/cytokine secretion, transcription factor engagement and more recently on the cellular metabolic phenotype (15). The rise of single-cell sequencing and of mass cytometry (CyTOF) are coming a long way to deciphering the functional diversity and plasticity of macrophages (16).

TISSUE MACROPHAGES IN METABOLIC PHYSIOLOGY AND PHYSIOPATHOLOGY

Efficient communication between insulin secreting and insulin target tissues (the pancreas, adipose tissue, the liver, and skeletal muscle) maintains metabolic homeostasis in response to physiological challenges that transiently vary glycaemia or lipaemia, such as feeding or fasting (3–5). Insulin resistance represents a partial breakdown in communication between these tissues, where insulin target tissues become resistant to insulin signaling, despite initial compensation by the pancreas. T2D represents a stage of complete to near-complete breakdown of communication where production of insulin no longer meets the body's requirement to regulate glycaemia. Each of these tissues has its specialized niche of macrophages with important physiological functions maintaining tissue integrity, more importantly the tissue macrophage population undergoes adaptation at each stage of developing T2D (3–5, 17, 18). The tissue macrophage responses have been shown to be extremely powerful mediators of insulin signaling, sensitivity, and resistance (**Figure 3**).

Pancreatic Islets Macrophages

Pancreatic islets, distributed within the exocrine pancreas, are micro-organs essential for systemic glucose homeostasis. β cells form the majority of the islet and respond to glucose, within

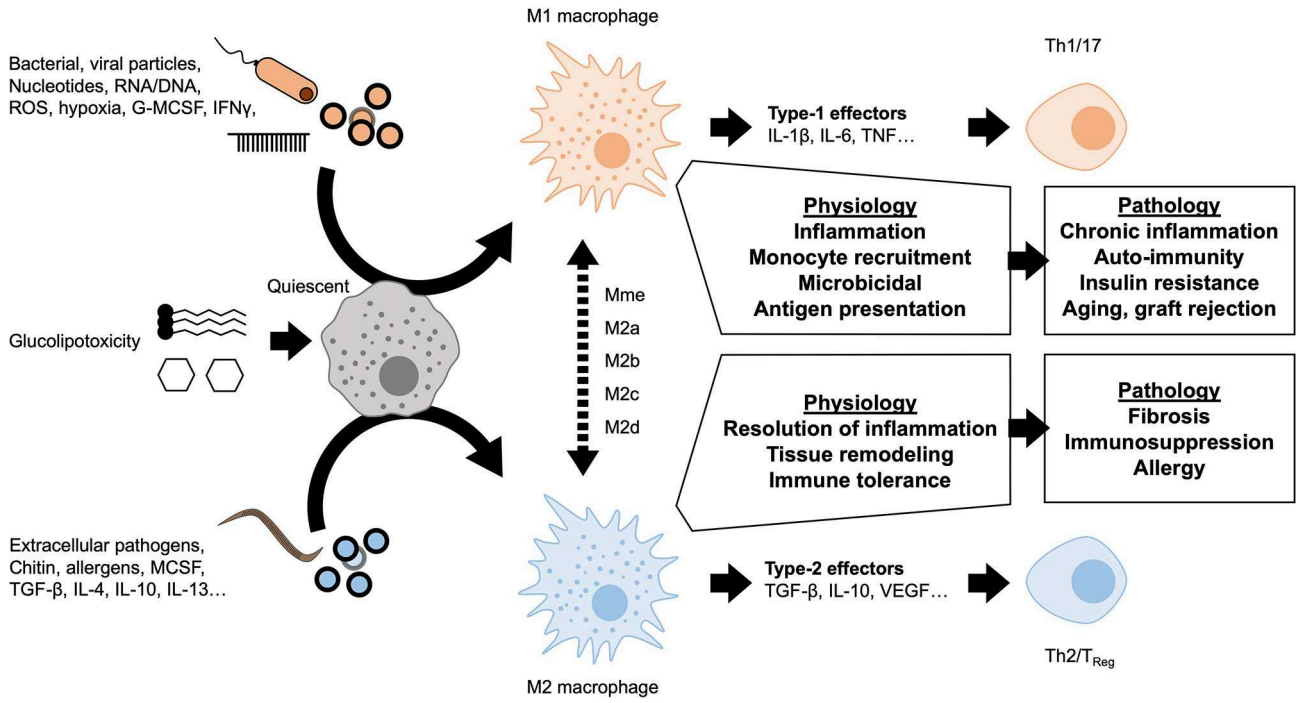

FIGURE 2 | Macrophage polarization and chronic inflammation. A variety of stimuli are known to induce either M1-like pro-inflammatory or M2-like anti-inflammatory polarization. These polarization states represent the extremes of a spectrum of activation profiles, dependent on nature of the stimulus and microenvironmental factors. Self-resolving inflammation is transient and considered a necessary physiological response in maintaining homeostasis and host-defense. If polarization is persistent, downstream signaling from macrophages also leads to lymphocyte polarization. Sustained dysregulated macrophage activation and lymphocytic polarization are important parts of a number of pathologies.

seconds, by secreting the appropriate amount of insulin required for optimal energy supply to insulin-sensitive tissues. Innate immune cells also form part of the pancreatic islet. Under steady-state, macrophages are the major innate immune cell in both mice and humans (10, 19–21). Over 20 years after their discovery, islet macrophage phenotype remains unclear. Unlike ATMs and liver macrophages, islet macrophages do not adhere to the M2 vs. M1 polarization paradigm associated with metabolic protection and dysfunction, respectively. Indeed, M1 markers (CD11c, MHC-II) are constitutively expressed by macrophages in healthy islets, they also highly express IL-1β, TNF-α, and the pro-inflammatory transcription factor interferon regulatory factor (IRF)-5 (10, 19, 22). Moreover, they do not express M2 markers (CD206), in contrast to stromal macrophages of the exocrine pancreas (19).

The role of macrophages in islet homeostasis has only begun to draw attention. *In situ* islet imaging revealed that macrophages are in close contact with both β cells and vasculature, in mice (23). Islet macrophages monitor β cell insulin secretion in response to glucose by detecting endogenous ATP that is co-released with insulin (24). In turn, macrophages may also directly provoke or enhance insulin secretion through production of factors such as retinoic acid (10). Interestingly, relative to any other tissue, β cells have the highest expression of the signaling IL-1 receptor 1 (IL-1R1), strongly indicating a physiological role for IL-1β in β cell function (25, 26). It is well-established that acute, but not chronic, exposure to IL-1β stimulates insulin secretion in mice and humans (27, 28). Underlying mechanisms remain unclear, but may involve an increase in insulin granule docking at the plasma membrane allowing enhanced exocytosis (27). Two studies confirm this hypothesis with transgenic murine models. β cell-targeted deletion of IL-1R1 impairs peripheral glucose tolerance *via* reduced glucose-stimulated insulin secretion (29). Other studies report that feeding induces a physiological rise in circulating IL-1β, potentiating postprandial insulin secretion (30). IL-1β secretion was attributed to peritoneal macrophages responding to glucose metabolism and bacterial products, released IL-1β in-turn acts on β cells (30). It has not been ruled out that islet-resident macrophages may also produce IL-1β post-prandially, indeed these macrophages may be the main source of IL-1β in the islet microenvironment. Taken together, these previous reports show that physiological IL-1β levels play a critical role in amplifying insulin secretion.

During obesity, increased production of insulin is required to maintain normal blood glucose levels. As a result, the number of β cells and islet size increase, mainly by local proliferation of pre-existing β cells (**Figure 3**). Therein, macrophages slowly accumulate and may play an important role in β cell adaptation to early weight gain and the development of insulin resistance. In that context, islet macrophages may license β cell mass expansion and the required angiogenesis during the first weeks of high fat diet and in early islet adaption of young Db/Db mice. Indeed, macrophage-depleted mice showed lower β cell replication rate,

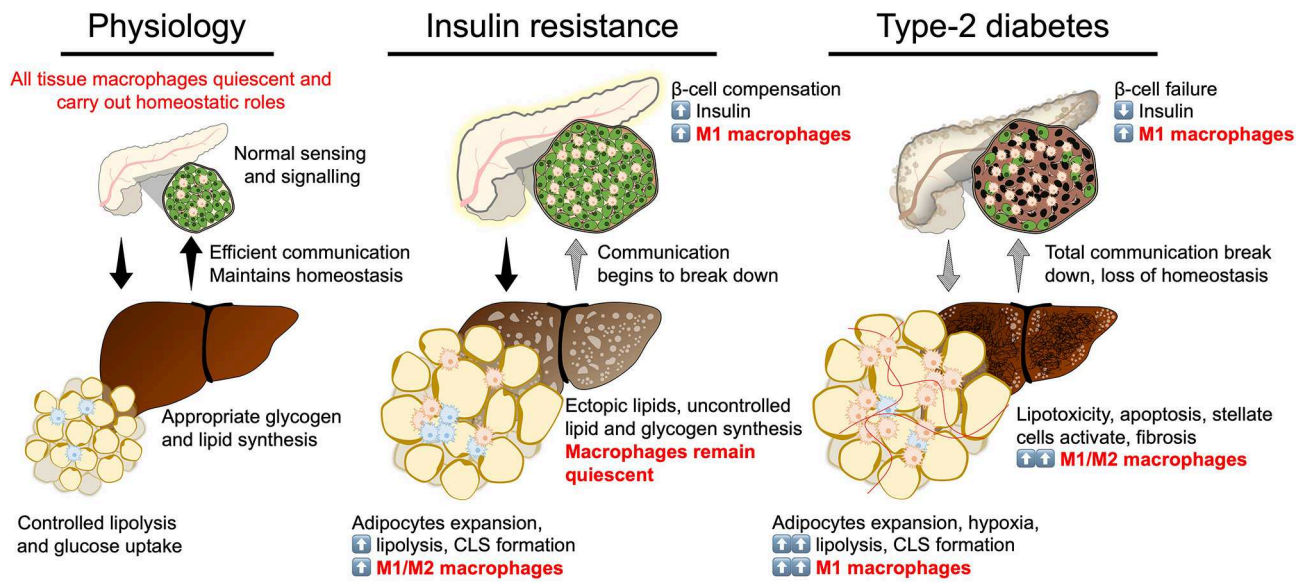

FIGURE 3 | Break down of insulin secretion and sensitivity in type-2 diabetes. At the physiological state glycaemic homeostasis is maintained by efficient communication between the insulin secreting organ, the pancreas, and insulin target organs (adipose tissue and liver). All tissues are populated by their respective tissue macrophages that participate in maintaining tissue homeostasis and physiological function. Insulin resistance is a breakdown of communication at insulin target tissues. At the onset of insulin resistance, macrophages accumulate in adipose tissue and pancreatic islets. Crown-like structures develop in adipose tissue with heterogeneously polarized macrophages and a decrease in adipocyte insulin sensitivity. Pancreatic islet size increases with increased β-cell number and increased macrophages. Increase in β-cell number allows compensatory insulin release to overcome insulin resistance. Increasing insulin resistance and systemic inflammation result in β-cell failure when insulin secretion no longer compensates for resistance and persistent hyperglycaemia develops. At the stage of type-2 diabetes, a complete breakdown in inter-organ communication occurs, insulin secretion drops and inflammatory macrophages permeate adipose tissue and the liver. Chronic inflammation, hyperglycaemia and dyslipidemia lead to the development of non-alcoholic steatohepatitis.

decreased insulin secretion and impaired glucose tolerance compared to controls (31). The promotion of β cell proliferation by islet macrophages could be mediated by the platelet-derived growth factor receptor (PDGF-R) signaling pathway (32).

When obesity becomes chronic, insulin secretion eventually no longer compensates for increased insulin demands, resulting in hyperglycemia and T2D. This β cell failure is associated with local islet inflammation and production of inflammatory effectors (IL-1β, TNF-α, CCL-2) (20, 26, 32–37). This phenomenon is associated with increased macrophages in the islet in diet-induced or genetically obese rodents and in patients with T2D (20, 31–33, 35, 37). Two distinct subsets of macrophages have been identified in the islet: resident macrophages and pro-inflammatory macrophages. Islet-resident macrophages ($CD11b^{+}Ly6C^{-}$ or $F4/80^{high}CD11c^{low}$) predominate at steady-state and pro-inflammatory macrophages ($CD11b^{+}Ly6C^{+}$ or $F4/80^{low}CD11c^{high}$) accumulate during the course of obesity (32, 33). While $CD11b^{+}Ly6C^{+}$ macrophages are recruited from monocytes, $F4/80^{low}CD11c^{high}$ macrophages proliferate *in situ*. In this context, chlodronate liposome macrophage depletion rescues glucose-induced insulin secretion in models of genetic obesity and in palmitate-infused mice (33). Interestingly, despite increasing islet macrophage number, diet-induced obesity does not markedly alter macrophage phenotype (19, 32). Another source of inflammatory factors that may participate in islet inflammation are endocrine cells themselves, including β cells. Indeed, RNA sequencing of islet cells from T2D patients revealed an inflammatory signature associated with β cell dysfunction relative to islet cells from healthy controls, this result was attributed not only to immune cells but also to endocrine cells fuelling local inflammation (38, 39). These results, somewhat contradictory, suggest that islet macrophages are not solely responsible for islet inflammation in obesity. More studies are required to fully define their phenotypes and to investigate the roles that other innate immune cells may play, such as innate lymphoid cells (ILC) and their potential role in regulating insulin secretion and β cell mass expansion (10).

Adipose Tissue Macrophages in Metabolic Homeostasis

AT is one of the first responders to alterations in energy balance. Physiologically AT regulates long term energy stores, appetite (through endocrine signaling) and body temperature (by providing insulation or even increasing thermogenesis in the case of brown adipose tissue). Adipose tissue macrophages (ATMs) generally present an M2 profile at steady state under physiological circumstances. They are characterized by expression of the mannose receptor CD206, CD301 alongside pan-macrophage markers such as F4/80 (in mice) CD14 (in humans) CD68 and CD11b. ATM homeostatic signaling includes expression of arginase 1 (ARG1), IL-10, and other type-2 effectors as well as catecholamines. The transcription factor peroxisome proliferator-activated receptor (PPAR)-γ is highly expressed in these cells and controls ATM oxidative metabolism and

capacity to cope with a lipid-rich environment. In this niche, ATMs interact with other immune cells and provide signals for activation or repression of B and T cells, neutrophils, natural killer cells, and ILCs (40).

ATMs maintain tissue homeostasis by removing dying adipocytes and debris from dead cells; this efferocytotic process maintains an anti-inflammatory environment. Indeed, murine adipose tissue presenting an excessive rate of dying adipocytes due to targeted activation of caspase 8 are characterized by an increased number of alternatively activated anti-inflammatory macrophages (M2, $CD206^+$), surrounding dead and dying adipocytes (41). This grouping of cells surrounding adipocytes in a ring-like structure are named crown-like structures (CLS). CLS are only occasionally found in lean AT. Under physiologic variation, AT homeostasis is challenged daily with periods of feeding, thus expansion and storage of lipids, or mobilization of stored-lipids during fasting or cold exposure. ATMs have enhanced lipid buffering capacities and this enables capturing lipids released from the dead adipocytes, also during physiological process such as weight loss, fasting-induced lipolysis (42), or thermogenesis (43). Interestingly, in obesity macrophage-mediated capture of excess lipids regulates systemic glucose tolerance. Lipids are stored within the macrophages and released into circulation in a controlled manner (44).

ATM lipid-buffering processes limit ectopic lipid storage, pro-inflammatory accumulation of lipids and systemic lipotoxicity/dyslipidemia. A program of lysosomal activity is activated in M2 ATMs to cope with environmental lipid overload. Interestingly, inhibition of lysosome biogenesis and consequently lipid accumulation and catabolism in ATMs decreases adipocyte lipolysis (45). More recently, novel pathways of lipid release independent of canonical lipolysis, have been described. Adipocytes release exosome-sized lipid-filled vesicles to be taken-up and stored by ATMs (46). The capture of lipids is facilitated by ATM expression of fatty acid transporter (CD36) and the lipid scavenger receptor MSR1 (45).

Much of the knowledge with regards to macrophage interactions with environmental lipids and their mechanisms of activation has come from the fields of atherosclerosis and the study of foam cells. Indeed, early studies carried out by Nagy et al. (47) brought to light the importance of such receptors as CD36, allowing macrophages to internalize oxidized lipids, which in turn act as nuclear receptor ligands (PPARγ in this case). The mechanisms described by Nagy et al. were amongst the earliest to elucidate links between metabolic stress, transcriptional regulation, and macrophage phenotypic plasticity.

The role of ATMs in thermogenesis is an emerging topic and pathways leading to the activating of ATMs are still under investigation (40). A novel population of macrophages involved in adipose tissue thermogenesis has been identified: sympathetic neuron associated macrophages (SAM) (48). These cells are morphologically different from ATMs and are located at fibers of the sympathetic nervous system in AT. Unlike ATMs, SAMs have the molecular machinery to uptake and catabolize norepinephrine which blunts catecholamine-induced lipolysis.

ATMs have also been associated with iron homeostasis, where intracellular iron is a source of free radicals and a cofactor for a number of proteins. Twenty-five percent of macrophages from lean adipose tissue are considered as ferromagnetic, i.e., iron-loaded and this proportion decreases with obesity (49). ATM iron recycling contributes to AT homeostasis, where an up-regulation of iron-related genes occurs during adipogenesis and an excess of iron contributes to adipocyte insulin resistance (50, 51).

ATMs play a more direct role in adipogenesis where alternatively activated macrophages form a niche for the development of adipocytes and in the vascularization of adipose tissue (52, 53). The accumulation of M2 ATMs in the CLS surrounding dead adipocytes leads to the recruitment of pre-adipocytes in response osteopontin (OPN). However, a recent study demonstrated that M2-like ATMs inhibit the proliferation of adipocyte progenitors through TGF-β signaling. A hallmark study by Buorlier et al. (53) characterized subcutaneous ATMs as being predominantly $CD206^+$, and to be the major source of matrix degrading enzymes, making them an essential part of tissue remodeling. In this same study, secreted factors from ATMs were found to promote angiogenesis and inhibit adipogenesis in stromal-vascular fraction progenitor cells (53, 54). Controlling angiogenesis is a key factor in the maintenance of tissue homeostasis as it limits the formation of hypoxic areas and insures appropriate irrigation supplying nutrients and oxygen to the microenvironment. In the light of the above work, the physiological phenotype of ATMs can be largely seen as protective and may, in the early stages of caloric excess, act to coordinate adipose tissue adaptation (53).

Finally, alternatively activated ATMs are characterized by their production of IL-10, an anti-inflammatory cytokine known for its important role as a modulator of insulin sensitivity (55). Indeed, acute IL-10 treatment improves global insulin sensitivity *in vivo* (56) and its expression is positively correlated with insulin sensitivity in humans (57). Surprisingly, the hematopoietic deletion of IL-10 does not promote obesity nor insulin resistance, suggesting that other factors and pathways are involved in the maintenance of AT metabolic health (58). Furthermore, ATMs can release exosomes containing miRNA, such as miR-155, that regulate insulin sensitivity. Such ATM-derived exosomes from lean mice improve glucose intolerance and insulin sensitivity when delivered to obese mice (59).

Adipose Tissue Macrophages and Metabolic Inflammation

Obesity is a complex pathology and a factor in the etiology of insulin resistance and T2D. The fundamental cause of obesity is chronic imbalance between energy expenditure and food intake leading to low-grade inflammation. Chronic low-grade inflammation is what is generally referred to when discussing metabolic inflammation, the starting point of which is the adipose tissue macrophage. An accumulation of inflammatory ATMs occurs in obesity and plays a key role in the pathogenesis of obesity-induced insulin resistance (**Figure 3**) (6, 7). Inflammatory ATMs correspond to the M1 subtype and are identified as $F4/80^+CD11b^+$ cells, also positive for CD11c and overexpressing IL-6, TNF-α, iNOS and the C-C chemokine receptor 2 (CCR2).

ATM accumulation in obesity occurs first due to *in situ* proliferation at CLS, and then by recruitment of circulating monocytes that differentiate into inflammatory macrophages (60). The first proliferative phase is driven by IL-4 signaling through Signal Transducer and Activator of Transcription (STAT)-6. Infiltrating macrophages increase upon CCL2 signaling to monocytes, several studies have demonstrated the importance of the CCR2/CCL2 axis in the recruitment of circulating monocytes (61). In addition, migratory capacity of macrophages is affected by obesity. Indeed, netrin-1, a laminin-related molecule known for its chemo-attractant/-repulsive properties, is induced by palmitate. It inhibits ATM migration to lymph nodes and consequently promotes ATM accumulation *in situ* (62).

The lipid-buffering capacity of ATMs is beneficial in early dysmetabolism and enhances a lysosomal program associated with M2 polarization (45), the abundance of lipids within ATMs impacts their polarization toward an M1 phenotype (63). Single-cell transcriptomic approaches confirm the heterogeneity of the ATMs, identifying three different macrophage populations in obese AT. Resident macrophages ($F4/80^{Lo}$) expressing CD206 are maintained in obese AT, whereas Ly6c expression characterizes the newly recruited macrophages (also $F4/80^{Hi}$). The pro-inflammatory subset of lipid-laden macrophages in CLS is characterized by the expression of CD9 (64). More recently, Jaitin and colleagues confirmed the phenotype and presence of $CD9^{+}$ lipid-laden macrophages at CLS. They report that $CD9^{+}$ cells counteract inflammation and adipocyte hypertrophy via the lipid receptor TREM2 (8). Proteomics analyses also identified specific ATM markers induced by stimuli reproducing the adipose tissue microenvironment with palmitate, insulin, and high levels of glucose (65). Such activation of ATMs gives rise to the metabolically activated macrophage (MMe), which is functionally and phenotypically distinct from classically activated M1 macrophages.

The importance of the pro-inflammatory capacity of the newly-recruited ATMs in the etiology of obesity is well established. Activated macrophages surround dead adipocytes and fuse to form multinucleate giant cells (66), an hallmark of chronic inflammation that correlates to insulin resistance (67). In 2008, Patsouris and colleagues demonstrated that the ablation of $CD11c^{+}$ cells during obesity restored insulin sensitivity by decreasing inflammatory markers (68). Interferon regulatory factor IRF5 is a pro-inflammatory transcription factor, commonly restricted to $CD11c^{+}$ cells, driving macrophage polarization toward an M1 phenotype (69), and is notably induced in ATMs in diet-induced obesity (70, 71).

Liver Macrophages in Metabolic Homeostasis

Liver resident macrophages, also called Kupffer cells (KCs), represent up to 80–90% of the whole body macrophage population and are characterized by the expression of canonical macrophage markers (F4/80, CD14, CD68, CD11b) as well as the C-type Lectin (Clec)-4F (5). Clec4f is the marker of *bona fide* KCs that are functionally distinct, specialized and self-renewing tissue-resident macrophages (72). KCs belong to the reticuloendothelial system of the liver, they are located close to blood vessels in lumen of hepatic sinusoids, they regulate hepatocyte proliferation and apoptosis upon injury and at steady-state they clear blood of aged erythrocytes and recycle iron by degrading hemoglobin (73). Their location is adapted to their function of clearance of the portal blood flow from pathogens, micro-organisms and cellular debris (74). KCs select and eliminate debris from blood through scavenger receptors and canonical PRRs expressed on the cell surface. Importantly, KCs impose immune tolerance in the liver, an organ constantly exposed to antigens and bacterial endotoxins from the intestine and portal blood. KCs maintain an anti-inflammatory environment by several mechanisms, secretion of IL-10, low expression of MHC-II and high expression of PDL-1, limiting antigen-presentation capacity and a powerfully inhibiting T-cells, respectively (75). Interestingly, even upon IFN-γ priming, KCs promote differentiation of T_{Regs}, a specialized immunoregulatory subset of T-cells that maintains immune tolerance (75, 76). At steady-state, KCs have limited interactions with distant non-immune cell types, because they are not typically motile cells. When microenvironmental communication is required, KCs secrete cytokines or signal to circulating monocytes to differentiate *in situ* (73).

Liver Macrophages in Metabolic Inflammation

Systemic extension of inflammation from AT is associated an increase of pro-inflammatory mediators in circulation and an increase in adiposity. Insulin resistance, persistent glucolipotoxicity, and systemic inflammation coincide in ectopic fat deposition, a major site of which is the liver. In obesity and T2D, the liver undergoes a spectrum of changes that range from benign steatosis to fibrosis and cirrhosis (77). This range of pathologies is known as non-alcoholic fatty liver disease (NAFLD), where lipotoxicity, inflammation and fibrogenesis characterize the more advanced stages of non-alcoholic steatohepatitis (NASH). Liver macrophages, KCs, are key actors in the progression of NASH, due to their pro-apoptotic and pro-inflammatory responses to lipotoxic hepatocytes and their capacity to activate matrix producing hepatic stellate cells (HSCs).

Ectopic fat deposition triggers activation of immune cells and an inflammatory environment which favors insulin resistance. Surprisingly, unbiased transcriptomic analysis revealed no differences in terms of expression of genes associated with a pro-inflammatory signature, between liver macrophages from lean and obese patients (similar data were obtained from mice fed an HFD for 9 weeks). Metabolic impairments are not associated with a pro-inflammatory activation of liver macrophages (78). However, the transcriptomic inflammatory signature is indeed variant between the stages of benign steatosis and NASH. At the transition between steatosis and NASH, liver macrophages target lipotoxic hepatocytes inducing their apoptosis and signal to HSCs to induce their activation (77). Chronic insults on the liver will result in fibrosis as an exuberant

scarring response to dead or dying hepatocytes, sustained fibrogenesis will in-turn affect liver function (77). Interestingly at the NASH stage, the liver macrophage pool is extremely heterogenous, with M1-like macrophages inducing hepatocyte apoptosis and M2-like macrophages promoting HSC activation and fibrogenesis (77, 79).

The pro-inflammatory transcription factor IRF5 has been shown to play a critical role in liver macrophages, mediating the transition between benign steatosis and NASH. Blunting IRF5 expression results in hepatoprotection through early upregulation of anti-apoptotic and immunoregulatory signaling, increasing T_{Reg} differentiation and IL-10 secretion upon hepatocellular stress (79). Recent research is delving into potential non-inflammatory or non-immune signaling efferent from KCs, notably effector molecules such as insulin-like growth factor-binding protein (IGFBP)-7, regulates insulin sensitivity in the context of obesity (80).

INITIATING AND SUSTAINING MACROPHAGE POLARIZATION IN T2D

Defining the extracellular metabolic and molecular signals associated with macrophage polarization in metabolic inflammation and insulin resistance is an area of active research. Candidate "metabolic" immunogens include lipids, hypoxia, cell death, and stress (42, 66, 81).

Ninety percent of ATMs are surrounding dead adipocytes in fat depots of genetically obese mice (82) suggesting that dead adipocytes are sources of DAMPs that lead to CLS formation and/or the accumulation of ATMs. Obese AT is also characterized by hypoxic areas and the expression of hypoxia-related genes, including HIF-1α. This transcription factor also promotes the pro-inflammatory capacities of ATMs in the context of obesity (83). Furthermore, lipolysis products and more generally lipids whose circulating levels are elevated in obesity, are extremely attractive candidates for the induction of an inflammatory response in ATMs. TLR-4 has been shown to be activated by nutritional fatty acids in macrophages, inducing pro-inflammatory signaling pathways (84). Macrophages can be activated by triglyceride-rich lipids, such as palmitate or very-low density lipoproteins (VLDL) which upregulate intracellular levels of ceramides and potentiate the pro-inflammatory response (85). Activation of the NLRP3-inflammasome by these mechanisms induces caspase-1-mediated cleavage of pro-IL-1β and pro-IL-18 into their active forms. Interestingly, saturated fatty acids such as palmitate have been shown to activate the NLRP3-inflammasome through an AMPK-autophagy-mitochondrial ROS signaling axis, leading to secretion of IL-1β and IL-18 (86). Importantly, IL-1β secretion *per se* is associated with insulin resistance. Indeed, IL-1β prevents insulin signaling through TNF-α-dependent and independent mechanisms (87). Once established, this pro-inflammatory environment favors the production of pro-inflammatory cytokines recruiting monocytes and other immune cells that sustain low-grade chronic inflammation.

Pro-inflammatory cytokines are key actors of the disruption of insulin signaling leading to insulin resistance (88). They act through paracrine mechanisms on insulin sensitive cells such as adipocytes. Physiologically, upon insulin binding to its receptor, the phosphorylation of tyrosine residues of insulin receptor substrate (IRS)-1 activates intracellular signaling pathways mediating insulin action (89). In the context of metabolic inflammation, JNK-1 and IKK are capable of interfering with insulin signaling by phosphorylating inhibitory serine/threonine residues of IRS-1. Insulin signaling is therefore disrupted (90). Similar pathways involving JNK-1 and IKK can be activated through the binding of fatty acids to TLRs. Moreover, IL-1β, which also signals through IKKβ and NFκB, favors insulin resistance by repressing IRS-1 expression at both transcriptional and post-transcriptional levels (91). Interestingly, IL-6 signaling inhibits insulin sensitivity through distinct mechanisms involving the JAK-STAT pathway that controls the transcription of its own suppressor, known as suppressors of cytokine signaling (SOCS), notably SOCS3. High levels of circulating IL6 induce increased expression of SOCS3 which physically interacts with tyrosine phosphorylated residues, and consequently inhibits IRS-1 binding to the insulin receptor (92).

METABOLIC MECHANISMS OF MACROPHAGE POLARIZATION

As with any other cell, macrophages have their own metabolic requirements and depend on the same well-characterized bioenergetic pathways as non-immune cells; these pathways are broadly classified into glycolytic or mitochondrial (**Figure 4**). In addition to pro-inflammatory signaling and transcriptional control, cellular metabolism is gaining recognition for the key role it plays in macrophage terminal differentiation. Mobilizing metabolic pathways does not solely produce energy but also dictates the magnitude of macrophage effector function (13). Early studies in immunometabolism characterized fundamental mechanisms fuelling macrophage function in model systems with canonical activators. Such foundation studies allowed clear association of bioenergetic profiles to polarization states. Current research is expanding on these paradigms through investigating bioenergetic profiles and metabolic adaptation of tissue-specific macrophage niches under physiological and pathological conditions and in response to diverse stimuli. Interestingly, the metabolic classification of macrophages was one of the first to be made, with the initial observation that M2 macrophages are able to metabolize arginine (93).

Metabolic Adaptation of Pro-inflammatory Macrophages

The enhanced glycolytic activity of the pro-inflammatory macrophages was observed decades ago (94) but the mechanisms underlying this process and its physiological significance were only recently described. It is a hallmark metabolic response in the polarization of macrophages toward an M1 phenotype (**Figure 4**). Glycolysis corresponds to the metabolic pathway responsible for the conversion of glucose into pyruvate, through 10 sequential enzyme-catalyzed reactions. This pathway gives rise to the production of ATP and NADH.

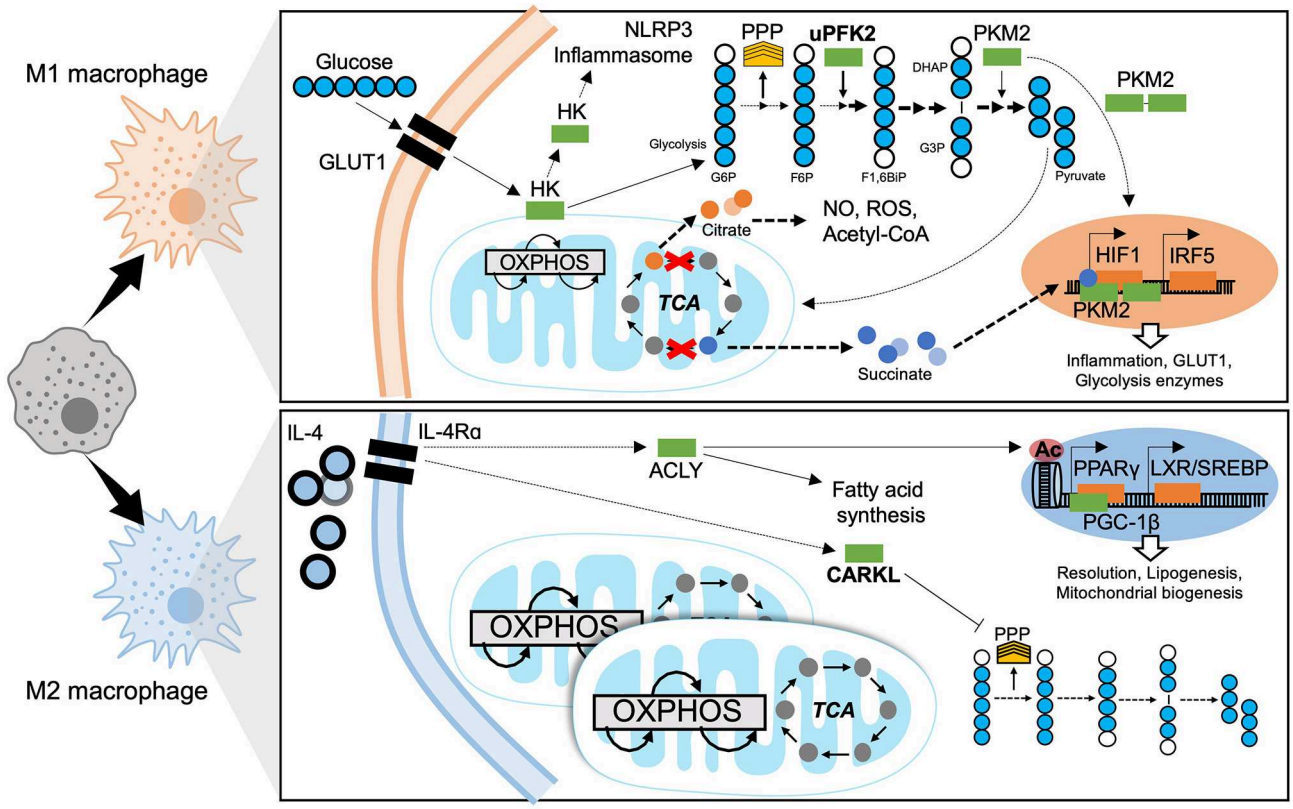

FIGURE 4 | Metabolic mechanisms of macrophage polarization. M1 macrophages are characterized by predominantly glycolytic metabolism. Glycolysis consists of breaking down a 6-carbon glucose molecule (where each carbon is depicted as a blue circle, white when phosphorylated) into 3-carbon sugars then into pyruvate, ATP, NADH, and H^+. The transcriptional programme that supports glycolysis is mediated by HIF1 and at least in part by IRF5. A Glucose substrate is provided by increased expression of the glucose transporter GLUT1. Meanwhile several glycolytic enzymes undertake non-canonical roles to support M1 effector functions. The mitochondrial tricarboxylic acid (TCA) cycle is disrupted, leading to accumulation of citrate and succinate which also enhance M1 effector function. The M2 macrophage has a fully intact TCA cycle, enhanced OXPHOS and increased mitochondrial biogenesis. ATP citrate lyase (ACLY) is activated downstream of IL4 signaling and enhances M2 effector functions through epigenetic mechanisms and producing substrates for lipogenesis. The sedoheptulose kinase (CARKL) represses the pentose phosphate pathway (PPP). Transcriptional programmes for M2 macrophage metabolism are mediated by PPARγ and LXR. GLUT1, Glucose transporter-1; HK, Hexokinase; NLRP3, NACHT, LRR, and PYD domains-containing protein; OXPHOS, oxidative phosphorylation; TCA, tricarboxylic acid cycle; PPP, pentose phosphate pathway; uPFK2, ubiquitous phosphofructokinase2; PKM2, pyruvate kinase isozyme 2; G6P, glucose-6-phosphate; F6P, fructose-6-phosphate; F1,6BiP, Fructose-1,6-biphosphate; G3P, glyceraldehyde-3-phosphate; DHAP, dihydroxyacetone phosphate; NO, nitrous oxide; ROS, reactive oxygen species; CoA, Coenzyme A; HIF1, hypoxia-inducible factor 1; IRF5, interferon regulatory factor 5; IL-4, interleukin 4; IL-4Rα, IL-4 receptor alpha; ACLY, ATP-citrate lyase; CARKL, carbohydrate kinase like/sedoheptulose kinase; Ac, acetylation mark; PPARγ, peroxisome proliferator-activated receptor gamma; LXR, liver X receptor; SREBP, sterol regulatory element binding protein; PGC-1β, PPARγ coactivator 1-beta.

Glycolytic metabolism facilitates pro-inflammatory differentiation to enable efficient bacterial killing (95) and the secretion of pro-inflammatory mediators. Experimental inhibition of glycolysis with 2-deoxy-glucose (2-DG) limits the pro-inflammatory macrophage response to LPS (96). The rapid induction of glycolysis is enhanced by the upregulation of glucose transporter (GLUT)-1 expression (97). The switch toward glycolytic metabolism is dependent on the transcription factor HIF-1α (98). Its stabilization in hypoxic conditions promotes anaerobic metabolism and enhanced transcription of genes encoding glycolytic enzymes, such as pyruvate dehydrogenase kinase (PDK) and hexokinase (HK) which catalyse glucose phosphorylation. By HIF-1α-independent mechanisms, the ubiquitous isoform of phosphofructokinase-2 (uPFK2) is induced in M1 macrophages. Whilst uPFK2 is a more active isoform of PFK2, its induction enhances glycolytic flux and favors the formation of fructose-2,6P_2 which allosterically activates PFK1, the enzymes catalyzing commitment to glycolysis (99). As well as HIF-1α-dependent mechanisms, studies of IRF5 risk-variants report that gain-of-function single nucleotide polymorphisms of IRF5 (associated with auto-immune disease) increase glycolysis and inflammatory signaling, basally and in response to LPS (100).

Some glycolytic enzymes have non-canonical roles in macrophages. Notably, pyruvate kinase isoenzyme 2 (PKM2), induced by LPS (101), can be found as a dimer. This dimer can translocate to nuclei and act as a coactivator for HIF-1 (**Figure 4**). Consequently, PKM2 participates in a positive feedback loop with the up-regulation of pro-inflammatory and glycolytic genes in response to HIF-1 activation (102). Moreover, HK1 can be

inhibited by bacterial products and then dissociate from the mitochondria, which activates the NLRP3 inflammasome and the downstream production of pro-inflammatory cytokines (103). Mechanisms of resolution of glycolytic programming have not yet been brought to light; however, a recent study by Ip et al. demonstrates that IL-10 signaling exerts its anti-inflammatory effects by inhibiting the translocation of GLUT1 to the membrane (104). As well as being a substrate for glycolysis, glucose also fuels the pentose phosphate pathway (PPP), required for the synthesis of nucleotides and NADPH destined for ROS production by NADPH oxidase. The PPP is also induced upon LPS stimulation and M1 polarization (105).

The Krebs/tricarboxylic-acid (TCA) cycle is a mitochondrial metabolic pathway enabling ATP production and provision of substrates for the electron transport chain (ETC) that supports oxidative phosphorylation (OXPHOS) (**Figure 4**). In the context of pro-inflammatory macrophages, the TCA cycle is disrupted at two key steps: (i) accumulation of citrate due to a decrease in isocitrate lyase expression and (ii) the accumulation of succinate. Mitochondrial efflux of citrate is enhanced in M1 macrophages. Citrate accumulation has functional relevance to inflammatory polarization, being required for the production of ROS, NO, and prostaglandins (106). Citrate also acts a substrate for transformation into acetyl-CoA, feeding fatty acid synthesis through the ATP-citrate lyase (ACLY) (107). Interestingly, inhibiting fatty acid synthesis by silencing fatty acid synthase (FAS) in myeloid cells, has been shown protective in diet-induced insulin resistance, hindering ATM recruitment and chronic inflammation in mice. This underlies the importance of lipid metabolism in the polarization and function of macrophages, and notably synthesis and composition of the plasma membrane (108). Finally, the accumulation of citrate leads to a decrease in the levels of cis-aconitate which is the precursor of itaconate, a well-described anti-inflammatory intermediate. Itaconate exerts its anti-inflammatory effects by inhibiting succinate dehydrogenase (SDH), ROS production, and the release of pro-inflammatory cytokines.

An itaconate negative feedback loop has been described in the context of LPS and IFNγ stimulation, where itaconate shuts down the inflammatory response (109, 110). On the other side, the accumulation of succinate favors SDH activity and production of mitochondrial ROS (111). Succinate can trigger the expression of IL-1β through stabilizing HIF-1α (112). Consequently, pro-inflammatory macrophages are characterized by an increase of glycolytic activity and decreased OXPHOS. Interestingly, acute LPS treatment induces a burst of oxidative metabolism in macrophages which increases the pool of available of acetyl-CoA. This process supports histone acetylation and the downstream transcription of pro-inflammatory genes (113). The shutdown of oxidative metabolism, a hallmark of M1 macrophages, occurs following longer LPS treatments.

Finally, amino acids, the immunometabolism of which is relatively less known, can also be metabolized and influence macrophage polarization. For example, glutamine catabolism feeds the TCA cycle by giving rise to α-ketoglutarate, which acts as a co-factor for histone modifying enzymes implicated in macrophage differentiation (114). Arginine is also metabolized into L-citrulline simultaneously to the production of NO by iNOS, favoring the killing of bacteria.

Metabolic Adaptation of Anti-inflammatory Macrophages

Mitochondrial respiration dominates the M2 polarized state. M2 macrophages are characterized by an intact, fully functional TCA cycle and enhanced OXPHOS (**Figure 4**). Fatty acid oxidation (FAO) and mitochondrial biogenesis are increased in a PPAR-γ-coactivator-1β (PGC-1β)-dependent manner (115). With FAO being the main source of substrates, glycolysis-fuelled OXPHOS is not required to maintain the M2 phenotype (116).

The molecular mechanisms linking the metabolic adaptations of M2 macrophages to their functions in tissue homeostasis remain largely unexplored. Interestingly, IL-4 is known to activate ACLY enhancing substrate formation for histone acetylation. This epigenetic modification enables the transcription of specific M2-genes (117). Other proposed mechanisms implicate the carbohydrate kinase-like protein (CARKL), a sedoheptulose kinase that regulates PPP. CARKL is down-regulated in response to LPS and highly expressed upon IL-4 stimulation (118). CARKL activity inhibits the PPP in the M2 state (**Figure 4**).

Glutamine metabolism also plays an important role in M2 polarization. The expression of Slc1a5, a glutamine transporter, is increased upon IL-4 stimulation (119). Glutamine catabolism, in addition to glucose metabolism, leads to the formation of UDP-GlcNAc that supports N-glycosylation, a process required for the expression of several M2 markers (120).

Lipid synthesis, mediated by LXR, is central to M2 effector function and resolution of inflammation (121). Upon pro-inflammatory activation, LXR-dependent lipogenesis is inhibited. LXR being a the pro-lipogenic nuclear receptor and transcription factor later engages the master regulator of lipogenesis, SREBP1 to mediate the production of anti-inflammatory lipids (i.e., eicosanoids, resolvins) (122).

Deciphering Metabolic Adaptations of Tissue Resident Macrophages and Insulin Resistance

The above fundamental findings in macrophage bioenergetics were largely established using *ex vivo* modeling systems (such as murine bone marrow- or human monocyte-derived macrophages) and in response to known polarizing agents. Whilst these mechanisms apply to a large proportion of macrophages, typically infiltrating macrophages, responses to complex metabolic stimuli and the heterogeneity of tissue resident macrophages remains to be addressed. Tissue-resident macrophages face nutrient competition, normoxic and hypoxic areas and interactions with other cells. They respond to complex stimuli rather than unique stimuli. The bioenergetic adaptations of tissue-resident macrophages in obesity and insulin resistance remain to be thoroughly elucidated.

Interestingly, ATMs in obesity have a unique hypermetabolic profile with both increased glycolysis and OXPHOS compared to lean ATMs, whilst maintaining a pro-inflammatory phenotype

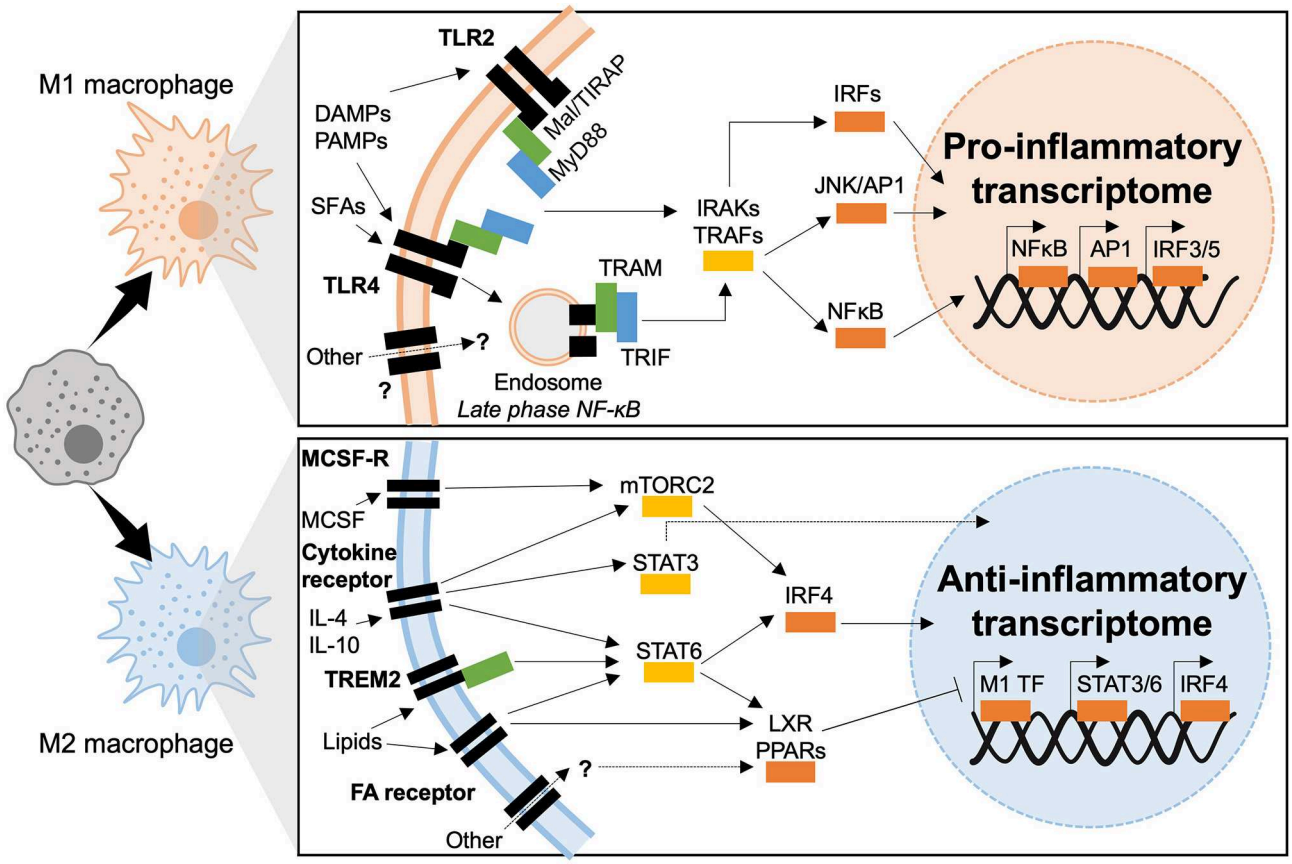

FIGURE 5 | Transcriptional mechanisms of macrophage polarization in T2D. M1 macrophages polarize in response to TLR2 or TLR4 ligation, downstream signaling is dependent of two adaptor complexes: Mal/TIRAP–MyD88 (TLR2 and TLR4) and TRAM–TRIF (TLR4). IRAK and TRAF signaling then dictate which transcriptional programmes are engaged, IRF3 IRF5, AP1, and NFκB have been shown to induce inflammatory polarization in T2D. M2 macrophages polarize downstream of cytokine and fatty acid receptor stimulation (also possible through other molecules such as TREM2). Intermediate signaling is largely through STATs and nuclear receptors (LXR and PPAR). STATs act as transcription factors or activate IRF4, whereas nuclear receptors act through transrepression of M1 transcription factors (M1 TF).

(123). More precisely, the pro-inflammatory capacity of the obese ATMs is mediated by glycolysis independently of HIF-1α (123). This bioenergetic profile is also distinct from peritoneal macrophages, despite the shared systemic glucolipotoxicity brought on by obesity. These observations underlie the specificity of metabolically activated macrophages and ATMs.

Hypoxic areas develop in AT upon inappropriate expansion in obesity and insulin resistance. Hypoxia and inadequate angiogenesis are attractive mechanisms leading to macrophage metabolic activation and their inflammatory polarization. Alternatively, the abundance of free fatty acids or lipolysis products in adipose tissue makes for a nutrient-/substrate-rich microenvironment. The effect of such lipid loading on macrophage metabolism and polarization remains to be investigated under iso- or hyper-caloric conditions. For example, the effect of obesity on macrophage glutamine metabolism remains to be investigated. Glutaminolysis is decreased in the AT of obese patients compared to lean subjects and glutamine levels in serum are decreased in patients with obesity or diabetes, suggesting an influential role for glutamine metabolism in ATM polarization (124).

TRANSCRIPTIONAL CONTROL OF MACROPHAGE POLARIZATION

Transcriptional control of macrophage polarization is well-characterized downstream of TLR ligation. Hallmark studies identified major TLR ligands as well as the key transcription factors that mediate inflammatory responses. Many of these pathways have been investigated in metabolic disease and are key mediators of macrophage activation in obesity, insulin resistance and T2D (**Figure 5**).

TLR-Dependent Inflammation in T2D

TLRs are highly-conserved transmembrane receptors expressed in and on macrophages. Their conservation is attributed to the evolutionary requirement to recognize structurally conserved

molecules and pathogens (125). Each TLR, from TLR1 to TLR13 recognizes specific ligands ranging from LPS, to nucleic acids, viral particles and chitin. Alongside their canonical roles in host-defense, several TLRs are implicated in metabolic inflammation and insulin resistance (126, 127). In this light, TLRs recognize not only infectious pathogens (through PAMPs) but also metabolic stressors or DAMPs associated with sterile inflammation and glucolipotoxicity.

The main TLRs implicated in diabetogenesis are TLR2 and TLR4. Engaging these two TLRs gives rise to chronic inflammation and insulin resistance through direct interference with insulin signaling (127–129). In macrophages TLRs 2 and 4 share common adaptor proteins, the myeloid differentiation primary response (MyD88) protein and Mal/TIRAP, that recruit IRAK kinases upon TLR engagement and dimerization. IRAK 1, 2, and 4 downstream signaling activates NFκB and Activator Protein (AP)-1. TLR4 also activates other downstream signaling. It is the only TLR that forms complexes with all adaptor proteins, Mal/TIRAP and MyD88, to initiate the early-phase NFκB response, the complex is then endocytosed and endosomal TLRs associate with TRAM and TRIF adaptors. Canonically, TRAM and TRIF set in motion the type-1 interferon response, transcriptionally mediated by Interferon Regulatory Factors (IRFs), AP-1 and late-phase NFκB activation. Both early and late phase action is required to sustain production of inflammatory cytokines (127–129). Co-ordinated action of TLRs, adaptor proteins and kinases result in the sustained activation of three major transcriptional programmes, headed by IRFs, AP-1, NFκB, and JAK-STAT.

Interferon Regulatory Factors

Initially characterized for their binding to virus-inducible enhancer elements on interferon coding regions, interferon regulatory factors (IRFs) are renowned for their control over innate immunity and type-1 interferon signaling. Also forming part of JAK-STAT signaling, IRFs respond to a number of DAMPs and PAMPs, mediate sterile inflammation (metabolic and auto-immune) and are also active in non-immune cells (e.g., adipocytes) (130, 131).

IRF family members are 300–500 amino acids long, share a conserved N-terminal DNA binding domain allowing binding to interferon sensitive regulatory elements. The C-terminal IRF association domain is variable and allows dimerization between the different IRFs (132). IRFs 1–5 and IRF9 control macrophage differentiation and polarization in response to PRR ligands, IRFs 3, 4, and 5 have been reported to play a role in metabolic inflammation (131).

IRF5 is responsible for M1 macrophage polarization, it is implicated in sterile inflammation and auto-immunity, namely rheumatoid arthritis where risk-variants contributing to the over-expression of IRF5 have been reported (131). In T2D, IRF5 contributes to macrophage activation and metabolic decline in both adipose tissue and in the liver.

In ATMs, IRF5 is highly expressed by $CD11c^{+}$ macrophages at CLS. Both CLS formation and IRF5 expression are strongly associated with AT inflammation, maladaptive adipocyte expansion and both local and systemic insulin resistance (70). Upon diet-induced obesity, mice with a myeloid-deficiency of IRF5 remain insulin sensitive despite increased adiposity. Visceral white adipose tissue in IRF5-deficiency is characterized by adaptive remodeling mediated by a *de facto* type-2 immune response, limiting adipocyte expansion and preventing loss of sensitivity to insulin's anti-lipolytic effect (70). Dysregulated expression of IRF5 is also causal in the progression to NASH. Throughout NAFLD, IRF5 mediates pro-apoptotic and inflammatory signaling from liver macrophages toward lipotoxic hepatocytes. Sustained inflammatory signaling and hepatocyte apoptosis result in scarring fibrogenesis in the liver (79).

IRF5 is the active transcription factor canonically downstream of TLR4. Interestingly, although the phenotypes of TLR4-deficiency and IRF5-deficiency are near identical under diet-induced obesity, the TLR4-IRF5 axis remains to be experimentally confirmed in the pathogenesis of T2D and its complications (133). Similarly downstream of TLR4, IRF3 promotes AT inflammation upon diet-induced obesity and inhibits adipose tissue browning. IRF3-deficient mice retain insulin sensitivity upon high-fat feeding and enhance AT browning (134).

In opposition to IRF3 and IRF5, IRF4 promotes macrophage M2 polarization and the resolution of inflammation (135). The metabolic phenotype observed in IRF4-deficient mice on HFD is accordingly aggravated (136). Myeloid-deficiency of IRF4 results in increased insulin resistance and adipose tissue inflammation when compared to IRF4-competent mice (136). Interestingly, IRF4 is nutritionally regulated by insulin signaling and by canonical transcription factors involved in metabolic signaling (e.g., FOXO1). Additionally, IRF4 regulates lipid handling in adipocytes, promoting lipolysis by facilitating lipase expression (130).

Activator Protein 1

AP-1 is a complex formed of the proto-oncogenes c-Jun and c-Fos that are essential for DNA binding. AP-1 activation responds to cytokine signaling and growth factors; it controls apoptosis, cell growth, and macrophage terminal differentiation to an M1-like phenotype (137).

AP-1 activity is dictated by post-translational modifications, notably translocation and/or dimerization of its subunits, by signaling from c-Jun N-terminal (JNK) and mitogen-activated protein kinases (MAPK). AP-1 activity is also regulated by the composition of its DNA binding dimer (Jun/Jun, Jun/Fos, bZIP) and through binding partners (138). AP-1 is canonically activated in response to PRR ligation, cytokine signaling and growth factors. In the case of metabolic inflammation AP-1 is responsive to saturated fatty acids (SFAs), namely palmitate (128). Macrophages exposed to palmitate release pro-inflammatory mediators in an AP-1 dependent manner (128).

AP-1 activity is also responsive in response to hormone signaling, where leptin increases binding of nuclear proteins to the AP-1 consensus sequence of the lipoprotein lipase (LPL) gene promoter. This activity increases macrophages expression of LPL, giving mechanistic insight into the

role of AP-1 in foam cell formation, atherogenesis and T2D (139).

The upstream kinases that activate AP-1 subunits have been extensively investigated in metabolic disease, namely JNKs. Mice-deficient for JNK1 and/or JNK2 remain metabolically healthy upon diet-induced obesity, mice gain less weight, are protected from insulin resistance and inflammation (140, 141). Interestingly, myeloid-specific deficiency of JNK, results in non-inflammatory obesity and a decrease in serum fatty acids. Studies indicate that myeloid-AP-1 is a key mediator of adipose tissue lipolysis upon diet-induced obesity (142).

Nuclear Factor-κB

NFκB is a transcription factor that promotes M1 polarization, it responds to a variety stress signals including: cytokines, redox stress, oxidized lipids, bacterial, or viral antigens (143–146). Dysregulated NFκB signaling occurs in a number of inflammatory conditions including T2D. NFκB is highly expressed in ATMs upon their M1/MMe differentiation and throughout the onset of insulin resistance. Furthermore, cytokines released by M1/MMe macrophages form an amplifying loop that recruits and polarizes other leukocytes at the site of inflammation.

Mice with a myeloid-deficiency of *Inhibitor of NFκB Kinase* (IKK-β), NFκB's canonical activator protein, display a diminished inflammatory response in diet-induced obesity and maintain systemic insulin sensitivity (147). Interestingly, hepatic deficiency of IKK-β only retains insulin sensitivity in the liver (not in muscle nor AT), indicating that the myeloid-derived IKK-β/NFκB is the main regulator of systemic metabolic homeostasis (147).

Signal Transducers and Activators of Transcription

A family of 7 transcription factors that regulate interferon signaling, Signal Transducers and Activators of Transcription (STATs), have well-established roles in apoptosis, proliferation, and differentiation of innate immune cells. Of note, STAT activity is particularly important in maintaining immune tolerance. STATs are activated downstream of cytokine, chemokine, and growth factor signaling. STAT dimerization and nuclear translocation is dependent on phosphorylation mediated Janus Kinase (JAK), together forming the JAK-STAT pathway.

STATs 1 and 5 promote M1-like signaling whereas STATs 3 and 6 promote M2-like signaling in macrophages (148–152). Interestingly the more recently described Mme phenotype is polarized independently of STAT1 activity (153).

STAT1 in macrophages is activated in response to high glucose and exerts pro-inflammatory signaling through epigenetic mechanisms. Of note, glucose-responsiveness of STAT1 has been reported in *in vitro* and *ex vivo* modeling, with little-to-no evidence being reported *in vivo* or from human studies of obesity, insulin resistance, and T2D (154, 155). To date no evidence links STAT5 activation *per se* to diabetic pathogenesis despite its known roles in inflammatory polarization.

STAT3 is strongly linked to the development of T2D and its complications, mainly with anti-inflammatory, metabolically protective properties. For example, STAT3 is a downstream target of the first-line T2D treatment, metformin. Metformin inhibits the differentiation of monocytes to macrophages and decreases their infiltration into atherosclerotic plaques through AMPK-mediated inhibition of STAT3 (156). Similarly, in insulin resistance and diet-induced obesity, protective effects of ABCA1/APOA1 activity are STAT3-dependent, as is the anti-inflammatory adipose tissue phenotype of mice with a myeloid-deficiency of JAK2 (157, 158).

STAT6, on its own, or in concert with the vasodilator-stimulated phosphoprotein (VASP) has immunoregulatory properties in the context of metabolic inflammation. The VASP-STAT axis has been described in mice with a myeloid-specific deficiency of VASP, mice were prone to hepatic inflammation and insulin resistance in a STAT6-dependent manner (159). Whereas, STAT6 deficiency predisposes mice to diet-induced obesity, oxidative stress, and adipose tissue inflammation (160).

Peroxisome Proliferator-Activated Receptors (PPARs)

PPARα, γ, and δ/β, are expressed at different levels in different tissues and vary across developmental stages. Highest expression levels are in the liver, skeletal, and cardiac muscle and in the spleen. PPARs are implicated in cellular metabolism, differentiation, development and more recently emerged as key regulators of inflammation.

In M1 macrophages PPAR-α inhibits the expression of pro-inflammatory mediators by negative regulation of AP-1 and NFκB. Several studies report the beneficial effects of PPAR-α activation in T2D and its complications. PPAR-α agonists have been applied in T2D patients and are beneficial in atherosclerosis, through inhibiting foam cell formation and inflammatory signaling. Beneficial effects are mediated by interfering with c-Fos and c-Jun interactions and by limiting lipid accumulation through repressing Fatty Acid Transport Protein (FATP)-1 (161–163).

PPAR-β/δ also acts on macrophage metabolism, regulating lipid efflux, fatty acid catabolism and beta-oxidation. PPAR-β/δ in macrophage regulates whole body energy dissipation and systemic responses to cholesterol; PPAR-β/δ activation occurs in response to dyslipidemia (164–166). In the pathogenesis of T2D, PPAR-β/δ plays a protective role controlling macrophage infiltration in adipose tissue and liver and promoting immune tolerance (M2 polarization) in ATMs acting downstream of STAT6 (167). Mice with a myeloid-deficiency of PPAR-β/δ display an aggravated metabolic phenotype upon diet-induced obesity.

PPAR-γ plays an important role in adipose physiology, adipocyte differentiation and maturation. Of the two known isoforms, PPAR-γ1 is expressed in macrophages and adipocytes whilst PPAR-γ2 is restricted to adipocytes (168). PPAR-γ1 enhances monocyte differentiation into M2 macrophages and is an inhibitor of inflammatory polarization, repressing MMP9,

IL-6, TNF-α, and IL-1β expression (161, 169, 170). In *in vitro* and *ex vivo* modeling, PPAR-γ inhibits M1 signaling associated with LPS+IFNγ stimulation, including iNOS, COX-2, and IL-12 (171–173). Importantly, macrophage PPAR-γ is also a downstream target of internalized lipids, and mediates expression scavenger receptors required for foam cell formation (47). Accordingly, PPAR-γ-deficient mice display impaired M2 maturation and develop exacerbated insulin-resistance and metabolic inflammation in diet-induced obesity (174, 175). Enhancing PPAR-γ activity with thiazolidinediones (TZDs) improves the metabolic phenotype in diet-induced obesity (176). Interestingly, reports of PPAR-γ overexpression demonstrate that mature adipocyte PPAR-γ is in-fact the main insulin-sensitizing component (overexpression phenotype is comparable to TZD treatment) (177). Little-to-no beneficial effects are observed upon diet-induced obesity when PPAR-γ is overexpressed in macrophage (177). Such over-/under-expression studies reveal divergent functions of PPAR-γ. Further mechanistic work is needed to precisely characterize the roles and regulation of this nuclear receptor and its different isoforms in different cell types and microenvironments.

With regards to mechanism of action, multiple mechanisms have been proposed, with the main one being *transrepression,* whereby PPAR-γ binds to active pro-inflammatory transcription factors and represses their function. Repressive mechanisms through interactions with nuclear receptor corepressor (NCoR) complexes have also been proposed (178).

Liver X Receptors

Liver X receptors (LXRs) exist in 2 isoforms, LXRα and LXRβ, both of which are lipid-activated and regulate macrophage inflammatory responses. To regulate transcription LXRs heterodimerise with Retinoid X Receptor (RXR) and bind to LXR response elements on the genome (179). LXRs, play important roles in T2D and in cardiovascular disease, promoting anti-inflammatory polarization and regulating macrophage lipid content.

LXR activation by oxysterol species and synthetic compounds allows cholesterol efflux from macrophages through the lipid transporters ACBCA1 and ACG1 (180). LXRs also directly repress transcription of pro-inflammatory genes and enhance transcription of anti-inflammatory genes in response to polarizing stimuli (181). Mechanistically, LXRs exert their effects by transrepression once they are sumoylated. This modification prevents LPS-dependent exchange of corepressors, thus maintaining LXR-mediated repression of inflammatory transcription factor activity (182). Several reports show the protective roles that LXRs have in metabolic inflammation and insulin resistance. Namely, LXR agonists act as insulin sensitizers and regulators of glycaemia through repressing hepatic gluconeogenesis (183–185).

Hypoxia Inducible Factor 1

Hypoxia inducible factor (HIF)-1 is a transcription factor with two subunits, α and β. HIF-1α is stabilized and its expression is increased in response to hypoxia, whereas HIF-1β is constitutively expressed and stabilized independently of oxygen levels (186). Under hypoxic conditions, HIF-1α translocates to the nucleus and dimerises with HIF-1β allowing binding to hypoxia response elements (HREs) on the genome and regulation of target gene expression (187). Under oxygen-poor conditions, HIF1 activation mediates a shift toward anaerobic respiration in cells where bioenergetic requirements are supported by glucose metabolism (188).

Myeloid-specific overexpression of HIF-1α leads to increased M1 polarization, inflammation and glycolysis in macrophages. Conversely, myeloid-specific deletion of HIF-1α impairs macrophage glycolysis and inflammatory polarization. In murine models of obesity, mechanisms of M1 polarization in adipose tissue macrophages are only partly dependent on HIF1 activation. Myeloid-specific deletion of HIF-1α results in decreased inflammatory signaling, decreased CLS formation and an ameliorated metabolic phenotype upon diet-induced obesity (189, 190).

EPIGENETIC CONTROL OF MACROPHAGE POLARIZATION

Epigenetic mechanisms control chromatin structure and conformation, factors that dictate the accessibility of genetic loci to transcription factors. Epigenetic remodeling, through transcriptional coregulators and epigenetic modifying enzymes (such as histone deacetylases or HDACs), regulates transcription factor activity. Understanding underlying epigenomic regulatory mechanisms can help develop new therapies, for example, by blocking an unwanted pathway or reprogramming macrophages to a more beneficial phenotype.

Rapid induction of an inflammatory transcriptional profile is a hallmark of macrophage activation required for an effective immune response. Under steady state, coregulator complexes bind to genomic regions of a broad repertoire of inflammatory genes to maintain macrophages in a quiescent state, this mechanism avoids deregulated inflammatory gene induction.

Coregulators function by first recognizing transcription factor activity and they then modulate this activity by establishing interactions with transcriptional machinery and chromatin (191, 192). Coregulators can be categorized as either coactivators or corepressors. Coactivators recognize and promote active transcription; corepressors however recognize and repress inactive transcription. However, this categorization of coregulator activity does not truly reflect the physiological or physiopathological situation, since coregulator activating or repressive function is highly context dependent. Coregulators establish cell type-dependent and ligand-dependent epigenomes by forming large multiprotein complexes that "write," "erase," or "read" reversible chromatin modifications associated with transcriptional activity (**Figure 6**). Although underlying mechanisms remain to be elucidated, convincing evidence places altered function or expression of coregulators at the center of dysregulated transcription inherent to disease-specific epigenomes.

Two such corepressors are the Nuclear Receptor Corepressor (NCoR1) and silencing mediator of retinoic acid and thyroid

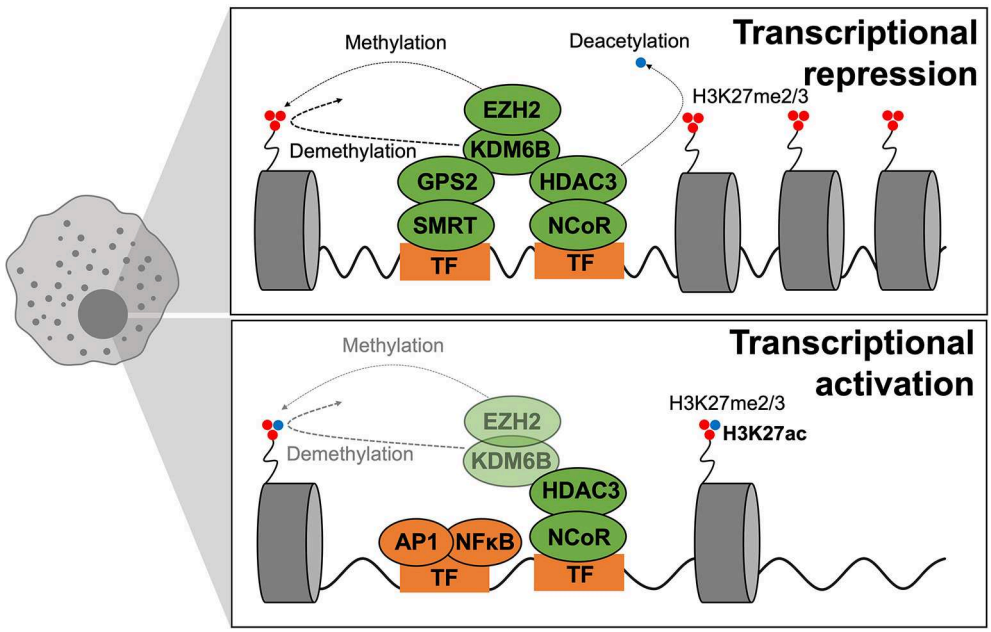

FIGURE 6 | Epigenetics of macrophage polarization in T2D. Epigenetic mechanisms that modulate transcription act on chromatin remodeling and altering DNA accessibility to transcriptional machinery. Modifications are in dynamic exchange where methylation and acetylation status of H3K27 dictate repression or activation of transcription, respectively. When chromatin is closed, methylation is dynamically altered by EZH2 (adding methyl groups) and KDMB6 (removing methyl groups), and the active transcription mark (H3K27ac) is removed through HDAC3 activity. GPS2–SMRT also participate in gene repression. During active transcription, the active transcription mark (H3K27ac) is maintained whilst EZH2–KDM6B play smaller roles. GPS2–SMRT are not present to exert repressive effects.

hormone receptor (SMRT or NCoR2) that interact with inflammatory transcription factors such as AP-1 and NFκB and in-turn bind to specific *genomic* regions to regulate transcription (192, 193). The classical view was that upon TLR4 stimulation, the NCoR complex is released from promoter/enhancer regions of inflammatory genes to promote, or de-repress, their transcription (194). However, in many cases this distinction does not truly reflect the *in vivo* situation, with context-specific microenvironmental cues dictating coregulator properties. In the context of macrophage polarization and T2D, the specific deletion of NCoR in macrophages caused the transcriptional activation of LXR, leading to the induction of lipogenic genes, which in-turn causes local anti-inflammatory effects by repressing NFκB (185). NCoR exerts pro-inflammatory actions in macrophages. Similarly, to NCoR, it was surprising that macrophages from HDAC3-deficient phenotypes were anti-inflammatory in two independent studies (195, 196). These findings are not consistent with earliest studies showing that HDAC3 and NCoR were shown to assemble a repressive complex *via* interaction with the NFκB subunit p50, necessary for the TLR tolerance phenomena where sustained TLR4 activation represses inflammatory gene expression (192). More mechanistic insights are required to better understand the specific action of NCoR1 and HDAC3.

In contrast, anti-inflammatory functions have been attributed to the SMRT/GPS2 (G-protein pathway suppressor-2) subunit/complex. In our recent study, we demonstrated that macrophage specific knockout of the GPS2 subunit exacerbates metabolic inflammation, aggravating glucose homeostasis under metabolic stress (197). The phenotype is associated with genomic features of the GPS2-repressive pathway, involving direct repression of the c-Jun subunit of AP-1. Considering all the recent studies, 2 sub-complexes may have different functions: GPS2/SMRT may have anti-inflammatory actions whilst NCoR/HDAC3 may act as pro-inflammatory machinery. This could explain the contradictory phenotypes of the respective KO models, despite both being initially classified as corepressor complexes.

Subcomplex specificities would allow controlling transcription of distinct gene clusters in response to a variety of signals and likely result from differential interactions with TFs, coregulators, and chromatin components (e.g., histones). This is exemplified by GPS2 actions in others cell types. In fact, the anti-inflammatory action of GPS2 is conserved in adipocytes by repressing CCL2 and IL6 (198, 199). While the main action of GPS2 in hepatocytes is to repress the metabolic nuclear receptor PPAR-α action (200). Hepatocyte-specific KO of GPS2 is then protective upon inflammatory stimulus while adipocyte- or macrophage-specific GPS2 deficiency is deleterious for whole body glucose homeostasis and exhibits exacerbated inflammation. These opposite functions are also observed in humans (197, 200, 201). These correlations are of importance because they point at the possibility that inappropriate GPS2 function could be linked to macrophage pathways that drive adipose tissue dysfunction and insulin resistance.

Other coregulators, such as Glutamate receptor-interacting protein (GRIP)-1, regulate macrophage programmed responses to IL-4 by acting as a coactivator for Kruppel-like factor (KLF)-4, a known driver of tissue-resident macrophage differentiation (202). Obese mice with conditional macrophage-specific deletion of GRIP1 develop inflammation and substantial macrophage infiltration in metabolic tissues, fatty livers, hyperglycemia and insulin resistance; recapitulating metabolic disease through GRIP-1's glutamate receptor-independent actions. Thus, coregulators such as GPS2, GRIP-1, NCoRs, and HDAC3 are critical regulators of macrophage reprogramming in metabolic disease. Their co-ordinated actions engage transcriptional mechanisms that coordinate the balance between macrophage polarization states and subpopulations to maintain metabolic homeostasis.

Epigenetic remodeling of specific histones is also a mark of macrophage activation states. Macrophage activation can be regulated by trimethylation of lysine residue 27 on histone 3 (a modification annotated as H3K27me3) via the action of lysine-specific demethylase 6B (KDM6B; also known as JMJD3). The histone mark H3K27me3 is represses transcription and is deposited by histone-lysine *N*-methyltransferase (EZH)-2, a subunit of the Polycomb Repressive Complex 2. Whereas, removal of this histone mark is mediated by the H3K27me3 demethylases KDM6A and KDM6B. Zhang et al. reported the critical role of the EZH2 histone methyltransferase modification in altering macrophage phenotype (203). EZH2 controls H3K27me3 deposition on the promoter of SOCS3, that encodes a cytokine signaling repressor. Accordingly, mice with a myeloid-specific deficiency of EZH2 exhibit attenuated macrophage activation and reduced inflammation under models of autoimmune disease. These findings make EZH2 an attractive target for other inflammatory diseases such as T2D.

The role of KDM6B in macrophage polarization is unclear. Pioneer studies have proposed that KDM6B is not necessary for the polarization of the pro-inflammatory macrophage phenotype in mice but is required for a proper anti-inflammatory response via the removal of H3K27me3 from the IRF4 promoter (204, 205). The absence of KDM6B completely blocks the induction of M2 macrophages in mice challenged with helminths or chitin, indicating that the role of KDM6B must be greater in M2 than in M1 macrophages (206). In contrast, Pro-inflammatory TLR4 gene activation was decreased in KDM6B-deficient macrophages. In line with these results, targeting KDM6B H3K27me3 demethylases with small-molecule inhibitors impairs inflammatory responses in human primary macrophages and could thus be of high pharmacological interest for the treatment of inflammatory diseases including T2D (207, 208). Interestingly, KDM6B also modulates expression of chemokines dependent of GM-CSF stimulation, which normally acts via STAT5-mediated and IRF5-mediated induction of a pro-inflammatory phenotype. Epigenetic signatures differ in disease states of chronic inflammation, such as T2D. KDM6B is one of the few epigenetic modifiers that could be directly involved in altering the epigenetic signature of macrophages. Gallagher et al. were the first to report on the role of KDM6B in controlling macrophage expression of IL-12 in a diabetic context (208). Proof-of-principle of these findings was achieved in a recent study where macrophages treated with a selective KDM6B inhibitor showed altered expression of pro-inflammatory cytokines (209). What remains to be determined are the degrees of contribution of nutrient overconsumption and obesity, insulin resistance, or hyperglycaemia to observed changes in histone methylation. A recent study proposes that altered DNA methylation is predominantly a consequence of adiposity, rather than a cause (210).

CONCLUSIONS: TOWARD FUNCTIONAL CLASSIFICATION, BIOENERGETICS AND NON-IMMUNE SIGNALING

Important advances have been made in the past decades characterizing the role of tissue macrophages in the development of insulin resistance. Indeed, macrophages are now seen as central actors in maintaining tissue and organism homeostasis in response to daily challenges of transient over- and under-nutrition; from inflammatory signaling necessary for insulin secretion, to the housekeeping roles they play in buffering AT lipolysis and their non-inflammatory signaling in NAFLD.

To date studies have largely focused on deciphering the molecular mechanisms that control macrophage responses to dysmetabolism, with a relatively restrictive categorization into M1-like vs. M2-like macrophages. Recent technological advances of single cell sequencing have allowed a much more in-depth characterization of tissue macrophage subsets that do not neatly adhere to the previously proposed dichotomies. Indeed in other fields of study, namely immune cell ontogeny, single cell sequencing has led to a thorough functional reclassification of innate immune subtypes (16). Such studies have particular value in characterizing macrophages in tissue niches that have been overlooked until recently, like pancreatic islet macrophages or sympathetic nervous system associated macrophages.

Such a shifting paradigm in macrophage functional classification can also be extended to their metabolic characterization, their bioenergetic requirements and adaptations to the specific challenges of insulin resistance. Numerous studies in infection and immunity have largely embraced bioenergetic adaptation as *bona fide* immune cell activation. Tissue macrophage bioenergetics remains to be elucidated, at the developmental stage, at steady state and at the onset of insulin resistance. Macrophage metabolism represents an attractive therapeutic target that will modulate inflammation without drastically altering effector functions by turning the immune response "on" or "off."

Following recent discoveries of non-immune and non-inflammatory signaling from macrophages, the scientific community has gained insight into non-canonical roles of the innate immune system. Further investigation into such homeostatic non-inflammatory signaling must be carried out in macrophages as well as related innate immune cells, such as dendritic cells, NK cells, and ILCs. As innate immunity, in all its diversity, is known to maintain homeostasis without necessarily engaging inflammation, steady state characterization,

and responses to physiological variation must be mapped to gain more basic insight into the deregulation of innate immune effector function that leads to metabolic pathology.

Despite consistently strong associations and mechanistic links between inflammation and insulin resistance there have been relatively few successful translational advances. Current anti-diabetic treatments aim to normalize glycaemia through various mechanisms and have been shown to also buffer systemic inflammation (e.g., TZDs, DPP-4 inhibitors, GLP-1 RAs). Such positive effects attribute improvement in the inflammatory profile to improved metabolic responses (211). Considering the overwhelming evidence that macrophage polarization is central to T2D pathology seemingly few clinical trials target inflammation in T2D.

To date anti-inflammatory strategies in clinical trials have targeted cytokines with neutralizing antibodies (e.g., anti-TNF, anti-IL1) or have applied agents with uncharacterised mechanisms (e.g., chloroquine, diacerein). Studies on these drugs have been promising, improving insulin sensitivity, secretion, or fasting blood glucose (212–214). The main obstacles to their routine application are the lack of long-term studies to evaluate efficacy and safety. Other hurdles to the translatability of anti-inflammatory approaches is the fact that inflammation in T2D is multifactorial, and the disease itself predisposes patients to a slew of complex complications and comorbidities (in which case the rise of precision medicine aims to identify mechanisms of response or those at-risk). Technical barriers also affect translational potential, for example clinical trials evaluate inflammation based on relatively non-specific circulating markers, such as CRP, which at best reflect systemic inflammation. Whereas, in preclinical studies scientists tend to evaluate tissue-specific inflammation, the extrapolation of which to human studies represents a substantial technical hurdle. Specific drug delivery to macrophages also represents a technical challenge and bypassing the cell-specificity leaves the door open to unexpected or unwanted side-effects. In light of the above work, promising approaches are slowly but surely increasing the translational potential of targeting inflammation in metabolic disease, for example the repurposing of well-tolerated drugs from other pathologies or fields, as was the case with anti-malarial chloroquine and hydroxychloroquine, and diacerein used to treat arthritis. In basic research, increasing attention is being placed earlier in disease course, where mechanisms that may delay or negate the natural course of T2D are being described and will soon provide bases for novel therapeutic targets. The development of small-molecule inhibitors or anti-sense oligonucleotides are increasingly attractive when targeting epigenetic or transcriptional pathways and are proving of increasing value to the clinical research community. Similarly, the search for metabolic immunogens or characterization of circulating immune cell populations will allow the development of predictive biomarkers of susceptibility to disease or risk-proxies of disease progression once insulin resistance has been established.

AUTHOR CONTRIBUTIONS

LO, ED, KD, NV, and FA wrote the review.

FUNDING

This work was supported by ATIP-AVENIR (2018) funding to ED, ERC (EpiFAT) and ANR (GlutaDiab) funding to NV, and EFSD and ANR-JCJC (MitoFLAME, ANR-19-CE14-0005) funding to FA.

REFERENCES

1. Shimobayashi M, Albert V, Woelnerhanssen B, Frei IC, Weissenberger D, Meyer-Gerspach AC, et al. Insulin resistance causes inflammation in adipose tissue. *J Clin Invest.* (2018) 128:1538–50. doi: 10.1172/JCI96139
2. Johnson AM, Olefsky JM. The origins and drivers of insulin resistance. *Cell.* (2013) 152:673–84. doi: 10.1016/j.cell.2013.01.041
3. Wu H, Ballantyne CM. Skeletal muscle inflammation and insulin resistance in obesity. *J Clin Invest.* (2017) 127:43–54. doi: 10.1172/JCI 88880
4. Rosso M, Kimbrough DJ, Gonzalez CT, Glanz BI, Healy BC, Rocca MA, et al. Cross-sectional study of smoking exposure: no differential effect on OCT metrics in a cohort of MS patients. *Mult Scler J Exp Transl Clin.* (2019) 5:2055217319828400. doi: 10.1177/2055217319828400
5. Jager J, Aparicio-Vergara M, Aouadi M. Liver innate immune cells and insulin resistance: the multiple facets of Kupffer cells. *J Intern Med.* (2016) 280:209–20. doi: 10.1111/joim.12483
6. Hotamisligil GS, Shargill NS, Spiegelman BM. Adipose expression of tumor necrosis factor-alpha: direct role in obesity-linked insulin resistance. *Science.* (1993) 259:87–91. doi: 10.1126/science.7678183
7. Weisberg SP, McCann D, Desai M, Rosenbaum M, Leibel RL, Ferrante AW Jr. Obesity is associated with macrophage accumulation in adipose tissue. *J Clin Invest.* (2003) 112:1796–808. doi: 10.1172/JCI200319246
8. Jaitin DA, Adlung L, Thaiss CA, Weiner A, Li B, Descamps H, et al. Lipid-associated macrophages control metabolic homeostasis in a Trem2-dependent manner. *Cell.* (2019) 178:686–98.e14. doi: 10.1016/j.cell.2019.05.054
9. Dong X, Liu J, Xu Y, Cao H. Role of macrophages in experimental liver injury and repair in mice. *Exp Ther Med.* (2019) 17:3835–47. doi: 10.3892/etm.2019.7450
10. Dalmas E, Lehmann FM, Dror E, Wueest S, Thienel C, Borsigova M, et al. Interleukin-33-activated islet-resident innate lymphoid cells promote insulin secretion through myeloid cell retinoic acid production. *Immunity.* (2017) 47:928–42.e7. doi: 10.1016/j.immuni.2017.10.015
11. Perdiguero EG, Geissmann F. The development and maintenance of resident macrophages. *Nat Immunol.* (2016) 17:2–8. doi: 10.1038/ni.3341
12. Stout RD, Jiang C, Matta B, Tietzel I, Watkins SK, Suttles J. Macrophages sequentially change their functional phenotype in response to changes in microenvironmental influences. *J Immunol.* (2005) 175:342–9. doi: 10.4049/jimmunol.175.1.342
13. O'Neill LA, Kishton RJ, Rathmell J. A guide to immunometabolism for immunologists. *Nat Rev Immunol.* (2016) 16:553–65. doi: 10.1038/nri.2016.70
14. Martinez FO, Gordon S. The M1 and M2 paradigm of macrophage activation: time for reassessment. *F1000Prime Rep.* (2014) 6:13. doi: 10.12703/P6-13
15. Mantovani A, Sica A, Sozzani S, Allavena P, Vecchi A, Locati M. The chemokine system in diverse forms of macrophage activation and polarization. *Trends Immunol.* (2004) 25:677–86. doi: 10.1016/j.it.2004.09.015

16. Ginhoux F, Schultze JL, Murray PJ, Ochando J, Biswas SK. New insights into the multidimensional concept of macrophage ontogeny, activation and function. *Nat Immunol.* (2016) 17:34–40. doi: 10.1038/ni.3324
17. Amouzou C, Breuker C, Fabre O, Bourret A, Lambert K, Birot O, et al. Skeletal muscle insulin resistance and absence of inflammation characterize insulin-resistant Grade I obese women. *PLoS ONE.* (2016) 11:e0154119. doi: 10.1371/journal.pone.0154119
18. Bhatt M, Rudrapatna S, Banfield L, Bierbrier R, Wang PW, Wang KW, et al. Evaluating the evidence for macrophage presence in skeletal muscle and its relation to insulin resistance in obese mice and humans: a systematic review protocol. *BMC Res Notes.* (2017) 10:374. doi: 10.1186/s13104-017-2686-6
19. Calderon B, Carrero JA, Ferris ST, Sojka DK, Moore L, Epelman S, et al. The pancreas anatomy conditions the origin and properties of resident macrophages. *J Exp Med.* (2015) 212:1497–512. doi: 10.1084/jem.20150496
20. Ehses JA, Perren A, Eppler E, Ribaux P, Pospisilik JA, Maor-Cahn R, et al. Increased number of islet-associated macrophages in type 2 diabetes. *Diabetes.* (2007) 56:2356–70. doi: 10.2337/db06-1650
21. Banaei-Bouchareb L, Gouon-Evans V, Samara-Boustani D, Castellotti MC, Czernichow P, Pollard JW, et al. Insulin cell mass is altered in Csf1op/Csf1op macrophage-deficient mice. *J Leukoc Biol.* (2004) 76:359–67. doi: 10.1189/jlb.1103591
22. Carrero JA, McCarthy DP, Ferris ST, Wan X, Hu H, Zinselmeyer BH, et al. Resident macrophages of pancreatic islets have a seminal role in the initiation of autoimmune diabetes of NOD mice. *Proc Natl Acad Sci USA.* (2017) 114:E10418–27. doi: 10.1073/pnas.1713543114
23. Zinselmeyer BH, Vomund AN, Saunders BT, Johnson MW, Carrero JA, Unanue ER. The resident macrophages in murine pancreatic islets are constantly probing their local environment, capturing beta cell granules and blood particles. *Diabetologia.* (2018) 61:1374–83. doi: 10.1007/s00125-018-4592-4
24. Weitz JR, Makhmutova M, Almaca J, Stertmann J, Aamodt K, Brissova M, et al. Mouse pancreatic islet macrophages use locally released ATP to monitor beta cell activity. *Diabetologia.* (2018) 61:182–92. doi: 10.1007/s00125-017-4416-y
25. Benner C, van der Meulen T, Caceres E, Tigyi K, Donaldson CJ, Huising MO. The transcriptional landscape of mouse beta cells compared to human beta cells reveals notable species differences in long non-coding RNA and protein-coding gene expression. *BMC Genomics.* (2014) 15:620. doi: 10.1186/1471-2164-15-620
26. Boni-Schnetzler M, Boller S, Debray S, Bouzakri K, Meier DT, Prazak R, et al. Free fatty acids induce a proinflammatory response in islets via the abundantly expressed interleukin-1 receptor *Endocrinology.* (2009) 150:5218–29. doi: 10.1210/en.2009-0543
27. Hajmrle C, Smith N, Spigelman AF, Dai X, Senior L, Bautista A, et al. Interleukin-1 signaling contributes to acute islet compensation. *JCI Insight.* (2016) 1:e86055. doi: 10.1172/jci.insight.86055
28. Zawalich WS, Zawalich KC. Interleukin 1 is a potent stimulator of islet insulin secretion and phosphoinositide hydrolysis. *Am J Physiol.* (1989) 256:E19–24. doi: 10.1152/ajpendo.1989.256.1.E19
29. Burke SJ, Batdorf HM, Burk DH, Martin TM, Mendoza T, Stadler K, et al. Pancreatic deletion of the interleukin-1 receptor disrupts whole body glucose homeostasis and promotes islet beta-cell de-differentiation. *Mol Metab.* (2018). doi: 10.1016/j.molmet.2018.06.003
30. Dror E, Dalmas E, Meier DT, Wueest S, Thevenet J, Thienel C, et al. Postprandial macrophage-derived IL-1beta stimulates insulin, and both synergistically promote glucose disposal and inflammation. *Nat Immunol.* (2017) 18:283–92. doi: 10.1038/ni.3659
31. Chittezhath M, Gunaseelan D, Zheng X, Hasan R, Tay VS, Lim ST, et al. Islet macrophages are associated with islet vascular remodeling and compensatory hyperinsulinemia during diabetes. *Am J Physiol Endocrinol Metab.* (2019) 317:E1108–120. doi: 10.1101/584953
32. Ying W, Lee YS, Dong Y, Seidman JS, Yang M, Isaac R, et al. Expansion of islet-resident macrophages leads to inflammation affecting beta cell proliferation and function in obesity. *Cell Metab.* (2019) 29:457–74 e5. doi: 10.1016/j.cmet.2018.12.003
33. Eguchi K, Manabe I, Oishi-Tanaka Y, Ohsugi M, Kono N, Ogata F, et al. Saturated fatty acid and TLR signaling link beta cell dysfunction and islet inflammation. *Cell Metab.* (2012) 15:518–33. doi: 10.1016/j.cmet.2012.01.023
34. Hasnain SZ, Borg DJ, Harcourt BE, Tong H, Sheng YH, Ng CP, et al. Glycemic control in diabetes is restored by therapeutic manipulation of cytokines that regulate beta cell stress. *Nat Med.* (2014) 20:1417–26. doi: 10.1038/nm.3705
35. Richardson SJ, Willcox A, Bone AJ, Foulis AK, Morgan NG. Islet-associated macrophages in type 2 diabetes. *Diabetologia.* (2009) 52:1686–8. doi: 10.1007/s00125-009-1410-z
36. Maedler K, Sergeev P, Ris F, Oberholzer J, Joller-Jemelka HI, Spinas GA, et al. Glucose-induced beta cell production of IL-1beta contributes to glucotoxicity in human pancreatic islets. *J Clin Invest.* (2002) 110:851–60. doi: 10.1172/JCI200215318
37. Jourdan T, Godlewski G, Cinar R, Bertola A, Szanda G, Liu J, et al. Activation of the Nlrp3 inflammasome in infiltrating macrophages by endocannabinoids mediates beta cell loss in type 2 diabetes. *Nat Med.* (2013) 19:1132–40. doi: 10.1038/nm.3265
38. Segerstolpe A, Palasantza A, Eliasson P, Andersson EM, Andreasson AC, Sun X, et al. Single-cell transcriptome profiling of human pancreatic islets in health and Type 2 diabetes. *Cell Metab.* (2016) 24:593–607. doi: 10.1016/j.cmet.2016.08.020
39. Mahdi T, Hanzelmann S, Salehi A, Muhammed SJ, Reinbothe TM, Tang Y, et al. Secreted frizzled-related protein 4 reduces insulin secretion and is overexpressed in type 2 diabetes. *Cell Metab.* (2012) 16:625–33. doi: 10.1016/j.cmet.2012.10.009
40. Kane H, Lynch L. Innate immune control of adipose tissue homeostasis. *Trends Immunol.* (2019) 40:857–72. doi: 10.1016/j.it.2019.07.006
41. Fischer-Posovszky P, Wang QA, Asterholm IW, Rutkowski JM, Scherer PE. Targeted deletion of adipocytes by apoptosis leads to adipose tissue recruitment of alternatively activated M2 macrophages. *Endocrinology.* (2011) 152:3074–81. doi: 10.1210/en.2011-1031
42. Kosteli A, Sugaru E, Haemmerle G, Martin JF, Lei J, Zechner R, et al. Weight loss and lipolysis promote a dynamic immune response in murine adipose tissue. *J Clin Invest.* (2010) 120:3466–79. doi: 10.1172/JCI42845
43. Nguyen KD, Qiu Y, Cui X, Goh YP, Mwangi J, David T, et al. Alternatively activated macrophages produce catecholamines to sustain adaptive thermogenesis. *Nature.* (2011) 480:104–8. doi: 10.1038/nature10653
44. Aouadi M, Vangala P, Yawe JC, Tencerova M, Nicoloro SM, Cohen JL, et al. Lipid storage by adipose tissue macrophages regulates systemic glucose tolerance. *Am J Physiol Endocrinol Metab.* (2014) 307:E374–83. doi: 10.1152/ajpendo.00187.2014
45. Xu X, Grijalva A, Skowronski A, van Eijk M, Serlie MJ, Ferrante AW Jr. Obesity activates a program of lysosomal-dependent lipid metabolism in adipose tissue macrophages independently of classic activation. *Cell Metab.* (2013) 18:816–30. doi: 10.1016/j.cmet.2013.11.001
46. Flaherty SE 3rd, Grijalva A, Xu X, Ables E, Nomani A, Ferrante AW Jr. A lipase-independent pathway of lipid release and immune modulation by adipocytes. *Science.* (2019) 363:989–93. doi: 10.1126/science.aaw2586
47. Nagy L, Tontonoz P, Alvarez JG, Chen H, Evans RM. Oxidized LDL regulates macrophage gene expression through ligand activation of PPARgamma. *Cell.* (1998) 93:229–40. doi: 10.1016/S0092-8674(00)81574-3
48. Pirzgalska RM, Seixas E, Seidman JS, Link VM, Sánchez NM, Mahú I, et al. Sympathetic neuron–associated macrophages contribute to obesity by importing and metabolizing norepinephrine. *Nat Med.* (2017) 23:1309–18. doi: 10.1038/nm.4422
49. Orr JS, Kennedy A, Anderson-Baucum EK, Webb CD, Fordahl SC, Erikson KM, et al. Obesity alters adipose tissue macrophage iron content and tissue iron distribution. *Diabetes.* (2014) 63:421–32. doi: 10.2337/db13-0213
50. Festa M, Ricciardelli G, Mele G, Pietropaolo C, Ruffo A, Colonna A. Overexpression of H ferritin and up-regulation of iron regulatory protein genes during differentiation of 3T3-L1 pre-adipocytes. *J Biol Chem.* (2000) 275:36708–12. doi: 10.1074/jbc.M004988200
51. Gabrielsen JS, Gao Y, Simcox JA, Huang J, Thorup D, Jones D, et al. Adipocyte iron regulates adiponectin and insulin sensitivity. *J Clin Invest.* (2012) 122:3529–40. doi: 10.1172/JCI44421
52. Lee YH, Petkova AP, Granneman JG. Identification of an adipogenic niche for adipose tissue remodeling and restoration. *Cell Metab.* (2013) 18:355–67. doi: 10.1016/j.cmet.2013.08.003
53. Bourlier V, Zakaroff-Girard A, Miranville A, De Barros S, Maumus M, Sengenes C, et al. Remodeling phenotype of human subcutaneous

adipose tissue macrophages. *Circulation.* (2008) 117:806–15. doi: 10.1161/CIRCULATIONAHA.107.724096
54. Pang C, Gao Z, Yin J, Zhang J, Jia W, Ye J. Macrophage infiltration into adipose tissue may promote angiogenesis for adipose tissue remodeling in obesity. *Am J Physiol Endocrinol Metab.* (2008) 295:E313–22. doi: 10.1152/ajpendo.90296.2008
55. Lumeng CN, Bodzin JL, Saltiel AR. Obesity induces a phenotypic switch in adipose tissue macrophage polarization. *J Clin Invest.* (2007) 117:175–84. doi: 10.1172/JCI29881
56. Kim HJ, Higashimori T, Park SY, Choi H, Dong J, Kim YJ, et al. Differential effects of interleukin-6 and−10 on skeletal muscle and liver insulin action *in vivo*. *Diabetes.* (2004) 53:1060–7. doi: 10.2337/diabetes.53.4.1060
57. Bluher M, Fasshauer M, Tonjes A, Kratzsch J, Schon MR, Paschke R. Association of interleukin-6, C-reactive protein, interleukin-10 and adiponectin plasma concentrations with measures of obesity, insulin sensitivity and glucose metabolism. *Exp Clin Endocrinol Diabetes.* (2005) 113:534–7. doi: 10.1055/s-2005-872851
58. Kowalski GM, Nicholls HT, Risis S, Watson NK, Kanellakis P, Bruce CR, et al. Deficiency of haematopoietic-cell-derived IL-10 does not exacerbate high-fat-diet-induced inflammation or insulin resistance in mice. *Diabetologia.* (2011) 54:888–99. doi: 10.1007/s00125-010-2020-5
59. Ying W, Riopel M, Bandyopadhyay G, Dong Y, Birmingham A, Seo JB, et al. Adipose tissue macrophage-derived exosomal miRNAs can modulate *in vivo* and *in vitro* insulin sensitivity. *Cell.* (2017) 171:372–84.e12. doi: 10.1016/j.cell.2017.08.035
60. Zheng C, Yang Q, Cao J, Xie N, Liu K, Shou P, et al. Local proliferation initiates macrophage accumulation in adipose tissue during obesity. *Cell Death Dis.* (2016) 7:e2167. doi: 10.1038/cddis.2016.54
61. Amano SU, Cohen JL, Vangala P, Tencerova M, Nicoloro SM, Yawe JC, et al. Local proliferation of macrophages contributes to obesity-associated adipose tissue inflammation. *Cell Metab.* (2014) 19:162–71. doi: 10.1016/j.cmet.2013.11.017
62. Ramkhelawon B, Hennessy EJ, Menager M, Ray TD, Sheedy FJ, Hutchison S, et al. Netrin-1 promotes adipose tissue macrophage retention and insulin resistance in obesity. *Nat Med.* (2014) 20:377–84. doi: 10.1038/nm.3467
63. Prieur X, Mok CY, Velagapudi VR, Nunez V, Fuentes L, Montaner D, et al. Differential lipid partitioning between adipocytes and tissue macrophages modulates macrophage lipotoxicity and M2/M1 polarization in obese mice. *Diabetes.* (2011) 60:797–809. doi: 10.2337/db10-0705
64. Hill DA, Lim HW, Kim YH, Ho WY, Foong YH, Nelson VL, et al. Distinct macrophage populations direct inflammatory versus physiological changes in adipose tissue. *Proc Natl Acad Sci USA.* (2018) 115:E5096–105. doi: 10.1073/pnas.1802611115
65. Kratz M, Coats BR, Hisert KB, Hagman D, Mutskov V, Peris E, et al. Metabolic dysfunction drives a mechanistically distinct proinflammatory phenotype in adipose tissue macrophages. *Cell Metab.* (2014) 20:614–25. doi: 10.1016/j.cmet.2014.08.010
66. Cinti S, Mitchell G, Barbatelli G, Murano I, Ceresi E, Faloia E, et al. Adipocyte death defines macrophage localization and function in adipose tissue of obese mice and humans. *J Lipid Res.* (2005) 46:2347–55. doi: 10.1194/jlr.M500294-JLR200
67. McNally AK, Anderson JM. Macrophage fusion and multinucleated giant cells of inflammation. *Adv Exp Med Biol.* (2011) 713:97–111. doi: 10.1007/978-94-007-0763-4_7
68. Patsouris D, Li PP, Thapar D, Chapman J, Olefsky JM, Neels JG. Ablation of CD11c-positive cells normalizes insulin sensitivity in obese insulin resistant animals. *Cell Metab.* (2008) 8:301–9. doi: 10.1016/j.cmet.2008.08.015
69. Weiss M, Byrne AJ, Blazek K, Saliba DG, Pease JE, Perocheau D, et al. IRF5 controls both acute and chronic inflammation. *Proc Natl Acad Sci USA.* (2015) 112:11001–6. doi: 10.1073/pnas.1506254112
70. Dalmas E, Toubal A, Alzaid F, Blazek K, Eames HL, Lebozec K, et al. Irf5 deficiency in macrophages promotes beneficial adipose tissue expansion and insulin sensitivity during obesity. *Nat Med.* (2015) 21:610–8. doi: 10.1038/nm.3829
71. Sindhu S, Thomas R, Kochumon S, Wilson A, Abu-Farha M, Bennakhi A, et al. Increased adipose tissue expression of interferon regulatory factor (IRF)-5 in obesity: association with metabolic inflammation. *Cells.* (2019) 8:E1418. doi: 10.3390/cells8111418
72. Scott CL, Zheng F, De Baetselier P, Martens L, Saeys Y, De Prijck S, et al. Bone marrow-derived monocytes give rise to self-renewing and fully differentiated Kupffer cells. *Nat Commun.* (2016) 7:10321. doi: 10.1038/ncomms10321
73. Ju C, Tacke F. Hepatic macrophages in homeostasis and liver diseases: from pathogenesis to novel therapeutic strategies. *Cell Mol Immunol.* (2016) 13:316–27. doi: 10.1038/cmi.2015.104
74. Burt AD, Ferrell LD, Hübscher SG. *MacSween's Pathology of the Liver, 7th ed* (2018).
75. Heymann F, Peusquens J, Ludwig-Portugall I, Kohlhepp M, Ergen C, Niemietz P, et al. Liver inflammation abrogates immunological tolerance induced by Kupffer cells. *Hepatology.* (2015) 62:279–91. doi: 10.1002/hep.27793
76. Yan ML, Wang YD, Tian YF, Lai ZD, Yan LN. Inhibition of allogeneic T-cell response by Kupffer cells expressing indoleamine 2,3-dioxygenase. *World J Gastroenterol.* (2010) 16:636–40. doi: 10.3748/wjg.v16.i5.636
77. Morrison MC, Kleemann R. Role of macrophage migration inhibitory factor in obesity, insulin resistance, type 2 diabetes, and associated hepatic co-morbidities: a comprehensive review of human and rodent studies. *Front Immunol.* (2015) 6:308. doi: 10.3389/fimmu.2015.00308
78. Morgantini C, Jager J, Li X, Levi L, Azzimato V, Sulen A, et al. Liver macrophages regulate systemic metabolism through non-inflammatory factors. *Nat Metab.* (2019) 1:445–59. doi: 10.1038/s42255-019-0044-9
79. Alzaid F, Lagadec F, Albuquerque M, Ballaire R, Orliaguet L, Hainault I, et al. IRF5 governs liver macrophage activation that promotes hepatic fibrosis in mice and humans. *JCI Insight.* (2016) 1:e88689. doi: 10.1172/jci.insight.88689
80. Xiao C, Stahel P, Morgantini C, Nahmias A, Dash S, Lewis GF. Glucagon-like peptide-2 mobilizes lipids from the intestine by a systemic nitric oxide-independent mechanism. *Diabetes Obes Metab.* (2019) 21:2535–41. doi: 10.1111/dom.13839
81. Rausch ME, Weisberg S, Vardhana P, Tortoriello DV. Obesity in C57BL/6J mice is characterized by adipose tissue hypoxia and cytotoxic T-cell infiltration. *Int J Obes.* (2008) 32:451–63. doi: 10.1038/sj.ijo.0803744
82. Murano I, Barbatelli G, Parisani V, Latini C, Muzzonigro G, Castellucci M, et al. Dead adipocytes, detected as crown-like structures, are prevalent in visceral fat depots of genetically obese mice. *J Lipid Res.* (2008) 49:1562–8. doi: 10.1194/jlr.M800019-JLR200
83. Boutens L, Stienstra R. Adipose tissue macrophages: going off track during obesity. *Diabetologia.* (2016) 59:879–94. doi: 10.1007/s00125-016-3904-9
84. Shi H, Kokoeva MV, Inouye K, Tzameli I, Yin H, Flier JS. TLR4 links innate immunity and fatty acid-induced insulin resistance. *J Clin Invest.* (2006) 116:3015–25. doi: 10.1172/JCI28898
85. Shin KC, Hwang I, Choe SS, Park J, Ji Y, Kim JI, et al. Macrophage VLDLR mediates obesity-induced insulin resistance with adipose tissue inflammation. *Nat Commun.* (2017) 8:1087. doi: 10.1038/s41467-017-01232-w
86. Wen H, Ting JP, O'Neill LA. A role for the NLRP3 inflammasome in metabolic diseases and did Warburg miss inflammation? *Nat Immunol.* (2012) 13:352–7. doi: 10.1038/ni.2228
87. Wen H, Gris D, Lei Y, Jha S, Zhang L, Huang MT, et al. Fatty acid-induced NLRP3-ASC inflammasome activation interferes with insulin signaling. *Nat Immunol.* (2011) 12:408–15. doi: 10.1038/ni.2022
88. Hotamisligil GS, Peraldi P, Budavari A, Ellis R, White MF, Spiegelman BM. IRS-1-mediated inhibition of insulin receptor tyrosine kinase activity in TNF-alpha- and obesity-induced insulin resistance. *Science.* (1996) 271:665–8. doi: 10.1126/science.271.5249.665
89. Haeusler RA, McGraw TE, Accili D. Biochemical and cellular properties of insulin receptor signalling. *Nat Rev Mol Cell Biol.* (2018) 19:31–44. doi: 10.1038/nrm.2017.89
90. Kanety H, Feinstein R, Papa MZ, Hemi R, Karasik A. Tumor necrosis factor alpha-induced phosphorylation of insulin receptor substrate-1 (IRS-1). Possible mechanism for suppression of insulin-stimulated tyrosine phosphorylation of IRS-1. *J Biol Chem.* (1995) 270:23780–4. doi: 10.1074/jbc.270.40.23780
91. Jager J, Gremeaux T, Cormont M, Le Marchand-Brustel Y, Tanti JF. Interleukin-1beta-induced insulin resistance in adipocytes through down-regulation of insulin receptor substrate-1 expression. *Endocrinology.* (2007) 148:241–51. doi: 10.1210/en.2006-0692

92. Wunderlich CM, Hövelmeyer N, Wunderlich FT. Mechanisms of chronic JAK-STAT3-SOCS3 signaling in obesity. *JAKSTAT*. (2013) 2:e23878. doi: 10.4161/jkst.23878
93. Munder M, Eichmann K, Modolell M. Alternative metabolic states in murine macrophages reflected by the nitric oxide synthase/arginase balance: competitive regulation by CD4+ T cells correlates with Th1/Th2 phenotype. *J Immunol.* (1998) 160:5347–54.
94. Oren R, Farnham AE, Saito K, Milofsky E, Karnovsky ML. Metabolic patterns in three types of phagocytizing cells. *J Cell Biol.* (1963) 17:487–501. doi: 10.1083/jcb.17.3.487
95. Pavlou S, Wang L, Xu H, Chen M. Higher phagocytic activity of thioglycollate-elicited peritoneal macrophages is related to metabolic status of the cells. *J Inflamm.* (2017) 14:4. doi: 10.1186/s12950-017-0151-x
96. Kellett DN. 2-Deoxyglucose and inflammation. *J Pharm Pharmacol.* (1966) 18:199–200. doi: 10.1111/j.2042-7158.1966.tb07853.x
97. Freemerman AJ, Johnson AR, Sacks GN, Milner JJ, Kirk EL, Troester MA, et al. Metabolic reprogramming of macrophages: glucose transporter 1 (GLUT1)-mediated glucose metabolism drives a proinflammatory phenotype. *J Biol Chem.* (2014) 289:7884–96. doi: 10.1074/jbc.M113.522037
98. Blouin CC, Page EL, Soucy GM, Richard DE. Hypoxic gene activation by lipopolysaccharide in macrophages: implication of hypoxia-inducible factor 1alpha. *Blood.* (2004) 103:1124–30. doi: 10.1182/blood-2003-07-2427
99. Rodriguez-Prados JC, Traves PG, Cuenca J, Rico D, Aragones J, Martin-Sanz P, et al. Substrate fate in activated macrophages: a comparison between innate, classic, and alternative activation. *J Immunol.* (2010) 185:605–14. doi: 10.4049/jimmunol.0901698
100. Hedl M, Yan J, Witt H, Abraham C. IRF5 is required for bacterial clearance in human M1-polarized macrophages, and IRF5 immune-mediated disease risk variants modulate this outcome. *J Immunol.* (2019) 202:920–30. doi: 10.4049/jimmunol.1800226
101. Palsson-McDermott EM, Curtis AM, Goel G, Lauterbach MA, Sheedy FJ, Gleeson LE, et al. Pyruvate kinase M2 regulates Hif-1alpha activity and IL-1beta induction and is a critical determinant of the warburg effect in LPS-activated macrophages. *Cell Metab.* (2015) 21:65–80. doi: 10.1016/j.cmet.2014.12.005
102. Luo W, Hu H, Chang R, Zhong J, Knabel M, O'Meally R, et al. Pyruvate kinase M2 is a PHD3-stimulated coactivator for hypoxia-inducible factor 1. *Cell.* (2011) 145:732–44. doi: 10.1016/j.cell.2011.03.054
103. Wolf AJ, Reyes CN, Liang W, Becker C, Shimada K, Wheeler ML, et al. Hexokinase is an innate immune receptor for the detection of bacterial peptidoglycan. *Cell.* (2016) 166:624–36. doi: 10.1016/j.cell.2016.05.076
104. Ip WKE, Hoshi N, Shouval DS, Snapper S, Medzhitov R. Anti-inflammatory effect of IL-10 mediated by metabolic reprogramming of macrophages. *Science.* (2017) 356:513–9. doi: 10.1126/science.aal3535
105. Baardman J, Verberk SGS, Prange KHM, van Weeghel M, van der Velden S, Ryan DG, et al. A defective pentose phosphate pathway reduces inflammatory macrophage responses during hypercholesterolemia. *Cell Rep.* (2018) 25:2044–52 e5. doi: 10.1016/j.celrep.2018.10.092
106. Infantino V, Convertini P, Cucci L, Panaro MA, Di Noia MA, Calvello R, et al. The mitochondrial citrate carrier: a new player in inflammation. *Biochem J.* (2011) 438:433–6. doi: 10.1042/BJ20111275
107. Infantino V, Iacobazzi V, Palmieri F, Menga A. ATP-citrate lyase is essential for macrophage inflammatory response. *Biochem Biophys Res Commun.* (2013) 440:105–11. doi: 10.1016/j.bbrc.2013.09.037
108. Wei X, Song H, Yin L, Rizzo MG, Sidhu R, Covey DF, et al. Fatty acid synthesis configures the plasma membrane for inflammation in diabetes. *Nature.* (2016) 539:294–8. doi: 10.1038/nature20117
109. Hooftman A, O'Neill LAJ. The immunomodulatory potential of the metabolite itaconate. *Trends Immunol.* (2019) 40:687–98. doi: 10.1016/j.it.2019.05.007
110. Lampropoulou V, Sergushichev A, Bambouskova M, Nair S, Vincent EE, Loginicheva E, et al. Itaconate links inhibition of succinate dehydrogenase with macrophage metabolic remodeling and regulation of inflammation. *Cell Metab.* (2016) 24:158–66. doi: 10.1016/j.cmet.2016.06.004
111. Quinlan CL, Orr AL, Perevoshchikova IV, Treberg JR, Ackrell BA, Brand MD. Mitochondrial complex II can generate reactive oxygen species at high rates in both the forward and reverse reactions. *J Biol Chem.* (2012) 287:27255–64. doi: 10.1074/jbc.M112.374629
112. Tannahill G, Curtis A, Adamik J, Palsson-McDermott E, McGettrick A, Goel G, et al. Succinate is a danger signal that induces IL-1β via HIF-1α. *Nature.* (2013) 496:238–42. doi: 10.1038/nature11986
113. Langston PK, Nambu A, Jung J, Shibata M, Aksoylar HI, Lei J, et al. Glycerol phosphate shuttle enzyme GPD2 regulates macrophage inflammatory responses. *Nat Immunol.* (2019) 20:1186–95. doi: 10.1038/s41590-019-0453-7
114. Liu PS, Wang H, Li X, Chao T, Teav T, Christen S, et al. alpha-ketoglutarate orchestrates macrophage activation through metabolic and epigenetic reprogramming. *Nat Immunol.* (2017) 18:985–94. doi: 10.1038/ni.3796
115. Vats D, Mukundan L, Odegaard JI, Zhang L, Smith KL, Morel CR, et al. Oxidative metabolism and PGC-1beta attenuate macrophage-mediated inflammation. *Cell Metab.* (2006) 4:13–24. doi: 10.1016/j.cmet.2006.05.011
116. Wang F, Zhang S, Vuckovic I, Jeon R, Lerman A, Folmes CD, et al. Glycolytic stimulation is not a requirement for M2 macrophage differentiation. *Cell Metab.* (2018) 28:463–75.e4. doi: 10.1016/j.cmet.2018.08.012
117. Covarrubias AJ, Aksoylar HI, Yu J, Snyder NW, Worth AJ, Iyer SS, et al. Akt-mTORC1 signaling regulates Acly to integrate metabolic input to control of macrophage activation. *Elife.* (2016) 5:e11612. doi: 10.7554/eLife.11612.024
118. Haschemi A, Kosma P, Gille L, Evans CR, Burant CF, Starkl P, et al. The sedoheptulose kinase CARKL directs macrophage polarization through control of glucose metabolism. *Cell Metab.* (2012) 15:813–26. doi: 10.1016/j.cmet.2012.04.023
119. Tavakoli S, Downs K, Short JD, Nguyen HN, Lai Y, Jerabek PA, et al. Characterization of macrophage polarization states using combined measurement of 2-deoxyglucose and glutamine accumulation: implications for imaging of atherosclerosis. *Arterioscler Thromb Vasc Biol.* (2017) 37:1840–8. doi: 10.1161/ATVBAHA.117.308848
120. Jha AK, Huang SC, Sergushichev A, Lampropoulou V, Ivanova Y, Loginicheva E, et al. Network integration of parallel metabolic and transcriptional data reveals metabolic modules that regulate macrophage polarization. *Immunity.* (2015) 42:419–30. doi: 10.1016/j.immuni.2015.02.005
121. Schulman IG. Liver X receptors link lipid metabolism and inflammation. *FEBS Lett.* (2017) 591:2978–91. doi: 10.1002/1873-3468.12702
122. Oishi Y, Spann NJ, Link VM, Muse ED, Strid T, Edillor C, et al. SREBP1 contributes to resolution of pro-inflammatory TLR4 signaling by reprogramming fatty acid metabolism. *Cell Metab.* (2017) 25:412–27. doi: 10.1016/j.cmet.2016.11.009
123. Boutens L, Hooiveld GJ, Dhingra S, Cramer RA, Netea MG, Stienstra R. Unique metabolic activation of adipose tissue macrophages in obesity promotes inflammatory responses. *Diabetologia.* (2018) 61:942–53. doi: 10.1007/s00125-017-4526-6
124. Ren W, Xia Y, Chen S, Wu G, Bazer FW, Zhou B, et al. Glutamine metabolism in macrophages: a novel target for obesity/Type 2 diabetes. *Adv Nutr.* (2019) 10:321–30. doi: 10.1093/advances/nmy084
125. Brennan JJ, Gilmore TD. Evolutionary origins of toll-like receptor signaling. *Mol Biol Evol.* (2018) 35:1576–87. doi: 10.1093/molbev/msy050
126. Ermis Karaali Z, Candan G, Aktuglu MB, Velet M, Ergen A. Toll-like receptor 2 (TLR-2) gene polymorphisms in type 2 diabetes mellitus. *Cell J.* (2019) 20:559–63. doi: 10.22074/cellj.2019.5540
127. Gupta S, Maratha A, Siednienko J, Natarajan A, Gajanayake T, Hoashi S, et al. Analysis of inflammatory cytokine and TLR expression levels in Type 2 diabetes with complications. *Sci Rep.* (2017) 7:7633. doi: 10.1038/s41598-017-07230-8
128. Haversen L, Danielsson KN, Fogelstrand L, Wiklund O. Induction of proinflammatory cytokines by long-chain saturated fatty acids in human macrophages. *Atherosclerosis.* (2009) 202:382–93. doi: 10.1016/j.atherosclerosis.2008.05.033
129. Rubartelli A, Lotze MT, Latz E, Manfredi A. Mechanisms of sterile inflammation. *Front Immunol.* (2013) 4:398. doi: 10.3389/fimmu.2013.00398
130. Eguchi J, Wang X, Yu S, Kershaw EE, Chiu PC, Dushay J, et al. Transcriptional control of adipose lipid handling by IRF4. *Cell Metab.* (2011) 13:249–59. doi: 10.1016/j.cmet.2011.02.005
131. Zhao GN, Jiang DS, Li H. Interferon regulatory factors: at the crossroads of immunity, metabolism, and disease. *Biochim Biophys Acta.* (2015) 1852:365–78. doi: 10.1016/j.bbadis.2014.04.030

132. Chen W, Royer WE Jr. Structural insights into interferon regulatory factor activation. *Cell Signal.* (2010) 22:883–7. doi: 10.1016/j.cellsig.2009.12.005
133. Orr JS, Puglisi MJ, Ellacott KL, Lumeng CN, Wasserman DH, Hasty AH. Toll-like receptor 4 deficiency promotes the alternative activation of adipose tissue macrophages. *Diabetes*. (2012) 61:2718–27. doi: 10.2337/db11-1595
134. Kumari M, Wang X, Lantier L, Lyubetskaya A, Eguchi J, Kang S, et al. IRF3 promotes adipose inflammation and insulin resistance and represses browning. *J Clin Invest*. (2016) 126:2839–54. doi: 10.1172/JCI86080
135. Gunthner R, Anders HJ. Interferon-regulatory factors determine macrophage phenotype polarization. *Mediators Inflamm.* (2013) 2013:731023. doi: 10.1155/2013/731023
136. Eguchi J, Kong X, Tenta M, Wang X, Kang S, Rosen ED. Interferon regulatory factor 4 regulates obesity-induced inflammation through regulation of adipose tissue macrophage polarization. *Diabetes.* (2013) 62:3394–403. doi: 10.2337/db12-1327
137. Ameyar M, Wisniewska M, Weitzman JB. A role for AP-1 in apoptosis: the case for and against. *Biochimie.* (2003) 85:747–52. doi: 10.1016/j.biochi.2003.09.006
138. Vesely PW, Staber PB, Hoefler G, Kenner L. Translational regulation mechanisms of AP-1 proteins. *Mutat Res*. (2009) 682:7–12. doi: 10.1016/j.mrrev.2009.01.001
139. Takahashi M, Yagyu H, Tazoe F, Nagashima S, Ohshiro T, Okada K, et al. Macrophage lipoprotein lipase modulates the development of atherosclerosis but not adiposity. *J Lipid Res.* (2013) 54:1124–34. doi: 10.1194/jlr.M035568
140. Hirosumi J, Tuncman G, Chang L, Gorgun CZ, Uysal KT, Maeda K, et al. A central role for JNK in obesity and insulin resistance. *Nature.* (2002) 420:333–6. doi: 10.1038/nature01137
141. Tuncman G, Hirosumi J, Solinas G, Chang L, Karin M, Hotamisligil GS. Functional *in vivo* interactions between JNK1 and JNK2 isoforms in obesity and insulin resistance. *Proc Natl Acad Sci USA.* (2006) 103:10741–6. doi: 10.1073/pnas.0603509103
142. Solinas G, Vilcu C, Neels JG, Bandyopadhyay GK, Luo JL, Naugler W, et al. JNK1 in hematopoietically derived cells contributes to diet-induced inflammation and insulin resistance without affecting obesity. *Cell Metab.* (2007) 6:386–97. doi: 10.1016/j.cmet.2007.09.011
143. Solinas G, Becattini B. JNK at the crossroad of obesity, insulin resistance, and cell stress response. *Mol Metab.* (2017) 6:174–84. doi: 10.1016/j.molmet.2016.12.001
144. Baker RG, Hayden MS, Ghosh S. NF-kappaB, inflammation, and metabolic disease. *Cell Metab.* (2011) 13:11–22. doi: 10.1016/j.cmet.2010.12.008
145. D'Ignazio L, Bandarra D, Rocha S. NF-kappaB and HIF crosstalk in immune responses. *FEBS J.* (2016) 283:413–24. doi: 10.1111/febs.13578
146. Xanthoulea S, Curfs DM, Hofker MH, de Winther MP. Nuclear factor kappa B signaling in macrophage function and atherogenesis. *Curr Opin Lipidol.* (2005) 16:536–42. doi: 10.1097/01.mol.0000180167.15820.ae
147. Arkan MC, Hevener AL, Greten FR, Maeda S, Li ZW, Long JM, et al. IKK-beta links inflammation to obesity-induced insulin resistance. *Nat Med.* (2005) 11:191–8. doi: 10.1038/nm1185
148. Wang N, Liang HW, Zen K. Molecular mechanisms that influence the macrophage M1-M2 polarization balance. *Front Immunol.* (2014) 5:614. doi: 10.3389/fimmu.2014.00614
149. Kovarik P, Stoiber D, Novy M, Decker T. Stat1 combines signals derived from IFN-gamma and LPS receptors during macrophage activation. *EMBO J.* (1998) 17:3660–8. doi: 10.1038/sj.emboj.7591120
150. Yamaoka K, Otsuka T, Niiro H, Arinobu Y, Niho Y, Hamasaki N, et al. Activation of STAT5 by lipopolysaccharide through granulocyte-macrophage colony-stimulating factor production in human monocytes. *J Immunol.* (1998) 160:838–45.
151. Yin Z, Ma TT, Lin Y, Lu X, Zhang CZ, Chen S, et al. IL-6/STAT3 pathway intermediates M1/M2 macrophage polarization during the development of hepatocellular carcinoma. *J Cell Biochem.* (2018) 119:9419–32. doi: 10.1002/jcb.27259
152. Gong M, Zhuo XZ, Ma AQ. STAT6 upregulation promotes M2 macrophage polarization to suppress atherosclerosis. *Med Sci Monit Basic.* (2017) 23:240–9. doi: 10.12659/MSMBR.904014
153. Coats BR, Schoenfelt KQ, Barbosa-Lorenzi VC, Peris E, Cui C, Hoffman A, et al. Metabolically activated adipose tissue macrophages perform detrimental and beneficial functions during diet-induced obesity. *Cell Rep.* (2017) 20:3149–61. doi: 10.1016/j.celrep.2017.08.096
154. Filgueiras LR, Brandt SL, Ramalho TR, Jancar S, Serezani CH. Imbalance between HDAC and HAT activities drives aberrant STAT1/MyD88 expression in macrophages from type 1 diabetic mice. *J Diabetes Complications.* (2017) 31:334–9. doi: 10.1016/j.jdiacomp.2016.08.001
155. Reardon CA, Lingaraju A, Schoenfelt KQ, Zhou G, Cui C, Jacobs-El H, et al. Obesity and insulin resistance promote atherosclerosis through an IFNgamma-regulated macrophage protein network. *Cell Rep.* (2018) 23:3021–30. doi: 10.1016/j.celrep.2018.05.010
156. Vasamsetti SB, Karnewar S, Kanugula AK, Thatipalli AR, Kumar JM, Kotamraju S. Metformin inhibits monocyte-to-macrophage differentiation via AMPK-mediated inhibition of STAT3 activation: potential role in atherosclerosis. *Diabetes.* (2015) 64:2028–41. doi: 10.2337/db14-1225
157. Tang C, Houston BA, Storey C, LeBoeuf RC. Both STAT3 activation and cholesterol efflux contribute to the anti-inflammatory effect of apoA-I/ABCA1 interaction in macrophages. *J Lipid Res.* (2016) 57:848–57. doi: 10.1194/jlr.M065797
158. Desai HR, Sivasubramaniyam T, Revelo XS, Schroer SA, Luk CT, Rikkala PR, et al. Macrophage JAK2 deficiency protects against high-fat diet-induced inflammation. *Sci Rep.* (2017) 7:7653. doi: 10.1038/s41598-017-07923-0
159. Lee WJ, Tateya S, Cheng AM, Rizzo-DeLeon N, Wang NF, Handa P, et al. M2 macrophage polarization mediates anti-inflammatory effects of endothelial nitric oxide signaling. *Diabetes.* (2015) 64:2836–46. doi: 10.2337/db14-1668
160. Ricardo-Gonzalez RR, Red Eagle A, Odegaard JI, Jouihan H, Morel CR, Heredia JE, et al. IL-4/STAT6 immune axis regulates peripheral nutrient metabolism and insulin sensitivity. *Proc Natl Acad Sci USA*. (2010) 107:22617–22. doi: 10.1073/pnas.1009152108
161. Shu H, Wong B, Zhou G, Li Y, Berger J, Woods JW, et al. Activation of PPARalpha or gamma reduces secretion of matrix metalloproteinase 9 but not interleukin 8 from human monocytic THP-1 cells. *Biochem Biophys Res Commun.* (2000) 267:345–9. doi: 10.1006/bbrc.1999.1968
162. Nakamachi T, Nomiyama T, Gizard F, Heywood EB, Jones KL, Zhao Y, et al. PPARalpha agonists suppress osteopontin expression in macrophages and decrease plasma levels in patients with type 2 diabetes. *Diabetes.* (2007) 56:1662–70. doi: 10.2337/db06-1177
163. Ye G, Gao H, Wang Z, Lin Y, Liao X, Zhang H, et al. PPARalpha and PPARgamma activation attenuates total free fatty acid and triglyceride accumulation in macrophages via the inhibition of Fatp1 expression. *Cell Death Dis.* (2019) 10:39. doi: 10.1038/s41419-018-1135-3
164. Lamichane S, Dahal Lamichane B, Kwon SM. Pivotal roles of peroxisome proliferator-activated receptors (PPARs) and their signal cascade for cellular and whole-body energy homeostasis. *Int J Mol Sci.* (2018) 19:E949. doi: 10.3390/ijms19040949
165. Riserus U, Sprecher D, Johnson T, Olson E, Hirschberg S, Liu A, et al. Activation of peroxisome proliferator-activated receptor (PPAR)delta promotes reversal of multiple metabolic abnormalities, reduces oxidative stress, and increases fatty acid oxidation in moderately obese men. *Diabetes.* (2008) 57:332–9. doi: 10.2337/db07-1318
166. Vosper H, Patel L, Graham TL, Khoudoli GA, Hill A, Macphee CH, et al. The peroxisome proliferator-activated receptor delta promotes lipid accumulation in human macrophages. *J Biol Chem.* (2001) 276:44258–65. doi: 10.1074/jbc.M108482200
167. Kang K, Reilly SM, Karabacak V, Gangl MR, Fitzgerald K, Hatano B, et al. Adipocyte-derived Th2 cytokines and myeloid PPARdelta regulate macrophage polarization and insulin sensitivity. *Cell Metab.* (2008) 7:485–95. doi: 10.1016/j.cmet.2008.04.002
168. Lefterova MI, Steger DJ, Zhuo D, Qatanani M, Mullican SE, Tuteja G, et al. Cell-specific determinants of peroxisome proliferator-activated receptor gamma function in adipocytes and macrophages. *Mol Cell Biol.* (2010) 30:2078–89. doi: 10.1128/MCB.01651-09
169. Jiang C, Ting AT, Seed B. PPAR-gamma agonists inhibit production of monocyte inflammatory cytokines. *Nature.* (1998) 391:82–6. doi: 10.1038/34184
170. Meier CA, Chicheportiche R, Juge-Aubry CE, Dreyer MG, Dayer JM. Regulation of the interleukin-1 receptor antagonist in THP-1 cells by ligands of the peroxisome proliferator-activated receptor gamma. *Cytokine.* (2002) 18:320–8. doi: 10.1006/cyto.2002.1945

171. Ricote M, Li AC, Willson TM, Kelly CJ, Glass CK. The peroxisome proliferator-activated receptor-gamma is a negative regulator of macrophage activation. *Nature.* (1998) 391:79–82. doi: 10.1038/34178
172. Chung SW, Kang BY, Kim SH, Pak YK, Cho D, Trinchieri G, et al. Oxidized low density lipoprotein inhibits interleukin-12 production in lipopolysaccharide-activated mouse macrophages via direct interactions between peroxisome proliferator-activated receptor-gamma and nuclear factor-kappa B. *J Biol Chem.* (2000) 275:32681–7. doi: 10.1074/jbc.M002577200
173. Welch JS, Ricote M, Akiyama TE, Gonzalez FJ, Glass CK. PPARgamma and PPARdelta negatively regulate specific subsets of lipopolysaccharide and IFN-gamma target genes in macrophages. *Proc Natl Acad Sci USA.* (2003) 100:6712–7. doi: 10.1073/pnas.1031789100
174. Odegaard JI, Ricardo-Gonzalez RR, Goforth MH, Morel CR, Subramanian V, Mukundan L, et al. Macrophage-specific PPARgamma controls alternative activation and improves insulin resistance. *Nature.* (2007) 447:1116–20. doi: 10.1038/nature05894
175. Hevener AL, Olefsky JM, Reichart D, Nguyen MT, Bandyopadyhay G, Leung HY, et al. Macrophage PPAR gamma is required for normal skeletal muscle and hepatic insulin sensitivity and full antidiabetic effects of thiazolidinediones. *J Clin Invest.* (2007) 117:1658–69. doi: 10.1172/JCI31561
176. Chinetti G, Fruchart JC, Staels B. Peroxisome proliferator-activated receptors (PPARs): nuclear receptors with functions in the vascular wall. *Z Kardiol.* (2001) 90(Suppl. 3):125–32. doi: 10.1007/s003920170034
177. Sugii S, Olson P, Sears DD, Saberi M, Atkins AR, Barish GD, et al. PPARgamma activation in adipocytes is sufficient for systemic insulin sensitization. *Proc Natl Acad Sci USA.* (2009) 106:22504–9. doi: 10.1073/pnas.0912487106
178. Ricote M, Glass CK. PPARs and molecular mechanisms of transrepression. *Biochim Biophys Acta.* (2007) 1771:926–35. doi: 10.1016/j.bbalip.2007.02.013
179. Kiss M, Czimmerer Z, Nagy L. The role of lipid-activated nuclear receptors in shaping macrophage and dendritic cell function: from physiology to pathology. *J Allergy Clin Immunol.* (2013) 132:264–86. doi: 10.1016/j.jaci.2013.05.044
180. Repa JJ, Berge KE, Pomajzl C, Richardson JA, Hobbs H, Mangelsdorf DJ. Regulation of ATP-binding cassette sterol transporters ABCG5 and ABCG8 by the liver X receptors alpha and beta. *J Biol Chem.* (2002) 277:18793–800. doi: 10.1074/jbc.M109927200
181. Fuentes L, Roszer T, Ricote M. Inflammatory mediators and insulin resistance in obesity: role of nuclear receptor signaling in macrophages. *Mediators Inflamm.* (2010) 2010:219583. doi: 10.1155/2010/219583
182. Ghisletti S, Huang W, Ogawa S, Pascual G, Lin ME, Willson TM, et al. Parallel SUMOylation-dependent pathways mediate gene- and signal-specific transrepression by LXRs and PPARgamma. *Mol Cell.* (2007) 25:57–70. doi: 10.1016/j.molcel.2006.11.022
183. Baranowski M, Zabielski P, Blachnio-Zabielska AU, Harasim E, Chabowski A, Gorski J. Insulin-sensitizing effect of LXR agonist T0901317 in high-fat fed rats is associated with restored muscle GLUT4 expression and insulin-stimulated AS160 phosphorylation. *Cell Physiol Biochem.* (2014) 33:1047–57. doi: 10.1159/000358675
184. Steffensen KR, Gustafsson JA. Putative metabolic effects of the liver X receptor (LXR). *Diabetes.* (2004) 53(Suppl. 1):S36–42. doi: 10.2337/diabetes.53.2007.S36
185. Li P, Spann NJ, Kaikkonen MU, Lu M, Oh DY, Fox JN, et al. NCoR repression of LXRs restricts macrophage biosynthesis of insulin-sensitizing omega 3 fatty acids. *Cell.* (2013) 155:200–14. doi: 10.1016/j.cell.2013.08.054
186. Wang GL, Jiang BH, Rue EA, Semenza GL. Hypoxia-inducible factor 1 is a basic-helix-loop-helix-PAS heterodimer regulated by cellular O2 tension. *Proc Natl Acad Sci USA.* (1995) 92:5510–4. doi: 10.1073/pnas.92.12.5510
187. Lewis JS, Lee JA, Underwood JC, Harris AL, Lewis CE. Macrophage responses to hypoxia: relevance to disease mechanisms. *J Leukoc Biol.* (1999) 66:889–900. doi: 10.1002/jlb.66.6.889
188. O'Neill LA, Pearce EJ. Immunometabolism governs dendritic cell and macrophage function. *J Exp Med.* (2016) 213:15–23. doi: 10.1084/jem.20151570
189. Fujisaka S, Usui I, Ikutani M, Aminuddin A, Takikawa A, Tsuneyama K, et al. Adipose tissue hypoxia induces inflammatory M1 polarity of macrophages in an HIF-1alpha-dependent and HIF-1alpha-independent manner in obese mice. *Diabetologia.* (2013) 56:1403–12. doi: 10.1007/s00125-013-2885-1
190. Takikawa A, Mahmood A, Nawaz A, Kado T, Okabe K, Yamamoto S, et al. HIF-1alpha in myeloid cells promotes adipose tissue remodeling toward insulin resistance. *Diabetes.* (2016) 65:3649–59. doi: 10.2337/db16-0012
191. Treuter E, Fan R, Huang Z, Jakobsson T, Venteclef N. Transcriptional repression in macrophages-basic mechanisms and alterations in metabolic inflammatory diseases. *FEBS Lett.* (2017) 591:2959–77. doi: 10.1002/1873-3468.12850
192. Glass CK, Saijo K. Nuclear receptor transrepression pathways that regulate inflammation in macrophages and T cells. *Nat Rev Immunol.* (2010) 10:365–76. doi: 10.1038/nri2748
193. Huang W, Ghisletti S, Perissi V, Rosenfeld MG, Glass CK. Transcriptional integration of TLR2 and TLR4 signaling at the NCoR derepression checkpoint. *Mol Cell.* (2009) 35:48–57. doi: 10.1016/j.molcel.2009.05.023
194. Treuter E, Venteclef N. Transcriptional control of metabolic and inflammatory pathways by nuclear receptor SUMOylation. *Biochim Biophys Acta.* (2011) 1812:909–18. doi: 10.1016/j.bbadis.2010.12.008
195. Chen X, Barozzi I, Termanini A, Prosperini E, Recchiuti A, Dalli J, et al. Requirement for the histone deacetylase Hdac3 for the inflammatory gene expression program in macrophages. *Proc Natl Acad Sci USA.* (2012) 109:E2865–74. doi: 10.1073/pnas.1121131109
196. Mullican SE, Gaddis CA, Alenghat T, Nair MG, Giacomin PR, Everett LJ, et al. Histone deacetylase 3 is an epigenomic brake in macrophage alternative activation. *Genes Dev.* (2011) 25:2480–8. doi: 10.1101/gad.175950.111
197. Fan R, Toubal A, Goni S, Drareni K, Huang Z, Alzaid F, et al. Loss of the co-repressor GPS2 sensitizes macrophage activation upon metabolic stress induced by obesity and type 2 diabetes. *Nat Med.* (2016) 22:780–91. doi: 10.1038/nm.4114
198. Drareni K, Ballaire R, Barilla S, Mathew MJ, Toubal A, Fan R, et al. GPS2 deficiency triggers maladaptive white adipose tissue expansion in obesity via HIF1A activation. *Cell Rep.* (2018) 24:2957–71 e6. doi: 10.1016/j.celrep.2018.08.032
199. Toubal A, Treuter E, Clement K, Venteclef N. Genomic and epigenomic regulation of adipose tissue inflammation in obesity. *Trends Endocrinol Metab.* (2013) 24:625–34. doi: 10.1016/j.tem.2013.09.006
200. Liang N, Damdimopoulos A, Goni S, Huang Z, Vedin LL, Jakobsson T, et al. Hepatocyte-specific loss of GPS2 in mice reduces non-alcoholic steatohepatitis via activation of PPARalpha. *Nat Commun.* (2019) 10:1684. doi: 10.1038/s41467-019-09524-z
201. Toubal A, Clement K, Fan R, Ancel P, Pelloux V, Rouault C, et al. SMRT-GPS2 corepressor pathway dysregulation coincides with obesity-linked adipocyte inflammation. *J Clin Invest.* (2013) 123:362–79. doi: 10.1172/JCI64052
202. Coppo M, Chinenov Y, Sacta MA, Rogatsky I. The transcriptional coregulator GRIP1 controls macrophage polarization and metabolic homeostasis. *Nat Commun.* (2016) 7:12254. doi: 10.1038/ncomms12254
203. Zhang X, Wang Y, Yuan J, Li N, Pei S, Xu J, et al. Macrophage/microglial Ezh2 facilitates autoimmune inflammation through inhibition of Socs3. *J Exp Med.* (2018) 215:1365–82. doi: 10.1084/jem.20171417
204. De Santa F, Totaro MG, Prosperini E, Notarbartolo S, Testa G, Natoli G. The histone H3 lysine-27 demethylase Jmjd3 links inflammation to inhibition of polycomb-mediated gene silencing. *Cell.* (2007) 130:1083–94. doi: 10.1016/j.cell.2007.08.019
205. Satoh T, Takeuchi O, Vandenbon A, Yasuda K, Tanaka Y, Kumagai Y, et al. The Jmjd3-Irf4 axis regulates M2 macrophage polarization and host responses against helminth infection. *Nat Immunol.* (2010) 11:936–44. doi: 10.1038/ni.1920
206. De Santa F, Narang V, Yap ZH, Tusi BK, Burgold T, Austenaa L, et al. Jmjd3 contributes to the control of gene expression in LPS-activated macrophages. *EMBO J.* (2009) 28:3341–52. doi: 10.1038/emboj.2009.271
207. Kruidenier L, Chung CW, Cheng Z, Liddle J, Che K, Joberty G, et al. A selective jumonji H3K27 demethylase inhibitor modulates the proinflammatory macrophage response. *Nature.* (2012) 488:404–8. doi: 10.1038/nature11262

208. Gallagher KA, Joshi A, Carson WF, Schaller M, Allen R, Mukerjee S, et al. Epigenetic changes in bone marrow progenitor cells influence the inflammatory phenotype and alter wound healing in type 2 diabetes. *Diabetes.* (2015) 64:1420–30. doi: 10.2337/db14-0872
209. Ntziachristos P, Tsirigos A, Welstead GG, Trimarchi T, Bakogianni S, Xu L, et al. Contrasting roles of histone 3 lysine 27 demethylases in acute lymphoblastic leukaemia. *Nature.* (2014) 514:513–7. doi: 10.1038/nature13605
210. Wahl S, Drong A, Lehne B, Loh M, Scott WR, Kunze S, et al. Epigenome-wide association study of body mass index, and the adverse outcomes of adiposity. *Nature.* (2017) 541:81–6. doi: 10.1038/nature20784
211. Pollack RM, Donath MY, LeRoith D, Leibowitz G. Anti-inflammatory agents in the treatment of diabetes and its vascular complications. *Diabetes Care.* (2016) 39(Suppl. 2):S244–52. doi: 10.2337/dcS15-3015
212. Stanley TL, Zanni MV, Johnsen S, Rasheed S, Makimura H, Lee H, et al. TNF-alpha antagonism with etanercept decreases glucose and increases the proportion of high molecular weight adiponectin in obese subjects with features of the metabolic syndrome. *J Clin Endocrinol Metab.* (2011) 96:E146–50. doi: 10.1210/jc.2010-1170
213. Larsen CM, Faulenbach M, Vaag A, Ehses JA, Donath MY, Mandrup-Poulsen T. Sustained effects of interleukin-1 receptor antagonist treatment in type 2 diabetes. *Diabetes Care.* (2009) 32:1663–8. doi: 10.2337/dc09-0533
214. Rekedal LR, Massarotti E, Garg R, Bhatia R, Gleeson T, Lu B, et al. Changes in glycosylated hemoglobin after initiation of hydroxychloroquine or methotrexate treatment in diabetes patients with rheumatic diseases. *Arthritis Rheum.* (2010) 62:3569–73. doi: 10.1002/art.27703

Conflict of Interest: The authors declare that the research was conducted in the absence of any commercial or financial relationships that could be construed as a potential conflict of interest.

The reviewer A-FB declared a shared affiliation, with no collaboration, with all of the authors, to the handling editor at the time of the review.

Appendix 2

Review published in August 2020, in International Journal of Molecular Sciences

International Journal of
Molecular Sciences

MDPI

Review

Metabolic and Molecular Mechanisms of Macrophage Polarisation and Adipose Tissue Insulin Resistance

Lucie Orliaguet, Tina Ejlalmanesh and Fawaz Alzaid *

Cordeliers Research Centre, INSERM, IMMEDIAB Laboratory, Sorbonne Université, Université de Paris, F-75006 Paris, France; lucie.orliaguet@gmail.com (L.O.); tina.ejlalmanesh@crc.jussieu.fr (T.E.)
* Correspondence: fawaz.alzaid@inserm.fr

Received: 13 July 2020; Accepted: 8 August 2020; Published: 10 August 2020

Abstract: Inflammation plays a key role in the development and progression of type-2 diabetes (T2D), a disease characterised by peripheral insulin resistance and systemic glucolipotoxicity. Visceral adipose tissue (AT) is the main source of inflammation early in the disease course. Macrophages are innate immune cells that populate all peripheral tissues, including AT. Dysregulated AT macrophage (ATM) responses to microenvironmental changes are at the root of aberrant inflammation and development of insulin resistance, locally and systemically. The inflammatory activation of macrophages is regulated at multiple levels: cell surface receptor stimulation, intracellular signalling, transcriptional and metabolic levels. This review will cover the main mechanisms involved in AT inflammation and insulin resistance in T2D. First, we will describe the physiological and pathological changes in AT that lead to inflammation and insulin resistance. We will next focus on the transcriptional and metabolic mechanisms described that lead to the activation of ATMs. We will discuss more novel metabolic mechanisms that influence macrophage polarisation in other disease or tissue contexts that may be relevant to future work in insulin resistance and T2D.

Keywords: adipose tissue; inflammation; insulin resistance; immunometabolism; macrophages; type-2 diabetes; T2D

1. Introduction: Physiology and Pathology of Adipose Tissue

The physiological role of adipose tissue (AT) is long-term energy storage in the form of fat, and depending on the AT depot, this fat also provides protection and insulation. AT is also an endocrine organ and responds to endocrine signalling to regulate appetite and to control systemic lipid homeostasis. Persistent overnutrition over time leads to adipose tissue expansion, phenotypic alterations and changes in sensitivity to hormone signalling.

AT is composed of two main fractions: the adipocyte fraction and the stromal vascular fraction (SVF). Adipocytes form the main component regulating energy stores and systemic lipid homeostasis. The SVF fraction is heterogenous in composition and changes over time in response to altered metabolic needs. The SVF is composed of mesenchymal progenitor/stem cells, preadipocytes, fibroblasts, endothelial cells, and immune cells including macrophages [1]. Macrophages represent one of the most dynamic cells in this fraction of adipose tissue and are key actors of inflammation and the development of insulin resistance.

Under physiological conditions, AT macrophages (ATMs) represent approximately 2% of the cells in AT. Throughout the development of obesity, insulin resistance and type-2 diabetes (T2D), ATMs increase in number to represent up to 50% of cells in AT [1]. The increase in ATM numbers is due to proliferation and the recruitment of circulating monocytes that differentiate in situ into macrophages. The increase in ATM number is accompanied by an altered phenotype. Whilst macrophages in the lean and metabolically healthy state are alternatively activated (M2-like or anti-inflammatory

phenotype), macrophages in the insulin resistant state are classically or metabolically activated (M1-like, pro-inflammatory or intermediate phenotypes) [2–4]. The increased number and change in polarisation are accompanied by an increase in pro-inflammatory cytokines, in the microenvironment and systemically.

This review will address the established inflammatory mechanisms implicated in adipose insulin resistance. Particular attention is drawn to the transcriptional-metabolic cross-talk in macrophages that optimises or mitigates AT adaptation to systemic and micro-environmental dysmetabolism. However, within the scope of inflammation and metabolic diseases, several questions remain unanswered. Namely the factors that initiate inflammation and ATM activation, such as hyperlipidaemia, hyperglycaemia, adipocyte death or release of exosomes. Similarly, the tissue specificity of macrophages remains to be studied in detail. Whilst progress has been made in defining cell lineages and differentiation trajectories, single-cell analyses and high density in situ analytical methods have only started to unravel the metabolic and transcriptional specificities of ATM subsets relative to other macrophages (monocyte-derived, peritoneal, Kupffer or red pulp). In this light, the current review brings together the established transcriptional and metabolic mechanisms that dictate macrophage effector functions and inflammatory polarisation in contexts relevant to insulin resistance and T2D.

2. Pathways Involved in Adipose Tissue Inflammation and Insulin Resistance

Studies in the 1990s drew the earliest links between inflammation and adipose tissue insulin resistance. Hotamisligil et al. and Uysal et al. demonstrated that the pro-inflammatory cytokine tumour necrosis factor (TNF) was highly expressed in AT of obese rodents and that this cytokine was causally linked to insulin resistance by direct interference with insulin receptor signalling [5–7].

Finding the precise triggers of this inflammatory response is an area of active research. However, expanding AT provides a number of potential cues that can influence macrophage polarisation, for example, adipocyte death or senescence, hypoxia, increased lipolysis or mechanical stress. Recent research has even implicated insulin resistance itself in the initiation of inflammation [8]. Indeed, it is important to note that in long-term diet-induced obesity, two phases of insulin resistance exist; an early phase that is independent of inflammation and an inflammation-dependent late phase [9].

More and more studies have implicated extracellular vesicles as important communication molecules between adipocytes and macrophages in the initiation or control of inflammation. These vesicles are exosomes released from adipocytes and from adipose tissue-derived mesenchymal stem cells and can influence insulin signalling, inflammation, and angiogenesis. Indeed, adipose exosomes carry hormones such as adiponectin, inflammatory adipokines (tumour necrosis factor, TNF; macrophage colony-stimulating factor, MCSF), fatty acid transporters (AFBP4) and miRNAs. Exosome composition varies between metabolic states and the different components have been predicted to regulate transforming growth factor (TGF)-beta and wnt/beta-catenin pathways [10].

3. Overview of Insulin Signalling, Resistance and the Onset of Type-2 Diabetes

Insulin exerts its effects through binding to its cell surface receptor, which undergoes autophosphorylation. Phosphorylation of three tyrosine residues is necessary for amplification of kinase activity that recruits insulin receptor substrate (IRS) proteins important for the signalling pathway. Downstream of these events, phosphatidylinositol-3-kinase (PI3K) and mitogen-activated protein kinase (MAP-kinase) mediate the metabolic and mitogenic actions of insulin in the cell [11].

Insulin resistance is a result of failure of one or more of these mechanisms, resulting in decreased glucose uptake, glycogen synthesis (mainly by the liver) and increased lipolysis in AT. Resulting hyperglycaemia and dyslipidaemia potentiate insulin secretion from the pancreas. If sustained, this vicious cycle results in beta cell failure, frank T2D and increased risk of complications and comorbidities. Chronic inflammation has been consistently implicated at every step of these changes [12–14]. Moreover, numerous studies have demonstrated that blunting the inflammatory response, mitigates metabolic decline, preserves glycaemic homeostasis or even reverses insulin resistance [14–16].

4. Molecular Mechanisms of Inflammation and Adipose Insulin Resistance

With ATMs being the central mediators of inflammation, much research has worked to decipher the mechanisms that control inflammatory polarisation and insulin resistance in the microenvironment. Multiple layers of regulation exist, from cell surface receptors to nuclear receptors, transcription factors and their co-regulators [17]. The multiple levels of complexity converge on the activation of two main inflammatory pathways: JNKs (c-Jun N-terminal kinases) and NFκB (nuclear factor kappa-light-chain-enhancer of activated B cells) [18–20]. These two pathways are active and exert their effects in both adipocytes and macrophages (Figure 1A).

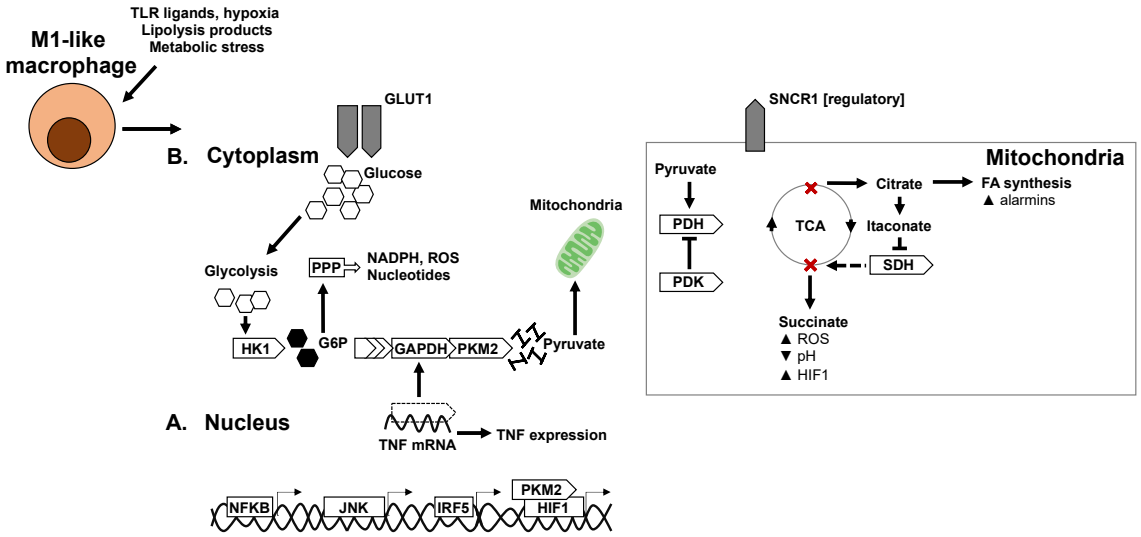

Figure 1. Transcriptional and metabolic adaptation of M1-like pro-inflammatory macrophages. Key transcription factors and enzymes that mediate pro-glycolytic and pro-inflammatory mechanisms in M1-like macrophages. (**A**) Transcriptional regulators of inflammation and macrophage metabolic adaptation. (**B**) Adaptation of metabolic pathways and enzymes in M1-like macrophages.

Activation of these pathways leads to the production of pro-inflammatory cytokines, chemokines and chemoattractants that promote the recruitment of monocytes. Once recruited to AT, monocytes are exposed to the inflammatory milieu and differentiate in situ. These monocyte-macrophages may be phenotypically and functionally distinct from resident macrophages and are termed infiltrating macrophages [21]. Infiltrating macrophages amplify the local and systemic inflammatory responses that contribute to impaired insulin signalling [22].

4.1. JNK Signalling in Adipocyte Insulin Resistance

JNK is expressed in myeloid cells and in insulin target cells. JNK activation in myeloid cells results in the transcription of pro-inflammatory mediators. JNK responds to a number of stimuli, including inflammatory cytokines, free fatty acids, or intracellular signalling, such as the unfolded protein response [23,24]. Importantly, in insulin-target cells, JNK activation can inhibit the insulin signalling pathway through serine-threonine phosphorylation and inhibition of IRS-1. This results in inhibiting PI3K/protein kinase B (PKB) signalling downstream of IRS1. This role was deciphered with the use of JNK1-deficient mice, specific to adipose tissue [25–27].

4.2. NFκB Signalling in Adipocyte Insulin Resistance

With regards to NFκB, under physiological conditions, NFκB proteins are retained in the cytoplasm by inhibitors of κB (IκBs). Regulated proteasomal degradation of IκBs allows the nuclear translocation of NFκB; this leads to the transcription of canonical inflammatory mediators, such as interleukin (IL)-6, TNF, interferons and importantly the monocyte chemoattractant protein-1 (CCL2/MCP1), which is

central to monocyte recruitment [28,29]. Adipocyte-specific IKKβ deletion and the proteins that mediate IκB degradation, results in a lack of responsiveness to fatty acids and a blunted inflammatory signature. Similarly, IKKβ overexpression in adipocytes decreases expression of anti-inflammatory molecules (leptin and adiponectin) [30].

4.3. Macrophage-Derived Cytokine Signalling and Adipose Tissue Inflammation

Innate immune cells, such as macrophages, mount their inflammatory responses following stimulation of pattern recognition receptors (PRRs). PRRs are composed of two main families: Toll-like and NOD-like receptors (TLRs and NLRs). These receptors span cell surface and intracellular membranes and are ligated by damage- or pathogen-associated molecular patterns (DAMPs or PAMPs). In the case of metabolic diseases, stimulation is by DAMPs generated by dysmetabolism, such as fatty acids, hyperglycaemia, cellular senescence or other stress signals [31].

Macrophages play a key role in amplifying inflammation in the adipose microenvironment. Once activated, secreted cytokines act both locally and peripherally to increase inflammation and insulin resistance [31]. Two main pathways are important actors of inflammation: the NLRP3 inflammasome and interferon signalling.

4.4. The NLRP3 Inflammasome: IL1B and IL18 Signalling

NLRP3 (gene encoding NALP3: NACHT, LRR and PYD domain-containing protein 3) is a NLR highly expressed in ATMs that forms a crown-like structure around senescent adipocytes upon diet-induced obesity [32]. NLRP3 and the adaptor protein ASC form a caspase-1 activating complex known as the NLRP3 inflammasome; the inflammasome complex is a sensor for metabolic homeostasis [33]. Activation of caspase-1 by this complex results in the maturation and release of IL1B and IL18; two potent inflammatory cytokines of the IL1 family. Mice deficient for NLRP3 are protected from diet-induced insulin resistance due to failure to form the inflammasome complex; similarly, therapeutic intervention for weight loss in obesity and T2D reduces expression of NLRP3 and its target cytokines [32].

IL1B is a key inflammasome product, a cytokine heavily involved in the development of T2D at multiple levels. Increased expression of IL1B is associated with insulin resistance as well as in the destruction of pancreatic beta cells in more advanced disease [34]. In AT, IL1B suppresses insulin signalling in adipocytes, exposure to IL1B results in decreased insulin stimulated glucose uptake and lipogenesis [35]. Glucose transporter (GLUT)-4 expression and translocation in adipocytes are also repressed [36,37].

IL1B exerts its effects by binding to its receptor and recruiting a coreceptor to form a heterodimer-receptor transmembrane complex. The cytoplasmic IL1R domain initiates intracellular signalling by recruiting the adaptor proteins MyD88 (myeloid primary response differentiation-88 protein) and IRAK (interleukin 1 associated kinase). Downstream of these adaptor proteins are the MAPK and NFκB signalling pathways, which are effectors of inflammation and insulin desensitisation.

IL18, another cytokine released by the inflammasome and member of the IL1 superfamily, is expressed in both immune and non-immune cells and is known to potentiate interferon signalling. Similar to IL1B, IL18 recruits the MyD88 adaptor protein and the inflammatory NFκB pathway. IL18 is released by AT and its circulating levels increase in obesity and T2D [38,39]. IL18 accelerates maturation of other immune cells, including T- and NK-cells, and enhances the production of other pro-inflammatory cytokines that exacerbate systemic inflammation in obesity and insulin resistance [40].

4.5. Macrophage-Derived IL6 and TNF Signalling

IL6 is an inflammatory cytokine involved in the development of insulin resistance [41]. IL6 expression characterises sepsis, mediating fever and the acute phase response. Mostly produced from macrophages, IL6 can also be released in small amounts by adipocytes; in AT, IL6 stimulates energy mobilisation and increases temperature. Upon interaction with its receptor, IL6 activates

the JAK1-STAT3 (Janus kinase-signal transducer and activator of transcription) pathway [42]. In AT during obesity and insulin resistance, IL6 exposure impairs insulin signalling by interfering with IRS phosphorylation, thus increasing adipocyte lipolysis, which promotes hepatic gluconeogenesis and insulin resistance [43–46]. Although physiological and positive effects of IL6 action have also been reported (increased satiety, leptin release, IL4R expression in macrophages), the aberrant IL6 expression in diet-induced obesity results in chronic activation of its inflammatory axis.

Tumour necrosis factor (TNF) is an inflammatory cytokine expressed in two forms: a transmembrane form that mediates autocrine and paracrine signalling; and a soluble form that mediates endocrine signalling. The levels of both forms are increased in AT in obesity and insulin resistance with the main source being ATMs [47,48]. TNF interacts with the receptors TNFR1 and TNFR2; both receptors can also be cleaved creating soluble forms thought to neutralise and clear soluble TNF from circulation [49]. Ligation of TNFR1 mediates the majority of effects on adipocytes [50]. TNFR2 has been shown to contribute in a limited manner to altering adipocyte function, notably reducing GLUT4, and IRS-1 and -2 expression, inducing apoptosis or contributing to JNK activation [51–53]. Both TNFRs exert their effects through signal transduction and adaptor protein recruitment. The effects of TNF include inducing adipocyte and pre-adipocyte apoptosis, with pre-adipocytes being more sensitive [54]. Signalling downstream of TNFR also includes activation of NFκB and MAPK cascades and are leading candidates for mediating TNF-related metabolic dysregulation [55,56]. TNF action is associated with suppression of the insulin receptors IRS-1, -2 and GLUT4, through multiple mechanisms, including proteasomal degradation, impaired translocation and direct transcriptional repression [57–59].

5. Transcriptional Control of ATM Polarisation

5.1. Signal Transducers and Activators of Transcription: JAK-STAT Signalling

The JAK family of proteins interact with cytokine and growth factor receptors and mediates signalling to STAT proteins. STATs are a family of seven proteins that form part of the interferon signalling system, and have a cell- and tissue-specific distribution [60–62]. The JAK-STAT axis controls a large number of metabolic pathways in AT and is dysregulated in diet-induced obesity and insulin resistance [42,63]. STATs expressed in M2-like macrophages have been implicated in buffering pro-inflammatory polarisation in T2D (Figure 2A), whereas STATs in M1-like macrophages have not been directly linked to T2D.

STAT activity is regulated by cytokines and growth factors, which once signalled to membranes initiate JAK-mediated phosphorylation of STATs allowing their dimerization and nuclear translocation. STAT1 and STAT5 induce M1-like polarisation of macrophages, whereas STAT3 and STAT6 induce M2 macrophage polarisation. Whilst macrophage STAT1 has not been reported to play a role in obesity or insulin resistance; in vitro and ex vivo studies demonstrated that STAT1 is activated in response to high glucose where a large epigenetic component is attributed to its function [64]. Similarly, no conclusive studies have linked STAT5 to T2D pathogenesis to our knowledge.

M2 polarising STATs are more closely associated to T2D. STAT3 is a downstream target of metformin. Metformin inhibits differentiation of monocytes to macrophages through AMPK-mediated inhibition of STAT3, which also resulted in decreased monocyte infiltration into atherosclerotic plaques and an ameliorated outcome in mice [65]. In other studies, a model of myeloid-specific deficiency of JAK2, reduced phosphorylation of STAT3 and led to a less inflammatory and healthier visceral AT phenotype upon diet-induced obesity and insulin resistance [66]. Mice deficient for STAT6 are more prone to diet-induced obesity and increase in oxidative stress and inflammation in AT, increasing susceptibility to insulin resistance and T2D [67].

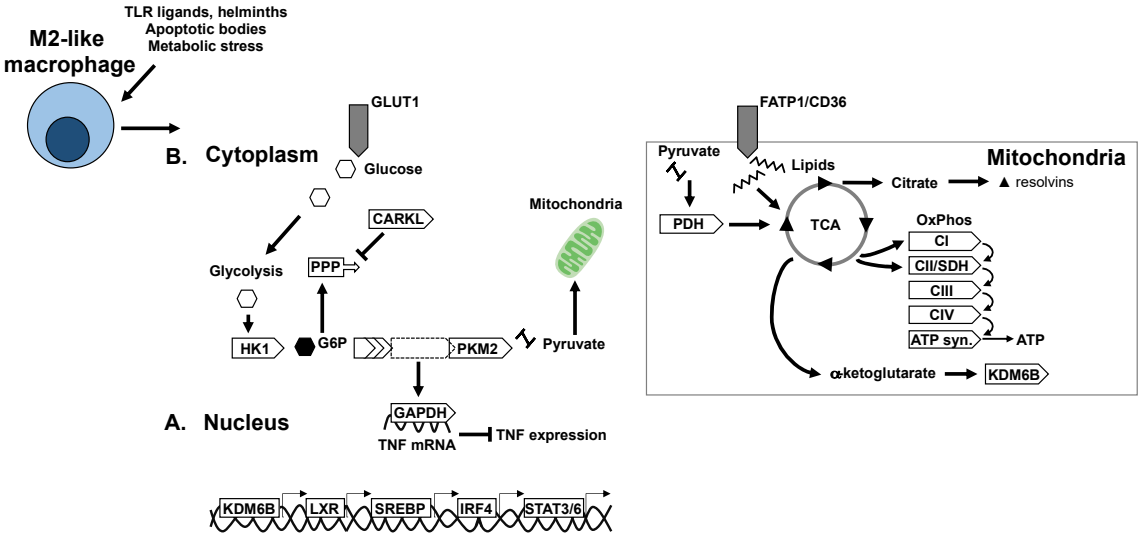

Figure 2. Transcriptional and metabolic adaptation of M2-like anti-inflammatory/pro-resolving macrophages. Key transcription factors and enzymes that mediate oxidative metabolism and immune-regulatory mechanisms in M2-like macrophages. (**A**) Transcriptional regulators of anti-inflammatory polarisation and macrophage metabolic adaptation. (**B**) Adaptation of metabolic pathways and enzymes in M2-like macrophages.

5.2. Type-1 Interferon Signalling and Transcription Control

The type-1 interferons (IFN) are a large family of proteins that regulate the multiple components of the immune system and were initially characterised as the host response to viral infection. IFNs signal danger to cells in proximity causing them to heighten their anti-viral defences [68]. However, over the years, several other roles have been attributed to IFNs, mainly in autoimmune and metabolic diseases. In macrophages, and other cells of the myeloid system, type-1 IFNs (IFNα, β, κ and ω) are expressed [69]. They are stimulated downstream of TLR-ligation, canonically by bacterial or viral stimuli, whereas the stimuli in metabolic diseases remain to be elucidated. Macrophage type-1 IFN expression is tightly regulated by two transcription factors, the IFN regulatory factors (IRF)-4 and -5.

Many studies have solidified the roles of these two transcription factors in the pathogenesis of T2D [70]. M1-like polarisation of macrophages is promoted by IRF5, whereas pro-resolution, M2-like polarisation is driven by IRF4 [71]. In ATMs, IRF5 is instrumental in mediating metabolic inflammation, leading to maladaptive AT expansion and the development of insulin resistance [14]. Mice with a myeloid-deficiency of IRF5 have improved metabolic homeostasis upon high-fat feeding, lower AT inflammation and redistribution of AT from the visceral depot towards the subcutaneous depot. This phenomenon is mediated by alternatively activated macrophages that restrict adipocyte growth and promote a hyperplasic and metabolically protective response upon diet-induced obesity. Interestingly this phenotype is comparable to that of TLR4-deficient mice, indicating that the TLR4–IRF5 axis of macrophage polarisation may be conserved in metabolic inflammation [72]. With regards to IRF4, deficiency in myeloid cells results in mice with exuberant AT inflammation and decreased insulin sensitivity when compared to IRF4-competent mice upon diet-induced obesity, despite no differences in weight gain [73]. Interestingly, IRF4 is also expressed in adipocytes, where it is required for lipolytic programming; mice lacking IRF4 in adipocytes are predisposed to increased weight gain and adiposity and deficient lipolysis [74].

6. Metabolic Mechanisms of Macrophage Polarisation

Macrophage cellular metabolism, or bioenergetic adaptation, also strongly influences effector functions. Canonically, pro-inflammatory polarisation is associated with glycolytic metabolism whereas anti-inflammatory or pro-resolution polarisation is associated with oxidative or mitochondrial

metabolism (Figures 1B and 2B). These metabolic pathways and the associated functions have been established in recent years with the application of model systems (such as bone marrow derived macrophages) treated with model immunogens or cytokines. The exact stressors in a diabetogenic context and the specific metabolic adaptations of tissue macrophages in situ remains to be fully deciphered. The particularity of diabetogenic conditions is the systemic abundance of metabolic substrates in hyperglycaemia and dyslipidaemia. Moreover, AT is particularly rich in lipids and lipolysis products at the onset of insulin resistance and thus ATMs are expected to have particular adaptations to this microenvironment and metabolic milieu (Table 1).

Table 1. Major adaptations in ATM polarisation states. When exposed to specific stimuli, macrophages undergo terminal differentiation into M1-like, M2-like or intermediate polarisation states. These states imply the activation of several transcriptional and metabolic pathways.

	Insulin Resistant State	**Insulin Sensitive State**
ATM polarisation	M1-like	M2-Like
Canonnical stimuli	Bacterial/viral stimuli (TLR/NLR ligands)	Helminths (TLR, lectin receptors)
Stimuli in T2D	Inflammatory cytokines/chemokines Free fatty acids, Hypoxia TLR/NLR ligands	Regulatory/Anti-inflammatory cytokines/chemokines Fatty acids, apoptotic bodies, CD36/FATP1 ligation Metformin, hormone signalling (leptin, adiponectin)
Pathway/TFs	JNK, NFKB, NLRP3, IRF5, HIF1	STAT3/6, IRF4, KDM6B, LXR, SREBPs
Cytokines/Chemokines	IL1B, IL18, IL6, TNF, IFNα, β, κ and ω	IL10, TGF, CCL1, IL1Ra *succinate
Glycolysis and PPP adaptation	• GAPDH releases nuclear break on TNF mRNA • ↘ CARKL, ↗ PPP • ↗ PPP provides substrates for protein and nucleotide synthesis • ↗ GLUT1 ↗ glucose uptake • ↗ HK1 supports NLRP3 inflammasome • ↗ Succinate stabilises HIF1 • PKM2 is coregulator for HIF1 • ↗ IRF5 ↗ AKT2 glycolysis	• GAPDH reatined in nucleas to bind TNF • ↗ CARKL ↘ PPP • ↗ Pyruvate towards mitochondria • mTORC sustains glycolysis
Mitochondria and oxidative metabolism	• ↘ Oxidative capacity • ↗ Citrate conversion to itaconate by ↗ IRG1 • ↗ Itaconate inhibits SDH • ↘ SDH ↗ succinate • ↗ Succinate ↘ pH ↗HIF1 • PDK inhibition of PDH • ↘ Pyruvate flux to mitochondria • Citrate subtrate for alarmin lipids • Succinate oxidation ↗ bactericidal ROS	• ↘ IRF5 ↗ efferocytosis • ↗ CD36/FATP1 ↗ Lipid uptake • ↗ PPARs/STAT6 ↗ Lipogenesis • ↗ lipid substrates for mitochondrial respiration and FAO • ↗ CPT1 ↗ substrates to mitochondria • TCA cycle is intact • OxPhos maintains redox balance • Secreted succinate has a regulatory effect in microenvironment • ↗ αKG cofactor for KDM6b • ↗ KDM6b ↗ anti-inflammatory programming

* succinate is a metabokine, metabolite signaling molecule.

6.1. Glycolysis in Macrophage Polarisation

Typically, in predominantly glycolytic macrophages, that are pro-inflammatory, the rapid influx of glucose is supported by upregulation and plasma membrane localisation of GLUT1 [75]. However, in some primary macrophage subsets, the increased uptake and metabolism of glucose has been shown to be dissociable from inflammation, notably in lipid-rich microenvironments such as in atherosclerotic plaques [76]. GLUT1 is indeed expressed in AT, and specifically in ATM, that forms crown-like structures over the course of diet-induced obesity, however a specific role for GLUT1 in ATM function or the development of insulin resistance remains to be validated (Figure 1).

Components of the glycolytic pathway have adjunct functions in macrophages, some components interact with transcriptional and inflammatory machinery to influence polarisation. Hexokinase (HK)-1 is a key enzyme that phosphorylates glucose to produce glucose-6-phosphate as the first step of glycolysis. In macrophages, HK1 promotes NLRP3 inflammasome formation and supports IL1B secretion, in collaboration with the mammalian target of rapamycin complex (mTORC)-1 [77].

The hypoxia sensor hypoxia-inducible factor (HIF)-1-α is an important link between glycolytic programming and inflammation. HIF1α is stabilised in macrophages by succinate, a metabolite of the

tricarboxylic acid (TCA) cycle that accumulates with increasing glycolytic flux [78]. The stabilisation of HIF1α allows its transcriptional activity to take place, inducing expression of GLUT1 as well as the expression of inflammatory mediators such as IL1B, with the pyruvate kinase isoenzyme (PKM)-2 as a coregulator. PKM2 canonically catalyses the last step of glycolysis, being responsible for net ATP and pyruvate production. In M1 macrophages, it also acts as a transcriptional coregulator [79,80]. The HIF1α pathway has itself been validated to play a role in metabolic diseases, where HIF1α deficient mice are protected against diet-induced obesity and insulin resistance.

Another glycolytic enzyme that influences inflammation is glyceraldehyde 3-phosphate dehydrogenase (GAPDH). GAPDH binds TNF at the mRNA level and post-transcriptionally represses its expression in monocytes [81]. When glycolysis is up-regulated, GAPDH is recruited to carry out its metabolic function, and this releases its break on TNF mRNA, allowing maturation and release of the cytokine in its active form.

The carbohydrate kinase-like (CARKL) protein is downregulated in classical macrophages. Downregulation channels the flux of glycolytic intermediates through the pentose phosphate pathway (PPP). Increased PPP activity generates substrates for protein and nucleotide synthesis, as well as the production of NADPH and NADPH oxidase-mediated ROS [82]. These activities support cytokine synthesis and generation of products necessary for bacterial killing.

As well as metabolic enzymes and metabolites that interact with inflammatory machinery, inflammatory transcription factors, namely IRF5, have been implicated in the control of cellular metabolism. Two separate mechanisms have been demonstrated for the role of IRF5 in cellular metabolism, the impairment of efferocytosis and the promotion of glycolysis. Seneviratne et al. demonstrated that IRF5 supports foam cell formation in atherosclerosis by inhibiting necrotic core formation, this would lead to an increase and possible overload of substrates in lipid-laden macrophages [83]. Conversely, genetic risk-variants that increase IRF5 expression are associated with increased glycolysis in bone-marrow derived macrophages [84]. Such mechanisms clearly work in parallel to IRF5's main function as a transcription factor promoting M1 polarisation.

Much less frequently, glycolysis has also been reported in alternatively activated macrophages. Precisely, macrophage stimulation with IL4 and MCSF leads to activation of mTORC2 and the upregulation of glycolysis through IRF4 [85]. However, a subtle difference in the glycolytic programming of alternatively activated macrophages is that glycolysis products are directed towards mitochondria rather than towards the PPP. This supports the TCA cycle and mitochondrial oxidative phosphorylation (OXPHOS); accordingly, other studies have shown that 2-deoxyglucose mediated inhibition of glycolysis also attenuates mitochondrial metabolism and M2 marker expression in response to IL4 [86].

6.2. Mitochondria and Mitochondrial Respiration in Macrophage Polarisation

Mitochondria have numerous functions beyond their roles in oxidative metabolism, such as dictating levels of oxidative stress, calcium signalling, apoptosis, and inflammation, as well as cellular and systemic metabolism. Altered mitochondrial function and reduced mitochondrial DNA have been reported in murine models of genetic obesity [87]; with decreases in mitochondrial activity also reported in human AT from obese individuals [88]. A general mechanism by which mitochondria contribute to inflammation is interaction with redox sensitive pathways in the cell. Mitochondrial dysfunction leads to aggravated inflammation through activation of redox-sensitive inflammatory mechanisms, such as NFκB or the NLRP3 inflammasome [89,90]. Mitochondrial dysfunction is also associated with accumulation of ectopic or excess lipids, interfering with insulin signalling and leading to adipocyte hypertrophy and hypoxia, respectively [91].

In terms of metabolism, mitochondria metabolise lipids as well as glycolysis end-products. Increased lipid uptake and oxidation characterise alternatively activated macrophages following IL4 stimulation [92]. Indeed, inhibition of fatty acid oxidation (FAO) or OXPHOS attenuates expression of M2 markers [93,94]. In the case of IL4 stimulation, metabolic reprogramming of M2 polarisation is

mediated by STAT6 and the peroxisome proliferator-activated receptor gamma (PPARγ), coactivator 1 beta (PGC1B) [95]. The substrates for FAO are exogenous lipids taken up by CD36 or are synthesised by lipogenic machinery of the cell. An additional important step for metabolising lipid imported into the cell by CD36 is their lipolysis by the lysosomal acid lipase (LAL). LAL deficiency or treatment by orlistat, a lipolysis inhibitor, decreases macrophage oxidative respiration and impairs alternative polarisation [96].

Fatty acid transporters (FATP1) and fatty acid binding proteins (FABP4/5) also influence macrophage polarisation [96,97]. Macrophage-deficiency of FATP1 biases cellular respiration towards glycolysis and primes polarisation towards a pro-inflammatory phenotype, which is reflected in vivo by an aggravated metabolic phenotype in diet-induced obesity. Interestingly, the deletion of FABP4/5 in macrophages results in a metabolically protective phenotype. This indicates that FABPs may contribute more to signal transduction from a dysmetabolic environment than to substrate provision for oxidative cellular respiration.

Mitochondrial enzymes themselves contribute to regulation of cellular metabolism and macrophage fate (Figure 2). Carnitine palmitoyl transferase (CPT)-1 is an enzyme essential for movement of substrates from the cytoplasm to the mitochondria for their metabolism. Overexpression of CPT1 increases FAO while decreasing triglyceride content and production of pro-inflammatory cytokines [98]. Alternatively, the loss of CPT2 in macrophages results in decreased FAO with no functional consequence on the IL4-stimulated alternative activation phenotype [94,99]. Similarly, etomoxir inhibition of FAO does not affect alternative activation of macrophages. Taken together these data indicate that CPT1 has specific properties that mediate anti-inflammatory/alternative polarisation, which may only be fuelled or potentiated by the other components of the CPT-FAO axis. Alternatively, FAO and CPT2 may play more significant roles in regulating redox status, or in tempering and resolving pro-inflammatory polarisation.

6.3. TCA Cycle and Intermediates in Macrophage Polarisation

The TCA cycle plays a central role in both pro- and anti-inflammatory polarization. Under classical activation, the TCA cycle is interrupted at two steps that result in decreased alpha-ketoglutarate (αKG) production and accumulation of succinate and citrate. Citrate is exported to the cytoplasm as a substrate for lipogenesis, where products are alarmins and pro-inflammatory mediators such as prostaglandin E2 and nitrous oxide [100]. Citrate can also be converted to itaconate through the enzyme immune responsive gene (IRG)-1. Itaconate is a metabolite that inhibits SDH and allows the accumulation of succinate [101]. The accumulation of succinate stabilizes HIF1α, which is an integral part of glycolytic and inflammatory programming. Moreover, in the presence of oxygen, succinate oxidation also provides a source of mitochondrial ROS necessary for anti-bacterial activity [102]. More recently another mechanism described autocrine as well as paracrine roles of succinate signalling, where succinate can be secreted by the succinate receptor (SUCNR)-1. In this context, a polarized macrophage can act on macrophages in the vicinity through succinate as a metabokine [103,104]. Interestingly, extracellular succinate plays a different role to intracellular succinate, as mice with SCNR1 deficiency in macrophages, develop a more aggravated metabolic response to high-fat feeding with a hyperinflammatory profile in AT [104].

αKG is a ketone derivative and intermediate of the TCA cycle, produced by oxidative decarboxylation of isocitrate or by oxidative deamination of glutamate. Several recent studies have revealed important roles of αKG in controlling macrophage polarization through metabolic and epigenetic mechanisms. A high αKG to succinate ratio promotes alternative (M2) activation of macrophages by engaging FAO and acting as a co-factor for the lysine demethylase (KDM)-6B [105]. High levels of αKG promote tolerance and resolution of inflammation after M1 polarisation.

Just upstream of the TCA cycle, pyruvate dehydrogenase kinase (PDK) hinders the transport of carbon substrates to the TCA cycle by repressing pyruvate dehydrogenase (PDH). This biases towards glycolysis and thus inflammation. Indeed, pharmacologic inhibitors of PDK mitigate inflammatory

polarization. In vivo myeloid-deficiency of PDK improves the metabolic phenotype of mice upon a high-fat diet with a decrease in AT inflammation and decreased ATM accumulation [106,107].

7. Nuclear Receptors and Transcriptional Control of Macrophage Metabolism

The main cellular pathways in lipogenesis and lipid metabolism are put in motion by the nuclear receptors PPARγ and PPARβ/δ. Deletion of either protein in macrophages inhibits alternative polarisation in response to IL4 [108]. In vivo and upon high fat feeding, the deletion of PPARγ or PPARβ/δ similarly results in mice with an exacerbated metabolic phenotype and increased adipose tissue inflammation [109].

Liver X receptors (LXRs) are also expressed in macrophages; they act as liposensors, regulating intracellular cholesterol content and controlling the expression of efflux transporters ABCA1 and ABCG1, and apolipoproteins APOE and APOC [110,111]. In vitro, LXR ligands inhibit the expression of inflammatory cytokines and promote the expression of arginase (ARG)-2, an enzyme characteristic of alternative polarisation that potentiates the anti-inflammatory response [112].

Sterol regulatory element binding proteins (SREBPs) are the master regulators of lipogenesis, especially de novo lipogenesis, promoting transcription of key enzymes for fatty acid synthesis (e.g., FASN, ACC, SCD1) [113]. However, their roles in immune cells are emerging, and have so far proven to be diverse. SREBP1 enhances expression of NLRP1A, a component of the NLRP3 inflammasome that culminates in the release of IL1B, as well as being necessary for signalling downstream of TLR4 [114,115]. SREBP1a does however have a dual role where it synthesises unsaturated anti-inflammatory fatty acids, or resolvin lipids. Despite its role in the expression of genes that lead to completion of inflammasome assembly, the loss of resolvins has a more important functional effect, where the response to TLR stimulation in vitro is of exaggerated inflammation [116]. In the context of insulin resistance and T2D, deficiency of the SREBP target gene fatty acid synthase (FASN) in macrophages leads to a hyperinflammatory and metabolically perturbed phenotype upon diet-induced obesity. This occurs as FASN plays such a crucial role in producing cellular lipids, including lipids that form the basis of membranes and their downstream signalling. Thus, the lack of FASN resulted in the production of disordered and functionally compromised membranes that aggravated macrophage responses [117]. Taken together, these data indicate that lipid metabolism in macrophages is complex and is of considerable functional importance. This field of work is still in its infancy in the domain of T2D and obesity, and could benefit from research into foam cell biology from the fields of atherosclerosis and cardiovascular disease.

8. Perspectives and Concluding Remarks

Here we have reviewed the roles and regulation of inflammation in the development of insulin resistance and in maladaptive AT function in obesity and T2D. Whilst transcriptional and molecular mechanisms linking inflammation to insulin resistance in AT have been extensively studied, several questions remain unanswered.

The factors that initiate ATM activation remain largely unknown in diabetogenesis. Several cues have been implicated, and are attractive candidates, such as fatty acids, hyperglycaemia or adipocyte death. However, these factors have all also been reported to be aggravated by, or to be downstream of inflammatory polarisation. Thus, defining the metabolic immunogens, or danger signals, that induce sterile inflammation in insulin resistance and T2D is an active area of research.

As we have largely focused on in this review, macrophages undergo extensive bioenergetic and metabolic adaptation to carry out their effector functions. Much progress has been made to determine the fundamental metabolic mechanisms that fuel macrophage polarisation; these early studies have largely been carried out in model systems with canonical PRR ligands. Future work could characterise the metabolic requirements of macrophages that populate specific tissue niches as well as macrophage activation in specific disease contexts.

Lastly, the translation aspects of fundamental research must be addressed. To date, a major challenge has been in the specific targeting of macrophages or other innate immune cells without affecting other cell types. Advances have been made in these domains, such as conjugation of bioactive molecules to antibodies targeting phenotypic cell surface receptors [118].

Author Contributions: F.A., L.O. and T.E. wrote the manuscript and drew the figures. All authors have read and agreed to the published version of the manuscript.

Funding: F.A.: L.O. and T.E. were supported by grants from the French National Agency of Research (ANR) for ANR MitoFLAME (ANR-19-CE14-0005) and the European foundation for the study of diabetes (EFSD)/Lilly grant (Characterisation of monocyte metabolism and bioenergetic responses in type-2 diabetes and risk of cardiovascular disease).

Conflicts of Interest: The authors declare no conflict of interest.

Abbreviations

T2D	Type-2 diabetes
AT	Adipose tissue
ATM	Adipose tissue macrophages
SVF	Stromal vascular fraction
TNF	Tumour necrosis factor
IRS	Insulin receptor substrate
PI3K	Phosphatidylinositol 3-kinase
MAPK	Mitogen-activated protein kinase
JNK	c-Jun N-terminal kinase
NFκB	Nuclear factor kappa-light-chain-enhancer of activated B cells
PKB	Protein kinase B
IκB	Inhibitors of κB
IL6	Interleukin 6
CCL2/MCP1	Chemokine (C-C motif) ligang 2/Monocyte chemoattractant protein 1
IKKβ	Inhibitor of nuclear factor kappa-B kinase subunit beta
PPR	Pattern recognition receptors
TLR	Toll-like receptors
NLR	NOD-like receptors
DAMP	Damage-associated molecular pattern
PAMP	Pathogen-associated molecular pattern
NLRP3	Gene encoding NACHT, LRR and PYD domains-containing protein 3
ASC	Apoptosis-associated speck-like protein containing a CARD
IL1B	Interleukin 1 beta
IL18	Interleukin 18
IL1R	Interleukin 1 receptor
MyD88	Myeloid primary response differentiation-88 protein
IRAK	Interleukin 1 associated kinase
JAK	Janus kinase
STAT	Signal transducer and activator of transcription
IL4R	Interleukin 4 receptor
TNFR	TNF receptor
AMPK	AMP-activated protein kinase
IFN	Interferon
IRF	Interferon regulatory factor
GLUT	Glucose transporter
HK	Hexokinase
mTORC1	Mammalian target of rapamycin complex
HIF1	Hypoxia inducible factor-1
TCA	tricarboxylic acid cycle
GAPDH	Glyceraldehyde 3-phosphate dehydrogenase

CARKL	Carbohydrate kinase-like
PPP	Pentose phosphate pathway
NADPH	Nicotinamide adenine dinucleotide phosphate
ROS	Reactive oxygen species
MCSF	Macrophage colony-stimulating factor
OXPHOS	oxidative phosphorylation
FAO	Fatty acid oxidation
IL4	Interleukin 4
LAL	Lysosomal acid lipase
FATP1	Fatty acid transporter 1
FABP	Fatty acid binding protein
CPT	Carnitine palmitoyl transferase
αKG	Alpha-ketoglutarate
SUCNR1	Succinate receptor
PDH	Pyruvate dehydrogenase
PDK	Pyruvate dehydrogenase kinase
PPAR	Peroxisome proliferator-activated receptor
ABCA1	ATP-binding cassette transporter sub-family A member 1
ABCG1	ATP-binding cassette transporter sub-family G member 1
APOE	Apolipoprotein E
APOC	Apolipoprotein C
ARG2	Arginase-2
SREBP	Sterol regulatory element binding protein
NLRP1A	Gene encoding NACHT, LRR and PYD domains-containing protein 1A
FASN	Fatty acid synthase

References

1. Bora, P.; Majumdar, A.S. Adipose tissue-derived stromal vascular fraction in regenerative medicine: A brief review on biology and translation. *Stem Cell Res. Ther.* **2017**, *8*, 145. [CrossRef] [PubMed]
2. Lumeng, C.N.; Deyoung, S.M.; Saltiel, A.R. Macrophages block insulin action in adipocytes by altering expression of signaling and glucose transport proteins. *Am. J. Physiol. Endocrinol. Metab.* **2007**, *292*, E166–E174. [CrossRef] [PubMed]
3. Castoldi, A.; Naffah de Souza, C.; Camara, N.O.; Moraes-Vieira, P.M. The Macrophage Switch in Obesity Development. *Front. Immunol.* **2015**, *6*, 637. [CrossRef] [PubMed]
4. Coats, B.R.; Schoenfelt, K.Q.; Barbosa-Lorenzi, V.C.; Peris, E.; Cui, C.; Hoffman, A.; Zhou, G.; Fernandez, S.; Zhai, L.; Hall, B.A.; et al. Metabolically Activated Adipose Tissue Macrophages Perform Detrimental and Beneficial Functions during Diet-Induced Obesity. *Cell Rep.* **2017**, *20*, 3149–3161. [CrossRef]
5. Hotamisligil, G.S.; Shargill, N.S.; Spiegelman, B.M. Adipose expression of tumor necrosis factor-alpha: Direct role in obesity-linked insulin resistance. *Science* **1993**, *259*, 87–91. [CrossRef]
6. Hotamisligil, G.S.; Arner, P.; Caro, J.F.; Atkinson, R.L.; Spiegelman, B.M. Increased adipose tissue expression of tumor necrosis factor-alpha in human obesity and insulin resistance. *J. Clin. Investig.* **1995**, *95*, 2409–2415. [CrossRef]
7. Uysal, K.T.; Wiesbrock, S.M.; Hotamisligil, G.S. Functional analysis of tumor necrosis factor (TNF) receptors in TNF-alpha-mediated insulin resistance in genetic obesity. *Endocrinology* **1998**, *139*, 4832–4838. [CrossRef]
8. Shimobayashi, M.; Albert, V.; Woelnerhanssen, B.; Frei, I.C.; Weissenberger, D.; Meyer-Gerspach, A.C.; Clement, N.; Moes, S.; Colombi, M.; Meier, J.A.; et al. Insulin resistance causes inflammation in adipose tissue. *J. Clin. Investig.* **2018**, *128*, 1538–1550. [CrossRef]
9. Lee, Y.S.; Li, P.; Huh, J.Y.; Hwang, I.J.; Lu, M.; Kim, J.I.; Ham, M.; Talukdar, S.; Chen, A.; Lu, W.J.; et al. Inflammation is necessary for long-term but not short-term high-fat diet-induced insulin resistance. *Diabetes* **2011**, *60*, 2474–2483. [CrossRef]
10. Gao, X.; Salomon, C.; Freeman, D.J. Extracellular Vesicles from Adipose Tissue-A Potential Role in Obesity and Type 2 Diabetes? *Front. Endocrinol.* **2017**, *8*, 202. [CrossRef]

11. Khamzina, L.; Gruppuso, P.A.; Wands, J.R. Insulin signaling through insulin receptor substrate 1 and 2 in normal liver development. *Gastroenterology* **2003**, *125*, 572–585. [CrossRef]
12. Dandona, P.; Weinstock, R.; Thusu, K.; Abdel-Rahman, E.; Aljada, A.; Wadden, T. Tumor necrosis factor-alpha in sera of obese patients: Fall with weight loss. *J. Clin. Endocrinol. Metab.* **1998**, *83*, 2907–2910. [CrossRef] [PubMed]
13. Kern, P.A.; Ranganathan, S.; Li, C.; Wood, L.; Ranganathan, G. Adipose tissue tumor necrosis factor and interleukin-6 expression in human obesity and insulin resistance. *Am. J. Physiol. Endocrinol. Metab.* **2001**, *280*, E745–E751. [CrossRef] [PubMed]
14. Dalmas, E.; Toubal, A.; Alzaid, F.; Blazek, K.; Eames, H.L.; Lebozec, K.; Pini, M.; Hainault, I.; Montastier, E.; Denis, R.G.; et al. Irf5 deficiency in macrophages promotes beneficial adipose tissue expansion and insulin sensitivity during obesity. *Nat. Med.* **2015**, *21*, 610–618. [CrossRef]
15. Yuan, M.; Konstantopoulos, N.; Lee, J.; Hansen, L.; Li, Z.W.; Karin, M.; Shoelson, S.E. Reversal of obesity- and diet-induced insulin resistance with salicylates or targeted disruption of Ikkbeta. *Science* **2001**, *293*, 1673–1677. [CrossRef]
16. Mayerson, A.B.; Hundal, R.S.; Dufour, S.; Lebon, V.; Befroy, D.; Cline, G.W.; Enocksson, S.; Inzucchi, S.E.; Shulman, G.I.; Petersen, K.F. The effects of rosiglitazone on insulin sensitivity, lipolysis, and hepatic and skeletal muscle triglyceride content in patients with type 2 diabetes. *Diabetes* **2002**, *51*, 797–802. [CrossRef]
17. Drareni, K.; Gautier, J.F.; Venteclef, N.; Alzaid, F. Transcriptional control of macrophage polarisation in type 2 diabetes. *Semin. Immunopathol.* **2019**, *41*, 515–529. [CrossRef]
18. Nakatani, Y.; Kaneto, H.; Kawamori, D.; Hatazaki, M.; Miyatsuka, T.; Matsuoka, T.A.; Kajimoto, Y.; Matsuhisa, M.; Yamasaki, Y.; Hori, M. Modulation of the JNK pathway in liver affects insulin resistance status. *J. Biol. Chem.* **2004**, *279*, 45803–45809. [CrossRef]
19. Bluher, M.; Bashan, N.; Shai, I.; Harman-Boehm, I.; Tarnovscki, T.; Avinaoch, E.; Stumvoll, M.; Dietrich, A.; Kloting, N.; Rudich, A. Activated Ask1-MKK4-p38MAPK/JNK stress signaling pathway in human omental fat tissue may link macrophage infiltration to whole-body Insulin sensitivity. *J. Clin. Endocrinol. Metab.* **2009**, *94*, 2507–2515. [CrossRef]
20. Baker, R.G.; Hayden, M.S.; Ghosh, S. NF-kappaB, inflammation, and metabolic disease. *Cell Metab.* **2011**, *13*, 11–22. [CrossRef]
21. Surmi, B.K.; Hasty, A.H. Macrophage infiltration into adipose tissue: Initiation, propagation and remodeling. *Future Lipidol.* **2008**, *3*, 545–556. [CrossRef] [PubMed]
22. Haase, J.; Weyer, U.; Immig, K.; Kloting, N.; Bluher, M.; Eilers, J.; Bechmann, I.; Gericke, M. Local proliferation of macrophages in adipose tissue during obesity-induced inflammation. *Diabetologia* **2014**, *57*, 562–571. [CrossRef] [PubMed]
23. Solinas, G.; Naugler, W.; Galimi, F.; Lee, M.S.; Karin, M. Saturated fatty acids inhibit induction of insulin gene transcription by JNK-mediated phosphorylation of insulin-receptor substrates. *Proc. Natl. Acad. Sci. USA* **2006**, *103*, 16454–16459. [CrossRef] [PubMed]
24. Ozcan, U.; Cao, Q.; Yilmaz, E.; Lee, A.H.; Iwakoshi, N.N.; Ozdelen, E.; Tuncman, G.; Gorgun, C.; Glimcher, L.H.; Hotamisligil, G.S. Endoplasmic reticulum stress links obesity, insulin action, and type 2 diabetes. *Science* **2004**, *306*, 457–461. [CrossRef]
25. Aguirre, V.; Uchida, T.; Yenush, L.; Davis, R.; White, M.F. The c-Jun NH(2)-terminal kinase promotes insulin resistance during association with insulin receptor substrate-1 and phosphorylation of Ser(307). *J. Biol. Chem.* **2000**, *275*, 9047–9054. [CrossRef]
26. Tanti, J.F.; Gremeaux, T.; Van Obberghen, E.; Le Marchand-Brustel, Y. Insulin receptor substrate 1 is phosphorylated by the serine kinase activity of phosphatidylinositol 3-kinase. *Biochem. J.* **1994**, *304*, 17–21. [CrossRef]
27. Gual, P.; Le Marchand-Brustel, Y.; Tanti, J.F. Positive and negative regulation of insulin signaling through IRS-1 phosphorylation. *Biochimie* **2005**, *87*, 99–109. [CrossRef]
28. Regnier, C.H.; Song, H.Y.; Gao, X.; Goeddel, D.V.; Cao, Z.; Rothe, M. Identification and characterization of an IkappaB kinase. *Cell* **1997**, *90*, 373–383. [CrossRef]
29. Covert, M.W.; Leung, T.H.; Gaston, J.E.; Baltimore, D. Achieving stability of lipopolysaccharide-induced NF-kappaB activation. *Science* **2005**, *309*, 1854–1857. [CrossRef]

30. Jiao, P.; Ma, J.; Feng, B.; Zhang, H.; Diehl, J.A.; Chin, Y.E.; Yan, W.; Xu, H. FFA-induced adipocyte inflammation and insulin resistance: Involvement of ER stress and IKKbeta pathways. *Obesity (Silver Spring)* **2011**, *19*, 483–491. [CrossRef]
31. Orliaguet, L.; Dalmas, E.; Drareni, K.; Venteclef, N.; Alzaid, F. Mechanisms of Macrophage Polarization in Insulin Signaling and Sensitivity. *Front. Endocrinol.* **2020**, *11*, 62. [CrossRef] [PubMed]
32. Vandanmagsar, B.; Youm, Y.H.; Ravussin, A.; Galgani, J.E.; Stadler, K.; Mynatt, R.L.; Ravussin, E.; Stephens, J.M.; Dixit, V.D. The NLRP3 inflammasome instigates obesity-induced inflammation and insulin resistance. *Nat. Med.* **2011**, *17*, 179–188. [CrossRef] [PubMed]
33. Schroder, K.; Zhou, R.; Tschopp, J. The NLRP3 inflammasome: A sensor for metabolic danger? *Science* **2010**, *327*, 296–300. [CrossRef] [PubMed]
34. Donath, M.Y.; Schumann, D.M.; Faulenbach, M.; Ellingsgaard, H.; Perren, A.; Ehses, J.A. Islet inflammation in type 2 diabetes: From metabolic stress to therapy. *Diabetes Care* **2008**, *31*, S161–S164. [CrossRef] [PubMed]
35. Lagathu, C.; Yvan-Charvet, L.; Bastard, J.P.; Maachi, M.; Quignard-Boulange, A.; Capeau, J.; Caron, M. Long-term treatment with interleukin-1beta induces insulin resistance in murine and human adipocytes. *Diabetologia* **2006**, *49*, 2162–2173. [CrossRef]
36. Gao, D.; Madi, M.; Ding, C.; Fok, M.; Steele, T.; Ford, C.; Hunter, L.; Bing, C. Interleukin-1beta mediates macrophage-induced impairment of insulin signaling in human primary adipocytes. *Am. J. Physiol. Endocrinol. Metab.* **2014**, *307*, E289–E304. [CrossRef]
37. Ballak, D.B.; Stienstra, R.; Tack, C.J.; Dinarello, C.A.; van Diepen, J.A. IL-1 family members in the pathogenesis and treatment of metabolic disease: Focus on adipose tissue inflammation and insulin resistance. *Cytokine* **2015**, *75*, 280–290. [CrossRef]
38. Wood, I.S.; Wang, B.; Jenkins, J.R.; Trayhurn, P. The pro-inflammatory cytokine IL-18 is expressed in human adipose tissue and strongly upregulated by TNFalpha in human adipocytes. *Biochem. Biophys. Res. Commun.* **2005**, *337*, 422–429. [CrossRef]
39. Zilverschoon, G.R.; Tack, C.J.; Joosten, L.A.; Kullberg, B.J.; van der Meer, J.W.; Netea, M.G. Interleukin-18 resistance in patients with obesity and type 2 diabetes mellitus. *Int. J. Obes.* **2008**, *32*, 1407–1414. [CrossRef]
40. Harms, R.Z.; Creer, A.J.; Lorenzo-Arteaga, K.M.; Ostlund, K.R.; Sarvetnick, N.E. Interleukin (IL)-18 Binding Protein Deficiency Disrupts Natural Killer Cell Maturation and Diminishes Circulating IL-18. *Front. Immunol.* **2017**, *8*, 1020. [CrossRef]
41. Feve, B.; Bastard, J.P. The role of interleukins in insulin resistance and type 2 diabetes mellitus. *Nat. Rev. Endocrinol.* **2009**, *5*, 305–311. [CrossRef] [PubMed]
42. Dodington, D.W.; Desai, H.R.; Woo, M. JAK/STAT—Emerging Players in Metabolism. *Trends Endocrinol. Metab.* **2018**, *29*, 55–65. [CrossRef] [PubMed]
43. Lagathu, C.; Bastard, J.P.; Auclair, M.; Maachi, M.; Capeau, J.; Caron, M. Chronic interleukin-6 (IL-6) treatment increased IL-6 secretion and induced insulin resistance in adipocyte: Prevention by rosiglitazone. *Biochem. Biophys. Res. Commun.* **2003**, *311*, 372–379. [CrossRef] [PubMed]
44. Perry, R.J.; Cardone, R.L.; Petersen, M.C.; Zhang, D.; Fouqueray, P.; Hallakou-Bozec, S.; Bolze, S.; Shulman, G.I.; Petersen, K.F.; Kibbey, R.G. Imeglimin lowers glucose primarily by amplifying glucose-stimulated insulin secretion in high-fat-fed rodents. *Am. J. Physiol. Endocrinol. Metab.* **2016**, *311*, E461–E470. [CrossRef] [PubMed]
45. Perry, R.J.; Camporez, J.G.; Kursawe, R.; Titchenell, P.M.; Zhang, D.; Perry, C.J.; Jurczak, M.J.; Abudukadier, A.; Han, M.S.; Zhang, X.M.; et al. Hepatic acetyl CoA links adipose tissue inflammation to hepatic insulin resistance and type 2 diabetes. *Cell* **2015**, *160*, 745–758. [CrossRef]
46. Sabio, G.; Das, M.; Mora, A.; Zhang, Z.; Jun, J.Y.; Ko, H.J.; Barrett, T.; Kim, J.K.; Davis, R.J. A stress signaling pathway in adipose tissue regulates hepatic insulin resistance. *Science* **2008**, *322*, 1539–1543. [CrossRef]
47. Beutler, B.; Greenwald, D.; Hulmes, J.D.; Chang, M.; Pan, Y.C.; Mathison, J.; Ulevitch, R.; Cerami, A. Identity of tumour necrosis factor and the macrophage-secreted factor cachectin. *Nature* **1985**, *316*, 552–554. [CrossRef]
48. Torti, F.M.; Dieckmann, B.; Beutler, B.; Cerami, A.; Ringold, G.M. A macrophage factor inhibits adipocyte gene expression: An in vitro model of cachexia. *Science* **1985**, *229*, 867–869. [CrossRef]
49. Gatanaga, T.; Hwang, C.D.; Kohr, W.; Cappuccini, F.; Lucci, J.A., 3rd; Jeffes, E.W.; Lentz, R.; Tomich, J.; Yamamoto, R.S.; Granger, G.A. Purification and characterization of an inhibitor (soluble tumor necrosis factor receptor) for tumor necrosis factor and lymphotoxin obtained from the serum ultrafiltrates of human cancer patients. *Proc. Natl. Acad. Sci. USA* **1990**, *87*, 8781–8784. [CrossRef]

50. Peraldi, P.; Hotamisligil, G.S.; Buurman, W.A.; White, M.F.; Spiegelman, B.M. Tumor necrosis factor (TNF)-alpha inhibits insulin signaling through stimulation of the p55 TNF receptor and activation of sphingomyelinase. *J. Biol. Chem.* **1996**, *271*, 13018–13022. [CrossRef]
51. Hotamisligil, G.S.; Arner, P.; Atkinson, R.L.; Spiegelman, B.M. Differential regulation of the p80 tumor necrosis factor receptor in human obesity and insulin resistance. *Diabetes* **1997**, *46*, 451–455. [CrossRef] [PubMed]
52. Pandey, M.; Tuncman, G.; Hotamisligil, G.S.; Samad, F. Divergent roles for p55 and p75 TNF-alpha receptors in the induction of plasminogen activator inhibitor-1. *Am. J. Pathol.* **2003**, *162*, 933–941. [CrossRef]
53. Cawthorn, W.P.; Sethi, J.K. TNF-alpha and adipocyte biology. *FEBS Lett.* **2008**, *582*, 117–131. [CrossRef] [PubMed]
54. Nisoli, E.; Briscini, L.; Giordano, A.; Tonello, C.; Wiesbrock, S.M.; Uysal, K.T.; Cinti, S.; Carruba, M.O.; Hotamisligil, G.S. Tumor necrosis factor alpha mediates apoptosis of brown adipocytes and defective brown adipocyte function in obesity. *Proc. Natl. Acad. Sci. USA* **2000**, *97*, 8033–8038. [CrossRef]
55. Kim, K.Y.; Kim, J.K.; Jeon, J.H.; Yoon, S.R.; Choi, I.; Yang, Y. c-Jun N-terminal kinase is involved in the suppression of adiponectin expression by TNF-alpha in 3T3-L1 adipocytes. *Biochem. Biophys. Res. Commun.* **2005**, *327*, 460–467. [CrossRef]
56. Chae, G.N.; Kwak, S.J. NF-kappaB is involved in the TNF-alpha induced inhibition of the differentiation of 3T3-L1 cells by reducing PPARgamma expression. *Exp. Mol. Med.* **2003**, *35*, 431–437. [CrossRef]
57. Stephens, J.M.; Lee, J.; Pilch, P.F. Tumor necrosis factor-alpha-induced insulin resistance in 3T3-L1 adipocytes is accompanied by a loss of insulin receptor substrate-1 and GLUT4 expression without a loss of insulin receptor-mediated signal transduction. *J. Biol. Chem.* **1997**, *272*, 971–976. [CrossRef]
58. Ruan, H.; Miles, P.D.; Ladd, C.M.; Ross, K.; Golub, T.R.; Olefsky, J.M.; Lodish, H.F. Profiling gene transcription in vivo reveals adipose tissue as an immediate target of tumor necrosis factor-alpha: Implications for insulin resistance. *Diabetes* **2002**, *51*, 3176–3188. [CrossRef]
59. Ruan, H.; Hacohen, N.; Golub, T.R.; Van Parijs, L.; Lodish, H.F. Tumor necrosis factor-alpha suppresses adipocyte-specific genes and activates expression of preadipocyte genes in 3T3-L1 adipocytes: Nuclear factor-kappaB activation by TNF-alpha is obligatory. *Diabetes* **2002**, *51*, 1319–1336. [CrossRef]
60. Schindler, C.; Darnell, J.E., Jr. Transcriptional responses to polypeptide ligands: The JAK-STAT pathway. *Annu. Rev. Biochem.* **1995**, *64*, 621–651. [CrossRef]
61. Richard, A.J.; Stephens, J.M. Emerging roles of JAK-STAT signaling pathways in adipocytes. *Trends Endocrinol. Metab.* **2011**, *22*, 325–332. [CrossRef]
62. Richard, A.J.; Stephens, J.M. The role of JAK-STAT signaling in adipose tissue function. *Biochim. Biophys. Acta* **2014**, *1842*, 431–439. [CrossRef] [PubMed]
63. Gurzov, E.N.; Stanley, W.J.; Pappas, E.G.; Thomas, H.E.; Gough, D.J. The JAK/STAT pathway in obesity and diabetes. *FEBS J.* **2016**, *283*, 3002–3015. [CrossRef] [PubMed]
64. Filgueiras, L.R.; Brandt, S.L.; Ramalho, T.R.; Jancar, S.; Serezani, C.H. Imbalance between HDAC and HAT activities drives aberrant STAT1/MyD88 expression in macrophages from type 1 diabetic mice. *J. Diabetes Complicat.* **2017**, *31*, 334–339. [CrossRef] [PubMed]
65. Vasamsetti, S.B.; Karnewar, S.; Kanugula, A.K.; Thatipalli, A.R.; Kumar, J.M.; Kotamraju, S. Metformin inhibits monocyte-to-macrophage differentiation via AMPK-mediated inhibition of STAT3 activation: Potential role in atherosclerosis. *Diabetes* **2015**, *64*, 2028–2041. [CrossRef]
66. Desai, H.R.; Sivasubramaniyam, T.; Revelo, X.S.; Schroer, S.A.; Luk, C.T.; Rikkala, P.R.; Metherel, A.H.; Dodington, D.W.; Park, Y.J.; Kim, M.J.; et al. Macrophage JAK2 deficiency protects against high-fat diet-induced inflammation. *Sci. Rep.* **2017**, *7*, 7653. [CrossRef]
67. Sajic, T.; Hainard, A.; Scherl, A.; Wohlwend, A.; Negro, F.; Sanchez, J.C.; Szanto, I. STAT6 promotes bi-directional modulation of PKM2 in liver and adipose inflammatory cells in rosiglitazone-treated mice. *Sci. Rep.* **2013**, *3*, 2350. [CrossRef]
68. Balkwill, F.R. Interferons: From molecular biology to man. Part 1. Genetics and molecular biology of the interferon system. *Microbiol. Sci.* **1986**, *3*, 212–215.
69. Kumaran Satyanarayanan, S.; El Kebir, D.; Soboh, S.; Butenko, S.; Sekheri, M.; Saadi, J.; Peled, N.; Assi, S.; Othman, A.; Schif-Zuck, S.; et al. IFN-beta is a macrophage-derived effector cytokine facilitating the resolution of bacterial inflammation. *Nat. Commun.* **2019**, *10*, 3471. [CrossRef]

70. Zhao, G.N.; Jiang, D.S.; Li, H. Interferon regulatory factors: At the crossroads of immunity, metabolism, and disease. *Biochim. Biophys. Acta* **2015**, *1852*, 365–378. [CrossRef]
71. Chen, W.; Royer, W.E., Jr. Structural insights into interferon regulatory factor activation. *Cell Signal.* **2010**, *22*, 883–887. [CrossRef]
72. Orr, J.S.; Puglisi, M.J.; Ellacott, K.L.; Lumeng, C.N.; Wasserman, D.H.; Hasty, A.H. Toll-like receptor 4 deficiency promotes the alternative activation of adipose tissue macrophages. *Diabetes* **2012**, *61*, 2718–2727. [CrossRef]
73. Eguchi, J.; Kong, X.; Tenta, M.; Wang, X.; Kang, S.; Rosen, E.D. Interferon regulatory factor 4 regulates obesity-induced inflammation through regulation of adipose tissue macrophage polarization. *Diabetes* **2013**, *62*, 3394–3403. [CrossRef]
74. Eguchi, J.; Wang, X.; Yu, S.; Kershaw, E.E.; Chiu, P.C.; Dushay, J.; Estall, J.L.; Klein, U.; Maratos-Flier, E.; Rosen, E.D. Transcriptional control of adipose lipid handling by IRF4. *Cell Metab.* **2011**, *13*, 249–259. [CrossRef]
75. Freemerman, A.J.; Johnson, A.R.; Sacks, G.N.; Milner, J.J.; Kirk, E.L.; Troester, M.A.; Macintyre, A.N.; Goraksha-Hicks, P.; Rathmell, J.C.; Makowski, L. Metabolic reprogramming of macrophages: Glucose transporter 1 (GLUT1)-mediated glucose metabolism drives a proinflammatory phenotype. *J. Biol. Chem.* **2014**, *289*, 7884–7896. [CrossRef]
76. Nishizawa, T.; Kanter, J.E.; Kramer, F.; Barnhart, S.; Shen, X.; Vivekanandan-Giri, A.; Wall, V.Z.; Kowitz, J.; Devaraj, S.; O'Brien, K.D.; et al. Testing the role of myeloid cell glucose flux in inflammation and atherosclerosis. *Cell Rep.* **2014**, *7*, 356–365. [CrossRef]
77. Moon, J.S.; Hisata, S.; Park, M.A.; DeNicola, G.M.; Ryter, S.W.; Nakahira, K.; Choi, A.M.K. mTORC1-Induced HK1-Dependent Glycolysis Regulates NLRP3 Inflammasome Activation. *Cell Rep.* **2015**, *12*, 102–115. [CrossRef]
78. Tannahill, G.M.; Curtis, A.M.; Adamik, J.; Palsson-McDermott, E.M.; McGettrick, A.F.; Goel, G.; Frezza, C.; Bernard, N.J.; Kelly, B.; Foley, N.H.; et al. Succinate is an inflammatory signal that induces IL-1beta through HIF-1alpha. *Nature* **2013**, *496*, 238–242. [CrossRef]
79. Koo, S.J.; Garg, N.J. Metabolic programming of macrophage functions and pathogens control. *Redox Biol.* **2019**, *24*, 101198. [CrossRef]
80. Palsson-McDermott, E.M.; Curtis, A.M.; Goel, G.; Lauterbach, M.A.R.; Sheedy, F.J.; Gleeson, L.E.; van den Bosch, M.W.M.; Quinn, S.R.; Domingo-Fernandez, R.; Johnston, D.G.W.; et al. Pyruvate Kinase M2 Regulates Hif-1alpha Activity and IL-1beta Induction and Is a Critical Determinant of the Warburg Effect in LPS-Activated Macrophages. *Cell Metab.* **2015**, *21*, 347. [CrossRef]
81. Millet, P.; Vachharajani, V.; McPhail, L.; Yoza, B.; McCall, C.E. GAPDH Binding to TNF-alpha mRNA Contributes to Posttranscriptional Repression in Monocytes: A Novel Mechanism of Communication between Inflammation and Metabolism. *J. Immunol.* **2016**, *196*, 2541–2551. [CrossRef]
82. Jha, A.K.; Huang, S.C.; Sergushichev, A.; Lampropoulou, V.; Ivanova, Y.; Loginicheva, E.; Chmielewski, K.; Stewart, K.M.; Ashall, J.; Everts, B.; et al. Network integration of parallel metabolic and transcriptional data reveals metabolic modules that regulate macrophage polarization. *Immunity* **2015**, *42*, 419–430. [CrossRef]
83. Seneviratne, A.N.; Edsfeldt, A.; Cole, J.E.; Kassiteridi, C.; Swart, M.; Park, I.; Green, P.; Khoyratty, T.; Saliba, D.; Goddard, M.E.; et al. Interferon Regulatory Factor 5 Controls Necrotic Core Formation in Atherosclerotic Lesions by Impairing Efferocytosis. *Circulation* **2017**, *136*, 1140–1154. [CrossRef]
84. Hedl, M.; Yan, J.; Abraham, C. IRF5 and IRF5 Disease-Risk Variants Increase Glycolysis and Human M1 Macrophage Polarization by Regulating Proximal Signaling and Akt2 Activation. *Cell Rep.* **2016**, *16*, 2442–2455. [CrossRef]
85. Huang, S.C.C.; Smith, A.M.; Everts, B.; Colonna, M.; Pearce, E.L.; Schilling, J.D.; Pearce, E.J. Metabolic Reprogramming Mediated by the mTORC2-IRF4 Signaling Axis Is Essential for Macrophage Alternative Activation. *Immunity* **2016**, *45*, 817–830. [CrossRef]
86. Tan, Z.; Xie, N.; Cui, H.C.; Moellering, D.R.; Abraham, E.; Thannickal, V.J.; Liu, G. Pyruvate Dehydrogenase Kinase 1 Participates in Macrophage Polarization via Regulating Glucose Metabolism. *J. Immunol.* **2015**, *194*, 6082–6089. [CrossRef]
87. de Mello, A.H.; Costa, A.B.; Engel, J.D.G.; Rezin, G.T. Mitochondrial dysfunction in obesity. *Life Sci.* **2018**, *192*, 26–32. [CrossRef]

88. Yin, X.; Lanza, I.R.; Swain, J.M.; Sarr, M.G.; Nair, K.S.; Jensen, M.D. Adipocyte Mitochondrial Function Is Reduced in Human Obesity Independent of Fat Cell Size. *J. Clin. Endocrinol. Metab.* **2014**, *99*, E209–E216. [CrossRef]
89. Escames, G.; Lopez, L.C.; Garcia, J.A.; Garcia-Corzo, L.; Ortiz, F.; Acuna-Castroviejo, D. Mitochondrial DNA and inflammatory diseases. *Hum. Genet.* **2012**, *131*, 161–173. [CrossRef]
90. Lopez-Armada, M.J.; Riveiro-Naveira, R.R.; Vaamonde-Garcia, C.; Valcarcel-Ares, M.N. Mitochondrial dysfunction and the inflammatory response. *Mitochondrion* **2013**, *13*, 106–118. [CrossRef]
91. Heilbronn, L.; Smith, S.R.; Ravussin, E. Failure of fat cell proliferation, mitochondrial function and fat oxidation results in ectopic fat storage, insulin resistance and type II diabetes mellitus. *Int. J. Obes. Relat. Metab. Disord.* **2004**, *28*, S12–S21. [CrossRef] [PubMed]
92. Tsao, C.H.; Shiau, M.Y.; Chuang, P.H.; Chang, Y.H.; Hwang, J. Interleukin-4 regulates lipid metabolism by inhibiting adipogenesis and promoting lipolysis. *J. Lipid Res.* **2014**, *55*, 385–397. [CrossRef] [PubMed]
93. Namgaladze, D.; Brune, B. Macrophage fatty acid oxidation and its roles in macrophage polarization and fatty acid-induced inflammation. *Biochim. Biophys. Acta* **2016**, *1861*, 1796–1807. [CrossRef] [PubMed]
94. Nomura, M.; Liu, J.; Rovira, I.I.; Gonzalez-Hurtado, E.; Lee, J.; Wolfgang, M.J.; Finkel, T. Fatty acid oxidation in macrophage polarization. *Nat. Immunol.* **2016**, *17*, 216–217. [CrossRef]
95. Vats, D.; Mukundan, L.; Odegaard, J.I.; Zhang, L.; Smith, K.L.; Morel, C.R.; Wagner, R.A.; Greaves, D.R.; Murray, P.J.; Chawla, A. Oxidative metabolism and PGC-1beta attenuate macrophage-mediated inflammation. *Cell Metab.* **2006**, *4*, 13–24. [CrossRef]
96. Huang, S.C.; Everts, B.; Ivanova, Y.; O'Sullivan, D.; Nascimento, M.; Smith, A.M.; Beatty, W.; Love-Gregory, L.; Lam, W.Y.; O'Neill, C.M.; et al. Cell-intrinsic lysosomal lipolysis is essential for alternative activation of macrophages. *Nat. Immunol.* **2014**, *15*, 846–855. [CrossRef]
97. Furuhashi, M.; Fucho, R.; Gorgun, C.Z.; Tuncman, G.; Cao, H.; Hotamisligil, G.S. Adipocyte/macrophage fatty acid-binding proteins contribute to metabolic deterioration through actions in both macrophages and adipocytes in mice. *J. Clin. Investig.* **2008**, *118*, 2640–2650. [CrossRef]
98. Calle, P.; Munoz, A.; Sola, A.; Hotter, G. CPT1a gene expression reverses the inflammatory and anti-phagocytic effect of 7-ketocholesterol in RAW264.7 macrophages. *Lipids Health Dis.* **2019**, *18*, 215. [CrossRef]
99. Namgaladze, D.; Brune, B. Fatty acid oxidation is dispensable for human macrophage IL-4-induced polarization. *Biochim. Biophys. Acta* **2014**, *1841*, 1329–1335. [CrossRef]
100. Zaslona, Z.; Serezani, C.H.; Okunishi, K.; Aronoff, D.M.; Peters-Golden, M. Prostaglandin E2 restrains macrophage maturation via E prostanoid receptor 2/protein kinase A signaling. *Blood* **2012**, *119*, 2358–2367. [CrossRef]
101. Lampropoulou, V.; Sergushichev, A.; Bambouskova, M.; Nair, S.; Vincent, E.E.; Loginicheva, E.; Cervantes-Barragan, L.; Ma, X.; Huang, S.C.; Griss, T.; et al. Itaconate Links Inhibition of Succinate Dehydrogenase with Macrophage Metabolic Remodeling and Regulation of Inflammation. *Cell Metab.* **2016**, *24*, 158–166. [CrossRef]
102. Mills, E.L.; Kelly, B.; Logan, A.; Costa, A.S.H.; Varma, M.; Bryant, C.E.; Tourlomousis, P.; Dabritz, J.H.M.; Gottlieb, E.; Latorre, I.; et al. Succinate Dehydrogenase Supports Metabolic Repurposing of Mitochondria to Drive Inflammatory Macrophages. *Cell* **2016**, *167*, 457–470.e413. [CrossRef]
103. Littlewood-Evans, A.; Sarret, S.; Apfel, V.; Loesle, P.; Dawson, J.; Zhang, J.; Muller, A.; Tigani, B.; Kneuer, R.; Patel, S.; et al. GPR91 senses extracellular succinate released from inflammatory macrophages and exacerbates rheumatoid arthritis. *J. Exp. Med.* **2016**, *213*, 1655–1662. [CrossRef]
104. Keiran, N.; Ceperuelo-Mallafre, V.; Calvo, E.; Hernandez-Alvarez, M.I.; Ejarque, M.; Nunez-Roa, C.; Horrillo, D.; Maymo-Masip, E.; Rodriguez, M.M.; Fradera, R.; et al. SUCNR1 controls an anti-inflammatory program in macrophages to regulate the metabolic response to obesity. *Nat. Immunol.* **2019**, *20*, 581–592. [CrossRef] [PubMed]
105. Liu, P.S.; Wang, H.; Li, X.; Chao, T.; Teav, T.; Christen, S.; Di Conza, G.; Cheng, W.C.; Chou, C.H.; Vavakova, M.; et al. alpha-ketoglutarate orchestrates macrophage activation through metabolic and epigenetic reprogramming. *Nat. Immunol.* **2017**, *18*, 985–994. [CrossRef] [PubMed]
106. Min, B.K.; Park, S.; Kang, H.J.; Kim, D.W.; Ham, H.J.; Ha, C.M.; Choi, B.J.; Lee, J.Y.; Oh, C.J.; Yoo, E.K.; et al. Pyruvate Dehydrogenase Kinase Is a Metabolic Checkpoint for Polarization of Macrophages to the M1 Phenotype. *Front. Immunol.* **2019**, *10*, 944. [CrossRef] [PubMed]

107. Meiser, J.; Kramer, L.; Sapcariu, S.C.; Battello, N.; Ghelfi, J.; D'Herouel, A.F.; Skupin, A.; Hiller, K. Pro-inflammatory Macrophages Sustain Pyruvate Oxidation through Pyruvate Dehydrogenase for the Synthesis of Itaconate and to Enable Cytokine Expression. *J. Biol. Chem.* **2016**, *291*, 3932–3946. [CrossRef]
108. Kang, K.; Reilly, S.M.; Karabacak, V.; Gangl, M.R.; Fitzgerald, K.; Hatano, B.; Lee, C.H. Adipocyte-derived Th2 cytokines and myeloid PPARdelta regulate macrophage polarization and insulin sensitivity. *Cell Metab.* **2008**, *7*, 485–495. [CrossRef]
109. Odegaard, J.I.; Ricardo-Gonzalez, R.R.; Goforth, M.H.; Morel, C.R.; Subramanian, V.; Mukundan, L.; Red Eagle, A.; Vats, D.; Brombacher, F.; Ferrante, A.W.; et al. Macrophage-specific PPARgamma controls alternative activation and improves insulin resistance. *Nature* **2007**, *447*, 1116–1120. [CrossRef]
110. Venkateswaran, A.; Laffitte, B.A.; Joseph, S.B.; Mak, P.A.; Wilpitz, D.C.; Edwards, P.A.; Tontonoz, P. Control of cellular cholesterol efflux by the nuclear oxysterol receptor LXR alpha. *Proc. Natl. Acad. Sci. USA* **2000**, *97*, 12097–12102. [CrossRef]
111. Joseph, S.B.; Bradley, M.N.; Castrillo, A.; Bruhn, K.W.; Mak, P.A.; Pei, L.; Hogenesch, J.; O'Connell, R.M.; Cheng, G.; Saez, E.; et al. LXR-dependent gene expression is important for macrophage survival and the innate immune response. *Cell* **2004**, *119*, 299–309. [CrossRef]
112. Marathe, C.; Bradley, M.N.; Hong, C.; Lopez, F.; Ruiz de Galarreta, C.M.; Tontonoz, P.; Castrillo, A. The arginase II gene is an anti-inflammatory target of liver X receptor in macrophages. *J. Biol. Chem.* **2006**, *281*, 32197–32206. [CrossRef] [PubMed]
113. Im, S.S.; Yousef, L.; Blaschitz, C.; Liu, J.Z.; Edwards, R.A.; Young, S.G.; Raffatellu, M.; Osborne, T.F. Linking lipid metabolism to the innate immune response in macrophages through sterol regulatory element binding protein-1a. *Cell Metab.* **2011**, *13*, 540–549. [CrossRef] [PubMed]
114. Lee, J.H.; Phelan, P.; Shin, M.; Oh, B.C.; Han, X.; Im, S.S.; Osborne, T.F. SREBP-1a-stimulated lipid synthesis is required for macrophage phagocytosis downstream of TLR4-directed mTORC1. *Proc. Natl. Acad. Sci. USA* **2018**, *115*, E12228–E12234. [CrossRef] [PubMed]
115. Varghese, J.F.; Patel, R.; Yadav, U.C.S. Sterol regulatory element binding protein (SREBP) -1 mediates oxidized low-density lipoprotein (oxLDL) induced macrophage foam cell formation through NLRP3 inflammasome activation. *Cell Signal.* **2019**, *53*, 316–326. [CrossRef] [PubMed]
116. Oishi, Y.; Spann, N.J.; Link, V.M.; Muse, E.D.; Strid, T.; Edillor, C.; Kolar, M.J.; Matsuzaka, T.; Hayakawa, S.; Tao, J.; et al. SREBP1 Contributes to Resolution of Pro-inflammatory TLR4 Signaling by Reprogramming Fatty Acid Metabolism. *Cell Metab.* **2017**, *25*, 412–427. [CrossRef]
117. Wei, X.; Song, H.; Yin, L.; Rizzo, M.G.; Sidhu, R.; Covey, D.F.; Ory, D.S.; Semenkovich, C.F. Fatty acid synthesis configures the plasma membrane for inflammation in diabetes. *Nature* **2016**, *539*, 294–298. [CrossRef] [PubMed]
118. Nejadmoghaddam, M.R.; Minai-Tehrani, A.; Ghahremanzadeh, R.; Mahmoudi, M.; Dinarvand, R.; Zarnani, A.H. Antibody-Drug Conjugates: Possibilities and Challenges. *Avicenna J. Med. Biotechnol.* **2019**, *11*, 3–23. [PubMed]

Résumé

Introduction

L'obésité, le diabète de type-2 (DT2) et l'inflammation métabolique

L'obésité est une pathologie métabolique caractérisée par un excès et une accumulation de masse grasse dans l'ensemble de l'organisme. Plus précisément, les individus avec un indice de masse corporelle (IMC) supérieur ou égal à 30kg/m^2 sont considérés comme obèses. L'obésité est dû à un déséquilibre entre les apports et les dépenses énergétiques. Aujourd'hui, les apports énergétiques ont tendance à augmenter du fait de la consommation d'aliments transformés et la sédentarisation impacte négativement les dépenses énergétiques.

L'obésité est un facteur de risque pour le développement de nombreuses pathologies, comme les complications cardiovasculaires, le DT2, la stéatose hépatique, certains cancers, l'apnée du sommeil… Par ailleurs, la fonction immunitaire est altérée chez des patients obèses, les rendant plus sensibles aux infections virales et bactériennes par exemple. L'obésité favorise la mise en place d'une résistance à l'insuline, qui, si elle est combinée à une altération de la sécrétion d'insuline par le pancréas, contribue au développement du DT2. On considère que l'obésité augmente de 30 à 53% le risque de développer un DT2 et environ 80-90% des patients DT2 sont en surpoids ou obèses. Tout comme l'obésité, le DT2 est un facteur de risque pour le développement de complications rénales, vasculaires… et représente la première cause de cécité dans le monde.

D'un point de vue épidémiologique, l'Organisation Mondiale de la Santé (OMS) considère l'obésité comme une pandémie, dont l'incidence augmente fortement dans le monde et notamment dans les pays en voie de développement. Aujourd'hui, 39% de la population mondiale est en surpoids et 13% sont obèses. De manière similaire, l'incidence du DT2 a été multipliée par quatre ces 30 dernières années, notamment dans les pays où l'obésité augmente. Par ailleurs, l'obésité et le DT2 altèrent la qualité de vie et sont associés à une espérance de vie plus courte.

Le tissu adipeux : un organe métabolique

Au cours de l'obésité, le tissu adipeux blanc (TA) augmente en taille suite au surplus énergétique. A l'inverse du TA viscéral, le TA sous-cutané ne semble pas être impliqué dans le

développement de l'obésité et de ses complications, il aurait plutôt un rôle protecteur (Porter).

Le TA est composé principalement d'adipocytes, de cellules mésenchymateuses, de fibroblastes mais aussi de cellules immunitaires qui forment un système spécifique au TA (Lynch Kane). Les adipocytes possèdent une gouttelette lipidique, qui occupe jusqu'à 90% du volume cellulaire. Cette gouttelette lipidique permet le stockage dynamique de lipides, sous forme de triglycérides. En période de surplus énergétiques, les adipocytes peuvent stocker des lipides, via la lipogenèse de novo ou l'estérification d'acides gras et lorsque les besoins énergétiques sont accrus, la lipolyse permet la libération d'acides gras dans la circulation. Par ailleurs, le TA sécrète des hormones métaboliques telles que la leptine, l'adiponectine ainsi que des cytokines pro-inflammatoires. Il est de fait considéré comme un organe endocrine.

Au cours de l'obésité, l'expansion du TA repose sur deux phénomènes : l'hyperplasie (augmentation en nombre) et l'hypertrophie (augmentation en volume) des adipocytes. Par ailleurs, il y a une augmentation du nombre de progéniteurs adipocytaires et les adipocytes expriment des marqueurs de stress cellulaire, notamment en lien avec l'hypoxie induite par des défauts de vascularisation. Enfin, le TA de patients obèses est caractérisé par un important infiltrat immunitaire, et notamment de macrophages, et par la mise en place d'un environnement pro-inflammatoire.

L'inflammation métabolique

Les premières preuves montrant un lien entre l'inflammation et le métabolisme remontent à 1993, lorsque Gökhan Hotamisligil et Bruce Spiegelman mettent en évidence une augmentation de l'expression de la cytokine pro-inflammatoire *tumor necrosis factor* α (TNFα) dans le TA de souris obèses. Les macrophages ont été identifiés comme principale source de cette production de TNFα, ainsi que d'autres molécules pro-inflammatoires (IL6 et l'oxyde nitrique synthase (iNOS)), dans un contexte obésogène. De plus, les macrophages s'accumulent considérablement dans le TA lors de l'obésité et lors de l'établissement d'une résistance à l'insuline. Ces données mettent en lumière la contribution de l'inflammation au cours de l'obésité, de l'insulino-résistance et du DT2. De ces observations, nait le concept d'inflammation métabolique, ou méta-inflammation, qui correspond à une inflammation stérile, chronique et de bas grade.

Les macrophages, des cellules de l'immunité innée

Les macrophages répondent rapidement aux signaux environnementaux. Ils détectent les changements de leur microenvironnement grâce à leurs récepteurs de surface cellulaires (les récepteurs *Toll like*). Une nomenclature dichotomique est communément utilisée pour décrire les états de polarisation du macrophage :

- Les macrophages de type M1 (activé classiquement) ayant une forte capacité microbicide, en réponse au lipopolysaccharide bactérien (LPS) et à l'interféron (IFN) γ. Ils produisent des cytokines pro-inflammatoires, telles que TNFα, IL6, IL1β, ainsi que des espèces réactives de l'oxygène (*reactive oxygen species* [ROS]) ;
- Les macrophages de type M2, les anti-inflammatoires (activé alternativement par l'IL4), sont impliqués dans la résolution de l'inflammation, ils produisent des médiateurs anti-inflammatoires, tels que l'IL10 et le *transforming growth factor-β* (TGFβ).

Alors que cette classification M1/M2 est toujours de rigueur, il existe sous cette dichotomie, un continuum de phénotypes divers de macrophages avec différentes réponses et intermédiaires. Les nouvelles classifications fonctionnelles représentent les macrophages polarisés selon une échelle progressive, entre le macrophage M1 et le M2.

Macrophages du TA : rôles physiologiques

Les macrophages jouent un rôle fondamental dans le maintien de l'intégrité du TA. Dans les conditions physiologiques, ces cellules présentent une polarisation de type M2 et sont caractérisées par l'expression de récepteurs CD206, CD301 à leur surface, en plus des marqueurs classiques des macrophages, tels que F4/80 (chez la souris), CD14 (chez l'Homme), CD11b, et CD68. De plus, ils expriment l'arginase 1 (ARG1), l'IL10 et le récepteur activé par les proliférateurs de péroxisomes (PPAR)-γ.

Les macrophages M2 participent à l'homéostasie du TA. Ils sont responsables du captage des lipides provenant des adipocytes mourants. Ces capacités de captage des lipides du milieu, contrôlé par CD36 et le *Macrophage scavenger receptor 1* (MSR1), sont mises à l'épreuve de façon quotidienne, lors des repas (expansion du tissu adipeux et stockage des lipides), mais aussi lors des périodes de jeûne, de perte de poids induisant la lipolyse, ou alors lors du relargage par les adipocytes d'exosomes enrichis en lipides. Ce stockage, puis relargage des lipides, contrôlé par les macrophages, est bénéfique pour l'homéostasie glucidique. Dans des contextes de stress métabolique, ces capacités limitent le dépôt de graisses ectopiques et la dyslipidémie systémique. Le captage et le stockage des lipides induisent la mise en place d'une activité lysosomale qui est essentielle au maintien de l'homéostasie du TA. De plus, les

macrophages favorisent le développement et la vascularisation du TA en contrôlant favorisant l'adipogenèse et l'angiogenèse, limitant la mise en place de zones hypoxiques.

Les macrophages M2 du TA sont impliqués notamment dans le maintien de la sensibilité à l'insuline, notamment via la production de l'IL10, une cytokine anti-inflammatoire dont l'expression est associée à une meilleure sensibilité à l'insuline.

Macrophages du TA : acteurs clé de l'inflammation métabolique

Si les macrophages participent activement à la physiologie du TA, il est aussi clairement établi qu'ils sont les principaux contributeurs de l'inflammation métabolique. En effet, ils produisent des cytokines pro-inflammatoires et s'accumulent au sein du tissu adipeux au cours de l'obésité. Les macrophages du TA de patients obèses sont dit « *metabolically activated* », ils produisent des cytokines pro-inflammatoires mais sont distincts des macrophages M1, de par leur profil transcriptomique et les marqueurs qu'ils expriment.

Les signaux induisant l'activation des macrophages vers un phénotype pro-inflammatoire et leur accumulation sont divers. L'apoptose des adipocytes, le stress oxydatif, les lipides circulants et l'hypoxie peuvent être perçus comme des signaux de danger, menant à l'activation des macrophages. L'accumulation des macrophages est liée à la fois à leur prolifération *in situ*, ainsi qu'à leur recrutement et rétention au sein du TA.

Au sein du TA de patients ou de souris obèses, on constate que les macrophages représentent une population hétérogène. On note une augmentation de *lipid-associated macrophages* (LAM) qui accumulent des lipides et limitent l'hypertrophie adipocytaires ainsi que la lipotoxicité. Certains sous-types de macrophages, exprimant CD9 et CD11c, sont responsables de la sécrétion de cytokines pro-inflammatoires, contribuant à l'insulino-résistance et à l'inflammation métabolique. Ainsi, au cours de l'obésité, les macrophages ont des rôles divers, à la fois bénéfiques mais aussi délétères pour le maintien de l'homéostasie métabolique.

Mécanismes d'activation des macrophages

De manière générale, l'activation et la polarisation des macrophages sont associées à un programme transcriptionnel spécifique, un remodelage épigénétique et des adaptations de leur métabolisme cellulaire.

Par exemple, le facteur de transcription *Interferon regulatory factor* (Irf) 5 orchestre la polarisation pro-inflammatoire des macrophages du TA. Outre l'activation de la transcription de facteurs pro-inflammatoires, Irf5 réprime l'expression de cytokines anti-inflammatoires. Ce facteur de transcription joue un rôle dans la progression de pathologies auto-immunes.

L'invalidation de ce facteur améliore la sensibilité à l'insuline de souris obèses et limite le développement de complications hépatiques associées au DT2.

En parallèle de la régulation transcriptionnelle des gènes cibles de l'inflammation, le métabolisme cellulaire joue un rôle prépondérant dans la différenciation des cellules immunitaires. Les voies métaboliques contribuent à la production d'énergie pour la cellule mais aussi à la mise en place de leurs fonctions effectrices.

Les macrophages de type M1 présentent une activité glycolytique renforcée, notamment grâce à la translocation membranaire du transporteur de glucose GLUT1. La fonction mitochondriale de ces macrophages est diminuée. En effet, le cycle de Krebs présente deux interruptions. On note tout d'abord une accumulation de citrate qui contribue à la synthèse d'acides gras qui servent de précurseurs pour la production de médiateurs lipidiques pro-inflammatoires et au remodelage membranaire. Par ailleurs, il y a une accumulation de succinate, qui favorise la stabilisation du facteur de transcription HIF1α, qui induit la transcription de gènes pro-inflammatoires. De plus, la glutamine est capturée par les macrophages et est métabolisée en direction du cycle de Krebs.

Historiquement, la classification des macrophages était basée sur le métabolisme de l'arginine dans les macrophages M2. Ces macrophages utilisent principalement l'oxydation des acides gras pour produire de l'énergie. La fonction oxydative de ces macrophages est augmentée, notamment du fait de la biogenèse mitochondriale.

La description des adaptations métaboliques des cellules immunitaires a initialement et principalement été menée dans des contextes *in vitro*. Cet axe de recherche est aujourd'hui en pleine expansion pour la compréhension de ces phénomènes dans des contextes *in vivo*, en tenant compte des spécificités des macrophages résidents et des microenvironnements associés. L'impact du microenvironnement tissulaire joue un rôle clé dans ces processus. Les macrophages du TA de patients obèses sont hypermétaboliques, avec une augmentation de la fonction glycolytique et de la respiration oxydative.

Ce projet de thèse est composé de trois axes. Nous nous sommes principalement intéressés au rôle d'IRF5 dans les adaptations métaboliques des macrophages. En parallèle, nous avons mené un projet sur le lien entre métabolisme cellulaire et polarisation des macrophages. Finalement, dans le cadre d'une collaboration, nous nous sommes penchés sur le métabolisme cellulaire des macrophages dans un autre contexte d'inflammation stérile.

Axe 1 : IRF5 et les adaptations métaboliques des macrophages au cours d'un stress métabolique

Hypothèse et objectifs du projet de thèse

Des études récentes ont mis en exergue le rôle d'IRF5 dans le contrôle de la fonction glycolytique des macrophages, dans des contextes d'auto-immunité ou bien d'infection virale. Considérant ces données et le rôle majeur d'IRF5 dans la pathogenèse de l'obésité, nous avons émis l'hypothèse qu'en réponse à un stress métabolique, IRF5 pouvait moduler les voies bioénergétiques des macrophages.

Les objectifs de cette thèse sont :

1. Evaluer les adaptations métaboliques IRF5-dépendantes des macrophages du TA au cours de l'obésité
2. Déterminer les mécanismes moléculaires associés à ces adaptations métaboliques,
3. Evaluer le potentiel translationnel du rôle d'IRF5 dans les adaptations métaboliques des macrophages chez des patients obèses et/ou diabétiques

Approche expérimentale

Des souris C57BL6/J ou bien spécifiquement invalidées pour IRF5 dans les macrophages (IRF5-KO) sont soumises à un régime gras pendant quatre semaines. Cette invalidation génétique est générée avec le système Cre-Lox. Pour étudier les adaptations métaboliques des macrophages, nous utiliserons une approche par cytométrie en flux avec un panel de marqueurs permettant d'identifier les macrophages du TA, de quantifier les substrats métaboliques et l'activité mitochondriale, ainsi que l'expression d'IRF5. En lien avec ces études, les fonctions glycolytique et mitochondriale des macrophages du TA seront évaluées par une analyse de flux métaboliques. L'approche mécanistique est réalisée grâce à des données transcriptomiques et des données publiques de séquençage après d'immunoprécipitation de chromatine (ChIP-seq) d'IRF5, et est validée in vitro. Enfin, des analyses similaires sont réalisées sur des biopsies de TA de patients obèses et/ou DT2, prélevées lors de chirurgie bariatrique.

Résultats

Afin de déterminer si les macrophages du TA adaptent leur métabolisme au cours d'un régime gras de façon IRF5-dépendante, nous avons analysé la fonction mitochondriale, la capture du glucose et le contenu lipidique des macrophages du TA de souris sauvages ainsi que l'expression d'IRF5 dans ces cellules. Si ces trois paramètres métaboliques sont modulés avec

le régime et indiquent une adaptation spécifique du métabolisme cellulaire, seule l'activité mitochondriale des macrophages est négativement corrélée avec l'expression d'IRF5. En appliquant le même schéma expérimental sur des souris IRF5-KO, nous démontrons que la respiration mitochondriale est augmentée dans les macrophages IRF5-KO, à la suite d'un régime gras. Cela suggère qu'IRF5 réprime la fonction mitochondriale des macrophages au cours d'un régime gras. Nous avons confirmé ces résultats *in vitro* avec un modèle de macrophages infiltrants. Au niveau transcriptionnel, on note un remodelage de l'expression des gènes associés au métabolisme cellulaire dans les macrophages IRF5-KO, confirmant le rôle d'IRF5 dans la respiration mitochondriale. De manière intéressante, les macrophages IRF5-KO présentent une surface de crêtes mitochondriales qui est augmentée par rapport aux macrophages contrôles. Ces crêtes sont des structures servant de support à l'ancrage des différents complexes protéiques impliqués dans le métabolisme oxydatif. Ces adaptations métaboliques favorisent un remodelage bénéfique du TA avec une meilleure sensibilité à l'insuline au cours du régime gras chez les souris IRF5-KO.

Afin de déterminer par quel(s) mécanisme(s) les macrophages IRF5-KO sont hyperoxydatifs, nous utilisons des données publiques de ChIP-seq d'IRF5 ainsi que nos données de transcriptomiques pour déterminer les gènes dont l'expression est régulée dans des contextes de stress métaboliques, en fonction de la fixation d'IRF5 à la chromatine. Nous avons identifié un gène cible : *Growth Hormone Inducible Transmembrane Protein* (GHITM). Ce gène joue un rôle dans le maintien des crêtes mitochondriales et son expression est négativement corrélée à celle d'IRF5. Par ailleurs, *in vitro*, nous validons la contribution de GHITM au phénotype hyperoxydatif des macrophages IRF5-KO. Finalement, des approches expérimentales similaires et l'utilisation de données publiques de séquençage sur des macrophages humains, nous ont permis de confirmer le rôle d'IRF5 dans les adaptations mitochondriales des macrophages du tissu adipeux de patients obèses et/ou diabétiques, via la répression de l'expression de GHITM.

Axe 2 : Influence du métabolisme cellulaire sur la polarisation des macrophages

La polarisation des macrophages est associée à un remodelage spécifique du métabolisme cellulaire. Cependant, il reste à déterminer si la modulation des voies métaboliques per se peut altérer la polarisation des macrophages.

Dans ce projet, nous utilisons un modèle in vitro de macrophages, que nous traitons avec des inhibiteurs de voies métaboliques. Par la suite, nous stimulons ces macrophages avec les activateurs canoniques associés avec les polarisations M1 et M2.

Dans ce contexte, nous démontrons que l'inhibition de certaines voies métaboliques altère la capacité de polarisation et d'activation des macrophages, mesurée par l'expression et la production de diverses cytokines.

Axe 3 : Métabolisme cellulaire des macrophages au cours des crises de goutte

Ces résultats sont issus d'une collaboration avec l'équipe de Dr Ea. Les crises de goutte représentent l'atteinte articulaire la plus courante. Il s'agit d'une inflammation douloureuse, aigüe, au niveau d'une articulation. D'un point de vue cellulaire, la présence de cristaux d'urate monosodique ou de pyrophosphate de calcium active le système immunitaire, et notamment les macrophages. Les macrophages peuvent phagocyter ces cristaux, activant le complexe protéique de l'inflammasome. Cette activation de l'inflammasome permet la sécrétion d'IL1b et le recrutement de neutrophiles.

Dans ce projet, il s'agit de déterminer les voies métaboliques impliquées dans l'inflammation induites par ces cristaux.

Ainsi, nous avons démontrer que l'activité glycolytique était modulée au cours du processus inflammatoires associés aux crises de goutte, notamment grâce à la translocation membranaire du transporteur de glucose GLUT1. Cette adaptation du métabolisme cellulaire est nécessaire à la production d'IL1b. Par ailleurs, l'inhibition *in vivo* de la capacité glycolytique des macrophages permet de l'imiter l'intensité des crises de goutte, chez la souris.

Conclusion

Ces résultats soulignent un rôle novateur pour IRF5. IRF5 a une fonction, non canonique, dans les adaptations métaboliques des macrophages au cours de l'obésité, indépendamment de son rôle inflammatoire. Le rôle d'IRF5 dans le contrôle du métabolisme cellulaire a notamment été récemment décrit dans les macrophages alvéolaires en réponse à une infection virale. Par ailleurs, des polymorphismes de surexpression d'IRF5 sont associés à une augmentation de la fonction glycolytique dans les monocytes humains.

En parallèle, nous avons démontré que le métabolisme cellulaire per se pouvait contrôler l'activation des macrophages. Par ailleurs, nous avons étudié les adaptations métaboliques

des macrophages dans un autre contexte d'inflammation stérile, à savoir l'arthrite induite par des cristaux. Dans ce contexte, nous avons mis en avant l'importance du métabolisme du glucose dans l'initiation du processus inflammatoire.

Ce projet de thèse qui s'inscrit à l'interface entre le métabolisme et l'immunologie, apporte un nouvel éclairage sur les adaptations métaboliques des cellules immunitaires. Les processus inflammatoires jouent un rôle clé dans la pathogenèse des maladies métaboliques. Une piste thérapeutique serait d'utiliser des stratégies anti-inflammatoires ou immuno-modulatrices. Ces approches sont actuellement en cours d'essais cliniques mais relèvent d'un coût financier important et d'une efficacité plutôt limitée. L'étude ciblée des voies métaboliques dans l'activation des cellules immunitaire s'avère être une piste thérapeutique intéressante. A noter que l'augmentation du métabolisme oxydatif des macrophages du TA améliore la sensibilité à l'insuline des souris obèses. Des approches similaires sont en cours d'étude dans le contexte de la sclérose en plaques et des transplantations de moelle osseuse.